Regulation of the μ-opioid receptor signalling in naturally occurring variants and phosphorylation site mutants

By

Marina Junqueira Santiago

A thesis submitted to Macquarie University

for the degree of

Doctor of Philosophy

Department of Biomedical Sciences

October 2015

MACQUARIE
University
Faculty of Medicine and
Health Sciences

Typeset in LaTeX 2_ε.

The work presented in this thesis is, to the best of my knowledge, original except as acknowledged in the customary manner. I hereby declare that I have not submitted this material, either in full or in part, for a degree at this or any other institution.

Marina Junqueira Santiago

Dedicated to my beloved partner, Luke Reid, who opened my eyes to a whole new world and taught me that everything is possible...

Acknowledgements

A large number of people were crucial directly or indirectly through this journey that has led to this thesis, and here I would like to show my gratitude for all their help and support.

First of all, I would like to thank God, without whom nothing is possible.

My special gratitude and thanks to my principal supervisor Prof. Mark Connor for this amazing opportunity and all the guidance throughout these years. I also would like to thank my associate supervisor Prof. Helen Rizos who was of great help during the final stage of my PhD candidature.

Many thanks to Prof. MacDonald Christie for providing some of the AtT20 cells used in this project, for allowing me access to Sydney University facilities to perform radioligand binding assays, and to Yan Ping Du and Cheryl Handford for the technical assistance and training.

Much appreciation to Natasha Grimsey from Auckland University for all her time and patience in helping me better understand molecular biology.

Thanks to all members of the Connor lab: Marika Heblinski, Rozhin Ashgari, Philip Bennallack, Jordyn Stuart, Dharmica Mistry, Courtney Breen, Amelia Edington, Max Camo, and a super special one to Alisa Knapman who shared this crazy opioid world with me. In addition, I would like to extend my gratitude to everybody in ASAM, especially Vivienne Lee, Erin Lynch, Nurul Farhana, Newsha Raoufi-Rad, Vanessa Tan and Varun Sreenivasan, who have helped me and made my days much more fun; I am going to miss you all.

It would be fitting to thank those people that, a long time ago, opened the doors to research and introduced me to this new exciting world. Therefore my thanks and appreciation to Prof. Alexandre Pyrrho, Prof. Sônia S Costa and for their lab members from Universidade Federal do Rio de Janeiro.

I grew up in a country where a very small percentage of the population have access to a high standard education. I would like to express my profound gratitude to my parents, Vânia M J Santiago and Fernando A D Santiago, for all their hard work and love that supported my education and dreams.

Finally, a very special thanks to Kerry and Stephen Reid for all their love and support, to my Aussie family who makes life much more fun, and my spiritual guides who are always with me. Couldn't have done this without you all!

List of Publications

Peer Reviewed Publications

1. Alisa Knapman, **Marina Santiago** and Mark Connor, "A6V polymorphism of the human μ-opioid receptor decreases signalling of morphine and endogenous opioids *in vitro*", *Br J Pharmacol*, available online, 2015

2. Alisa Knapman, **Marina Santiago** and Mark Connor, "Buprenorphine signalling is compromised at the N40D polymorphism of the human μ opioid receptor *in vitro*", *Br J Pharmacol*, Vol.171, pp.4273-4288, 2014

3. Alisa Knapman, **Marina Santiago**, Yan Ping Du, Philip Bennallack, MacDonald Christie and Mark Connor, "A continuous, fluorescence-based assay of μ-opioid receptor activation in AtT-20 cells", *J Biomol Screen*, Vol.18, pp.269-276, 2013

Conference Presentations and Posters

1. **Marina Santiago**, Alisa Knapman, and Mark Connor, "Signalling pathway-selective consequences of the common μ-opioid receptor variants A6V and N40D", *Australasian Society of Clinical and Experimental Pharmacologists and Toxicologists (ASCEPT)and the Molecular Pharmacology of GPCRs (MPGPCR) meeting*, 2014

2. **Marina Santiago**, YanPing Du, MacDonald Christie and Mark Connor, "Desensitization of the μ-opioid receptor in intact AtT20 cells: is C-terminal phosphorylation essential?", *International Narcotics Research Conference (INRC)*, 2013

3. **Marina Santiago**, YanPing Du, MacDonald Christie and Mark Connor, "μ-Opioid receptor homologous and heterologous desensitization: Is C-terminal phosphorylation essential?", *Gordon Research Conference on Molecular Pharmacology*, 2013

4. **Marina Santiago**, YanPing Du, MacDonald Christie and Mark Connor, "Activation and acute desensitization of μ-opioid receptor wild-type and mutants with deleted phosphorylation sites", *Australasian Society of Clinical and Experimental Pharmacologists and Toxicologists (ASCEPT)*, 2012

5. **Marina Santiago**, Philip Bennallack and Mark Connor, "Desensitization of acute μ-opioid receptor signalling measured using a continuous membrane potential assay", *Australasian Neuroscience Society (ANS) Conference*, 2011

Abstract

Opioid drugs are highly effective for the treatment of moderate to severe nociceptive pain. They exert their analgesic and rewarding effects primarily by signalling through the μ-opioid receptor (MOPr). The focus of this project was to better understand MOPr signalling regulation by investigating natural variants of MOPr and MOPr phosphosite mutants.

Isogenic, stably transfected mouse pituitary adenoma (AtT20) cell lines expressing eight naturally occurring human MOPr variants and four phosphomutants were created. Opioid-stimulated changes in membrane potential were measured using a membrane potential-sensitive dye, while receptor phosphorylation of Ser377 residue was determined by Western Blot and whole-cell ELISA was used to obtain the receptor surface loss dynamics.

The N-terminal MOPr variants, A6V and N40D, are the most common single-nucleotide polymorphisms found worldwide. Their signalling regulation was quite similar to the wild-type MOPr in each assay, where buprenorphine was the opioid with the most variance observed. In AtT20-hMOPr-L85I cells morphine mediated internalisation was not as substantial as previously reported, while the second intracellular loop (ICL2) polymorphism R181C dramatically impacted receptor ability to signal by affecting opioid affinity and probably G protein binding. The majority of the third intracellular loop (ICL3) variants had detrimental effect in receptor signalling and regulation which indicates the important role this region plays in G protein activation. In addition the multiple phosphorylation mutants also affected membrane expression

which was related to endoplasmic reticulum sequestration and possible changes in receptor stability. Finally, deleting all the putative phosphorylation sites in the human MOPr C-terminal domain did not greatly influence homologous desensitisation of the membrane potential signal, yet completely abolished internalisation as expected. In contrast heterologous desensitisation was deeply compromised in some mutants of the ICL3 while total phosphorylation deletion of the C-terminal was the only variant to increase desensitisation of somatostatin signalling. Interestingly buprenorphine induced signalling had a quite different profile across the variants, and morphine and methadone signalling were more affected by the ICL3 changes when compared to opioid peptides and buprenorphine.

Overall, these results support the hypothesis of multiple mechanisms involved in regulation of MOPr, where ICL2 and ICL3 are crucial for G protein signalling, and receptor phosphorylation is not necessary for receptor desensitisation. In addition, this work highlights the profound effect of rare polymorphisms on opioid response at the molecular level, which is likely to contribute to the significant inter-individual variability observed with opioid therapy.

List of Abbreviations

AC	Adenylyl Cyclase
β_2AR	β_2-Adrenergic Receptor
β-FNA	β-Funaltrexamine
BSA	Bovine Serum Albumin
cAMP	Cyclic Adenosine Monophosphate
CA	Calcium Assay
CaMKII	Calcium/Calmodulin-Dependent Protein Kinase II
CHO	Chinese Hamster Ovary
Con A	Concanavalin A
CRC	Concentration Response Curve
DAMGO	[D-Ala^2,N-MePhe^4,Gly-ol]-enkephalin
DMSO	Dimethyl Sulfoxide
DNA	Deoxyribonucleic Acid
DOPr	δ-Opioid Receptor
ECL	Extracellular Loop
Endo-2	Endomorphin-2
ER	Endoplasmic reticulum
ERK	Extracellular Signal-Related Kinase
GIRK	G Protein-Coupled Inwardly Rectifying Potassium Channel
GPCR	G Protein Couple Receptor
GRK	G Protein Receptor Kinase

HA-tag	Human Influenza Hemagglutinin Tag
HBSS	Hank's Balanced Salt Solution with HEPES
HEK	Human Embryonic Kidney
ICC	Immunocytochemistry
ICL	Intracellular Loop
hMOPr	Human μ-Opioid Receptor
LC	Locus Coeruleus
ME	Met-Enkephalin
mMOPr	Mouse μ-Opioid Receptor
MOPr	μ-Opioid Receptor
MPA	Membrane Potential Assay
PKA	Protein Kinase A
PKC	Protein Kinase C
PMA	Phorbol-12-myristate-13-acetate
PTM	Post-Translational Modification
PTX	Pertussis Toxin
rMOPr	Rat μ-Opioid Receptor
RFU	Relative Fluorescence Units
RGS	Regulator of G Protein Signalling
SEM	Standard Error of the Mean
SNP	Single-Nucleotide Polymorphism
SST	Somatostatin
TM	Transmembrane
WT	Wild-Type

Contents

1

General Introduction and Outline

Opioids are widely used clinically because of their unique analgesic properties, which are largely mediated by the activation of the μ-opioid receptor (MOPr)[233]. Adverse effects, in addition to tolerance and dependence, bring limitations to opioid therapy; however opioids are still largely prescribed considering the absence of superior or even equivalent therapeutic options for moderate to severe pain. Better understanding of the molecular mechanisms involved in MOPr signalling and regulation is essential for developing improved drugs with less unwanted effects.

Furthermore, the study of pharmacogenomics has enriched our understanding of genetic mutations which can affect opioid drugs pharmacokinetics and pharmacodynamics. Genetic variation of some enzymes of the CYP450 superfamily is well established to be responsible for some variability in response to opioids[269,304,305]; however MOPr polymorphisms also need to be considered. A large number of human μ-opioid

receptor (hMOPr) single-nucleotide polymorphisms (SNPs) have been previously reported[180,326], and aside from many studies of the most common SNP allele A118G (N40D) , only a few studies have analysed the molecular mechanisms behind the other SNPs. While rare polymorphisms do not attract the attention of clinical studies, the effect of amino acid changes in receptor signalling and regulation may help to elucidate the importance of receptor regions and, together with the most common polymorphisms, may add to the complex inter-individual variability in opioid response which is a major clinical problem.

1.1 Hypotheses and Aims

This project is based on two main hypotheses:

I. Single-nucleotide polymorphism can differentially regulate hMOPr function, which could contribute to inter-individual variability in opioid analgesics response

II. Phosphorylation of the hMOPr regulates receptor signalling being an important component for desensitisation

By studying expression, signalling, desensitisation, phosphorylation and receptor surface loss of hMOPr SNPs and phosphosite mutants of different regions of the receptor, I aimed to assess signalling and regulation differences between variants and wild-type receptor, in addition to examine the functional importance of specific receptor regions.

1.2 Thesis Outline

This thesis contains eight main chapters including one introductory, one experimental methodology and five results chapters.

- Introductory chapter
  - Chapter 2 briefly covers the importance of opioid drugs and literature review pertinent to this thesis

- Experimental methodology
  - Chapter 3 describes the details of experimental procedures used throughout this PhD project.
- Experimental results and discussions
  - Chapter 4 documents the use of a new non-invasive, real-time kinetics technique to assess MOPr homologous and heterologous desensitisation. This chapter also examine the effect of kinase modulators in desensitisation.
  - In Chapter 5, the investigation of the effect of two common SNPs of the hMOPr N-terminal on signalling and regulation is presented.
  - Chapter 6 documents the study of two rare SNPs; one SNP in the first transmembrane domain which has been linked to a total loss of function, and one SNP in the second intracellular loop that promotes morphine induced endocytosis.
  - In Chapter 7, signalling and regulation is assessed using six hMOPr variants of the third intracellular loop. Three variants are SNPs and the other three are phosphosite mutants, where serine and/or threonine were substituted to alanine.
  - Chapter 8 study focused on determining the importance of phosphorylation of the hMOPr C-terminal tail in signalling and desensitisation by using a C-terminal total phosphosite deleted receptor.
  - Chapter 9 contains a summary of important findings, in addition to discussing some limitations and further directions to the present work.
- Appendices
  - Appendices A and B contain information regarding products, recipes, equipment and suppliers used.

- Appendix C contains information not included in Chapter 3 regarding vectors and transfections performed during this project.
- Appendix D contains important controls regarding kinase modulators used in Chapter 4.
- Appendix E and F contain biosafety approvals, biosafety workshop certificate and radiation safety certificate that were obtained to carry out experiments reported in this thesis.

2

Introduction

In this introductory chapter a review of some of the important aspects involving opioid drugs, therapy and receptors will be presented. This PhD project is focused on the molecular mechanisms of the μ-opioid receptor, therefore attention will be given to review μ-opioid receptor structure, signalling and regulation.

Contents

2.1 Introduction to Opioids

The use of opium for its rewarding and therapeutic effects is described in many historical documents, but modern opioid pharmacology was only born after morphine isolation in the beginning of the Nineteenth century[47]. Since then a large number of studies in this area has been published, especially in the last fifty years after opioid receptors and peptides were recognised, and cloning opioid receptors together with genetic manipulations became possible[266]. Recent technological advances enabled the performance of a variety of functional assays in addition to conformational studies of opioid receptors; however, until today, many aspects of opioid signalling regulation are still unclear.

2.1.1 Endogenous Opioid Peptides and Opioid Receptors

In 1954, Beckett and Casy[26] reviewed the information available and reported drug-receptor mechanisms involving the action of opioids. At that time a large number of opioids were already synthesised and not only agonists were found, but also antagonist and mixed agonist-antagonist drugs[47]. The varying effect observed for these opioid drugs not only raised the question regarding multiple opioid receptors[227,276], but also the use of antagonists supported the existence of endogenous opioids[3].

The opioid receptor family contains four members: μ, κ and δ opioid receptors, and the opioid like nociceptin receptor. The μ-opioid receptor (MOPr) and the κ-opioid receptor (KOPr) were first described by Martin et al. (1976)[228] and were named after the agonists morphine and ketocyclazocine, respectively. Lord et al. (1977)[212] assessed binding properties in vas deferens homogenates and determined the existence of a different opioid receptor from previously described MOPr and KOPr. Hence they proposed the existence of the δ-opioid receptor (DOPr, named after the tissue). These three receptors genes were cloned in the early 90's, which enabled investigating these receptors in recombinant systems, where binding and functional properties of the recombinant and endogenous receptors were found to be equivalent[62,114,176,177,363]. Furthermore, the advent of cloning techniques facilitated the search for related opioid receptors based on sequence homology, and this led to the successful identification of nociceptin receptor (NOPr), also known as opioid receptor like-1[48,244]. It is noteworthy that some studies supported the division of the main opioid receptors into subtypes; however evidence is lacking[4,77]. In this thesis I will only be using the current NC-IUPHAR approved nomenclature as discussed by Cox et al. (2015)[86].

Having mentioned the opioid receptor family, it is important to highlight that none of the aforementioned receptors are orphans. Endogenous opioid ligands have been identified in brain extracts almost simultaneously to the description of the three classical opioid receptors, and in mammals three main precursors are known: proenkephalins, prodynorphin and pro-opiomelancortin (POMC)[47,266]. Many opioid peptides have been reported but some examples are: met-enkephalin (ME) and leu-enkephalin which are

derived from proenkephalins and they bind preferably to the DOPr[159]; prodynorphin gives rise to dynorphin A and B which are KOPr ligands[135]; and last POMC is the precursor of many important physiological peptides including β-endorphin which has higher affinity for the MOPr[85]. Remarkably, none of the opioid peptides bind exclusively to one opioid receptor, and they present negligible affinity for NOPr[82]. Endomorphin-1 and endomorphin-2 are opioid peptides isolated from brain extracts which present a high selectivity and affinity for the MOPr. However, interestingly the evidence for endomorphins precursor is missing even after a full human proteomic search; therefore they are putative endogenous peptides[337,366]. Nociceptin also called orphanin FQ was identified as the endogenous ligand of NOPr with the pro-prenociceptin precursor[239,289]. NOPr will not be discussed further, as it has a pharmacological profile and behaviour considerably distinct from classical opioid receptors[263].

The use of endogenous opioid peptides as an analgesic drug *in vivo* is limited by the profound enzymatic degradation when systemically administered[143,144]. Therefore a number of enkephalin analogues was developed with modified C and N-terminal and this was found to significantly decrease enzymatic breakdown in addition to modifying peptide selectivity[144]. Unfortunately, even with modifications, the pharmacokinetic profile of these peptides was still quite disadvantageous compared with opioid analgesics such as morphine. Thus the use of these synthetic peptides is largely restricted to research. One enkephalin synthetic analogue [D-Ala^2,N-MePhe^4,Gly-ol]-enkephalin, known as DAMGO, has been largely used in research, as it is a stable peptide and highly selective for MOPr[151]. DAMGO, β-endorphin and endomorphin-2 were used in the present work and their chemical structures, together with met-enkephalin, are presented in Figure 2.1. Note that β-endorphin is a relatively long peptide containing 31 amino acids compared to five amino acids for met-enkephalin and four for endomorphin-2.

In addition to the endogenous and synthetic peptides, food-derived opioid peptides also called exorphins have been identified. Casein, a milk protein, and gliadin, a gluten-derived protein, are examples of proteins that, digested by enzymes, release peptides

with opioid activity. Interestingly, these peptides may affect gut function[246] including predisposing susceptible individuals to inflammatory and systemic oxidation[342]. The effect of these food-derived peptides in human endogenous opioidergic systems is not well understood and further research is necessary to determine if they play any physiological role[338].

Met-enkephalin

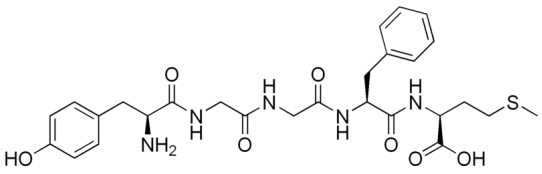

DAMGO

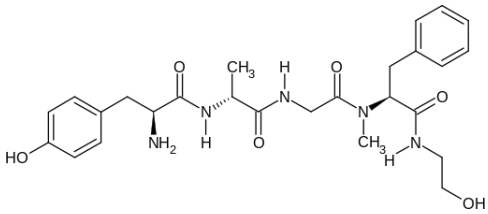

Endomorphin-2

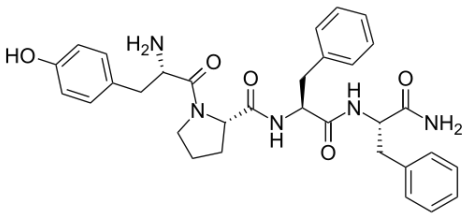

β-endorphin

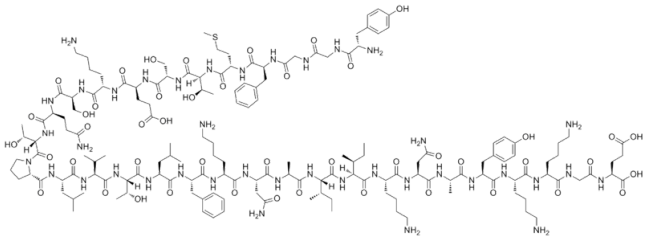

Figure 2.1. Chemical structures of opioid peptides used in this project, in addition to met-enkephalin

2.1.2 Opioid Analgesics and their Clinical Relevance

Since morphine was first extracted from the opium poppy, numerous opioid drugs became available. These drugs can be classified according to the effect on the receptor; however this classification is avoided here considering function selectivity, where some agonists may be full agonists in one pathway but partial in another pathway. Therefore in Table 2.1 some of the available μ-opioid receptor drugs are listed according to the mode of synthesis, a generally accepted classification. In addition, the chemical structures for the four non-peptide opioid agonists used in this project, together with two antagonists, are presented in Figure 2.2.

The majority of the opioid analgesics available for clinical use are relatively MOPr selective compounds[288]. Morphine affinity is higher for MOPr, however it is still able

Table 2.1. Examples of opioid drugs classified according to synthesis process

Naturally occuring compounds	Semi-synthetic compounds	Synthetic compounds
Morphine	Buprenorphine	Methadone
Codeine	Oxycodone	Fentanyl
Papaverine	Heroin	Pentazocine
Thebaine	Hydromorphone	Tapentadol

Adapted from Pathan and Williams (2012) [266]

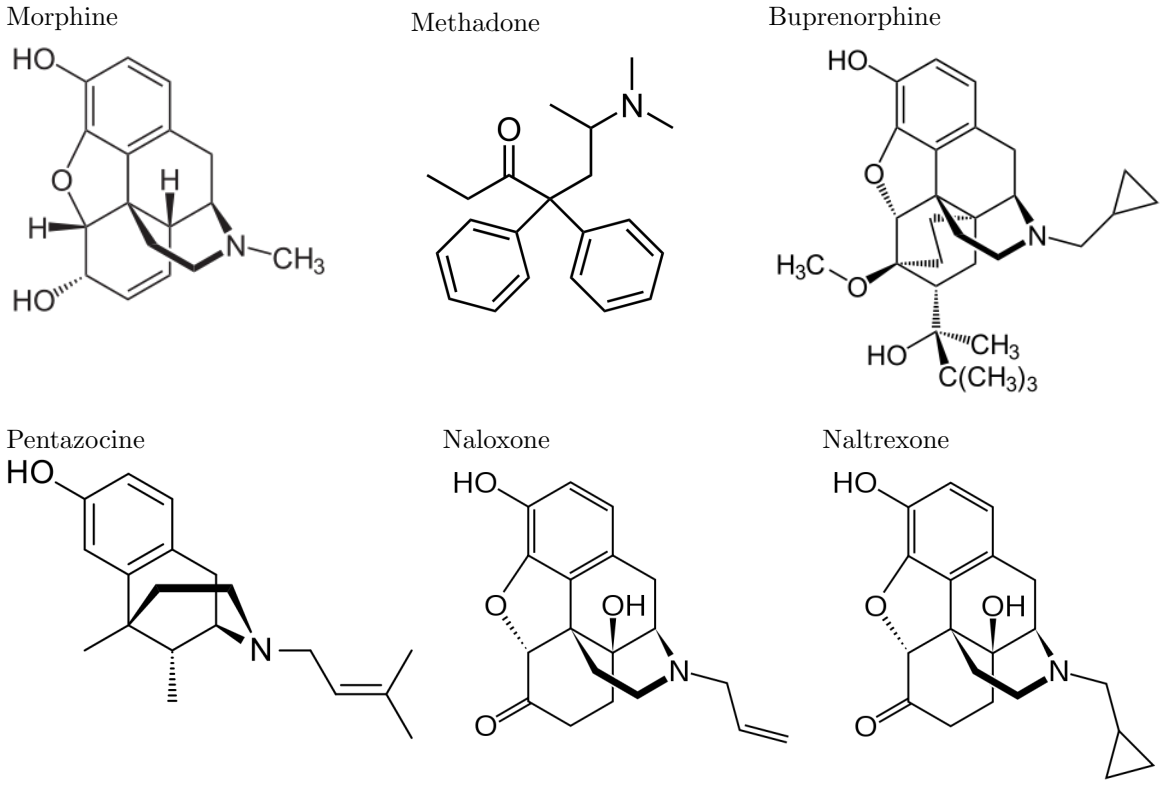

Figure 2.2. Chemical structures of opioid analgesics used in this project and two opioid antagonists.

to bind to KOPr and DOPr, but with a much lower affinity, and pentazocine and buprenorphine are non-selective drugs [288]. Interestingly buprenorphine is a low intrinsic activity agonist at MOPr and antagonist at DOPr and KOPr [215].

The relevance of opioids drugs in current medical practices is irrefutable. Opioids are the most effective drugs available for the treatment of pain, thus therapeutic guidelines not only in Australia, but in most countries recommend the use of opioids for moderate to strong pain [145,252,299]. Opioids are well established for the treatment

of acute pain in many conditions, and chronic pain of terminally ill patients. However, only recently under much controversy has the long-term use of opioids for chronic noncancer pain been accepted[299]. In the U.S., chronic nonmalignant pain affects approximately 116 million Americans[245]. This gives a good estimate of how these new guidelines increase dramatically the number of patients taking opioids, and emphasises the importance of developing better drugs with safer profiles, with fewer adverse effects and reduced potential to develop tolerance and dependence.

In Australia, a range of opioid analgesics are commercialized for oral, transdermal and intravenous administration. The most commonly prescribed opioid for analgesia is codeine combined with paracetamol, probably because of low restriction, and it is followed by tramadol, oxycodone, buprenorphine, morphine and fentanyl[149]. In the absence of new developed drugs with lower adverse effects, the pharmaceutical industries are developing new combinations such as oxycodone and naloxone to decrease constipation, a very common side effect[49].

It is noteworthy that opioid drugs are highly effective in the treatment of nociceptive pain (somatic and visceral); however pain can also comprise a different component which is neuropathic. This type of pain which arises from damaged or dysfunctional nerves was initially described as 'opioid resistant' but neuropathic pain is now known to respond to opioids; however, higher doses are generally required, which increase the probability of bothersome adverse effects[10,111,252]. Tramadol is usually recommended before stronger opioids as its serotonergic and noradrenergic effects may be beneficial[109]. Nevertheless, guidelines support the use of antidepressants (tricyclic antidepressants and duloxetine) or anticonvulsants (pregabalin and gabapentin) as better options for treating neuropathic pain[252,308,309].

2.1.3 Overview of Opioid Neurobiology

The endogenous opioid system plays an important role in modulating analgesia, reward (which is involved with food intake and drug addiction), and emotional and stress responses[29]. Moreover, this complex neuromodulatory system is also involved

in autonomic control including respiration, gastrointestinal motility and thermoregulation[283,302], thus explaining many of the opioid adverse effects such as respiratory depression[40] and constipation[46,188].

Before the identification of each specific opioid receptor, it was already clear that different opioid receptors were present in the central nervous system (CNS)[270,319,336], and their distribution was not uniform[191]. Since then many studies have reported the presence of opioid receptors throughout the CNS[52,222,223], and these receptors also occur at lower concentration in the peripheral tissue such as the sensory and enteric nerves, cardiovascular and immune systems[44,188,328,329].

Besides being widely distributed throughout the CNS, high expression of opioid receptors occurs in the periaqueductal grey (PAG), locus coeruleus (LC) and rostral ventral medulla, and also in the substancia gelatinosa of the dorsal horn, which is extremely important region for transmission of pain impulses from the periphery[266]. Molecular cloning and sequencing of opioid receptor cDNA enabled *in situ* hybridisation studies, which together with other techniques, ascertained the distinct expression pattern for the three classical opioid receptors , where MOPr have the highest overall expression and a distinguishing high density in the LC, striatum, thalamus and PAG regions of mammalian CNS[222,223,268]. Both opioid receptors expression and the synthesis of their endogenous peptides are variable; a recent study had demonstrated the presence of enkephalins and dynorphins in the dorsal horn while β-endorphin was undetectable[230]. As expected, many regions expressing opioid receptors are in the neuronal circuit of pain modulation, which was recently reviewed by Ossipov et al. (2010)[258]. The analgesic effect reported for MOPr agonists are mainly attained by directly inhibiting nociceptive afferents in the periphery, or indirectly increasing neuronal activity in the inhibitory descending pathway.

MOPr has been associated with physiological functions including analgesia, gastrointestinal motility and social behaviour[213,226,323]. The advances in gene technology also allowed disruption of the MOPr expression in mouse models which defined the

main role this receptor plays in analgesia. Interestingly, in MOPr knockout mice, morphine not only fails to promote analgesia but also tolerance, reward effect, physical dependence and adverse effects such as respiratory depression and constipation[126,233,301]. These findings emphasise the complexity of developing an ideal analgesic drug, because, in this case the desired and undesired effects are produced by activation of the same receptor type.

Analgesia, motor control, reward and emotion are some of the physiological functions correlated to DOPr[72,150]. In contrast to MOPr, morphine analgesic effect was not affected in DOPr knockout mice, but analgesic tolerance to morphine did not develop[376]. Likewise, analgesic response of KOPr knockout mice to morphine treatment was similar to wild-type mice; reward was also unaffected but the severity of withdrawal syndrome was reduced[320]. KOPr also has important physiological roles including analgesia, immunomodulation and behaviour control[53,89]. By studying physiological pain between knockouts MOPr, DOPr and KOPr mice, Martin et al. (2003)[226] reported an antinociceptive opioid tone differentially regulated by the three classical opioid receptors. Together these studies confirm not only the importance of the endogenous opioid system in physiological function, but also support the crucial role of the MOPr in opioid analgesic therapeutic response.

2.1.4 Overview of Opioid Tolerance, Dependence and Addiction

The history of opium abuse dates back to ancient times, and soon after the isolation of morphine, it was clear that the potential to abuse morphine was similar to opium[47]. Since then, large efforts have concentrated on finding an ideal opioid which has high analgesic properties but low abuse potential. Interestingly, heroin is a failed attempt at developing such an ideal opioid.

A great deal of confusion surrounds the terms tolerance, dependence and addiction. Tolerance is related to the decrease in drug effectiveness after repeated exposure. Under chronic opioid treatment, patients report a necessity of increasing drug dose to maintain

level of analgesia; besides the most common cause being disease related increased pain, dose escalating is also known to be caused by tolerance development[110,275]. Opioid tolerance is also classified as acute or chronic. Perioperative and postoperative analgesia are regularly achieved by using opioids, and patients may very rapidly develop tolerance. Therefore, these situations offer good evidence of acute opioid tolerance in the clinical scenario[6,178]. Many studies into tolerance also look at opioid induced hyperalgesia (OIH), which is the increase of perception of certain painful stimuli with opioid treatment[6,123]. OIH is a extremely controversial topic which was critically discussed by Bantel et al. (2015)[25]. A good body of clinical evidence for chronic tolerance in analgesia is lacking, as the majority of the work does not differentiate between increase in pain associated with the underlying condition and real tolerance[18].

Nevertheless, a large amount of animal work have demonstrated the development of tolerance after prolonged opioid treatment; and the development of tolerance to some of opioid side effects is well documented[110]. Many studies had demonstrated that different factors contribute to the development of tolerance, for example, it is known that different opioids as well as different route of administration can produce varying degrees of tolerance and cross-tolerance[264,267,348]. These not only enable opioid rotation therapy to manage chronic pain with less dose escalation, but also indicate that development of a drug that has high analgesic potency and low tolerance potential may be possible[136,322]. In addition, varying levels of tolerance have been reported to different opioid circuits. While tolerance to opioid induced-constipation does not usually develop[107], which can become a problem for appropriate management of chronic pain, tolerance may occurs to respiratory depression in a lower rate than euphoric effects, consequently increasing the risk of overdose in opioid abuse[354].

Physical dependence is related to adaptations of the body to the long-term administration of a drug. It is well characterised by detection of withdrawal symptoms when a drug is ceased. Addiction is a multi-faceted condition which is related to the rewarding effects of the drug. There are psychological and neurobiological factors involved in the possible development of addiction[186]. Therefore, many drugs can cause physical dependence however drugs that can produce positive reinforcement tend to be abused.

Because opioids have powerful rewarding properties it has a high potential for abuse. The neurophysiology of opioid in the rewarding circuit was recently reviewed by Fields and Margolis (2015)[121].

Opioid maintenance therapy is available in many countries including Australia. In this therapy, opioid addicts commonly replace illegal opioid use with buprenorphine or methadone, which are opioids with prolonged effect, with the objective of decreasing disease transmission through needle sharing, relieving cravings and blocking euphoric effects associated with opioid intake[170,234]. Note that opioid abuse not only includes the use of the heroin, but also other drugs such as oxycodone which is becoming a major problem in many countries[142,146].

A number of studies reported the role of the endogenous opioid system in substance abuse. This system is actually involved in the addiction process of many substances including alcohol, nicotine and cannabinoids[106,341]. For this reason, polymorphisms of the MOPr, especially A118G(N40D), have been of great interest in addiction studies; nevertheless, besides a large number of studies in the common A118G polymorphism, results are too conflicting to draw any conclusion[248,249,300].

In summary, all three opioid receptors are involved in many important physiological processes. However, after genetic manipulation, it became clear that the MOPr is the main receptor responsible not only for the analgesic effect, but also for tolerance, dependence and the rewarding properties of opioid drugs. The focus of this project was the regulation of MOPr signalling, and although desensitisation, phosphorylation and internalisation are likely to be involved in chronic exposure tolerance, the aim will be to understand molecular mechanisms underlying acute MOPr regulation.

2.2 μ-Opioid Receptor Structure

Function and structure are two very tightly correlated topics. For a long time studying function of receptors was an easier task than trying to determine their complex conformations. Fortunately, with the latest advances in G protein coupled receptor crystallography, we might understand how MOPr structure, conformational changes

and interaction with effectors produce varying signalling profile for different drugs.

2.2.1 G Protein Coupled Receptors

Opioid receptors are G protein couple receptors (GPCRs)[290], which is the largest family of membrane receptors in the human genome, encoding for nearly 800 different receptors[34]. Furthermore, GPCRs are important pharmacological targets, approximately 30-40% of the drugs available on the market act on these receptors[73,255]. The human μ-opioid receptor (hMOPr) gene *OPRM1* codes for a 400 amino acids structure that, like all GPCRs, has seven-transmembrane (TM) α-helices, with an extracellular N-terminal, where multiple N-glycosylation can be found, and an intracellular C-terminal tail containing many putative phosphorylation sites (Figure 2.3). It belongs to the GPCR rhodopsin-like subfamily, also known as class A. This classification was based on sequence and structural similarities; however, sequence homology is limited to a few conserved amino acid residues and motifs[14,124]. In contrast, the sequence homology between the integrants of the opioid receptor family are very high, and phylogenetic analysis had also reported significant similarity between opioid, somatostatin and GPCR neuropeptide receptor families[169].

GPCRs undergo conformation changes upon extracellular stimuli, these changes produce heterotrimeric G protein activation which evokes signal transduction[161]. This perfectly orchestrated signal transmission from the outside to the inside of the cell is largely dependent on the receptor structure and the subtype of G protein it preferentially activates[255]. The heterotrimeric G protein is formed by the three subunits α, β and γ, where 21 Gα, 6 Gβ and 12 Gγ subunits subtypes have been identified in human[255]. G proteins were grouped according to Gα subunit similarities, typically there are four main families: Gα_s, G$\alpha_{i/o}$, G$\alpha_{q/11}$ and G$\alpha_{12/13}$[24]. Activation of G proteins is dependent on the release of GDP from the Gα subunit and replacement by a GTP, this results in the dissociation of the active Gα and G$\beta\gamma$ subunits. G proteins are GTPase enzymes; they hydrolyse GTP into GDP switching 'off' the signal transduction pathway. Note that some factors can influence this important step, including regulators of G protein signalling (RGS) which accelerates the enzymatic process.

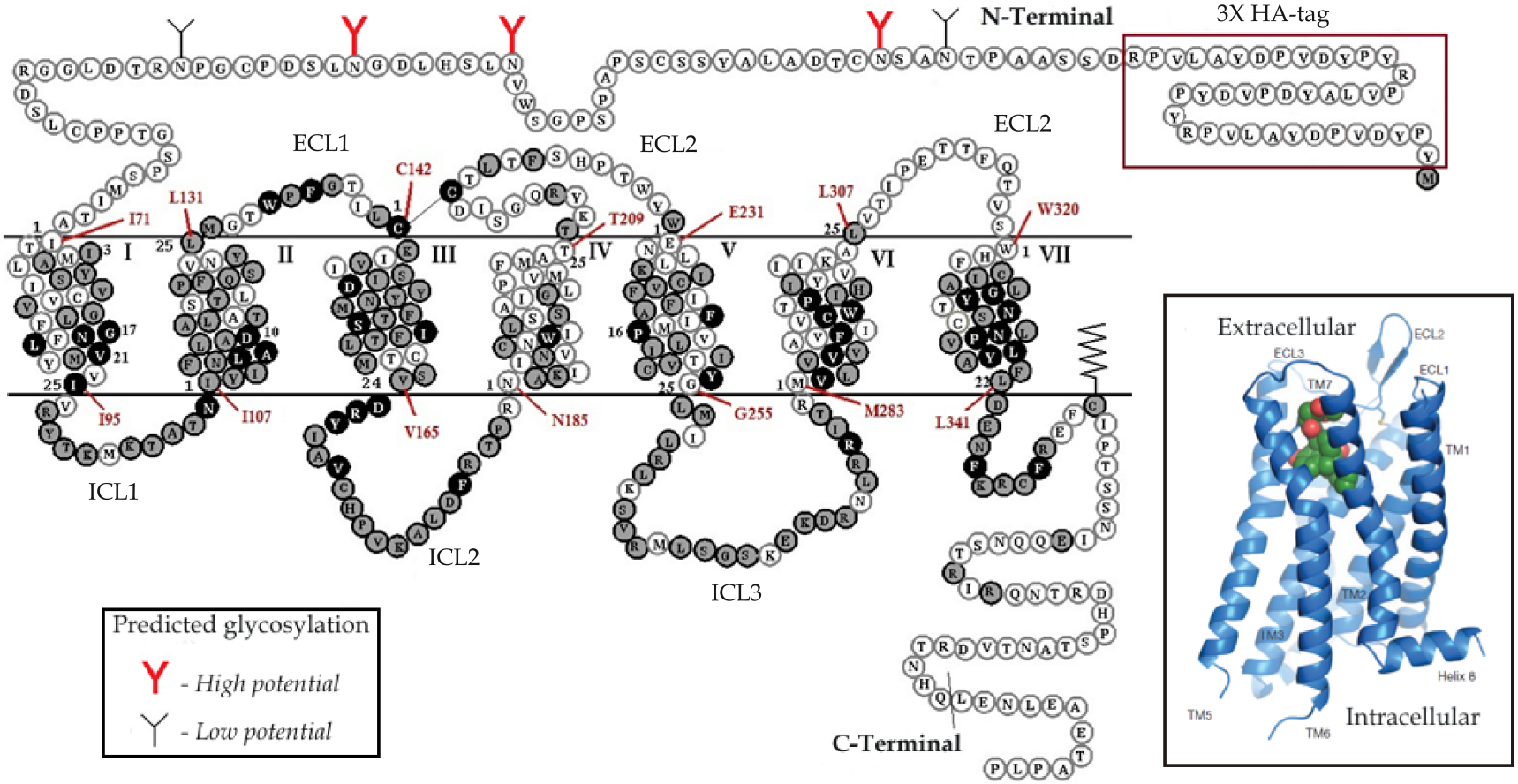

Figure 2.3. Serpentine structure of the human μ-opioid receptor showing triple HA tag attached to the N-terminal and predicted glycosylation sites. Class A GPCR highly conserved residues are in black and opioid receptors family conserved residues are in grey. Crystal structure overview for the mouse μ-opioid receptor bound to antagonist β-funaltrexamine (green/red) is illustrated in the box. Adapted serpentine figure from Center for Opioid Research and Design (CORD)[83] and crystal structure reproduced from Manglik et al. (2012)[220].

2.2.2 The μ-Opioid Receptor Crystal Structure

In 2000, Palczewski et al.[261] published the first GPCR crystal structure of bovine rhodopsin. Nevertheless, it took another 7 years and many advances in GPCR crystallography techniques to determine the crystal structure of the first ligand-activated GPCR, the β_2-adrenergic receptor (β_2AR)[65,284,296]. As highlighted by Rosenbaum et al. (2009)[297], some of the intrinsic characteristics of GPCRs impose challenges for crystallography which include low expression in native tissues, in addition to thermal and proteolytic instability. Manglik et al. (2012)[220] published the crystal structure of the mouse μ-opioid receptor (mMOPr) utilising many of the methods developed to overcome the challenges above. The N and C-terminal are extremely disordered regions thus they were truncated to increase proteolytic stability. The majority of the third intracellular loop was substituted for T4 lysozyme which stabilises TM5/TM6 region and also increases proteolytic stability. The receptor was expressed in Sf9 cells for a higher yield, and it was also bound to the antagonist β-funaltrexamine (β-FNA) to increase thermal (conformation) stability. Therefore, the mMOPr crystal structure is in the inactive conformation; and it is important to recognise that, considering the modifications to increase receptor stability, it actually determines native-like pharmacological and biophysical characteristics[297].

The overall view of the mMOPr bound to β-FNA is shown in Figure 2.3, where the position determined for the seven TM α-helices was illustrated. The mMOPr binding pocket for the antagonist used comprised residues in the TM3, TM5, TM6 and TM7 domains, and, compared to previous GPCR crystal structures, the pocket was remarkably deep but wide and open, which may explain the rapid dissociation constants observed for MOPr ligands[220]. Interestingly, out of the 14 residues that possibly interact with the bound antagonist, nine of them, which have a more direct interaction with β-FNA, are conserved in DOPr and KOPr. Nevertheless, it is expected that different opioids would have different positioning in the pocket, consequently, other residues are probably involved in binding interactions and may be responsible for varying receptor conformational changes[314]. One important point often ignored and highlighted by Bonner et al. (2000)[39] is that some residues may affect receptor

activation but not ligand binding, therefore when analysing receptor mutations it is important to avoid drawing conclusions based only on binding experiments. Another interesting feature of the mMOPr binding pocket is the absence of a highly charged surface, as observed for the chemokine receptor CXCR4; this possibly results in polar and non-polar interactions between the receptor and opioid drugs.

The MOPr crystal structure was able to confirm the previously predicted extracellular disulfide bond between Cys140, in the interface of the first extracellular loop (ECL) and TM2, with Cys217, in ECL2[220,372]. The intracellular interactions reported in the crystal structure involved the highly conserved DRY motif. A salt bridge was reported between the adjacent residues Asp164 and Arg165, in addition to two polar interactions, one between Asp164 and Arg179 and the second one between Arg165 and Thr279, in the distal region of the third intracellular loop (ICL). Considering that the structure reported is in the inactive state, and substitution of the Thr279 to a Lys produced a constitutive active receptor[154], the polar interaction Arg165-Thr279 is probably important for stabilising the receptor in an inactive conformation.

The ICLs and ECLs are flexible and were too disordered to be well characterised by crystallography; therefore, limited information was generated regarding these regions of the MOPr crystal structure. A previous study using mutagenesis techniques has determined the importance of MOPr ECLs for ligand selectivity, which is probably due to exclusion not binding mechanisms[238]. The high resolution crystal structure of the hDOPr highlighted the hydrogen-bond networking involving mainly the ICL3 but also ICL2 and C-terminal tail; these regions are probably responsible to stabilise the receptor in the inactive state[115]. All the residues described in hDOPr structure are conserved in hMOPr; hence, hDOPr ICL3 'close' conformation in the inactive state would probably be observed in hMOPr. Another interesting finding from this hDOPr study is the description of the sodium pocket formed by 16 amino acids; where 15 are highly conserved class A GPCR residues, similarly observed for the allosteric site of β_{2A}AR[115,209]. It is established that sodium is a negative allosteric modulator of the opioid receptors by probably stabilising the receptor in its inactive conformation[317]. It is likely that the allosteric sodium pocket in MOPr resembles the one described for

hDOPr.

2.2.3 G Protein Binding and Activation

The MOPr, similarly to many GPCRs, presents different affinity states for bound and unbound G protein[32,298,352]. Therefore, in the absence of G proteins, the mMOPr crystal structure is not only in the inactive conformation, but also in the low agonist affinity state. In general, the activation mechanism of GPCR is accepted to start at the agonist binding site and propagate downwards G protein binding site; however, the opposite has also been proposed, where intracellular changes are first observed which results in structural changes that propagate upwards[108]. Furthermore, crystal structure of β_2-adrenergic receptor in the inactive state was similar to the receptor bound to an agonist but without G protein interaction. This indicated that, at least for this GPCR, the interaction between receptor and agonist was not enough to stabilise the receptor in the active state, which highlights the crucial role played by G proteins[298].

GPCRs have dynamic structures, the intra and extracellular domains are reasonably flexible and even the transmembrane membrane helices can move, which is extremely important for transmitting information from the extracellular to the intracellular regions. Unfortunately, the MOPr crystal structure in the active state is not available. Nevertheless, some information from the β_2AR active conformation bound to a nanobody, which mimics a G protein interaction, may be useful in proposing an MOPr active state. Interactions between the nanobody and the β_2AR was determined, where a pocket formed by TM3, TM5, TM6 and TM7 interacted with a part of the nanobody. In addition, a different region of the nanobody interacted with cytoplasmic interface of TM5 and TM6. The conformational switch region was identified for the β_2AR which contains three highly conserved residues Ile121 (TM3), Pro211 (TM5) and Phe282 (TM6)[285]; these are represented in the MOPr by residues Ile157 (TM3), Pro246 (TM5) and Phe291 (TM6). Therefore, if following the dynamics of the β_2AR, an outward movement of TM5 and TM6 in addition to an inward displacement of TM7 and TM3 would be expected in the active state of MOPr bound to G protein. Movement of these TMs would produce a change in the intracellular regions which

is probably necessary for signal transduction. MOPr molecular dynamics simulations proposed an increase in the flexibility of ICL3 induced by morphine, which is probably crucial for G protein activation[315]; this actually may be related to the change in the 'closed' conformation reported for the hDOPr. Mutations of many residues across the TM and intracellular domains have confirmed the importance of these regions for ligand binding and G protein signalling; some of these regions will be further discussed in later chapters[180,315]. An intriguing finding from Claude et al. (1996)[74] showed that mutating a highly conserved serine in the TM4 of the MOPr resulted in opioid antagonists acting as agonists in CHO cells; this revealed the important role some individual amino acids play to receptor conformation and signalling transduction.

The classical view that ligand interaction with the receptor produces one active state is now known to be a very simplistic model. Many studies support the existence of multiple agonist specific receptor states, where the conformational change induced by agonist binding produce many intermediate states which would explain bias-agonism[108,132]. This notion is further supported by molecular dynamics simulations of the MOPr, as shown by Shim et al. (2013)[318], and the difficulty of obtaining a ligand-bound GPCR crystal structure of an active conformation[285]. Furthermore, recent studies have demonstrated that prolonged exposure to opioids produce a higher affinity reversible conformation of the MOPr, which partially involves phosphorylation of the C-terminal[32,33]. Therefore, evidence suggests that MOPr may be stabilised in varying conformations, however how these different conformations affect receptors signalling and regulation still need to be better understood; remarkably, this may open new possibilities for drug development.

2.2.4 μ-Opioid Receptor Oligomerisation

Interestingly, the mMOPr crystal structure revealed that this receptor was mainly crystallised as parallel dimers, and to a less extent formed oligomers of higher order observed through a different dimer interface[220]. Association between TM5 and TM6 helices was the most common interaction, while TM1, TM2 and helix 8 were involved in interdimeric interaction. Moreover, it was predicted that dimers interacting through

TM5 and TM6 interface would not be able to couple to G proteins due to steric blockage, while tetramers could couple to two G proteins. In contrast, a recent molecular dynamics simulation proposed homodimers formation mainly between interfaces TM5/TM5 and TM1-TM2/TM5-TM6 but G protein coupling was not studied[278].

A large number of studies reported the involvement of MOPr in the formation not only of homodimers, but also heteromers. The heteromer formed between MOPr and DOPr has attracted much attention, as binding and function of these protomers[†] were reported to be distinct from the protomers of homodimers as reviewed by Stockton et al. (2012)[332]. In another recent review, Costantino et al. (2012)[84] reported the role of opioid receptors heteromers in analgesia and highlighted the possibility of targeting these complexes to obtain greater pharmacological effects in the treatment of pain and opioid addiction. It is noteworthy that heteromers between MOPr and non-opioid receptor have also been reported, where activation of one protomer interfered with signalling and regulation of the other[272,345]. Interestingly, a mMOPr brain atlas reported by Erbs et al. (2015)[113] has demonstrated regions where MOPr and DOPr are co-expressed such as the hippocampus, higher probability of heteromer formation, while in the forebrain these opioid receptors are rarely co-expressed in the same neurons. In spite of the recent enthusiasm around opioid homo and heteromers, it is necessary to emphasise that a previous study ascertained that MOPr can signal as a monomer[192].

2.2.5 Post-Translational Modifications

Changes to a protein that occur during or after protein biosynthesis are called post-translational modifications (PTMs). Here glycosylation, phosphorylation and palmitoylation, three PTMs which typically occurs in GPCRs, will be discussed with focus on the MOPr.

A very common PTM, which is important for protein structure, function and stability, is N-glycosylation[8]. The hMOPr has five predicted glycosylation sites, and NetNGlyc 1.0 Software[1] predicts that three of them have a high potential of being glycosylated (Figure 2.3). Although the precise pattern of MOPr glycosylation is not

[†]A protomer is the structural unit of an oligomeric protein

known, MOPr is definitely glycosylated. Western Blot analysis of MOPr detects a molecular weight which is higher than expected, based on the amino acid sequence of the receptor, and when treated for N-deglycosylation with PNGase F, MOPr migrates as expected[155,156]. Interestingly, Huang et al. (2008)[155] had determined a varying rMOPr glycosylation profile in different areas of the brain, which may have functional importance. Another area of interest involving N-glycosylation is the study of the common hMOPr single-nucleotide polymorphism (SNP) A118G (N40D). In this variant a putative glycosylation site is deleted which consequences are still not well understood. This polymorphism is one of the natural hMOPr variants studied in the present work, and it will be further discussed in Chapter 5.

In the β_2AR crystal structure, a C-terminal (helix 8) cysteine was covalently bound to a palmitic acid[65]. A similar palmitoylation was predicted for the MOPr (Figure 2.3) but a previous mutagenesis study in rMOPr could not confirm this hypothesis[60]. Furthermore, this PTM was not reported for all opioid receptors crystal structures; nevertheless, helix 8 was observed to be parallel to the membrane similarly to the palmitoylated β_2AR[138,220,359]. Noticeably, a recent report by Zheng et al. (2012)[375] proposed a palmitoylation of the rMOPr cysteine 170 which may facilitate homodimerisation and G protein coupling.

Phosphorylation is known to alter function and activity of many proteins. It is established that the MOPr is phosphorylated in the C-terminal tail as reviewed recently by Mann et al. (2015)[221]; however, phosphorylation of other intracellular domains needs investigation. Immunological and mass spectrometric analysis ascertained many phosphorylation sites in the C-terminal; while mutagenesis work predicted phosphorylation at specific serine, threonine and tyrosine residues of other regions as shown in Figure 2.4 and Table 2.2. In HEK293 cells expressing MOPr, C-terminal phosphorylation can be constitutive or agonist induced. Two sites were determined to be constitutively phosphorylated, Ser263 and Thr370[63,102], where Thr370 is further phosphorylated by agonist binding. In addition to Thr370, residues in STANT and TSST clusters are also agonist phosphorylated, and DAMGO phosphorylation compared to

morphine is more robust and widespread[63,102,195]. Previously reported phosphorylation sites are described in Table 2.2; however, it is noteworthy that some of the sites were identified using mutagenesis technique which is a great tool to identify function alteration. Nevertheless, the use of this technique to confirm a phosphorylation site may be misleading, as amino acid substitution may lead to a change in conformation or interference with other factors; therefore, if changes are observed, it is not necessarily a consequence of absence of phosphorylation. One example is the Thr394 residue which has previously been reported to be phosphorylated by mutagenesis analysis[259] but high resolution mass spectrometric analysis were not able to detect phosphorylation of this site[63,195,247].

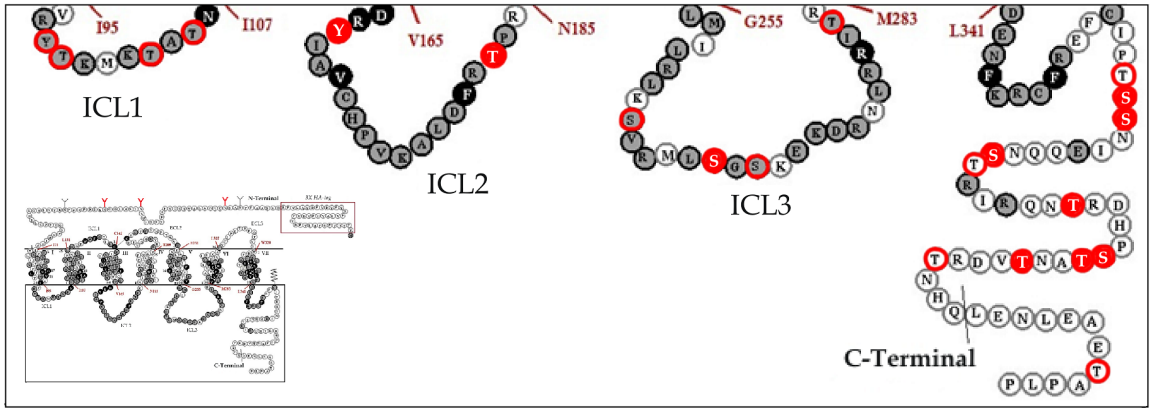

Figure 2.4. Enlarged serpentine structure of the human μ-opioid receptor intracellular domains showing potential phosphorylation sites highlighted in red. The full red circles mark residues previously reported to be phosphorylated. One tyrosine residue in the base of TM2 and one in the base of TM7/helix8 have also been reported to be phosphorylated but are not shown in this illustration. Further information is presented in Table 2.2. Adapted figure from Center for Opioid Research and Design (CORD)[83].

In view of the fact that phosphorylation of particular residues may regulate different functions, determining which kinases are involved in phosphorylation of specific residues becomes important for characterising receptor function. Chen et al. (2013)[63] in addition to identifying the C-terminal phosphorylation sites Ser356, Thr357, Ser363, Thr370 and Ser375 by mass spectrometry, also determined *in vitro* calcium/calmodulin-dependent protein kinase II (CaMKII), protein kinase C (PKC) and G protein receptor

kinase 2 (GRK2) binding profile. The ICL3 and C-terminal tail were significantly phosphorylated by these kinases, in contrast to ICL2, where phosphorylation produced did not reach significance. Moreover, the specific phosphorylated residues were also tested against the kinases above, and results are presented in Table 2.2. The efficiency of an agonist in phosphorylating Ser375 residue correlates well with β-arrestin 2 recruitment and receptor endocytosis[171,236]. Interestingly, Ser375 is the primary site in a hierarchical phosphorylation also involving Thr370, Thr376 and Thr379 residues, and recruitment of GRK2/3, which is characteristic of DAMGO but not morphine treatment, is essential for efficient phosphorylation of these sites. Furthermore, MOPr can be heterologously phosphorylated by PKC activators and other receptors such as substance P and $NPFF_2$ receptors[102,163,247]

Considering that in the present work I only used human MOPr, it is noteworthy that the majority of studies in C-terminal phosphorylation used rat or mouse MOPr, and small interspecies differences at this region are observed. A difference which must be highlighted is the absence of the last threonine of the TSST cluster (Figure 2.4); this residue was one of the five phosphorylation sites identified in the rMOPr C-terminal by mass spectrometry[63]; therefore, it is important to consider the effect of the absence of one of the two characterised phosphorylation sites in the TSST cluster. The role of this cluster phosphorylation is still not well established however recent studies have examined this region in desensitisation studies of rodent MOPr with some interestingly results[33,364]. A study in hMOPr by Mouledous et al. (2012)[247] indicated that in the TSS cluster only Ser358 was phosphorylated; however, phosphorylation was very low and too close to detection limit, only able to be detected after exposure to the high efficacy agonist DAMGO. Note that as a consequence of two amino acids deletion at the N-terminal of rodents MOPr, human MOPr amino acids are always numbered two sites above.

Further studies are needed not only to better characterise the PTMs that occur in MOPr but also to determine the role of these modification in MOPr function. Phosphorylation is the most studied PTM in MOPr and further information is presented in Section 2.4.

Table 2.2. Summary of MOPr phosphorylation sites, proposed kinase involved and key findings

mMOPr Site[+]	Key observations	Kinase	Cell type	Reference
ICL1				
Tyr106	Increased DAMGO potency by heterologous dephosphorylation of constitutive phosphorylated residue (MG)	Tyrosine kinase	*X. laevis* oocytes	McLaughlin and Chavkin (2001)[235]
ICL2				
Tyr166	Increased DAMGO potency by heterologous dephosphorylation of constitutive phosphorylated residue (MG)	Tyrosine kinase	*X. laevis* oocytes	McLaughlin and Chavkin (2001)[235]
Thr180	Mutation to alanine blocked DAMGO induced homologous desensitisation (MG)	GRK3	*X. laevis* oocytes	Celver et al. (2001)[57]
ICL3				
Ser266	Substitution by alanine or proline affected DAMGO induced desensitisation/ G protein coupling (MG)	CaMKII	*X. laevis* oocytes/ HEK293	Koch et al. (1997,2000)[184,185]
TM7[++]				
Tyr336	Mutation to phenylalanine caused a significant decrease in AC activation after chronic exposure to morphine (MG)	Src kinase	HEK293	Zhang et al. (2009)[370]
C-term				
TSST cluster	DAMGO and morphine induced phosphorylation of this cluster (MS)		HEK293	Lau et al. (2011)[195]
	Low phosphorylation of hMOPr Ser358 (Ser356 in mouse); apparently increased by DAMGO (MS)		SH-SY5Y	Mouledous et al. (2012)[247]
	DAMGO and morphine induced phosphorylation of Ser356 and Thr357 (MS)	PKC*	HEK293	Chen et al. (2013)[63]
Ser363	Constitutive phosphorylation (IM)		HEK293	Doll et al. (2011)[102]
	Phosphorylated by PKC (MS)	PKC*	CHO	Feng et al. (2011)[116]
	Constitutive phosphorylation (MS)		HEK293	Lau et al. (2011)[195]
	Constitutive phosphorylation, but no distinction between hMOPr Ser365 and Thr366 was possible (MS)		SH-SY5Y	Mouledous et al. (2012)[247]
	Constitutive phosphorylation (MS)	PKC*/ CaMKII*	HEK293	Chen et al. (2013)[63]
	Constitutive phosphorylation (IM)	PKC	HEK293 & mouse brain	Illing et al. (2014)[163]

Continued on page 27

[+] Studies used mouse, rat and human MOPr, however the analogue site for mouse is showed. Note that in human the amino acid number is different by two when compared to rodents. [++] According to crystal structure[220], but has been shown as part of C-terminal by some studies[356]. * *In vitro* peptide phosphorylation. Analysis by mass spectrometry (MS), immunodetection (IM) or mutagenesis (MG).

Table 2.2. Summary of MOPr phosphorylation sites, proposed kinase involved and key findings. Continued from page 26

mMOPr Site[+]	Key observations	Kinase	Cell type	Reference
C-term				
Thr370	DAMGO, PMA but not morphine induced phosphorylation (IM)	PKC (heterologous)	HEK293	Doll et al. (2011)[102]
	Phosphorylation mediated by DAMGO but also morphine in a much lower extent (MS)		HEK293	Lau et al. (2011)[195]
	Phosphorylation mediated by DAMGO (GRK2/3) and only by morphine when GRK2/3 overexpressed. GRK5/6 not involved (IM)	GRK2/3	HEK293	Doll et al. (2012)[103]
	Heterologously phosphorylated by $NPFF_2$ receptor activation (MS)		SH-SY5Y	Mouledous et al. (2012)[247]
	Constitutive; and also morphine and DAMGO induced phosphorylation (MS)	CaMKII*	HEK293	Chen et al. (2013)[63]
	Phosphorylation diminished if Ser375 deleted (IM)	GRK2/3	HEK293	Just et al. (2013)[171]
	Substance P receptor activation and PMA heterologously activated PKC which phosphorylated Thr370 (IM)	PKCα (heterologous)	HEK293	Illing et al. (2014)[163]
STANT cluster	DAMGO and morphine induced phosphorylation of Ser375 (IM)	GRK2	HEK293	Schulz et al. (2004)[311]
	Morphine and DAMGO induced Ser375 phosphorylation (IM)	Not PKC	HEK293	Doll et al. (2011)[102]
	This cluster phosphorylation abundance is the major difference between morphine and DAMGO phosphorylation profile (MS)		HEK293	Lau et al. (2011)[195]
	Ser375 phosphorylation mediated by morphine (GRK5) and DAMGO (GRK2/3)(IM/MG)	GRK2/3 GRK5	HEK293 & mouse brain	Doll et al. (2012)[103]
	hMOPr Ser377, Thr378 heterologously phosphorylated by $NPFF_2$ receptor activation (MS)	GRK2	SH-SY5Y	Mouledous et al. (2012)[247]
	Morphine and DAMGO induced phosphorylation of Ser375 (MS)	GRK2	HEK293	Chen et al. (2013)[63]
	Ser375 primary site but Ser376 (very delayed) and Thr379 (slightly delayed) also phosphorylated (IM)	GRK2/3	HEK293	Just et al. (2013)[171]
Thr394	Mutation to alanine affected homologous desensitisation induced by DAMGO (MG)	Possibly GRK2	CHO	Pak et al. (1997)[259]

[+] Studies used mouse, rat and human MOPr, however the analogue site for mouse is showed. Note that in human the amino acid number is different by two when compared to rodents. * *In vitro* peptide phosphorylation. Analysis by by mass spectrometry (MS), immunodetection (IM) or mutagenesis (MG).

2.3 μ-Opioid Receptor Signalling

GPCRs are promiscuous proteins, not only because they bind to a large variety of ligands, but also because they couple with many partners. Signalling transduction via G proteins was recognised early into GPCR investigations, however recently G protein independent pathways have been described where the previously characterised regulatory proteins known as β-arrestins were found to play an important role in GPCR signalling transduction[200].

2.3.1 G Protein Dependent Signalling

MOPr preferentially stimulates G_{o1}, G_{o2}, G_{i2}, G_{i3} and G_z, however some studies have also demonstrated that it also couples to G_{i1}, G_{15} and G_{16} less efficiently or without clear functional significance[75]. Therefore, MOPr couples to the inhibitory $G_{i/o}$ proteins which are also known as pertussis toxin-sensitive G proteins as treatment with this toxin disrupts signalling by catalysing the ADP-ribosylation of $G\alpha_{i/o}$[50,76]. A large number of effectors have been identified for MOPr-G protein pathway, here adenylyl cyclase (AC) inhibition, G protein-coupled inwardly rectifying potassium channel (GIRK) activation and voltage-dependent calcium channel (I_{Ca}) inhibition will be discussed; however, activation of voltage-gated potassium channels (K_v)[344], MAPKs[197], PI3K/Akt[218] and mobilisation of calcium from endoplasmic reticulum[76] amongst others have also been linked to the complex G protein dependent MOPr signalling cascade (Figure 2.5).

Cyclic adenosine monophosphate (cAMP) is a crucial second messenger involved in the regulation of many biological processes. It is synthetised by AC, then activation or inhibition of this enzyme by GPCRs controls the downstream cascade dependent on cAMP levels. The inhibitory G proteins activated by opioid receptors produce AC inhibition, thus activation of AC via G_s or forskolin[†] exposure, would be blunted if opioid receptors were to be activated in parallel[74,182,358]. Under inflammatory conditions, such as tissue injury, complex molecular mechanisms occur; not only AC is activated by many inflammatory mediators such as prostaglandins, but also MOPr is upregulated

[†]Forskolin is largely used in research to heterologously activate AC

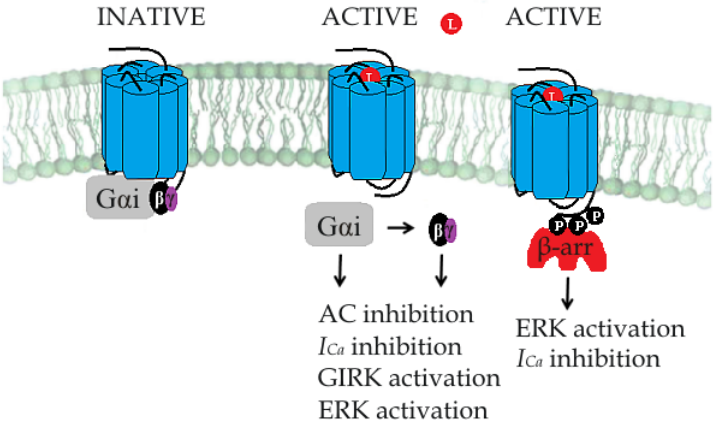

Figure 2.5. MOPr G protein dependent and independent signalling and examples of effectors. MOPr bound to G proteins in the high affinity inactive state, followed by activation produced by opioid ligand (red) which leads to conformational changes of the MOPr. Active receptor can activate the heterotrimeric G proteins dependent and/or β-arrestin dependent signalling. Examples of effectors for each pathway are presented. AC, adenylyl cyclase; I_{Ca}, voltage-dependent calcium channel; G protein-coupled inwardly rectifying potassium channel, GIRK; extracellular signal-regulated kinase, ERK.

and transported from the dorsal root ganglion to primary afferent neuron terminals. There, activated by endogenous or analgesic opioids, MOPr signalling inhibits AC leading to a directly or indirectly suppression of calcium and sodium currents, which in addition to decreasing propagation of action potentials, it diminishes release of substance P, an excitatory proinflammatory neuropeptide[330]. Many studies have reported the crucial role inhibition of AC plays in peripheral MOPr analgesic effect, which is largely related to decreased activation of protein kinase A (PKA)[158]. PKA is a cAMP-dependent kinase which is associated with increase in nociception by phosphorylation of ion channels. Interestingly, many AC subtypes have been identified, and isoform selective compounds have been investigated as possible pharmacological targets for many conditions including neuropathic pain[273]. PKA independent cAMP signalling has also been reported, one example is the direct modulation of voltage-channels (I_h) which inhibited by MOPr would reduce neuronal excitability[165].

It is noteworthy that a well recognised adaptation following chronic opioid treatment is the upregulation of adenylyl cyclase activity, also known as superactivation.

This phenomenon is correlated to MOPr function, as it was not detected in the brain of MOPr knockout mice[233] and it has been mainly studied for morphine treatment; however, other opioids also produce superactivation[19]. Interestingly this adaptation is also observed for other $G_{i/o}$ coupling receptors, such as cannabinoid receptor CB1, and a number of molecular mechanisms have been proposed, including regulation of AC by $G\beta\gamma$ subunits and differential regulation of varying AC isozymes[69]. Zhang et al. (2009 and 2013)[370,371] suggested that the change from AC inhibition to activation is related to recruitment and activation of Src kinase by chronic treatment with opioids. This would be responsible for tyrosine kinase phosphorylation of MOPr residue Tyr336 and activation of a noncanonical signalling pathway. Therefore, AC superactivation is probably multifactorial and, in combination with other cellular adaptations reviewed by Christie (2008)[69], forms a complex web of molecular mechanisms involved in cellular tolerance which may be involved not only in opioid tolerance and withdrawal, but also in synaptic plasticity.

Activation of MOPr results in the separation of the heterotrimeric G proteins. Multiple $G\beta\gamma$ subunits directly binds to GIRKs producing their opening which leads to membrane potential hyperpolarisation[78]. Considering the tight relation between G protein and GIRK activation, measuring membrane potential change is a sensible way of measuring MOPr signalling, without much external interference which may be observed if effector is further downstream the complex signalling cascade. Genetic manipulation of GIRK expression had demonstrated the importance of this effector in opioid induced membrane potential hyperpolarisation in LC neurons[339], and more importantly, the crucial role GIRK plays in opioid induced analgesia by inhibitory regulation of neuronal excitability[162,225,250]. The role GIRK plays in CNS expressed MOPr has been long accepted; however, only recently Nockemann et al. (2013)[250] was able to demonstrated the importance of GIRK channel for peripheral opioid-mediated analgesia. Interestingly, MOPr is absent in mouse peripheral neurons, differently from rat and human, and this not only explain conflicting data around this matter, but also highlight some important interspecies differences which can cause much confusion.

The increase of intracellular calcium concentration evokes the release of excitatory

neurotransmitters, such as substance P and tachykinins, which are important contributors to transmission of pain. MOPr inhibits calcium channels primarily of voltage-gated group (I_{Ca}); therefore, negatively modulates the release of neurotransmitters and propagation of action potential centrally and peripherally[196,328]. The role of G protein in modulating I_{Ca} was reviewed by Dolphin (2003)[104] where the $\beta\gamma$ subunits were described to bind to the channel inhibiting its opening. Evidence for MOPr functional coupling with I_{Ca} is available not only in recombinant systems, but also in rodent native neurons from brain regions such as LC and PAG[41,80,164]. It is important to point out that in addition to the direct effect of G proteins in I_{Ca}, these channels can also be indirectly modulated by other effectors activated by MOPr, as mentioned above for cAMP.

2.3.2 G Protein Independent Signalling

The ability of GPCRs to signal independently from G proteins reinforces the already extremely complex GPCR signalling mechanisms. The active conformation of the majority of the GPCRs can interact not only with G proteins, but also with G protein receptor kinases (GRK) and β-arrestins[202]. Initially described as important proteins for GPCR desensitisation, endocytosis and recycling, GRKs and β-arrestins roles have expanded dramatically when they were characterised as signalling transducers[292]. Lefkowitz and Shenoy (2005)[202] reviewed β-arrestins signalling transduction involving MAPKs, tyrosine kinases, Akt, PI3 kinases and NFκB. The GRK pattern of phosphorylation is known to work as a 'barcode' that regulates β-arrestins function, and a recent study in β_2AR demonstrated that while GRK2 phosphorylation is important for β-arrestin mediated internalisation, activation of extracellular signal-regulated kinase (ERK) pathway by β-arrestin is observed only under GRK6 phosphorylation[292]. This supports the hypotheses that phosphorylation patterns can stabilise β-arrestin in distinct functional conformations, and highlights that while recruitment assays indicate β-arrestin interaction with GPCR, it does not necessarily indicates signalling via this pathway.

The role of β-arrestins in MOPr signalling transduction is still not well defined.

Miyatake et al. (2009)[242] reported ERK activation by morphine and DAMGO via G protein and β-arrestin 2-dependent pathways in astrocytes, which is involved in cell proliferation. The role GRK3 and β-arrestin 2 in ERK activation by fentanyl was also reported in striatal neurons[217]. Note that activation of the MAPK cascade regulates cellular processes such as proliferation and cell-cell communication. Iegorova et al. (2010)[160] suggested MOPr G protein independent signalling modulation of P-type calcium channels via scaffolding proteins or protein-protein interaction; however, they did not exclude the possibility of opioid direct channel interaction. Another study also determined an important role for β-arrestin 2 in activating c-Src, a kinase necessary for inhibiting I_{Ca}[349]. Taken together these studies suggested that MOPr may activate ERK and modulate calcium channels via β-arrestin dependent pathway; nevertheless, evidence is lacking regarding other effectors (Figure 2.5).

2.4 μ-Opioid Signalling Regulation

Opioid tolerance and dependence are linked to the activation of the MOPr[233]; however, the exact cellular mechanisms underlying these well characterised clinical phenomena are still elusive. It is known that a very complex network of regulatory processes occur after even a single dose of opioid, and with chronic treatment cellular tolerance is observed[19,356]. Nevertheless, *in vivo* tolerance is not a direct consequence of only cellular tolerance, as many complex regulatory mechanisms at both cellular and neural circuit are likely to contribute to it[69]. The most studied regulatory process is desensitisation, which is characterised by a decrease in receptor signalling with persistent stimulation[199]. The focus of this review will be on molecular mechanisms of acute desensitisation involving phosphorylation and internalisation. Figure 2.6, from a thorough recent review of MOPr regulation by Williams et al. (2013)[356] illustrates regulatory processes in addition to the time line for each process.

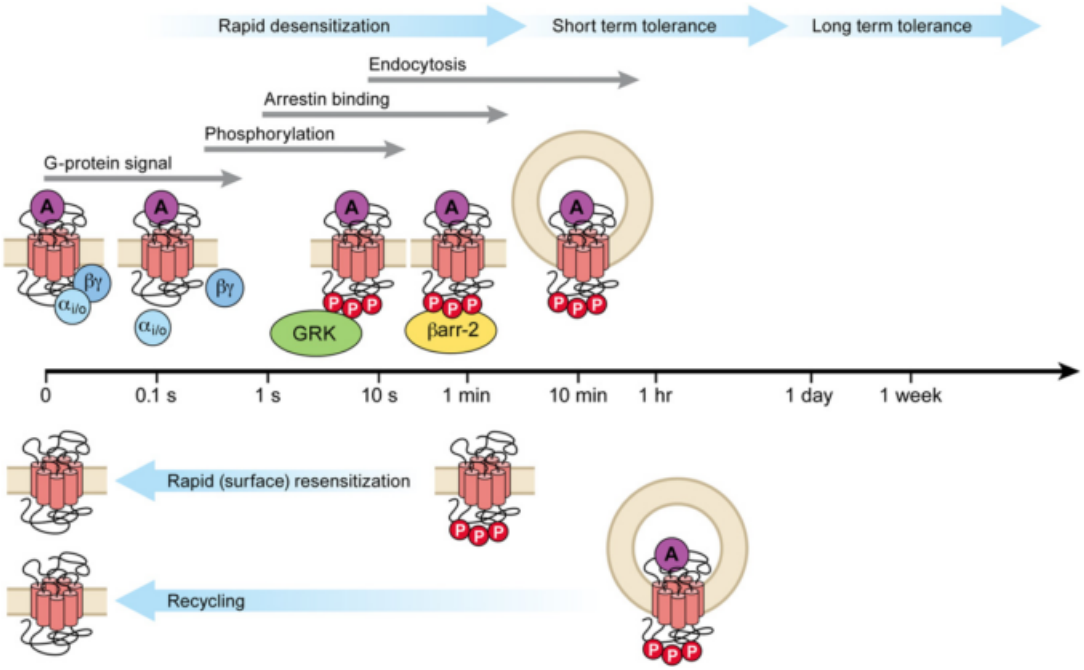

Figure 2.6. General scheme and time line (log scale) for MOPr signalling regulation processes after binding of a high efficacy agonist such as DAMGO. After agonist induced conformational change, G protein activation is the fastest step, followed by GRK phosphorylation which facilitates arrestin binding, and arrestin recruits the machinery necessary for endocytosis. Under the time scale rapid surface resensitisation by dephosphorylation and the slower recycling process are illustrated. This figure is reproduced from Williams et al. (2013)[356] and the authors characterised rapid desensitisation until signal steady state (approximately 5 minutes) followed by short-tolerance and long-tolerance.

2.4.1 Desensitisation

A rapid decrease in agonist induced signalling to levels similar to unstimulated is observed with many GPCRs, despite continues drug exposure. This phenomenon termed desensitisation was observed since early GPCR studies and interested many researches, as both receiving and terminating GPCR signals is important for cellular homeostasis[201]. In early desensitisation studies, the observation that desensitised β_2AR migrated slower in SDS-PAGE gels than non-agonist exposed receptors[327], led to the investigation and confirmation of receptor phosphorylation. Initially, GRK2 was identified and proposed to be responsible for phosphorylation, and thus desensitisation; however, soon it became clear that a 'cofactor' was missing, later identified and named β-arrestin

(to differentiate from visual arrestin)[30]. Since then, a large number of kinases have been demonstrated to phosphorylate GPCRs, including the extremely important regulatory kinases G protein receptor kinases (GRK). In addition, different subtypes of arrestins have been identified where non-visual arrestins, known as β-arrestin 1 and 2, are also crucial regulatory proteins. After a large number of studies, the classical model for GPCR desensitisation was determined to involve receptor phosphorylation by GRKs which increased the affinity of the activated receptor for cytosolic β-arrestins. β-arrestins would then disrupt coupling of G proteins, consequently, producing signalling desensitisation[190]. This GPCR desensitisation model was soon challenged, considering that some agonists does not recruit β-arrestin as efficiently but still lead to profound desensitisation. Moreover, a recent study highlighted that phosphorylation is not essential for β-arrestin biding to some GPCRs[133]. Studies of MOPr desensitisation support the idea of a complex interplay of factors which culminate in desensitisation, and the mechanisms involved are agonist-selective probably as a result of different active conformations[175].

Desensitisation can be characterised as homologous or heterologous in nature. Homologous desensitisation is the reduced signalling restricted to one subtype of GPCR, while heterologous desensitisation occurs when one subtype of GPCR is activated producing reduced signalling of other GPCRs, which share similar signalling pathway. At the present work, acute homologous and heterologous signalling desensitisation induced by DAMGO and morphine were investigated.

Homologous desensitisation of MOPr signalling has been reported after treatment with many different agonists, and it has been measured using many different effectors. Recording of opioid effects on ion channels is one of the best methods to determine receptor desensitisation, as it is direct and with good temporal resolution. LC neurons contain mainly MOPr of the opioid receptors family in addition to GIRK; hence, these neurons have been largely used to study MOPr desensitisation. Morphine acute desensitisation has been the focus for much controversy; while high efficacious agonists, such as DAMGO and met-enkephalin (ME), were consistently reported to promote a

significant desensitisation in LC neurons, morphine acute desensitisation was not significant[5,20]. Nevertheless, in HEK293 cells expressing MOPr and GIRK, morphine and DAMGO promoted a rapid desensitisation of GIRK signalling[167], and similar results are observed in AtT20 cells[364]. Also in AtT20 cells, homologous desensitisation of the inhibition of I_{Ca} produced by DAMGO and morphine was significant and similar between these agonists[41]. Likewise, rapid desensitisation in the $[Ca^{2+}]_i$ was observed for both morphine and DAMGO in HEK293 cells[71].

Heterologous desensitisation after opioid exposure has been previously reported for α_2-adrenergic receptor and somatostatin receptor(s) in LC neurons[35,211], and natively expressed somatostatin receptor(s) in AtT20 cells transfected with MOPr[364]. Curiously, heterologous desensitisation in response to noradrenaline was observed in immature rat LC neurons, but not in mature which was correlated to a decrease in GRK2 levels during aging process[211]. Heterologous desensitisation will be further discussed in Chapter 4.

Desensitisation, together with adaptations such as AC superactivation and down-regulation, are likely to be mechanisms underlying tolerance after chronic opioid exposure[69]. Levitt and Williams (2012)[203], in a study of rat LC neurons, suggested that desensitisation and cellular tolerance are separate processes, but desensitisation also contributes to behavioural tolerance because it was affected by PKC inhibitor modulation of morphine desensitisation.

2.4.2 Desensitisation and Phosphorylation

The fact that GPCR phosphorylation increases β-arrestin affinity is a clear indication of the importance of phosphorylation for G protein signalling regulation and G protein independent signalling[292]. However what happens to signalling desensitisation if kinases are modulated or phosphorylation sites are deleted?

The intracellular region of hMOPr have 21 putative phosphorylation sites, where more than half have been reported to be phosphorylated (Figure 2.4, Table 2.2). It is clear that the majority of the phosphorylation sites are in the C-terminal tail, which has been extensively characterised; however, some isolated sites in the ICLs have also

been described.

Table 2.2 also summarises kinases involved in the phosphorylation of many residues. Modulation of kinase activity has been largely used to determine the influence of a certain kinase in MOPr desensitisation; basically, two different approaches have been utilised: genetic and chemical manipulation. In the first one, kinase activity can be partially (knockdown) or completely (knockout) disrupted[23], or increased by overexpression[367]. In the second one, chemical compounds can be used to activate or inhibit kinases, which can be selective but often they are promiscuous affecting many different kinases[13,167]. β-arrestin levels were also genetically manipulated in many studies to better determine this adaptor role, in addition to separate phosphorylation and β-arrestin function[94].

Of the ICL phosphorylation sites, only two have been linked to desensitisation: Thr180 and Ser266 (mMOPr). In *Xenopus laevis* oocytes and AtT20 cells, Thr180 substitution to alanine affected DAMGO induced MOPr desensitisation which requires GRK3 and β-arrestin 2. However, cells were washed for 10 minutes between one hour treatment and challenge; thus, many factors could affect these results, as in one hour adaptations can already be present and prolonged wash allow many regulatory processes to occur[56,57]. In addition, phosphorylation of this site was not detected using a phosphosite specific antibody after DAMGO treatment[271]. The Ser266 residue, in the third ICL, has been described to be the primary site of CaMKII phosphorylation, and alteration to alanine or proline attenuated receptor desensitisation[185]. This site will be further discussed in Chapter 7 as it is affected by the hMOPr SNP S268A.

Two recent studies have assessed the effect of C-terminal tail phosphorylation in desensitisation by mutagenesis of different serine and/or threonine residues. Birdsong et al. (2015)[33] reported a significant decrease in ME induced sustained desensitisation observed after alanine substitution of both TSST and STANT clusters, but isolated mutation of either clusters did not affect signal reduction; desensitisation was measured using whole cell voltage clamp in MOPr knockout brain slices[†] injected with viral plasmid containing MOPr variant sequence. Note that the term sustained desensitisation

[†]mediodorsal nucleus of the thalamus neurons

was used to describe desensitisation measured by challenging opioid response after stimulus, while acute desensitisation was measured by signal decay after opioid stimulus. In this paper, acute desensitisation was not significantly different in the thalamus neurons where sustained desensitisation was measured, but in LC neurons mutation of both clusters attenuated desensitisation by ME. The second study was performed in AtT20 cells transfected with wild type mMOPr and three phosphosite deleted variants by alanine substitution[364]. Morphine and ME induced sustained desensitisation (measured as described above) was unaffected in two mutants with multiple important phosphorylation sites deleted. Only the total deletion of C-terminal phosphorylation sites abolished ME desensitisation; however, morphine induced desensitisation was also unaffected. Morphine induced desensitisation was reduced by PKC inhibitor, as previously reported, and interestingly this inhibitor abolished desensitisation in the total phosphosite deleted mutant. Therefore these studies suggest a crucial role for C-terminal tail phosphorylation in ME stimulated desensitisation, while PKC activity is more important for morphine.

The correlation between PKC activity and morphine tolerance is supported by a number of *in vivo* studies, where inhibition of PKC attenuates tolerance[37,153,321]. Bailey et al. (2004)[21] investigated these findings at the molecular level and determined that activation of PKC by a phorbol ester increased opioid induced desensitisation, which could be reversed by PKC inhibition. Remarkably, morphine which was previously determined to cause a very low desensitisation, compared to DAMGO and methadone in LC neurons[20], in the presence of a PKC activator produced a significant rapid desensitisation. A later study has not only determine PKCα as the subtype responsible for this increased desensitisation in LC neurons, but also ascertained that this process was independent of GRK2 by using a GRK2 dominant negative mutant[23]. This crucial role played by PKC in morphine desensitisation is not observed for DAMGO, which, in contrast, is GRK2 dependent[23,167].

Phosphorylation independent GRK2/3 activity has also been suggested to affect MOPr desensitisation of GIRK signalling by competing with the channel for the G$\beta\gamma$ subunits[286]. This is a quite different mechanism that needs to be considered, especially,

for opioid agonists such as DAMGO. This opioids produce a robust phosphorylation by GRK2/3; therefore, efficiently recruiting these kinases.

It is noteworthy that desensitisation has been measured in many different ways which can significantly affect results obtained. With this in mind, Arttamangkul et al. (2015)[13] compared two different desensitisation measurements, acute and sustained desensitisation which was mentioned above, and concluded that in LC neurons results obtained for both measurements probably involves distinct factors; consequently, varying results may be expected. Two other points need to be considered: difference in cell type and receptor expression. Desensitisation has been studied in many different cell lines including LC neurons, HEK293 and AtT20 cells. Atwood et al. (2011)[15] compared mRNA levels of important proteins for GPCR signalling and regulation in HEK293, AtT20, BV2 and N18 cells; the difference is astonishing and would be surprising not to affect GPCRs function. In addition, level of expression of MOPr which can be natively expressed, as in LC neurons, or heterologously expressed may interfere with measurements. In a review, Connor et al. (2004)[79] highlighted how a large receptor reserve can mask desensitisation, especially if using high concentration of a highly efficacious agonist. Although receptor reserve is generally linked to heterologous systems, LC neurons were also reported to present a reasonable receptor reserve for high efficacy agonists[79,294].

The MOPr and β-arrestin binding is enhanced by phosphorylation of the C-terminal tail, which is related to GRK2/3 activation and phosphorylation of MOPr STANT cluster[63,171]. Chu et al. (2008)[71], by manipulating β-arrestin activity in HEK293 cells, demonstrated the importance of this adaptor for DAMGO induced acute desensitisation, however morphine stimulated desensitisation was β-arrestin independent. In contrast, a desensitisation study in LC neurons of β-arrestin knockout mouse demonstrated that absence of β-arrestin 2 did not affect acute desensitisation induced by ME when compared to wild-type counterpart; however, faster resensitisation was observed[95]. Moreover, cellular tolerance and impaired resensitisation detected after chronic morphine exposure in wild-type LC neurons did not occur in β-arrestin 2 knockout, and resensitisation was reversed to normal in wild-type neurons after GRK2 inhibition.

In a *in vivo* model of β-arrestin 2 knockout, cellular tolerance development is compromised but not withdrawal[36,80]; together these support the role of β-arrestin 2 and GRK2 phosphorylation in adaptations involved in tolerance, but not opioid dependence development after chronic morphine exposure.

Chapters 4 and 8 will further discuss the role of phosphorylation in desensitisation.

2.4.3 Desensitisation and Internalisation

The conformational changes after agonist binding promote GRK phosphorylation of GPCRs that facilitates β-arrestin binding. The complex GPCR-β-arrestin traffics into clathrin-coated pits promoted by β-arrestin-clathrin direct interaction in combination with other factors, such as action of clathrin adapter complex AP-2 which is recruited by β-arrestin[194,347]. The formation of vesicles, known as early endosomes, is facilitated by a GTPase protein called dynamin which fission the vesicles from the membrane surface. β-arrestins have also been implicated in the dynamin endocytosis step, as phosphorylation of dynamin is crucial for this protein activity, and dynamin phosphorylation is dependent on Src kinase which in turn is activated by β-arrestin signalling[216,240]. The endocytosis machinery, described until now, is highly conserved across GPCRs; however, once internalised two different patterns are observed which are classified as class A or class B according to β-arrestin interaction. MOPr, β_2AR and dopamine D1A receptor are class A receptors, they do not bind to visual arrestins and have a higher affinity for β-arrestin 2 than β-arrestin 1[216,368]. GPCRs of this class present a very fast β-arrestin dissociation once internalised, while class B receptors form a much stronger bound complex with β-arrestin; consequently, the complex is observed in later endosomes. It has been proposed that this difference in interaction with β-arrestin is part of the complex mechanism which define if receptors are to be recycled or degraded, where class A is more likely to recycle, while class B is highly degraded. The phosphorylation 'barcode' previously mentioned to be important to determine β-arrestin signalling, also seems to play a role in determining the stability of the receptor-β-arrestin complex[251].

Early studies in regulation of opioid receptor internalisation were reviewed by Von

Zastrow et al. (2003)[347], they outlined the above conserved mechanisms for opioid peptides (Figure 2.7), and the inability of morphine to engage the endocytosis machinery after acute and chronic exposure. More recent publications have ascertained that morphine is an example of a opioid which does not engage in phosphorylation of the STANT cluster as effectively as DAMGO; therefore, the difference in β-arrestin promoted rapid internalisation[171,195]. A good correlation between agonist induced mMOPr Ser375 phosphorylation, β-arrestin 2 recruitment and internalisation was determined for a large range of opioids by Mcpherson et al. (2010)[236].

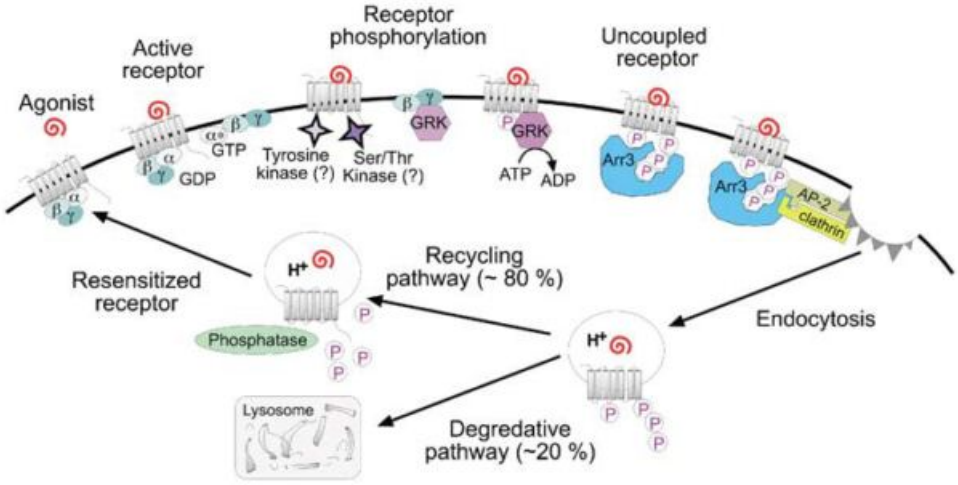

Figure 2.7. Generally accepted μ-Opioid receptor regulatory pathway after an internalising agonist such as DAMGO. Note that the majority of the receptors are recycled as expected for β-arrestin class A receptors. This figure is reproduced from Connor et al. (2004)[79].

The interconnection between phosphorylation, β-arrestin recruitment, internalisation and resensitisation can be misleading. An agonist's ability to rapidly internalise GPCRs was thought to contribute to receptor acute desensitisation as receptors would not signal from inside the cell[117], and this was consistent with the lower morphine desensitisation profile observed in LC neurons. Endocytosis mediated by opioid peptides was proposed to increase resensitisation and slow rate of desensitisation, as observed in the recombinant HEK293 cells by Law et al. (2000)[196]. The sustained phosphorylation of Ser375 by morphine after opioid removal, in contrast to DAMGO, which is internalised and dephosphorylated, was first thought to prevent resensitisation and, therefore, promoting morphine mediated desensitisation which could be related to

tolerance. Nevertheless, recent evidence ascertained that MOPr can be adequately dephosphorylated at membrane level and receptor can be recovered[95,102,279]. In transfected HEK293 cells, MOPr Ser375 and Thr370 residues are rapidly dephosphorylated after agonist removal, and it is independent of endocytosis as using an internalisation inhibitor, concanavilin A, did not affect the rapid dephosphorylation normally observed[102]. In 2006, Arttamangkul et al.[11] demonstrated that recovery from desensitisation is not affected by inhibition of internalisation in LC neurons, and in β-arrestin knockout LC neurons recovery was faster after ME exposure than in wild type. A recent study in AtT20 cells transfected with MOPr variant, in which phosphorylation sites at C-terminal STANT cluster were deleted, the receptor failed to internalise but did not affect desensitisation[364]. Therefore, aside from being mechanistically related, desensitisation, endocytosis and resensitisation are not necessarily correlated, and, clearly, endocytosis is not a regulatory process necessary for acute receptor desensitisation and resensitisation.

The notion that acute desensitisation and internalisation are distinct regulatory processes is further supported by their time course. Acute desensitisation is a faster process than internalisation. Johnson et al. (2006)[167] reported DAMGO induced maximum desensitisation of GIRK signalling in approximately 5 minutes, while at 10 minutes internalisation was far from complete in HEK293 cells expressing rMOPr. In LC neurons, although acute desensitisation of DAMGO induced GIRK activation was slightly slower than reported in HEK293, receptor loss was still much slower[20]. Furthermore, DAMGO induced MOPr desensitisation measured via I_{Ca} inhibition in AtT20 cells transfected with mMOPr is consistent with above reports[41]; then, overall, DAMGO induced internalisation reaches steady state before 30 minutes and half-time is somewhat around 5 minutes, while according to Williams et al. (2013)[356] review, rapid desensitisation reaches steady state by 5 minutes.

The correlation between endocytosis and cellular tolerance was reported by Finn and Whistler (2001)[122], where a chimera construction that facilitated morphine endocytosis reduced cellular tolerance and cAMP superactivation after prolonged morphine

exposure. Although there is weak evidence to correlate internalisation and acute desensitisation[11], endocytosis and resensitisation may contribute to the complex adaptation mechanisms involved in tolerance and dependence[69,229]. Interestingly, a recent study had demonstrated that MOPr recycling, which can modify receptor surface numbers, is not only regulated by opioids but also may be physiologically cross-regulated by substance P neurokinin 1 receptor signalling transduction[43]. Paradoxically, substance P, a pro-nociception neurotransmitter, induced an increase in MOPr recycling and resensitisation in trigeminal ganglion neuron after fentanyl and DAMGO, but not morphine, and it was dependent on PKC activation and phosphorylation of Ser363 and Thr370. This emphasises not only the importance of heterologous signalling pathways in MOPr regulation, but also the agonist-selective heterologous modulation, where in mice fentanyl mediated acute tolerance was diminished while morphine was unaffected.

Last, the importance of subcellular compartments must be highlighted as morphine induced significant MOPr internalisation in dendrites of nucleus accumbens neurons, in contrast to the low endocytosis in the same neuron cell bodies[140]. Endocytosis by morphine was also observed in striatal neurons[141] and in the hMOPr SNP L85I[287], which emphasises that not only distinct molecular mechanisms across different cell types, but also how a small change in receptor structure could affect endocytosis machinery. The L85I polymorphism will be further discussed in Chapter 6.

In conclusion, recent methodology advances enabled assessing desensitisation, phosphorylation and internalisation in many different systems and under varying conditions. Phosphorylation and endocytosis are much better understood then desensitisation which is a much more complex regulatory process. It is clear that regulatory processes are agonist-selective and this highlights the importance of characterising the functional importance of receptor regions and varying active conformations stabilised by each agonist; this knowledge will probably explain how varying opioids recruit differential regulatory processes and may supply a valuable clue on how to develop an improved opioid drug[175].

2.5 Functional Selectivity at the MOPr

Functional selectivity, also termed biased agonism and ligand direct signalling, is supported by the notion that a specific agonist binding stabilises varying active conformations of GPCRs, which can lead to activation of selected pathways and different regulation. Raehal et al. (2011)[281] reviewed biased agonism at the MOPr *in vivo* and *in vitro*, and they described bias signalling and regulation at many different levels. Phosphorylation, internalisation and desensitisation have been previously discussed, here focus will be on β-arrestin versus G protein functional selectivity.

Although β-arrestin biased agonism is a quite recent concept, it already clarified the intriguing pharmacological variance between β-blockers[292]. Many MOPr studies have looked at agonist mediated β-arrestin recruitment, but, unfortunately, evidence of β-arrestin signalling under varying opioid agonist treatment is lacking. Endomorphin-2 was determined to be β-arrestin biased, based on an operational model of pharmacological agonism, and, interestingly, it induced faster GIRK signalling desensitisation than DAMGO[294]. This was following the study by McPherson et al. (2010)[236] which reported β-arrestin 2 recruitment bias between a large number of opioids and determined the endomorphins to be the most β-arrestin-biased of a range of opioids tested.

Many studies using β-arrestin 2 knockout mice reported a reduction in adverse effects and tolerance, in addition to increase of morphine induced anti-nociception in these genetic modified animals compared with the wild type[80,280,281]. In contrast, the analgesic effect of morphine in knockdown Gα_i mice was diminished[282,306]. Combined this information supports the notion of G protein dependent analgesia and β-arrestin 2 dependent adverse effects. Nevertheless, it is important to note that opioid withdrawal was not determined to be β-arrestin 2 dependent[80], and rewarding properties by morphine is enhanced in these rodents; therefore, the development of a novel opioid drug biased towards G protein signalling with less adverse effects may alarmingly increase dependence and abuse. Interestingly, a G protein-biased MOPr ligand, named TRV130, is in clinical trials[101]. A preclinical model with a small group of healthy man demonstrated that molecular studies may be translated to the clinics, as greater

analgesia with less adverse effects were reported with TRV130 when compared with morphine[324].

2.6 Genetic Variants of the Human μ-Opioid Receptor

Since the identification and cloning of the MOPr gene *OPRM1*, a large number of studies have used genetic manipulation to construct MOPr variants to study signalling and regulation. However, naturally occurring variants have also been identified which are classified as splice variants or single nucleotide polymorphisms (SNPs).

Alternative splicing of *OPRM1* has been described for mice, rats and humans. A number of N and C-terminal hMOPr splice variants were identified, and differences in signalling and/or regulation were reported[262,361]. It is noteworthy that only a few studies from the same research group identified hMOPr splice variants; therefore, a larger body of evidence is necessary not only to determine frequency of expression, but also to identify *in vivo* functional relevance associated to their expression.

A large number of SNPs in the coding region of *OPRM1* have been identified, and they have been thoroughly reviewed by Knapman and Connor (2015)[180]. The A118G (N40D) allele variant is the most studied SNP. A large number of clinical and molecular studies have analysed this polymorphism as it is very common in some populations and have been associated with lower pain threshold and drug addiction[248]. This variant together with C17T (A6V), another common N-terminal variant, are assessed and discussed in Chapter 5. In addition to these two common SNPs, five rare polymorphisms will also be assessed in this work. The R181C polymorphism was previously characterised by a study as a total loss of function, while L85I was able to be internalised by morphine stimulus[287]. The hMOPr SNPs R260H, R265H and S268P are third intracellular loop mutations and have been reported to affect signalling[180]. The study of MOPr SNPs may help to elucidate MOPr molecular mechanisms, in addition to corroborate with known genetic factors involving pharmacokinetics[304] to explain the well

recognised inter-individual variability in opioid response. Note that in the present work the term polymorphism was used for all naturally occurring variants independently of frequency.

Therefore, by studying naturally occurring mutations of MOPr, together with targeted mutations of putative phosphorylation sites, I hope to gain a greater understanding of the mechanisms underlying receptor signalling and regulation.

3

Experimental Methodology

This chapter contains experimental protocols used throughout this work. Wherever required, a brief explanation of the basic principle is provided. Information regarding recipes, materials and equipment utilised can be checked in Appendix A, and information regarding suppliers in Appendix B.

Contents

3.1 Cell Culture

The work presented in this thesis was carried out using cultured cells to research molecular pharmacology of the MOPr. AtT20 cells, immortalised mouse pituitary adenoma cells, were the main cell type used for this work, while Human Embryonic

Kidney 293 (HEK293) cells were used for control experiments. It is important to note that none of the cell lines used in this project constitutively express MOPr, therefore all data obtained is through heterologous expression.

All the cell culture related procedures were performed under sterile conditions and adhered to the requirements of the Office of the Gene Technology Regulator (OGTR) for dealing with genetic modified organisms. Biosafety approvals obtained to work with genetic modified organism are shown on Appendix E.

3.1.1 AtT20 Cells

AtT20 cells are mouse pituitary adenoma cells. The adherent type of this cell line was chosen for this project because it constitutively expresses functional G protein-coupled inwardly rectifying potassium channels (GIRKs). GIRKs play an important role in maintaining the resting membrane potential and excitability of cells, which is crucial for the main signalling assay performed during this work (section 3.5). In addition, AtT20 cells also constitutively express somatostatin receptors, which allow ready study of heterologous desensitisation.

AtT20 wild-type cells were purchased from ATCC and all AtT20 cells expressing mouse MOPr were a gift from Prof. MacDonald Christie from Sydney University.

3.1.1.1 Growth Condition

AtT20 cells were cultured in complete growth medium, which consists of 10% fetal bovine serum (FBS) and 1% of penicillin-streptomycin in high glucose Dulbecco's Modified Eagle Medium (DMEM). Selection antibiotics were added to the transfected cells medium and will be further discussed in section 3.3. The cultures were grown and maintained in a humidified incubator at 37 ^{o}C with 5% CO_2 in air atmosphere.

3.1.1.2 Propagation

AtT20 cells grew attached to the bottom of the flask and complete growth medium was changed every 2-3 days. They were round in shape after seeding and in 1-2 days

became more elongated in normal growth condition. Cells were passaged to a new flask when confluency reached ∼70-80%.

Passaging involved rinsing the cells with phosphate-buffered saline (PBS), then adding trypsin-EDTA and incubating for ∼2 minutes, followed by complete growth medium, centrifugation to pellet cells (@ 1000 rpm for 5 min), aspiration of medium, resuspension of cells pellet in complete growth medium and reseeding.

Trypsin, a serine protease, is used in tissue culture to detach cells by cleaving the extracellular matrix that attaches cells to the flask. EDTA, a chelating agent, increases trypsin enzymatic activity by neutralising calcium and magnesium ions that obscure the peptide bonds on which trypsin acts.It is important to stop enzymatic reaction with complete growth medium; otherwise the continuous digestion can lead to cell death. FBS contains protease inhibitors, for that reason complete growth media is used to stop trypsin reaction, and also PBS is used to remove any remaining medium before adding trypsin-EDTA.

Reseeding was done according to expected usage of cells. In a long-term propagation only ∼ 0.1mL of 5mL resuspension is used.

Every time cells were passaged, an increase in passage number was recorded. In this project, cells were used up to 20 passages from transfection.

3.1.1.3 Storage

Cell lines were stored frozen in liquid nitrogen tanks. This enables not only long-term storage and transportation but also the maintenance of batches with low passage numbers.

Freezing cells involved the same steps as propagation, with the exception that when resuspending cells a freezing medium was used. Freezing medium consists of 20% FBS, 5% DMSO and 75% DMEM.

When freezing cells, ice crystals form and can puncture the plasma membrane, leading to cell death. DMSO, a cryoprotectant agent, is used to partially solubilise the membrane (making it less prone to puncture) and also decreases formation of crystals. Cells from a T75 flask were carefully resuspended in 2mL of ice-cold freezing medium

and transferred to a labelled cryo-vial (1mL per Symport cryo-vial). Cryo-vials were placed inside an ice-cold Mr. Frosty™[†] and transferred into a -80 ^{o}C freezer for at least 4 hours, and then to a liquid nitrogen tank. Information regarding frozen cell line and location in tanks was recorded in the liquid nitrogen registry.

3.1.1.4 Thawing

The thawing procedure is stressful to frozen cells, and using good technique and working quickly ensures a high proportion of cells survive this procedure.

Cells were removed from liquid nitrogen tanks and quickly (<1 minute) thawed in 37 ^{o}C water bath. DMSO is toxic to the cells above 4 ^{o}C for this reason a rapid procedure was crucial. Then, cells were added drop-wise to a T75 flask containing 10mL of complete growth medium without selection antibiotics. In order to remove cryoprotectant agent, 24 hours after seeding or whenever cells were completely attached, medium was changed to complete growth medium plus selection antibiotics.

3.1.1.5 Assay Condition

All assays performed during this project were done after overnight serum starvation by incubating samples in L15 medium supplemented with 1% FBS, 1% of penicillin-streptomycin and glucose to 15mM at 37 ^{o}C in air atmosphere. Serum starvation was used to put the cells in a similar proliferative state across all assays.

3.1.2 HEK293 Cells

HEK293 cells are largely used as a vehicle for the expression of recombinant proteins in the literature. In this project, these cells were only used for sets of control experiments. They do not natively express GIRKs.

[†]Mr. Frosty™ is filled with isopropranol and designed to regulate the rate of temperature drop to 1 ^{o}C.min^{-}1

3.1.2.1 Growth, Thaw, Propagation and Storage

HEK293 cells were grown, propagated, stored and thawed in similar way to AtT20 cells. These cells grew in a slightly faster rate, then medium was changed more often than with AtT20. In addition, 10% instead of 5% DMSO was used to prepare freezing medium.

3.2 Gene Construction and Transformation

In this project, 12 variants of the hMOPr and four variants of the mMOPr were analysed. The human variants were constructed in collaboration with Dr. Alisa Knapman, and were synthetised by GenScript.

The mouse variants were constructed, transformed and transfected by Prof. MacDonald Christie lab members at the University of Sydney.

3.2.1 μ-Opioid Receptor Constructs

DNA constructs were synthesized according to sequences outlined in this subsection and inserted in the cloning site HindIII-BamHI of the pCDNA5/FRT/TO vector (see subsection C.1.3) by GenScript.

All designed DNA sequences contain an 'adequate' Kozac consensus and encode a triple human influenza hemagglutinin tag (HA-tag) attached to the N-terminal of the MOPr (green font in hMOPr-WT sequence Figure 3.1).

3.2.1.1 hMOPr-WT

The most common hMOPr variant, encoded by the *OPRM1* gene, was used to construct the hMOPr-WT sequence. This sequence was optimised by GenScript for good expression yields in a heterologous system and is shown in Figure 3.1.

```
   1  AAGCTTGCCA  CCATGTATCC  TTATGATGTG  CCTGACTATG  CTCTGGTCCC
  51  ACGATATCCC  TACGATGTGC  CCGACTACGC  TCTGGTCCCA  CGATACCCTT
 101  ATGACGTGCC  AGATTACGCA  CTGGTGCCCA  GAGACAGCTC  CGCCGCTCCT
 151  ACCAACGCCT  CTAATTGCAC  AGATGCACTG  GCCTATTCTA  GTTGTAGTCC
 201  AGCCCCCTCT  CCTGGCAGTT  GGGTGAACCT  GTCCCACCTG  GACGGCAATC
 251  TGTCTGATCC  ATGCGGACCC  AACAGGACCG  ACCTGGGCGG  AAGAGATTCC
 301  CTGTGCCCTC  CCACAGGAAG  TCCCTCAATG  ATCACAGCAA  TCACTATTAT
 351  GGCCCTGTAC  TCTATTGTCT  GCGTGGTCGG  GCTGTTTGGC  AACTTCCTGG
 401  TCATGTACGT  CATCGTGCGG  TATACCAAGA  TGAAAACAGC  CACTAACATC
 451  TACATCTTCA  ACCTGGCCCT  GGCAGACGCA  CTGGCTACCT  CAACACTGCC
 501  TTTTCAGAGC  GTCAACTATC  TGATGGGAAC  ATGGCCATTC  GGGACTATCC
 551  TGTGCAAGAT  CGTGATCAGC  ATCGATTACT  ACAACATGTT  CACCAGTATC
 601  TTCACCCTGT  GCACAATGTC  AGTGGACCGA  TACATTGCTG  TCTGTCACCC
 651  AGTGAAGGCA  CTGGATTTCC  GAACACCCAG  GAACGCAAAA  ATCATTAACG
 701  TCTGCAATTG  GATTCTGAGC  AGCGCCATTG  GGCTGCCTGT  GATGTTTATG
 751  GCTACCACAA  AGTACCGCCA  GGGCAGCATC  GACTGTACTC  TGACCTTCTC
 801  CCATCCAACA  TGGTATTGGG  AGAACCTGCT  GAAAATTTGC  GTGTTCATCT
 851  TTGCTTTCAT  TATGCCCGTC  CTGATCATTA  CCGTGTGCTA  CGGACTGATG
 901  ATCCTGCGCC  TGAAGTCCGT  GCGAATGCTG  AGCGGGTCCA  AGGAGAAAGA
 951  TCGGAATCTG  AGGAGAATCA  CTCGCATGGT  GCTGGTGGTC  GTGGCCGTGT
1001  TCATCGTGTG  CTGGACCCCC  ATTCACATCT  ATGTCATCAT  TAAGGCTCTG
1051  GTGACAATCC  CTGAAACTAC  CTTTCAGACC  GTGAGCTGGC  ATTTCTGCAT
1101  TGCTCTGGGC  TACACCAACT  CCTGTCTGAA  TCCTGTGCTG  TATGCATTTC
1151  TGGACGAGAA  CTTCAAAAGA  TGCTTTCGGG  AATTCTGTAT  CCCAACATCC
1201  TCTAACATTG  AACAGCAGAA  TTCTACTAGG  ATCAGGCAGA  ACACCAGGGA
1251  TCATCCCAGT  ACTGCCAATA  CCGTGGACCG  AACCAACCAT  CAGCTGGAAA
1301  ACCTGGAAGC  CGAGACCGCC  CCTCTGCCAT  AAGGATCC
```

Figure 3.1. Human μ-Opioid receptor wild-type sequence. Kozac consensus underlined, HA-tag highlighted in green and initiation codon in purple.

3.2.1.2 hMOPr-A6V

This SNP occurs in position 17 of the *OPRM1* gene. The change of a C to a T in the second position of the codon results in a change from alanine to valine (highlighted in cyan in Figure 3.2).

```
  51  ACGATATCCC  TACGATGTGC  CCGACTACGC  TCTGGTCCCA  CGATACCCTT
 101  ATGACGTGCC  AGATTACGCA  CTGGTGCCCA  GAGACAGCTC  CGCCGTTCCT
 151  ACCAACGCCT  CTAATTGCAC  AGATGCACTG  GCCTATTCTA  GTTGTAGTCC
```

Figure 3.2. Sequence of the mutated codon in hMOPr-A6V

3.2.1.3 hMOPr-N40D

This SNP is in position 118 of the *OPRM1* gene. The change of an A to a G in the first position of the codon results in a change from asparagine to aspartic acid (highlighted in cyan in Figure 3.3).

```
151  ACCAACGCCT  CTAATTGCAC  AGATGCACTG  GCCTATTCTA  GTTGTAGTCC
201  AGCCCCCTCT  CCTGGCAGTT  GGGTGAACCT  GTCCCACCTG  GACGGCGATC
251  TGTCTGATCC  ATGCGGACCC  AACAGGACCG  ACCTGGGCGG  AAGAGATTCC
```

Figure 3.3. Sequence of the mutated codon in hMOPr-N40D

3.2.1.4 hMOPr-L85I

This SNP is originally a change of a C to an A in position 253 of the *OPRM1* gene, resulting in a change from leucine to isoleucine. However with the optimisation of the hMOPr-WT, the codon used was CTG, and the nucleotide change would lead to methionine not isoleucine. Therefore the nucleotide on position 255 was also changed from G to C to result in the expected amino acid change (highlighted in cyan in Figure 3.4).

```
301  CTGTGCCCTC  CCACAGGAAG  TCCCTCAATG  ATCACAGCAA  TCACTATTAT
351  GGCCCTGTAC  TCTATTGTCT  GCGTGGTCGG  GATCTTTGGC  AACTTCCTGG
401  TCATGTACGT  CATCGTGCGG  TATACCAAGA  TGAAAACAGC  CACTAACATC
```

Figure 3.4. Sequence of the mutated codon in hMOPr-L85I

3.2.1.5 hMOPr-R181C

This SNP is originally a change of a C to a T in position 541 of the *OPRM1* gene, resulting in a change from arginine to cysteine. However with the optimisation of the hMOPr-WT, the codon used was CGA, and the nucleotide change would lead to a stop codon not cysteine. Therefore the nucleotide on position 543 was also changed from A to T to result in the expected amino acid change (highlighted in cyan in Figure 3.5).

```
601  TTCACCCTGT  GCACAATGTC  AGTGGACCGA  TACATTGCTG  TCTGTCACCC
651  AGTGAAGGCA  CTGGATTTCT  GTACACCCAG  GAACGCAAAA  ATCATTAACG
701  TCTGCAATTG  GATTCTGAGC  AGCGCCATTG  GGCTGCCTGT  GATGTTTATG
```

Figure 3.5. Sequence of the mutated codon in hMOPr-R181C

3.2.1.6 hMOPr-R260H

This SNP is in position 779 of the *OPRM1* gene. The change of a G to an A in the second position of the codon results in a change from arginine to histidine (highlighted in cyan in Figure 3.6).

```
851  TTGCTTTCAT  TATGCCCGTC  CTGATCATTA  CCGTGTGCTA  CGGACTGATG
901  ATCCTGCACC  TGAAGTCCGT  GCGAATGCTG  AGCGGGTCCA  AGGAGAAAGA
951  TCGGAATCTG  AGGAGAATCA  CTCGCATGGT  GCTGGTGGTC  GTGGCCGTGT
```

Figure 3.6. Sequence of the mutated codon in hMOPr-R260H

3.2.1.7 hMOPr-R265H

This SNP is originally a change of a G to an A in position 794 of the *OPRM1* gene, resulting in a change from arginine to histidine. However, with the optimisation of the hMOPr-WT, the codon used was CGA, and the nucleotide change would lead to glutamine not cysteine. Therefore the nucleotide on position 795 was also changed from A to C to result in the expected amino acid change (highlighted in cyan in Figure 3.7).

```
851  TTGCTTTCAT  TATGCCCGTC  CTGATCATTA  CCGTGTGCTA  CGGACTGATG
901  ATCCTGCGCC  TGAAGTCCGT  GCACATGCTG  AGCGGGTCCA  AGGAGAAAGA
951  TCGGAATCTG  AGGAGAATCA  CTCGCATGGT  GCTGGTGGTC  GTGGCCGTGT
```

Figure 3.7. Sequence of the mutated codon in hMOPr-R265H

3.2.1.8 hMOPr-S268P

This SNP is originally a change of a T to a C in position 802 of the *OPRM1* gene, resulting in a change from serine to proline. However with the optimisation of the hMOPr-WT, the codon used was AGC, which does not even contain a T. Therefore

the whole codon was changed to CCT to result in the expected amino acid change (highlighted in cyan in Figure 3.8).

```
851  TTGCTTTCAT  TATGCCCGTC  CTGATCATTA  CCGTGTGCTA  CGGACTGATG
901  ATCCTGCGCC  TGAAGTCCGT  GCGAATGCTG  CCTGGGTCCA  AGGAGAAAGA
951  TCGGAATCTG  AGGAGAATCA  CTCGCATGGT  GCTGGTGGTC  GTGGCCGTGT
```

Figure 3.8. Sequence of the mutated codon in hMOPr-S268P

3.2.1.9 hMOPr-S268A

The codon AGC, that codes amino acid on position 268 of the *OPRM1* gene, was modified to GCT to introduce a serine to alanine point mutation (highlighted in cyan in Figure 3.9).

```
851  TTGCTTTCAT  TATGCCCGTC  CTGATCATTA  CCGTGTGCTA  CGGACTGATG
901  ATCCTGCGCC  TGAAGTCCGT  GCGAATGCTG  GCTGGGTCCA  AGGAGAAAGA
951  TCGGAATCTG  AGGAGAATCA  CTCGCATGGT  GCTGGTGGTC  GTGGCCGTGT
```

Figure 3.9. Sequence of the mutated codon in hMOPr-S268A

3.2.1.10 hMOPr-3S/A

Three codons of the *OPRM1* gene were modified to change all 3rd loop amino acid serine to alanine (highlighted in cyan in Figure 3.10).

```
851  TTGCTTTCAT  TATGCCCGTC  CTGATCATTA  CCGTGTGCTA  CGGACTGATG
901  ATCCTGCGCC  TGAAGGCCGT  GCGAATGCTG  GCTGGGGCCA  AGGAGAAAGA
951  TCGGAATCTG  AGGAGAATCA  CTCGCATGGT  GCTGGTGGTC  GTGGCCGTGT
```

Figure 3.10. Sequence of the mutated codons in hMOPr-3S/A

3.2.1.11 hMOPr-3ST/A

Four codons of the *OPRM1* gene were modified to change all 3rd loop serine and threonine amino acids to alanine (highlighted in cyan in Figure 3.11).

```
851  TTGCTTTCAT  TATGCCCGTC  CTGATCATTA  CCGTGTGCTA  CGGACTGATG
901  ATCCTGCGCC  TGAAGGCCGT  GCGAATGCTG  GCTGGGGCCA  AGGAGAAAGA
951  TCGGAATCTG  AGGAGAATCG  CTCGCATGGT  GCTGGTGGTC  GTGGCCGTGT
```

Figure 3.11. Sequence of the mutated codons in hMOPr-3ST/A

3.2.1.12 hMOPr-CST/A

Eleven codons of the *OPRM1* gene were modified to change all C-terminal serine and threonine amino acids to alanine (highlighted in cyan in Figure 3.12).

```
1151  TGGACGAGAA  CTTCAAAAGA  TGCTTTCGGG  AATTCTGTAT  CCCAGCAGCC
1201  GCTAACATTG  AACAGCAGAA  TGCTGCCAGG  ATCAGGCAGA  ACGCCAGGGA
1251  TCATCCCGCA  GCTGCCAATG  CCGTGGACCG  AGCCAACCAT  CAGCTGGAAA
1301  ACCTGGAAGC  CGAGGCCGCC  CCTCTGCCAT  AAGGATCC
```

Figure 3.12. Sequence of the mutated codons in hMOPr-CST/A

3.2.2 Transformation and Plasmid DNA Preparation

Genetic transformation is a technique where a host organism takes in a foreign DNA and expresses the foreign gene. This technique was essential for propagating and maintaining plasmids which were important to obtain enough plasmid DNA for transfections.

Alpha-select gold efficiency *Escherichia coli* competent cells were thawed on ice, 25μL added to a sterile 2059 tube and mixed with 0.1-1μg of plasmid DNA. To make the cell passively permeable to DNA, the mix was heat shocked in 42 ^{o}C water bath for 45 seconds with gentle agitation, then placed in ice for 2 minutes. LB broth (500μL) without ampicillin were added and cells were incubated in a shaking incubator (200-250rpm) at 37 ^{o}C for 30-60 minutes, thus cells started growing and expressing ampicillin resistance gene. 100μL of this mix were spread onto one LB-ampicillin (100μL/mL) plate and a sterile loop used to inoculated onto another plate using the streaking technique, once dried, plates were flipped over and incubated overnight at 37 ^{o}C. On the second day, two isolated bacteria colonies were picked, each inoculated into 10mL of LB-ampicillin broth then placed in a shaking incubator (150-200 rpm) overnight at 37 ^{o}C. On the last day, PureLink® quick plasmid miniprep kit was used to purify

plasmids from cultures as per manufacturer's protocol.

Glycerol stock was also made for long-term storage by mixing 250μL of 50% glycerol (cryoprotectant agent) and ~600μL of overnight culture and transferred to -80 ^{o}C freezer.

DNA purity was assessed using NanoDrop™ 2000 spectrophotometer where a ratio (A260/A280) of ~1.8 is generally accepted as 'pure' for DNA. As a result all samples where ratio was ~1.8 were considered for transfection.

In addition, DNA electrophoresis was performed to check for successful transformation. Plasmid DNA was restricted digested using BamHI and HindIII, and incubated at 37 ^{o}C for 2 hours. Digested sample and 1Kb promega ladder mixed with loading dye were loaded in a 0.8% agarose gel, prepared with GelRed™(1:10,000) and TAE buffer, then were run for 30-60 minutes at 80V. Gel was imaged using Gel Doc™ EZ System (UV tray) and only digested plasmids with a band size of ~1300bp were considered for transfection.

3.3 Transfections

Flp-In System was transfected into an AtT20 wild-type cell line and then hMOPr were integrated using that system. The Flp-In™ System information presented in this section was obtained from Life Technologies™ manuals. More information on Flp-In™ System vectors and transfection related results are presented in Appendix C.

All transfections performed had a negative control where no plasmid DNA was added to the transfection mixture. If these cells did not die during selection, all transfections done in that experiment were discarded.

3.3.1 LacZeo2/FRT: Generating a FlpIn™ AtT20 Cell Line

Generating a stable cell line which expresses genetic variants in a manner where comparison between variants was easier to perform has always been a challenge. The Flp-In™ System allows integration and expression of a gene of interest in mammalian cells at a specific genomic location, this enables generating isogenic stable cell lines.

Therefore this system was selected to transfect all hMOPr variants into AtT20 cells.

The introduction of a Flp Recombinase Target (FRT) site into the genome of AtT20 WT cells was the first step to produce a Flp-In™ System. This site is present in the FRT/*lac*Zeo 2 vector which also expresses a fusion protein containing β-galactosidase (*lacZ* gene) and the Zeocin™ resistance marker.

Before starting transfection, it was important to determine the minimum Zeocin concentration to kill the WT cells, thus a kill curve for Zeocin™ was performed (see result on Appendix C) and 150μg/mL was decided the optimal concentration for selection.

Cells were plated in a 6-well plate at high confluency 24 hours before transfection. The FRT/lacZeo 2 plasmid was linearised using the ScaI restriction enzyme (incubated for 2 hours at 37 ^{o}C) and mixed with transfection agent Fugene HD (3:1 and 4:1 ratio to DNA) and DMEM to 100μL. Mixture was incubated at room temperature (RT) for 10 minutes and then added drop-wise to cells. They were incubated at 37 ^{o}C with 5% CO_2 in air atmosphere for 48 hours after which selection started. Selection medium was changed every 3-4 days until foci were identified. Zeocin-resistant foci were isolated using glass cylinders and isolated clones were tested for β-galactosidase activity using the Beta-Glo Assay System (see results on Appendix C), where clone 2 with medium activity, called AtT20 Flp-In 2, was selected for this project. Ideally screening for number of integrants should have been done, however after many months spent trying to get a Southern Blot to work only the positive control was observed. To try to avoid single integration, in case of multiple-integrants, after transfection of hMOPr plasmids Zeocin selection was performed for all variants and, as expected for a full integration, they were sensitive (see Appendix C for vector details).

3.3.2 μ-Opioid Receptor Variants

The constructs presented on section 3.2 were integrated into the genome via Flp recombinase-mediated DNA recombination at the FRT site[254]. Once the AtT20 Flp-In™ cell line was created, subsequent generation of Flp-In™ cell lines expressing hMOPr variants was rapid and efficient.

The selected clone AtT20 Flp-In 2 was plated in a 6-well plate at high confluency 24 hours before transfection. Fugene HD [†] (3:1 or 4:1 ratio to 3μg total DNA), pOG44 plasmid (9:1 ratio to gene of interest DNA, see pOG44 information on Appendix C), gene of interest plasmid and DMEM were mixed, incubated at RT for 10 minutes then added drop-wise to wells. Cells were incubated at 37 ^{o}C with 5% CO_2 for 48 hours and then selection started. Selection was done using 100μg/mL of Hygromycin according to kill curve performed previously (see result on Appendix C). Selection medium was changed every 3-4 days until colonies were growing. The Flp-In™ System permits rapid and efficient transfection and polyclonal selection of stable expression cell lines, hence isolating clones was not necessary.

Clones expressing different hMOPr variants were assayed for opioid response after 5 passages and then frozen down as previously described.

3.4 Radioligand Binding Assay

Radioligand binding assay was performed using intact stably transfected cells and [^{3}H]-DAMGO to determine surface hMOPr expression.

3.4.1 Experimental Procedure

Approximately 24 hours before the assay, cells were detached from flask as described on Section 3.1 and resuspended in L15 supplemented medium. Cells were counted with Countess® automated cell counter and 2 x 10^5 cells were plated per well of a poly-D-lysine pre-coated 48-well plate and incubated overnight at 37 ^{o}C in air atmosphere . On the day of the assay, cells were gently washed twice with wash buffer (50mM Tris-Cl - pH 7.4) and incubated with [^{3}H]-DAMGO concentrations ranging from 0.125 to 16nM for 2 hours on ice to reach steady state. Non-specific binding was determined in the presence of unlabelled 10μM naloxone. After incubation, cells were gently rinsed three times with ice-cold wash buffer and digested with 100μL of 1N NaOH for 30 minutes at RT. Then samples were neutralised with 100μL of 1N HCl per well and

[†]Fugene HD ratio changed when new batch was purchased or after long-term storage

the whole volume collected into scintillation vials. To determine bound ligand, 3mL of scintillation fluid was added per vial, samples were thoroughly mixed and counts were obtained using a MicroBeta® counter.

Out of the 48 wells, three were separated to determine protein concentration per well. These wells were treated as above without radioligand until last wash and RIPA buffer was used to extract proteins from wells. Protein concentration in these samples was determined with Pierce™ BCA Protein Assay Kit as per manufacturer's instructions.

It is important to point out that naloxone was used to determine non-specific binding (NSB) because as previously reported[51], it is best to choose a drug that is chemically different from the radioligand. This avoids the possibility of the drug inhibiting 'specific' but non-receptor binding sites.

Three technical and at least three biological replicates were performed when collecting radioligand binding data for this thesis. Note that technical replicates are replicates that share the same sample (repeated measurements), while biological replicates use different samples; i.e. different passage number and/or day.

3.4.2 Data Analysis

Receptor density (B_{max}) and affinity(K_D) were calculated using GraphPad Prism Software one site (specific binding) equation and disintegrations per minute (DPM) data. This data was determined by converting counts per minute (CPM) using specific activity of [^{3}H]-DAMGO (49.2Ci/mmol). Receptor density in fmol/mg was quantified using B_{max} and protein concentration obtained. Specific binding in fmol/mg total protein was plotted in GraphPad Prism also using the one site (specific binding) equation. Statistical tests on B_{max} and K_D were performed and significance was assessed with Student t-test, $p<0.05$ was considered significant. Note that each mutant was compared with hMOPr-WT, no comparison between mutants was made.

3.5 FLIPR®Membrane Potential Assay

Experiments in this section were developed by Prof. Mark Connor's group and were published in the journal:

Alisa Knapman, **Marina Santiago**, Yan Ping Du, Philip Bennallack, MacDonald Christie and Mark Connor, "A continuous, fluorescence-based assay of μ-opioid receptor activation in AtT20 cells", *J Biomol Screen*, Vol.18, pp.269-276, 2013

The FLPR® Membrane Potential Assay (MPA) Kit allows observation of real-time membrane potential changes. The product used in this project contains a proprietary fluorescence blue dye combined with a quencher which is claimed to provide high quality screening data that shows good correlation with manual patch clamp assays (data provided by Molecular Devices).

This kit is able to detect ion channel modulation and as cellular membrane potential changes, the fluorescence signal decrease or increase. Dye follows the positively charged ions, then when cell depolarise, fluorescence signal intensity increases as dye follows the ions inside the cell, while during hyperpolarisation dye signal decrease as it goes out of the cell (see Figure 3.13) . This happens because outside the cell there are quenching molecules, which reduce background fluorescence and improve the signal-to-noise ratio.

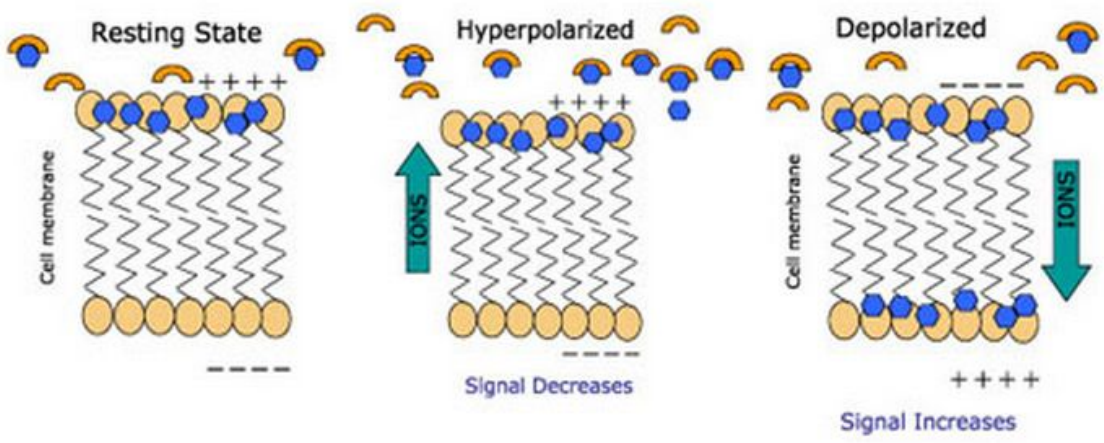

Figure 3.13. The FLPR® Membrane Potential Assay Kit: Fluorescence intesity changes with increase or decrease in cellular membrane potential. Blue circles represent fluorescent dye and semi-circles quencher. Reproduced from Molecular Devices product information.

The blue dye was purchased in bulk, and reconstituted with low-potassium HBSS

(see recipe on Appendix A), aliquoted and frozen in -80 ^{o}C. Dye was used either at the concentration recommended by the manufacturer or diluted by 50% - this made no difference to the results.

FlexStation® 3 Microplate reader can simultaneously read and pipet therefore is uniquely suited to capture the fast kinetics associated with this assay. SoftMax Pro 5.4 microplate reader software is used to run FlexStation® 3. Experimental software setup parameters used with this kit that were unchanged throughout this project are presented in Table 3.1.

Table 3.1. Membrane potential assay experimental setup paramenters

Read Mode	Fluorescence (RFUs) Bottom Read
Wavelength (nm)	530 (Ex) 565 (Em) 550 (Cutoff)
Sensitivity	Reading: 6 (normal) PMT sensitivity: Medium
Timing	Interval: 2 sec
Assay Plate Type	96 well Costar blk/clrbtm
Compound Source	Greiner 96 Vbtm plate
Auto Calibrate	On
Auto Read	Off

A concentration response curve (CRC) was obtained for somatostatin (SST) and the following opioids: morphine, DAMGO, buprenorphine, methadone, pentazocine, endomorphin-2, β-endorphin and fentanyl. Note that not all opioids mentioned were used in all MOPr variants.

Homologous desensitisation data was collected for all clones using morphine and DAMGO, in addition to the heterologous desensitisation with SST. Buprenorphine and endomorphin-2 data were only collected for clones hMOPr-WT, hMOPr-A6V and hMOPr-N40D. When kinase modulators phorbol-12-myristate-13-acetate (PMA) and staurosporine were used, an extra incubation of 10 minutes was performed before first

addition of opioid. Both kinase modulators needed DMSO for solubilisation, but the final concentration of DMSO was not more than 0.01% and control experiments revealed that this concentration produced no detectable change on membrane potential.

At least two technical and five biological replicates were done when collecting signalling data for this thesis using MPA kit (exception Chapter 4). In addition, the background fluorescence of cells without dye or dye without cells were analysed in many assays and were always negligible.

3.5.1 Concentration Response Curve: Experimental Procedure

On the day before the assay, cells were detached from flask and resuspended in supplemented L15 as described on Section 3.1. Approximately 1 x 10^5 cells in 90μL were seeded per well of a sterile, black wall, clear bottom 96-well plate using an automated multi-channel pipette, and incubated at 37 ^{o}C overnight. The reconstituted dye was thawed and 90μL of dye was loaded per well (180μL total) and incubated for 1 hour inside FlexStation® 3 set to 37 ^{o}C; this incubation is essential to achieve resting membrane potential steady state signal. During this time serial drug dilutions of drugs cited above in HBSS were prepared and loaded to a V-shape 96-well plate according to experimental protocol designed.

Once started the run, data was collected every 2 seconds, drug added at 120 seconds and total run time was 300 seconds. In addition to the experimental parameters in Table 3.1, concentration response curve parameters are shown in Table 3.2.

Pertussis toxin (PTX) and naloxone controls were carried out with all hMOPr transfected cell lines. The above details were altered when PTX or naloxone were added. In particular, PTX was added to wells at final concentration 200ng/mL when seeding cells in 96 well plate (overnight pre-treatment). An extra compound transfer of 20μL to 1μM naloxone final concentration at 300 seconds were done; furthermore total running time was changed to 420 seconds in both control experiments.

Table 3.2. Concentration response curve additional experimental parameters

Timing	Time: 300 sec
Compound Transfer - T1	Pipette Height: 190μL Volume: 20μL Rate: 2 ($\sim$31μL/sec) Time Point: 120 sec
Triturate Assay Plate - T1	Volume: 30μL Cycles: 3 Height: 160μL

3.5.2 Concentration Response Curve: Data Analysis

Raw data collected in RFUs was exported in .txt format and analysed using Microsoft Excel. First, baseline average was calculated for each sample using the last 30 seconds previous to drug addition. Then, percentage remaining from baseline for each time point collected was determined, being 100% no change from baseline. This was followed by a vehicle correction, as every time vehicle was added there was a small baseline drop even if only HBSS was used; this is why during experimental design every column had a blank (HBSS addition). The minimum RFU reading of each run (maximum hyperpolarisation) was defined, and then averaged with the reading before and the reading after. Last, the difference between the baseline (100%) and this maximum hyperpolarisation average, Δ fluorescence (%), was pasted in GraphPad Prism software. It has the capability of averaging the technical replicates and plotting a concentration response curve containing the standard error of the mean (SEM), in addition to calculating $p\text{EC}_{50}$ and maximum response (E_{max}) of the 'treatment'. The equation fitted to the results was the non-linear regression log(inhibitor) vs. response - variable slope (four parameters), with the bottom constrained to zero (Y=Bottom + (Top-Bottom)/(1+$10^{(LogIC50-X)*HillSlope}$).

Statistical tests were performed using GraphPad Prism. E_{max} and $p\text{EC}_{50}$ values derived from individual experiments were compared using unpaired Student's t-test, $p<0.05$ was considered significant. Note that each mutant was compared with hMOPr-WT, no comparison between mutants was made. Comparisons between maximum

agonist responses amoung drugs were made by comparing E_{max} values derived from individual experiments using one-way analysis of variance (*ANOVA*) followed by Student's *t*-test, corrected for multiple comparisons using the Bonferroni method, $p<0.05$ was considered significant.

3.5.3 Desensitisation: Experimental Procedure

In this assay, to quantify the degree of desensitisation a saturating agonist concentration was added after the desensitising stimulus. In homologous desensitisation assay the same drug was used in both additions, while in the heterologous assay somatostatin (SST) was added after opioid stimulus. Desensitisation time course was performed by changing the time between the two additions (5, 10, 20, 30 and 40 minutes)

Experimental procedures for desensitisation assay were very similar to those used in concentration response curve assays; the only differences are the parameters and drug dilutions. The additional parameters used for this assay are shown in Table 3.3. Drug dilutions are not detailed as they are simple mathematical calculations.

Table 3.3. Desensitisation additional experimental parameters

Interval between additions (min)		**5**	**10**	**20**	**30**	**40**
Timing	Time(sec):	720	1020	1620	2220	2820
Compound Transfer - T1	Pipette Height(μL):	190	190	190	190	190
	Volume(μL):	20	20	20	20	20
	Rate:	2	2	2	2	2
	Time Point(sec):	120	120	120	120	120
Triturate Assay Plate - T1	Volume(μL):	30	30	30	30	30
	Cycles:	3	3	3	3	3
	Height(μL):	160	160	160	160	160
Compound Transfer - T2	Pipette Height(μL):	210	210	210	210	210
	Volume(μL):	20	20	20	20	20
	Rate:	2	2	2	2	2
	Time Point(sec):	420	720	1320	1920	2520
Triturate Assay Plate - T2	Volume(μL):	30	30	30	30	30
	Cycles:	3	3	3	3	3
	Height(μL):	190	190	190	190	190

3.5.4 Desensitisation: Data Analysis

As per CRC data, raw data collected in RFUs was exported in .txt format and analysed using Microsoft Excel. The first steps are the same as per CRC analysis until calculating Δ fluorescence (%). Then desensitisation is calculated as a percentage of the difference between the result obtained with the saturation concentration with and without stimulus. For instance, if DAMGO without stimulus results in a % change of 27.9 and DAMGO with stimulus produces a change of 23.0% then % desensitisation is 17.6. Results were calculated for each time point and analysed in GraphPad Prism where a desensitisation time course was plotted using the non-linear regression equation for one-phase association with Y0 constrained to zero. Significance was assessed with two-way *ANOVA*, $p<0.05$ was considered significant. In addition, maximum desensitisation (D_{max}) and $t^1/_2$ values derived from individual experiments were compared using unpaired Student's *t*-test, $p<0.05$ was considered significant. Note that each mutant was compared with hMOPr-WT, no comparison between mutants was made.

Decline in the MOPr signalling was also analysed by fitting the 40 minutes decay after stimulus to a one-phase association. Time constant (τ) and maximum decay/recovery (R_{max}) values derived from individual experiments were obtained and also compared using unpaired Student's *t*-test, $p<0.05$ was considered significant.

3.6 Phosphoprotein Detection by Western Blot

Western blot is a widely used analytical technique which can detect specific proteins in a sample. Briefly, proteins are extracted from cells, quantified, separated by electrophoresis and then blotted to a membrane where proteins can be immuno detected using specific antibodies. In this project a phosphosite-specific antibody was used to determine hMOPr phosphorylation of serine 377 (Ser377) under opioid treatment, and the detailed procedures are described in this section.

At least three biological replicates were performed for each experiment.

3.6.1 Protein Extraction and Quantification

AtT20 cells expressing HA-tagged hMOPr were grown in regular growth condition[†] until reaching 80-90% confluency, then medium was changed to complemented L15 and cells incubated overnight at 37 ^{o}C in air atmosphere. Before starting extraction, RIPA buffer containing phosphatase inhibitors (PhosStop) were thawed and protease inhibitors added as described on Appendix A. Drug dilution was prepared using HBSS and L15 (from cells) in a 1:1 ratio and 1μM concentration to mimic membrane potential assay medium conditions and stimulus on desensitisation assay respectively. Remaining cell medium was aspirated and a new one with drugs added then incubated at 37 ^{o}C in air atmosphere for 5 or 30 minutes. Desensitisation assay indicated that these two time points were optimal to produce sub maximum and maximum (plateau) desensitisation. The reaction was stopped by placing plate on ice, washing cells twice with ice-cold PBS and adding ice-cold complete RIPA buffer. After 10 minutes incubation on ice, plates were scrapped and sample transferred to a cold microtube and incubated for additional 2 hours at 4 ^{o}C on a rotating mixer for further cell lysis and protein extraction. Then lysate was centrifuged at 14,000xg for 15 minutes at 4 ^{o}C to separate total protein (supernatant) from cellular debris (pellet), and total protein quantified using Pierce™ BCA Protein Assay Kit according to manufacturer's protocol.

3.6.2 Gel Electrophoresis, Transfer, Blocking and Detection

Proteins 10-30μg[‡] were mixed with LDS loading buffer, reducing agent and water to 10μL, incubated at RT for 10 minutes (GPCR/membrane proteins typically aggregate upon heating) and separated using SDS-polyacrylamide gel electrophoresis . A 10% Bio-rad pre-stained mini gel with 15 wells was used; this enabled visualising the protein without needing dyes such as coomassie blue. Then after loading all samples and marker (Precision Plus Western C or Dual Color), gel was run at 70V for 10 minutes and then 150V using Mini-PROTEAN® System, and gel image was obtained using GelDoc EZ

[†]Initially a T225 were used with 1mL RIPA, then it was scaled down to a T75 with 300μL and last it was scaled down again to a well of a 6-well plate with 50μL.

[‡]30μg of buprenorphine treated samples were loaded per lane as hMOPr S267 phosphorylation very low

System and Image Lab™ software (Bio-Rad).

Proteins were transferred to a mini polyvinylidene difluoride (PVDF) membrane. These membranes have a high binding capacity, are stronger and have better retention of adsorbed protein than nitrocellulose, which enables multiple re-probing of blots. Proteins were tranfered with Trans-Blot® Turbo™ Transfer System following manufacturer's protocol for mixed molecular weight protein (7 minutes).

Blots were rinsed with TBST (see Appendix A for recipe), blocked with blocking buffer (5% skim milk in TBST) for 1 hour at RT to avoid non-specific binding of antibodies, and followed by incubation with primary antibody overnight at 4 ^{o}C. On the next day, blot was washed three times with TBST, incubated with HRP conjugated secondary antibody for 1 hour at RT, followed by three washes and finally detection using Clarity Western ECL substrate (1.5mL for 5 minutes), ChemiDoc™ MP System and Image Lab™ software. Information on antibodies used and dilutions are pesented in Table 3.4, for further details, see AppendixA.

Table 3.4. Antibodies used for Western Blot

Antibody	**Antibody Dilution**	**Dilution Buffer**
Anti-pSer377 MOPr (Rb)	1:1,000	3% BSA in TBST
Anti-HA (Mouse)	1:2,000	5% skim milk
Anti-GAPDH (Rb)	1:2,500	5% skim milk
Anti-mouse HRP	1:5,000	5% skim milk
Anti-rabbit HRP	1:5,000-10,000	5% skim milk

Background was clearer when blocking with 5% skim milk; however, when antibody was diluted in 3%BSA (generally phosphosite-specific antibodies), membrane was rinsed three times before adding primary. When blots were reprobed, primary and secondary antibodies were stripped with ReBlot Plus Strong antibody stripping solution between phospho and total antibodies and stripping efficiency was found to be optimum when incubated for 20 minutes at RT. After stripping, membranes were re-blocked with blocking buffer (5 and 30 minutes) at RT and re-probed. All blot incubations and washes were done on a rocking platform.

AtT20 WT cell extract was used as a negative control (background determination) for MOPr antibodies.

3.6.3 Data Analysis

Images obtained were analysed using volume tools from Image Lab™ software. Area measured for each protein analysed was constant throughout the analysis (Figure 3.14) and global background subtraction method was performed. Analysis table was exported to Microsoft Excel where results were normalised. Phosphoprotein volume (pSer377) was divided by total protein volume (HA), then normalised to value of response of MOPr-WT to DAMGO. GAPDH was used as a loading control.

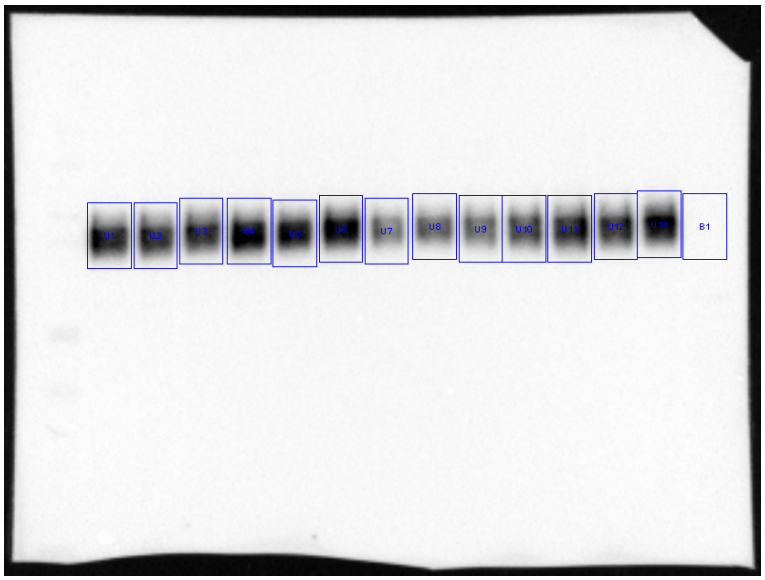

Figure 3.14. Example of blot analysis using Image Lab ™ volume tools. Intensity of band inside each rectangle is measured and background (B1) subtracted from each sample (U1-13). AtT20 cells expressing hMOPr variants samples immunodetected with primary antibody HA-tag and secondary antibody mouse-HRP.

Western blot results were plotted and analysed using GraphPad Prism software. One-sample t-test (hypothetical value = 100) and unpaired t-tests were used to compare mean values obtained from individual experiments, $p<0.05$ was considered significant. Note that each mutant was compared with hMOPr-WT, no comparison between mutants was made.

3.7 Immunocytochemistry

Immunocytochemistry (ICC) is a common molecular biology technique utilising antibodies to localise specific proteins in cells. In this project, the protein of interest was the hMOPr and the antibody used anti-HA, which is highly specific.

3.7.1 Experimental Procedures

Sterile coverslips were coated with poly-D-lysine and placed in 24-well plate, then cells in supplemented L15 were seeded in low confluency and incubated overnight at 37 ^{o}C. On the day of the assay, first part of procedure was the same as per internalisation assay without DAPI (volumes adjusted for 24-well plate). Then, after washing off HA-488-conjugated, procedure was repeated starting with re-fixing and followed by a permeabilisation/blocking step (1%BSA and 0.25% Triton-X-100 in PBS) for 1 hour at RT. Primary HA antibody diluted in 1%BSA/PBST (see Appendix A) was incubated for 1.5 hours at RT. Then three washes with PBST were performed followed by incubation with secondary anti-mouse Alexa Fluor 594 in 1%BSA/PBST for 1 hour at RT. Five washes were performed, excess liquid removed and coverslips placed sample-side down onto one drop of ProLong® Gold reagent with DAPI on a glass slide. After 24 hours curing at RT in the dark, coverslips were sealed with clear nail polish and allowed to dry. Coverslips were cleaned and images obtained using a Leica confocal microscope.

3.7.2 Data Analysis

Images were analysed using Image J 1.47v (National Institute of Health, USA) software and no statistical tests were performed as for the purpose of this experiment only visual comparison was required.

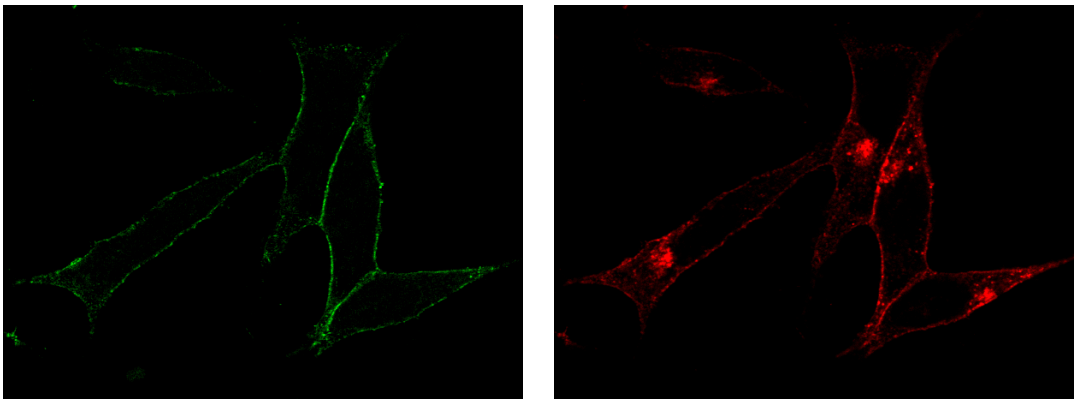

(A) **(B)**

Figure 3.15. Fluorescence confocal images of AtT20 cells expressing hMOPr-WT treated with DAMGO for 30 minutes then fixed and stained according to protocol on Section 3.7. **(A)** Image obtained under a 488nM laser excitation. HA-488 conjugated antibody was used before permeabilisation. **(B)** Image obtained under a 594nM laser excitation. Anti-HA primary and Alexa-594 secondary antibody were used after permeabilisation. Note that fixation did not permeabilise membrane to HA-488 conjugated antibody.

3.8 Quantification of Cell Surface Receptor Assay

In order to complement desensitisation and Western Blot data, cell surface MOPr after morphine and DAMGO treatment was assessed. This is a whole cell enzyme-immunosorbent assay (ELISA), where cells were treated, fixed and immunoprobed for hMOPr on the cells' surface.

It is important to point out that immunocytochemistry experiments indicated that HA antibody did not cross cell membrane after fixation with 4% paraformaldehyde (PFA), therefore only extracellular epitopes were detected (Figure 3.15).

At least three technical and four biological replicates were performed for this assay.

3.8.1 Experimental Procedures

On the day before the assay, AtT20 cells expressing HA-tagged hMOPr were plated according to membrane potential assay protocol with the exception that only ~8-9 x 10^4 cells in 80μL were loaded per well. After overnight incubation, drug dilutions were prepared in HBSS in a 2X concentration, added to plate in a 1:1 ratio, followed by a 5 or 30 minutes incubation at 37 ^{o}C. Then, plate was placed in ice for a couple of minutes,

drug solution removed and 40μL of fixative 4%PFA solution loaded. Fixation was performed on ice for 5 minutes followed by incubation at RT for further 10 minutes before washing three times with ice-cold PBS. Cells were blocked with 31μL of 1% BSA in PBS for 1 hour at RT on a rocking platform, then solution was thoroughly removed and cells incubated in the dark on a rocking platform at RT for 1.5 hours with 31μL of anti-HA-488 conjugated (1:1,000 in blocking solution). Primary antibody was removed and cells counter stained with 5μg/mL of DAPI in PBS for 15 minutes at RT. Last, wells were rinsed five times with PBS, 50μL PBS loaded per well and plate read using PHERAstar FS microplate reader (filters 485,520 and 360,460) and MARS Data Analysis software (BMG Labtech).

Controls for this experiment were:

- AtT20 WT cells (non transfected) with conjugated antibody[†] (Fluorescence negative control)
- AtT20 hMOPr cells without conjugated antibody (Fluorescence negative control, if above not available)
- AtT20 hMOPr cells without conjugated antibody and DAPI. (DAPI Negative Control)

3.8.2 Data Analysis

Data collected was exported to Microsoft Excel and analysed according to protocol supplied by Dr. Natasha Grimsey from Auckland University. First, fluorescence negative control average reading was subtracted from fluorescence data, and the same was calculated using DAPI negative control and DAPI data (Background subtraction). Fluorescence data was then divided by DAPI data to correct for cell number and normalised such that vehicle treatment was 100%.

[†]After many replicates these reading were always similar to AtT20 hMOPr cells without antibody, hence I stopped performing this control.

GraphPad Prism was utilised to generate graphs and perform statistical tests. Significance was assessed in three different ways: with two-way *ANOVA* and unpaired Student *t*-tests, $p<0.05$ was considered significant. Note that each mutant was compared with hMOPr-WT, no comparison between mutants was made.

- To determine if the change in amount of membrane receptors was significant different from baseline, each value obtained was compared to the hypothetical value 0 using one-sample *t*-tests, $p<0.05$ was considered significant.
- To determine if the change in amount of membrane receptors was significant higher than the lowest concentration of the same drug, the higher concentrations values were compared to the lowest concentration for each variant using repeated measures one-way *ANOVA* followed by Student's *t*-test, corrected for multiple comparisons using the Bonferroni method, $p<0.05$ was considered significant.
- To compare results between variant and hMOPr-WT two-way *ANOVA*, corrected for multiple comparisons using the Bonferroni method was used, $p<0.05$ was considered significant.

4

Desensitisation and Kinase Modulators

This chapter describes investigations on μ-opioid receptor (MOPr) desensitisation using FLPR® Membrane Potential Assay (MPA) kit to obtain real-time response of MOPr to opioid agonists (homologous desensitisation) and somatostatin (heterologous desensitisation)[181]. Some of the desensitisation work presented in this chapter has been published (Knapman et al. [2013][181]) and here I only present the experiments I designed and performed. In addition, the role of kinase modulators on morphine and DAMGO induced desensitisation was assessed using this non-invasive assay. Results presented in this chapter were obtained from wild-type mouse MOPr (mMOPr) and human MOPr (hMOPr).

Contents

4.1 Introduction

Desentisation is thought to be one of many complex events related to the development of opioid tolerance; however, it is very important to differentiate both processes. As described on Chapter 2, rapid opioid desensitisation is related to a fast loss of receptor responsiveness after short agonist exposure, while tolerance happens after a longer exposure, which can be only several hours (acute tolerance) to days or weeks[93].

An ideal signalling-dependent cell-based functional assay is accurate and produces comprehensive data. GPCR signalling consists of a series of spatial and temporal events, which start extremely fast after ligand-binding and change with time; therefore it has been a challenge to develop assays that fulfil requirements to capture all the dimensions of this signalling. The majority of published work on MOPr reported desensitisation measured with biochemical assays or electrophysiological techniques[41,211,369]. Many widely used biochemical assays are limited; for example by using purified membranes, many proteins important for receptor regulation may have been washed out; furthermore, these assays generally only analyse few time points, consequently, a large chance of missing important events. Electrophysiology techniques such as patch-clamping, is able to detect rapid changes in cell kinetics however they are

relatively invasive experiments. Experiments in this chapter used a non-invasive technique, yet it is important to point out that the experimental protocol of this assay is somewhat different from recent reported desensitisation experiments, since cells cannot be washed between drug additions; nevertheless non-wash experiments had previously been reported[257]. As described on experimental Section 3.5, rapid opioid desensitisation is measured by comparing response of a saturating opioid concentration with or without stimulus; moreover, to supplement desensitisation data signal decay after opioid exposure was also measured.

It is established that kinases regulate the function of G-protein coupled receptors (GPCR) by phosphorylating intracellular residues and leading to many events, such as β-arrestin recruitment[120] and internalisation[98]. This enzymatic process is receptor specific. G protein receptor kinase (GRK) and second-messenger kinases such as protein kinase C (PKC) constitute the two major kinase families involved in MOPr phosphorylation[118,119,190].

Zhang et al.[369], in 1996, provided some of the first evidence of the involvement of PKC on MOPr desensitisation and phosphorylation, together with the idea that different phosphorylation patterns may contribute to MOPr desensitisation. They reported that activation of PKC was associated with desensitisation of DAMGO-induced MOPr signalling in *Xenopus* oocytes co-expressing cDNAs encoding the MOPr and GIRK1; in addition, they also confirmed an associated increase in hMOPr phosphorylation stably transfected in CHO cells. Since then, there has been lots of interest in PKC-dependent phosphorylation of MOPr and the role of this in modulating opioid tolerance. It is not completely clear whether PKC phosphorylates MOPr directly or indirectly[221], however it is involved in the constitutive phosphorylation of residue Serine 363[163] and also in the heterologous phosphorylation of threonine 370 (Thr370) of the mMOPr[102,116]. Smith et al. (2007)[321] determined that out of all PKC isoforms only α, γ and ϵ appeared to be involved with morphine tolerance in mice. PKCα isoform has been identified as responsible for the selective and dose dependent phosphorylation of Thr370 by activation of PKC by phorbol esters or heterologous activation of substance P receptors[43,163]. In addition, morphine also uses PKCϵ pathway to induce ERK phosphorylation and

MOPr desensitisation[374].

In locus coeruleus (LC) neurons, desensitisation of mMOPr signalling by morphine was increased by phorbol-12-myristate-13-acetate (PMA) which is a PKC activator[21,22]. Moreover, inhibition of PKC by staurosporine reduced phosphorylation and desensitisation of mMOPr induced by morphine but not by DAMGO in HEK-293 cells also expressing G protein-couple inwardly rectifying potassium channel (GIRK)[167]. These studies indicated that morphine desensitisation is dependent on PKC activation but DAMGO is dependent on GRK pathway. This is an area of controversy as in a recent study PMA did not increase morphine induced desensitisation[13].

The purpose of these experiments was to examine rapid MOPr desensitisation and to determine PKC involvement in this process using a real-time kinetic assay in whole AtT20 cells[181]. Homologous desensitisation by DAMGO and morphine, and somatostatin receptor(s) heterologous desensitisation of somatostatin receptor signalling with both opioids were assessed.

4.2 Results

4.2.1 Membrane Potential Assay in AtT20 Expressing μ-Opioid Receptor

In this chapter, DAMGO and morphine induced membrane potential hyperpolarisation was measured using membrane potential assay kit as described on Section 3.5. As shown in Figure 4.1, morphine can rapidly hyperpolarise cells by activating GIRK channels in a concentration-dependent manner. Maximum response was achieved with 300nM and interestingly only the 10nM response rapidly returned to resting membrane potential. Note that each result was obtained from an individual well at the same time, as FlexStation® 3 can read 8 wells every 2 seconds. Therefore, by not using the same cell population to obtain more than one concentration point, we eliminated any possibility of the first concentration of agonist desensitise the response to subsequent concentrations when obtaining concentration response curve measurements.

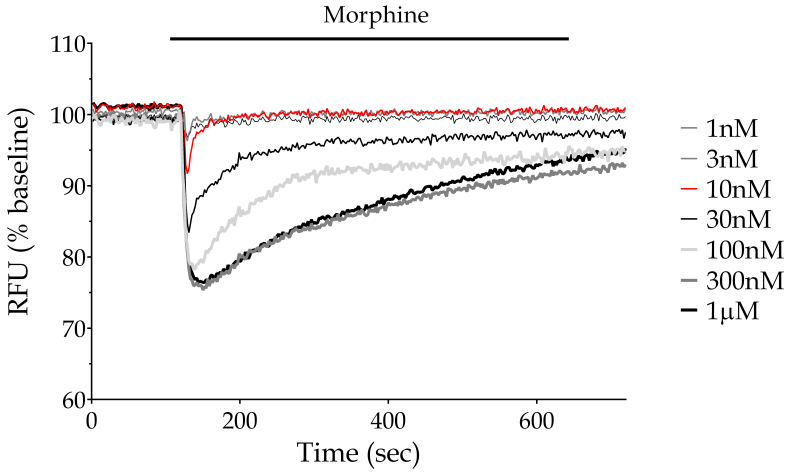

Figure 4.1. Traces of AtT20-mMOPr response to varying morphine concentrations (1nM, 3nM, 10nM, 30nM, 100nM, 300nM and 1μM). Negligible hyperpolarisation observed for the two lower concentrations, while last two concentrations reached maximum hyperpolarisation. Interesting 10nM morphine (red trace) led to a very steep return to resting membrane potential.

The opioid-induced hyperpolarisation was abolished by overnight pre-treatment of the cells with 200ng/mL pertussis toxin, an inhibitor of $G_{i/o}$ protein signalling. The opioid induced hyperpolarisation was also rapidly and completely reversed by the opioid antagonist naloxone (Figure 4.2).

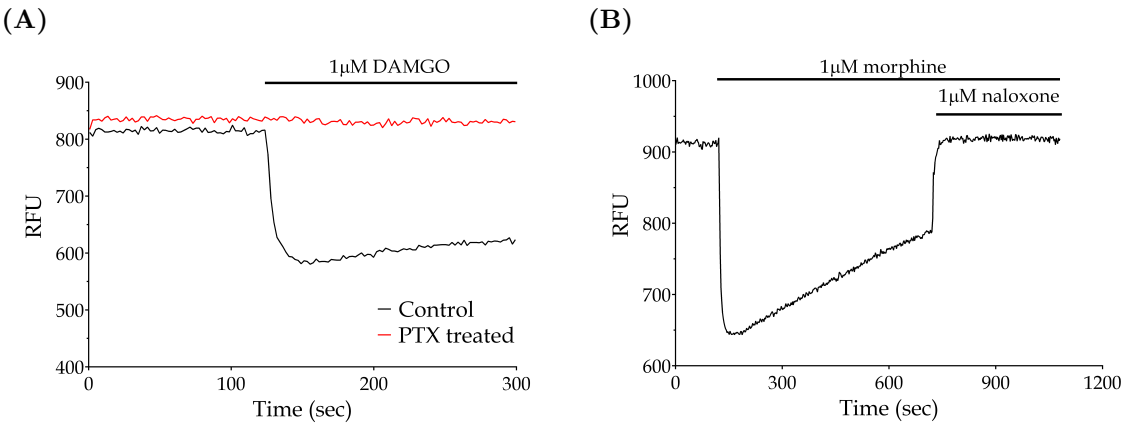

Figure 4.2. (A) Traces of fluorescence signal from AtT20-mMOPr cells exposed to DAMGO after overnight incubation with 200ng/mL pertussis toxin (PTX - red trace) or vehicle (black trace). PTX prevented opioid induced hyperpolarisation **(B)** Trace from AtT20-mMOPr cells illustrating hyperpolarisation after 1μM morphine treatment and fast signal reversal (depolarisation) with opioid antagonist (1μM naloxone).

4.2.2 Desensitisation of μ-Opioid Receptor Signalling in AtT20 Cells

To assess agonist-dependent homologous mMOPr desensitisation, cells were incubated with morphine stimulus (1μM) and then challenged with saturating concentration of 10μM (Figure 4.3**(A)**; see Section 3.5 for experimental details). In a similar manner, to assess heterologous desensitisation, cells were incubated with morphine stimulus (1μM) but on this assay challenged with 1μM somatostatin (SST)(Figure 4.3**(B)**). Desensitisation time-course was determined by challenging at different time points (5, 10, 30 and 40 minutes) and comparing maximum hyperpolarisation obtained. A significant decline in responses were observed over time as shown in Figure 4.4, where the percentage difference between expected response (vehicle stimulus) and obtained response (morphine stimulus) for each time point were plotted and one-phase exponential association function fitted. The maximum homologous desensitisation obtained was 72% (95% confidence interval, [CI] 67-76%) and t$^1/_2$ of 5.7 min ([CI] 4.8-7.0 min). A smaller decline in the somatostatin response was observed (30%; CI, 27-34%) however the t$^1/_2$ was similar (t$^1/_2$ of 5.3 min ([CI] 3.8-8.6 min).

To examine decline in the MOPr signal, one-phase exponential association was fitted to each data collected for 40 minutes after morphine stimulus (before challenge) in AtT20-mMOPr. Signal decay was similar to previously reported in LC neurons[20] with a time constant (τ) of less than 10 minutes (491$\pm$77 sec) and t$^1/_2$ 385$\pm$55 sec ($\pm$SEM, n=5). Interestingly, t$^1/_2$ for signal decay and desensitisation time course are similar.

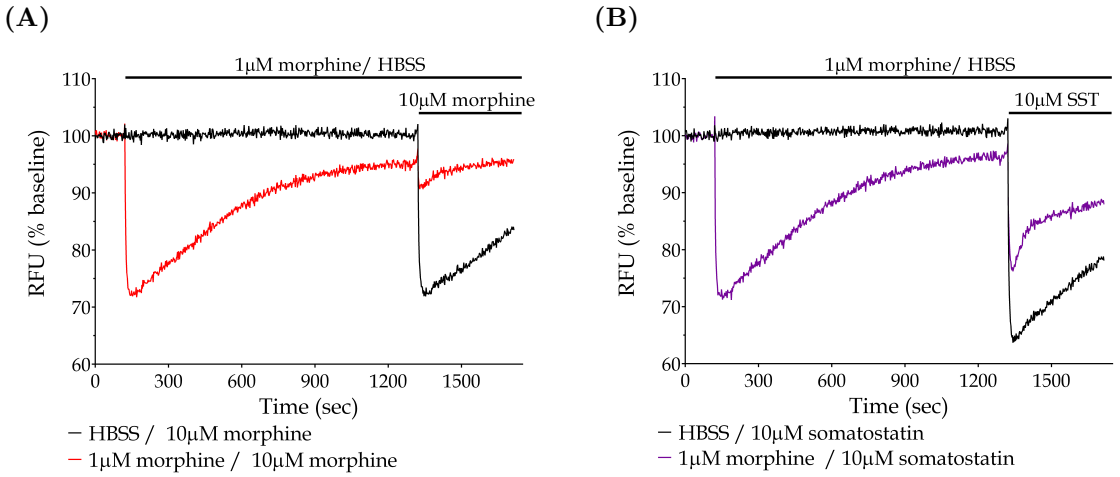

Figure 4.3. Homologous and heterologous mMOP desensitisation in AtT20 cells. Traces showing that a continuous exposure to 1μM morphine reduces the response to a subsequent addition of a high concentration of morphine or somatostatin (SST). **(A)** Example of homologous desensitisation experiment where 10μM morphine challenge was performed 20 minutes after first addition of morphine (grey trace) or vehicle (black trace).**(B)** Example of heterologous desensitisation experiment where 1μM SST challenge was performed 20 minutes after first addition of morphine (grey trace) or vehicle (black trace).

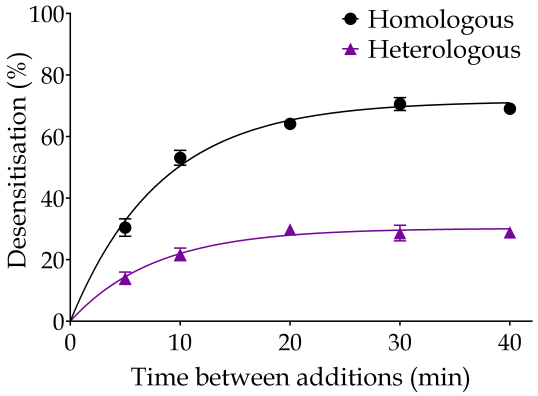

Figure 4.4. Homologous and heterologous desensitisation time course. Exposing the cells to 1μM morphine desensitise not only mMOPr but also somatostatin receptor(s) signal over time. One-phase exponential function fitted, maximum homologous desensitisation 72% and heterologous 30%. Data are expressed as a percentage desensitisation from vehicle control, and represent the mean ±SEM of three to eight determinations, each in duplicate or triplicate.

4.2.3 Preliminary Data: Concentration Response Curve and Desensitisation with PKC Activator

To evaluate the role of PKC in the opioid response, cells were incubated for 10 minutes with phorbol ester phorbol-12-myristate-13-acetate (PMA) to stimulate PKC activation prior to opioid exposure. Figure 4.5 shows traces for one concentration of morphine and DAMGO in one experiment and also for the normalised pooled results for all four biological replicates of one concentration of morphine and DAMGO. Treatment with PMA for 10 minutes prior to opioid exposure did not alter maximum hyperpolarisation for stimulus and rechallenge additions of both opioids, however a slightly increase in the rate of recovery was observed. DMSO was added to HBSS in the same concentration as in PMA solution to eliminate possibility of differences observed being caused by solvent.

Morphine and DAMGO concentration response curves were fitted using first opioid addition maximum hyperpolarisation (Figure 4.6). *ANOVA* analysis found a significant variance between morphine results (p=0.0117), however this is unlikely to have any biological significance. E_{max} and EC_{50} are presented in Table 4.1 showing that efficacy and potency were similar between vehicle and PMA treatments (p value >0.05 for all control versus PMA comparisons, Student's *t*-test).

Table 4.1. Efficacy and potency for morphine and DAMGO in AtT20 cells expressing mMOPr incubated with PMA for 10 minutes.

Opioid	**E_{max}(%)**		**EC_{50}(nM)**	
	Control	PMA	Control	PMA
Morphine	27±2	25±1	29±5	35±7
DAMGO	29±1	29±1	3±7	3±5

n=3-4, ±SEM

To determine concentrations where signal desensitisation was observed, a saturating opioid concentration (10μM) was added after each stimulus concentration. The hyperpolarisation produced by the saturating concentration of drug was plotted against the stimulus concentration of drug (Figure 4.7). Morphine concentrations of less than 10nM

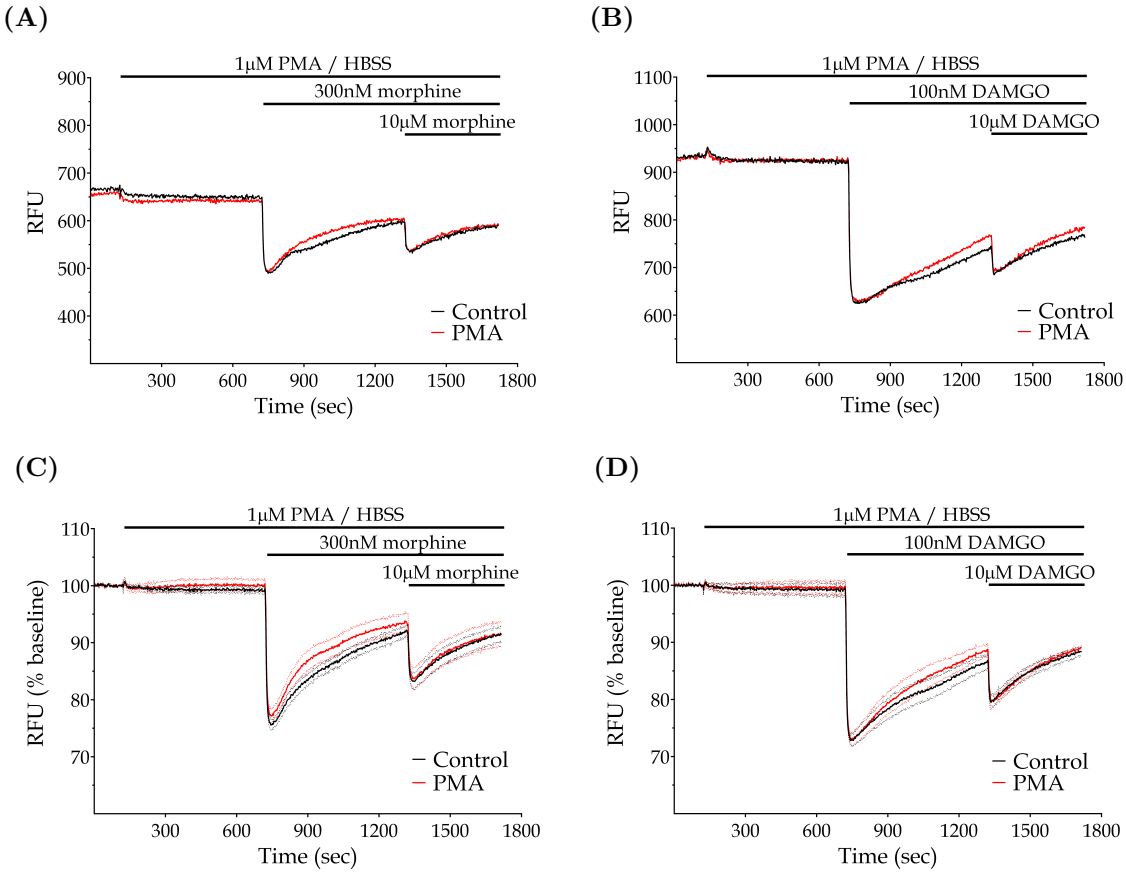

Figure 4.5. Homologous mMOPr desensitisation after opioid stimulus and rechallenge (10μM) in AtT20 cells pre-incubated for 10 minutes with HBSS (black trace) or 1μM PMA (red trace). **(A)** Traces show fluorescence recorded from populations of AtT20 cells during application of morphine stimulus (300nM) and saturating concentration (10uM).**(B)** Traces show fluorescence recorded from populations of AtT20 cells during application of DAMGO stimulus (100nM) and saturating concentration (10uM). **(C)** and **(D)** Average reading of four biological replicates normalised to baseline clearly shows receptor signalling desensitisation induced by morphine and DAMGO respectively (SEM - faint line).

and DAMGO of less than 3nM produced no desensitisation, as concentration of stimulus increased there was a concentration dependent reduction in the response to the challenge concentration. No significant difference between PMA or vehicle treatment was found with morphine (two-way *ANOVA*, p=0.15), however DAMGO curves were slightly different (two-way *ANOVA*, p=0.005) which is unlikely to have any biological relevance. Note that 10nM morphine, 1nM and 3nM DAMGO caused hyperpolarisation but no desensitisation.

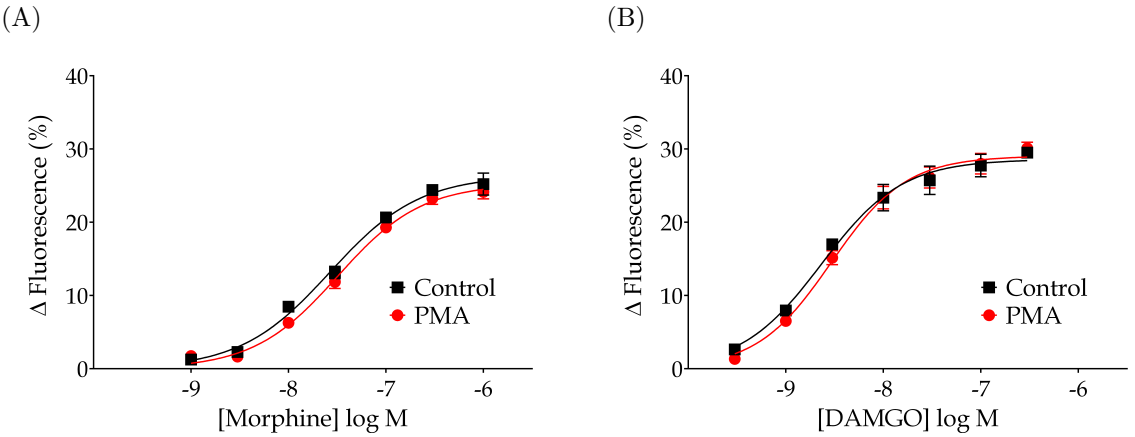

Figure 4.6. Concentration response curve after incubation for 10 minutes with 1μM PMA or HBSS (control) in AtT20 cells expressing mMOPr-WT. **(A)** Response to morphine stimulus at varying concentrations **(B)** Response to DAMGO stimulus at varying concentrations. Note that morphine potency and efficacy is lower than DAMGO. Data represent the mean ± SEM of pooled data from 3-4 independent determinations performed in triplicate.

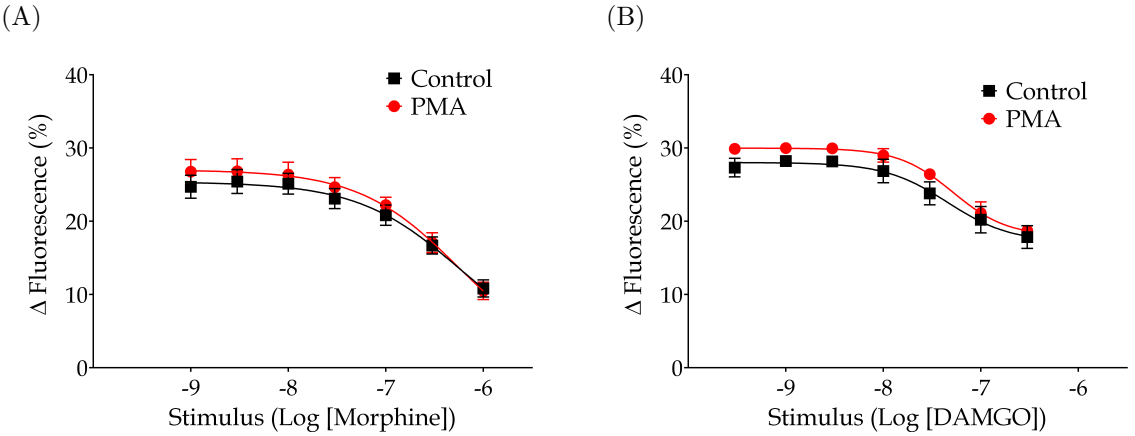

Figure 4.7. Response to saturating concentration (10μM) of opioids after stimulus with or without incubation for 10 minutes with 1μM PMA in AtT20 cells expressing mMOPr-WT. **(A)** Morphine treatment. **(B)** DAMGO treatment. Data represent the mean ± SEM of pooled data from 3-4 independent determinations performed in triplicate.

The rate of signal decay after first opioid exposure was apparently faster when pre-incubated with 1μM PMA than with vehicle (HBSS)(Figure 4.5). To analyse this, a one-phase association was fitted to the recovery data and recovery time constant (τ) obtained for concentrations with a higher than 5% RFU (% baseline) signal (Table 4.2). No statistical significance was found between control and PMA recovery time

constant for both opioids when each point was analysed using Student t-test (p>0.05). However if a concentration response curve was produced using time constant values, it became clear that PMA treated cells had a significant faster recovery rate when exposed to higher morphine concentrations (Figure 4.8(A), two-way *ANOVA*, p=0.0055, n=4), while DAMGO recovery was similar (Figure 4.8(B), two-way *ANOVA*, p=0.48, n=2-3).

Table 4.2. Recovery time constant (τ) for PMA or vehicle treated after morphine or DAMGO exposure.

[Opioid]	Morphine		DAMGO	
	Control (sec)	PMA (sec)	Control (sec)	PMA (sec)
3nM	*	*	49±8	49±6
10nM	26±2	20±6	145±37	109±32
30nM	44±12	45±11	322±133	275±96
100nM	117±20 (4)	93±21	606±189	498±138
300nM	321±33	225±41	786±99	767±52
1μM	481±64	320±36		

* Signal lower than 5% RFU (% baseline). Data expressed as τ ± SEM (n=4)

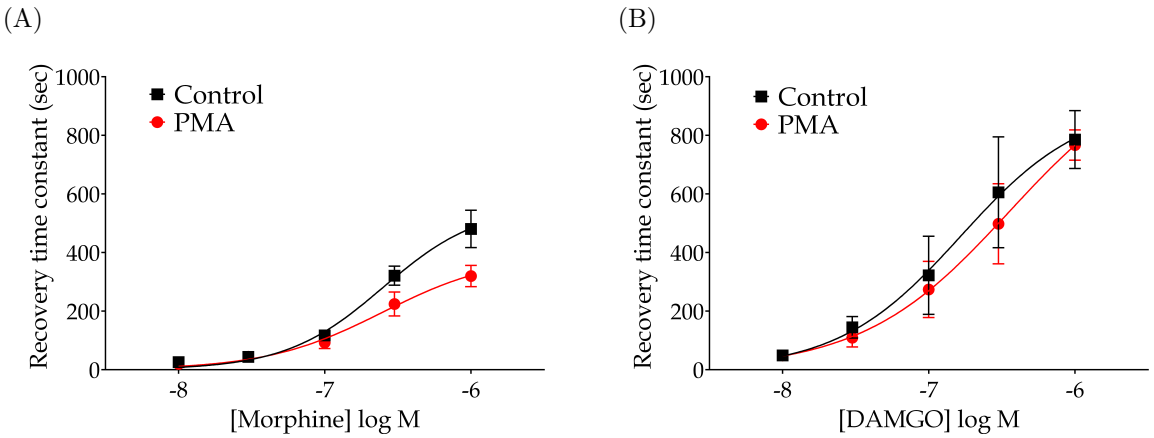

Figure 4.8. Recovery time constant (τ) concentration response curve after incubation for 10 minutes with 1μM PMA or HBSS (control) in AtT20 cells expressing mMOPr-WT. Recovery time constant to **(A)** morphine and **(B)** DAMGO stimulus at varying concentrations. Data represent the mean ± SEM, n=4.

4.2.4 Opioid-mediated Desensitisation and PKC Activator

The effects of PMA on homologous and heterologous desensitisation of MOPr signalling were assessed in AtT20 expressing mMOPr or hMOPr. Based on results above a stimulus concentration of 100nM DAMGO and 300nM morphine was chosen for use with PMA because these concentrations had recovery time constant of approximately five minutes.

Figure 4.9 shows traces of morphine and DAMGO induced homologous and heterologous desensitisation in AtT20-mMOPr. Signal decay after morphine pick hyperpolarisation was slightly faster with PMA incubation (τ of 169±13 sec) compared with control (τ of 282±36 sec; n=8, t-test p=0.0115). Even though visually DAMGO recovery also appeared somewhat faster, recovery time constant variance was not statistically significant (480±70 sec [control]; 369±53 sec [PMA]; t-test p=0.2286, n=7).

AtT20-hMOPr when preincubated with PMA and then exposed to morphine presented a faster recovery than control (τ of 265±61 sec [control]; 121±10 sec [PMA]; t-test p=0.0487; n=5), differently from DAMGO whose signal decay was similar between treatments (897±110 sec [control]; 590±194 sec [PMA]; t-test p=0.2081; n=5).

Homologous and heterologous desensitisation (± SEM, n=4-9) in AtT20 expressing mouse or human MOPr is summarised in Figure 4.10. Morphine and DAMGO induced homologous desensitisation was similar for mouse and human MOPr (t-test,p>0.05). Heterologous desensitisation caused by DAMGO was greater than produced by morphine (mMOPr t-test, p=0.0007). There was no difference between vehicle or PMA treated results for all conditions tested (t-test, p>0.05).

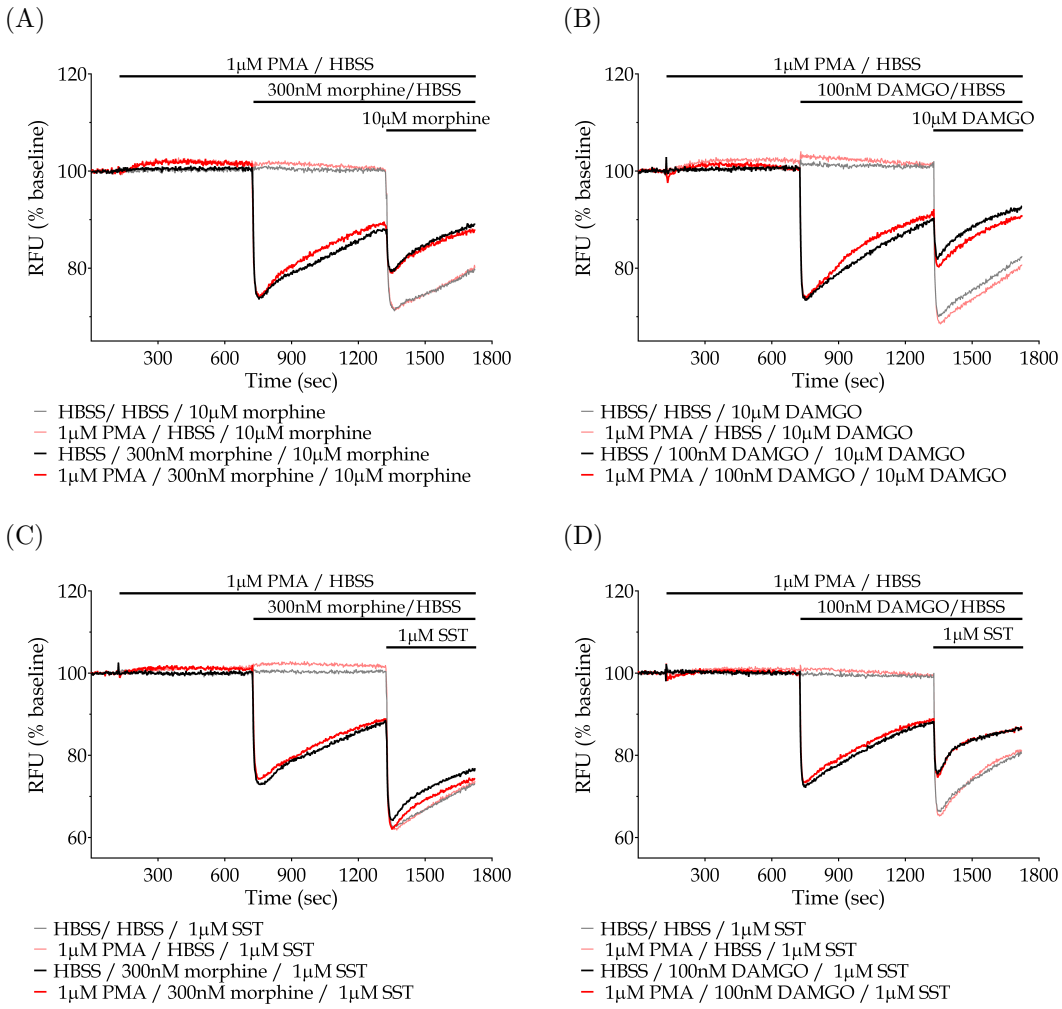

Figure 4.9. Representative traces of homologous and heterologous desensitisation after PKC activation. AtT20-mMOPr were incubated for 10 minutes with 1μM PMA before exposure to opioid for another 10 minutes before challenged with opioid (10μM) or somatostatin (1μM). **(A)** Morphine-induced homologous desensitisation. **(B)**DAMGO-induced homologous desensitisation. **(C)** Morphine-induced heterologous desensitisation. **(D)** DAMGO-induced heterologous desensitisation.

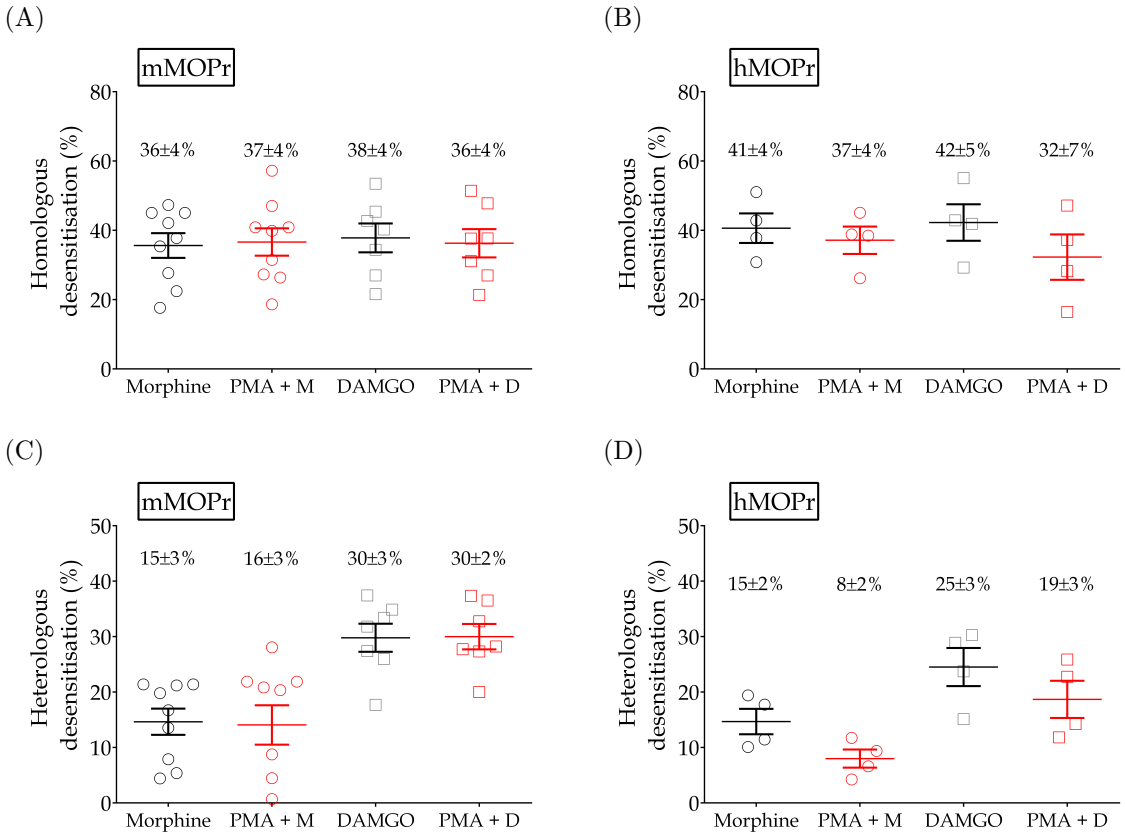

Figure 4.10. Modulation of PKC activity by PMA on homologous and heterologous desensitisation. Pre-treatment of cells expressing mMOPr or hMOPr with 1μM PMA did not significantly affect desensitisation by morphine (M) or DAMGO (D) (t-test, p>0.05). **(A)** Homologous desensitisation in AtT20-mMOPr. **(B)** Homologous desensitisation in AtT20-hMOPr. **(C)** Heterologous desensitisation in AtT20-mMOPr. **(D)** Homologous desensitisation in AtT20-mMOPr. Data represent the mean ±SEM, n=4-9.

4.2.5 Opioid Desensitisation and Staurosporine

To further study the role of PKC on MOPr desensitisation, the effect of staurosporine, a kinase inhibitor, was assessed using the same protocol as per PKC activation.

Figures 4.11(A) and 4.11(B) show representative traces of homologous desensitisation induced by morphine and DAMGO. Because staurosporine by itself inconsistently produced an apparent membrane hyperpolarisation, the response to opioids in the presence of staurosporine could appear to be slightly greater.

Recovery rate with morphine and DAMGO was not influenced by staurosporine treatment. In AtT20 expressing mMOPr, signal decay after 300nM morphine exposure was not different when cells preincubated with PMA or vehicle (291±59 sec [control], 244±43 sec [staurosporine]; t-test p=0.5351, n=6), the same was observed with 100nM DAMGO (451±100 sec [control], 406±120 sec [staurosporine]; t-test p=0.7803, n=5). In agreement with above data, activating PKC in AtT20 cells expressing hMOPr did not affect morphine (265±61 sec [control]; 181±42 sec [staurosporine]; *t*-test p=0.2926, n=5) or DAMGO (831±92 sec [control]; 500±122 sec [staurosporine]; *t*-test p=0.0624, n=5) decline in the hMOPr signalling.

Morphine and DAMGO induced homologous desensitisation are presented in Figure 4.11(C) and 4.11(D) respectively. Desensitisation induced by DAMGO and morphine in both mouse and human expressing cells was not different in the presence of staurosporine (*t*-test, p>0.05). Furthermore, heterologous desensitisation induced by morphine or DAMGO in AtT20-hMOPr was not affected by staurosporine (Figure 4.12, *t*-test, p>0.05).

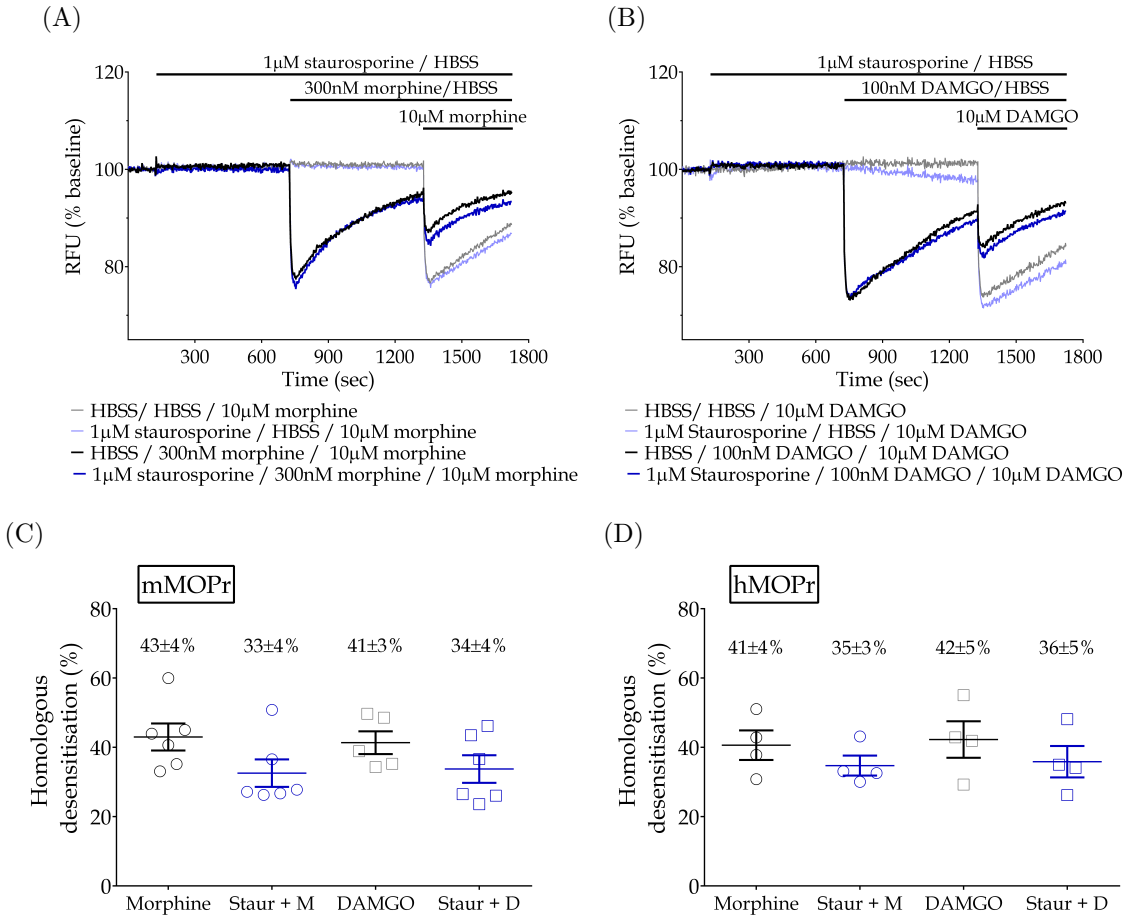

Figure 4.11. Effect of kinase modulation by staurosporine on homologous desensitisation. AtT20-MOPr cells were incubated for 10 minutes with 1μM staurosporine before exposure to opioid for another 10 minutes and then challenged with opioid (10μM). **(A)** Representative traces of morphine-induced homologous desensitisation in AtT20-mMOPr. **(B)** Representative traces of DAMGO-induced homologous desensitisation in AtT20-mMOPr. Note that staurosporine slightly increased opioid hyperpolarisation; however a decrease in signal with staurosporine alone was also observed. **(C)** Homologous desensitisation in AtT20-mMOPr. **(D)** Homologous desensitisation in AtT20-hMOPr. No statistical significant difference between vehicle (black) and staurosporine (blue) treated cells results were found (t-test, p>0.05). (C) and (D) data represent the mean ±SEM, n=4-6.

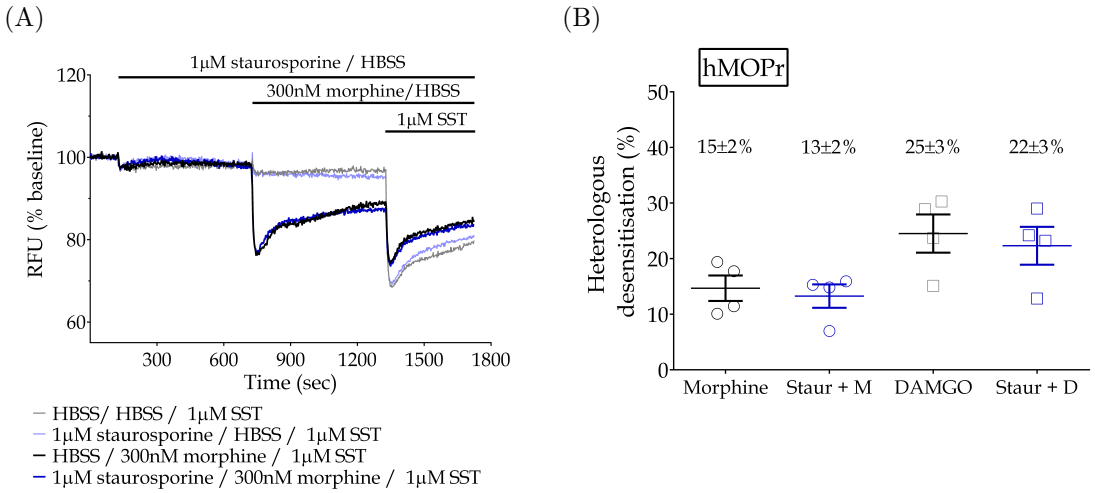

Figure 4.12. Modulation of kinase activity by staurosporine on heterologous desensitisation. AtT20-hMOPr cells were incubated for 10 minutes with 1μM staurosporine before exposure to opioid for another 10 minutes anf then challenged with 1μM somatostatin (SST). **(A)** Representative traces of morphine-induced heterologous desensitisation in AtT20-hMOPr. **(B)** Heterologous desensitisation in AtT20-hMOPr. Staurosporine treatment did not affect heterologous desensitisation (t-test, p>0.05). Data represent the mean ±SEM, n=4.

4.2.6 Kinase Modulators and Membrane Potential Signal

PMA and staurosporine caused an unpredictable decrease in fluorescence in some experiments. This hyperpolarisation was slow and continuous, and evident after 10 minutes incubation. Figure 4.13 shows two experiments were a pronounced drop in fluorescence was observed after 20 minutes incubation with 1μM PMA (8 %) and 1μM staurosporine (5 %). At 10 minutes, opioid maximum response was similar between vehicle and PMA or staurosporine treated; in contrast, at 20 minutes hyperpolarisation recorded was higher when cells were exposed to kinase modulators; remarkably, a decrease in fluorescence signal at 20 minutes was also recorded with cells incubated with PMA and staurosporine but vehicle treated. Because this change in membrane potential caused by the kinase modulators tested was inconsistent even across same day experiments, normalisation was not used.

To distinguish if these effects were influenced by the expression of MOPr, PMA and staurosporine response was assessed in AtT20 WT cells (Figure 4.14). PMA and staurosporine produce a decline in fluorescence during prolonged incubation, which is

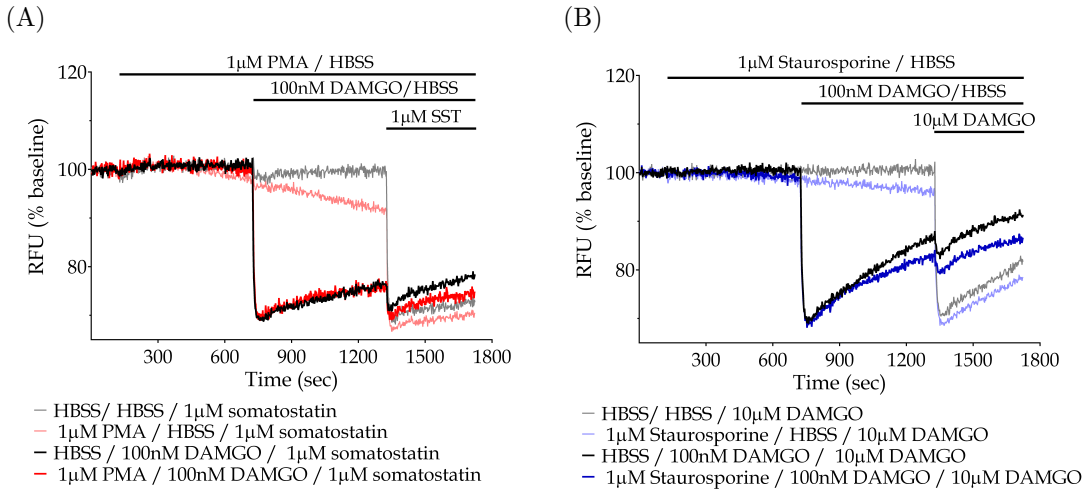

Figure 4.13. Traces showing examples of assays in AtT20 expressing hMOPr where incubation with PMA and staurosporine caused a large signal decrease. **(A)** Heterologous desensitisation with 100nM DAMGO stimulus and 1μM somatostatin (SST) challenge, incubated with vehicle (black traces) or PMA (red traces). Fluorescence decreased with PMA by itself. **(B)** DAMGO induced Homologous desensitisation incubated with vehicle (black traces) or 1μM staurosporine (blue traces). Fluorescence also decreased with staurosporine by itself.

independent of MOPr expression. To minimise this interference, pre-incubations with these drugs were limited to 10 minutes.

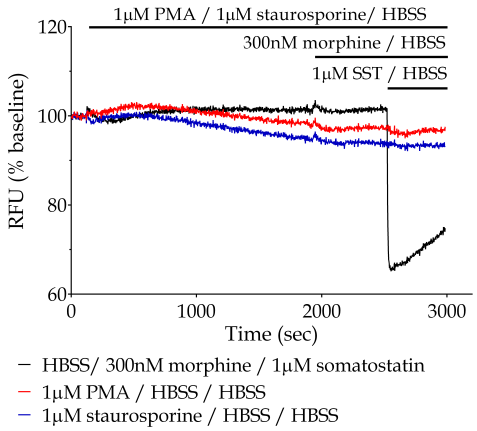

Figure 4.14. Example traces of AtT20 WT cells response to PMA (red trace) and staurosporine (blue trace) incubated for 48 minutes. Fluorescence readings decreased during incubation with both kinase modulators, however only PMA had a small increase immediately after exposure. Somatostatin and morphine was used as a positive and negative control respectively (black trace).

4.3 Discussion

Desensitisation of MOPr signalling has been assessed using many different techniques, but few can achieve a great temporal resolution. This study provides a novel non-invasive way of measuring real-time opioid induced desensitisation of GIRK channel signalling. By stimulating the AtT20 cells expressing MOPr with morphine or DAMGO, a fast membrane potential hyperpolarisation followed by decay (depolarisation) was observed. We measured the decrease of response by determining decay rate constant (τ), and desensitisation by challenging cells with a saturating opioid concentration after stimulus. Somatostatin receptor(s) heterologous desensitisation could also be studied by challenging cells with a high concentration of SST instead of opioid.

In a work published by our group, Knapman et al.[181] demonstrated a good correlation between the results for efficacy and potency of many opioid agonists using this proprietary membrane potential dye when compared to previous studies of GIRK activation in AtT20 cells and native neurons[70,164]. Not mentioned in our publication but showed here, morphine 10nM hyperpolarisation signal was relatively different from other concentrations as it has a very fast recovery to membrane potential resting state. RGS proteins are involved in negative regulation of GPCRs including MOPr[127,340]; they could be involved in this fast recovery, as they accelerate the intrinsic GTPase activity of G_α leading to heterotrimeric complex re-association. Atwood et al.[15] have revealed by mRNA microarray analysis that AtT20 cells express statistically significant levels of RGS14, 20 and Snx13; where RGS20 (RGSZ1) and a family member of RGS14 have already been reported to interact with the MOPr[128,360]. Further research is needed to confirm this involvement and assess if there are any correlation between the above finding, RGS proteins and desensitisation, as 10nM did not cause hMOPr signal desensitisation.

In this study, using the continuous membrane potential dye assay, a time dependent homologous and heterologous rapid desensitisation induced by morphine was examined, with maximum desensitisation of 72% and 30% respectively. This difference confirms that homologous desensitisation was not only caused by GIRK channel desensitisation

as heterologous desensitisation of SST receptor(s) signal was much lower, indicating that GIRKs are still available to signal but are not being activated by opioid receptor G proteins $\beta\gamma$ subunits. Pertussis toxin completely abolished opioid signalling in this assay, indicating the involvement of $G_{i/o}$ proteins.

In these AtT20-MOPr cells used, morphine has a lower maximal effect than DAMGO which suggests a relatively low receptor density. This is important as receptor reserve can interfere with desensitisation readings as previously shown[79].

This new assay is well suited to measure signal decay after opioid exposure, since continuous kinetic signal is detected before and after expected receptor endocytosis, and even through receptor resensitisation and recycling. Recovery $t^1/_2$ of 385±55 sec measured after morphine exposure is consistent with previously reported for LC neurons[20]. However, maximum desensitisation was equivalent to DAMGO, which is higher than reported in the same study for morphine but similar to a report in HEK293 expressing MOPr[167]. The similarities between signal decay and desensitisation time course, in addition to the partial exclusion of GIRK channel desensitisation, supports the possibility that the majority, if not all, of the changes in membrane potential observed are related to MOPr desensitisation.

Morphine induced rapid desensitisation has been the focus of much controversy. Johnson et al. (2006)[167] reported 73±6% desensitisation to morphine measured by patch clamp in transfected HEK293 cells, which is equivalent to the work presented here. Moreover, in another study using AtT20 cells, morphine produced rapid desensitisation of the inhibition of voltage-dependent calcium channel current (I_{Ca})[41]. These findings contradict many reports from LC neurons[20] and HEK293 cells[353] where little to none rapid desensitisation was produced by morphine. Note that LC neurons were previously reported to have MOPr reserve[79,294]. Furthermore, a recent study analysed desensitisation in the mouse ventral tegmental area and found that morphine did not desensitise nerve terminal MOPr[214]. Interestingly, morphine-induced rapid desensitisation can be observed in LC neurons[21] and in nerve terminals of the ventral tegmental area[214] only if PKC is activated by a heterologous source, such as another receptor or phorbol esters. PKC activation was assessed in AtT20-MOPr cells where

incubation for ten minutes with PMA did not increase homologous desensitisation. In contrast, rate of signal decay with 300nM and 1μM morphine was faster in both mouse and human MOPr transfected cells with PMA. This is an interesting finding as some studies have reported desensitisation by measuring signal decay[13,20,21]. However, at least in the assay here assessed, this does not represent a good MOPr desensitisation measure in the presence of PMA and staurosporine, because both kinase modulators tested in this project changed membrane potential independently of MOPr expression, and if samples were incubated with PMA for longer than 10 minutes this could considerably influence results. It is possible that the short incubation with PMA is responsible for the variance in desensitisation results when compared to other studies; nevertheless, PMA can phosphorylate mMOPr Thr370 residue to a reasonable extent in 10 minutes[163]. To complement all arguments mentioned above, a recent study by Arttamangkul et al. (2015)[13] reported that two ways of measuring desensitisation can result in different findings, in addition to proposing that known PKC-activators may interfere with measurements of opioid induced hyperpolarisation through mechanisms that may be unrelated to PKC activation.

DAMGO induced desensitisation has not been shown to be influenced by PKC activators as this agonist is linked to GRK not PKC activity[23,167]. This high efficacy agonist did induce a similar hMOPr signalling desensitisation via GIRK to morphine in both mouse and human MOPr, and PKC modulation by PMA did not affect desensitisation and signal decay results.

AtT20 cells natively express four of five known somatostatin receptors[15,265] which, like MOPr, are GPCRs coupled to inhibitory G proteins. In this project, this knowledge was used to analyse signal 'interference' between somatostatin and μ-opioid receptors as they use similar transduction pathways and are phosphorylated by PKC and GRKs[312]. The ability of somatostatin receptor(s) to signal through GIRK after DAMGO and morphine stimulus was examined. Heterologous desensitisation was detected for both agonists, where DAMGO had a higher impact than morphine. Pfeiffer et al. (2002)[272] reported the formation of heterodimers between MOPr and SST_{2A} receptor when co-expressed in HEK293 cells. They demonstrated that cross-phosphorylation caused by

DAMGO treatment to the SST_{2A} receptor may be responsible for heterologous desensitisation of ERK and adenylyl cyclase signalling, however SST_{2A} receptor was not co-internalised by DAMGO. MOPr is phosphorylated by GRK2, GRK3 and GRK5 and a clear difference between GRKs recruitment and agonist used exists; higher efficacy opioids recruit GRK2/3 while lower efficacy recruit GRK5[103,134,171]. Interestingly, phosphorylation of SST_{2A} receptor by 1μM SST-14 is also related to GRK3/4 but not GRK5[274]. Therefore, in agreement with Pfeiffer et al. (2002)[272] where a cross-phosphorylation is probably caused by GRKs, it is possible that recruitment of GRK2/3 by DAMGO is probably the responsible for the difference observed between DAMGO and morphine induced heterologous desensitisation. The mechanisms involving heterologous desensitisation still need to be better elucidated.

Raveh et al. (2010)[286] added an interesting possibility to this complex desensitisation mechanism, they reported that by stimulus-specific and phosphorylation independent GRK2 can sequestrate $\beta\gamma$ subunits away from GIRK channels in HEK293 cells. This could be involved in heterologous desensitisation, and also explain the different between DAMGO and morphine as GRK phosphorylation role is more prominent with DAMGO. However, it does not clarify homologous desensitisation as the ability of morphine and DAMGO to induce desensitisation is relatively similar.

Modulation of PKC activity by PMA on heterologous desensitisation was also examined and activating PKC did not change results when compared with control. SST_{2A} receptor can undergo heterologous PKC mediated phosphorylation in CHO-KI cells[207], but if this phosphorylation also happens in AtT20 cells it did not change GIRK signal heterologous desensitisation profile.

In another part of this study, MOPr signalling desensitisation was assessed in the presence of staurosporine, a promiscuous kinase inhibitor which at a 1μM concentration inhibits many kinases[174]. Signal decay (τ) in addition to homologous and heterologous desensitisation induced by morphine or DAMGO did not vary between vehicle and staurosporine treated AtT20-MOPr cells. This is another area of controversy as in HEK293-MOPr cells staurosporine reduced desensitisation by morphine but

not DAMGO[167], while in LC neurons, it did not change met-enkephalin desensitisation response but increased rate of recovery[12]. It is intriguing that inhibition of a large number of kinases does not affect desensitisation, and raise the question if phosphorylation does really play a role in desensitisation; nevertheless, staurosporine does not inhibit many GRKs.

To support the finding using staurosporine and PMA in this chapter, the activity of these kinase modulators was confirmed as shown in Appendix D.

In the face of so many variant findings it is clear that not only we are looking at a very complex mechanism that can be deeply influenced by the way data is collected and analysed, but also cell-type examined. PKC activity is abnormal in a number of different cancers[172], therefore it can be expected that AtT20, an adenoma pituitary cell line, presents a different PKC activity to native cells (LC neurons) or non-tumour cell lines (HEK293). PKCα mutations in pituitary adenomas have been reported; for instance, one study examined the human D294G mutation which caused a loss-of-function by preventing PKC to efficiently bind to cellular membrane[377]. Therefore, we could speculate that a mutation of native proteins could lead to higher basal PKC activity, explaining why morphine induced desensitisation is higher in AtT20-MOPr cells without the need to activate PKC. Basal level of Thr370 phosphorylation in AtT20 cells was investigated, but unfortunately this antibody did not work even for positive controls. Another possible explanation are the differences in proteins expression between cell types; not only MOPr levels could be different but also PKC subtypes and even G protein subtypes. A report of AtT20 and HEK293 cells mRNA microarray analysis[15] showed a relevant difference in PKC subtypes, and more importantly AtT20 only had statistically significant mRNA levels for one subtype(G_{i2}) of the 5 G proteins (G_{o1}, G_{o2},G_{i2} , G_{i3}, G_z) that MOPr preferentially stimulates[75].

In conclusion, comparing MOPr desensitisation results in different cell types which have been measured and analysed in various ways is a complicated task. Nevertheless, an assay was developed with good temporal resolution and similar results to the ones previously reported for this cell type. More importantly, it will enable a good and uncomplicated comparison between various human MOPr desensitisation expressed in

AtT20 FlpIn cells, which is the main objective of this project.

5

Regulation of N-terminal SNPs of hMOPr

This chapter focuses on the study of two high prevalence N-terminal human μ-opioid receptor (hMOPr) single nucleotide polymorphisms (SNPs), known as A6V and N40D. This study was started in CHO-KI cells by Dr. Alisa Knapman and continued by myself in AtT20 cells. In addition to some results that have already been published (Knapman et al. [2014,2015][182,183]), desensitisation, phosphorylation and surface receptor loss are presented here.

Contents

5.1 Introduction

A large number of studies have shown the effect of inherited genetic variation in drug response. Mutations that can interfere with some opioids pharmacokinetics have long been identified[100,269,304], though the question remains whether hMOPr SNPs play a role in patient response variance. This study assessed molecular mechanisms of A6V and N40D variants which are common N-terminal SNPs of the hMOPr (Figure 5.1).

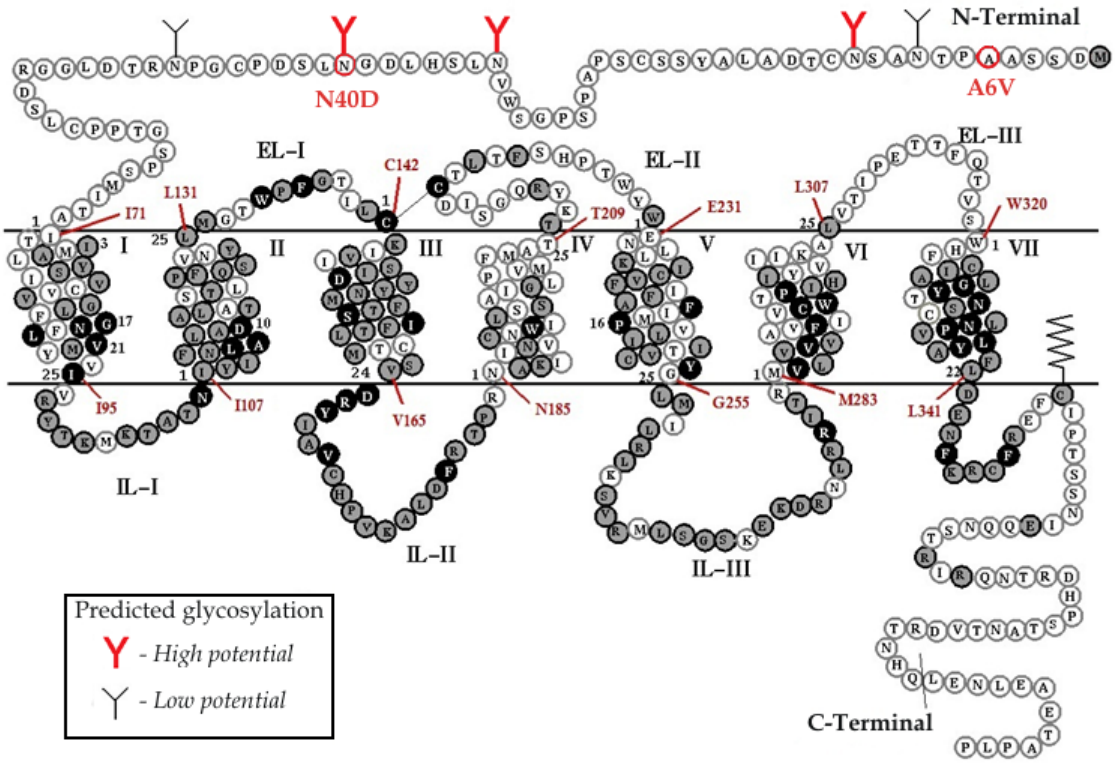

Figure 5.1. Serpentine structure and amino acid sequence of the human μ-opioid receptor wild-type. N-terminal amino acids altered by SNPs A6V and N40D are highlighted in red. Note that N40D polymorphism deletes predicted glycosylation.

The most studied polymorphism of the OPRM1 gene is A118G, which results in an asparagine to aspartic acid substitution (N40D), therefore a loss of a predicted glycosylation site. N40D allele variant has a low frequency in sub-Saharan Africans (0.8%) and African Americans (2.2%) but a high frequency among Caucasians (11-17%) and Asians (27-48%)[248]. C17T is another exon 1 polymorphism resulting in an amino acid change from alanine to valine (A6V). A6V variant has an allelic frequency distribution somewhat inverse to N40D as it is common in African-American and northern Indian populations (up to 20%) but is rare in Caucasian and east Asian populations (less than 1%)[88,180,335]. Both SNPs are frequent enough to be clinically interesting and they have been implicated in drug abuse[180]; therefore, becoming extremely interesting candidates for functional studies.

The clinical significance of the A6V polymorphism is still not well understood as only a small number of reports have investigated this variant, and most of them had insufficient statistical power to reach a reliable conclusion. A recent large study reported a higher use of cocaine, alcohol and tobacco in HIV positive African American women with the polymorphic homozygous genotype (T:T), but no difference with the heterozygous genotype (C:T)[90]. An intriguing finding was that opioid use was not statistically different between the genotypes; however, the prevalence of opioid abuse was low in the study cohort, thereby making it impossible to detect subtle effects of the A6V polymorphism[90]. Regarding MOPr-A6V signalling *in vitro*, only three studies have assessed this polymorphism; one of these few studies was performed by our group, and a part of the work presented in this chapter was published (Knapman et al. [2015][183]). A study in HEK293 cells expressing A6V polymorphism in a MOPr splice variant backbone (MOR1A-A6V) showed unchanged morphine and DAMGO induced internalization, however a higher DAMGO efficacy, but not morphine, measured by calcium influx; when compared to receptor with same backbone but without point mutation[287]. A later report examined DAMGO, endomorphin-1 and Leu-enkephalin mediated inhibition of forskolin-induced change in cAMP-dependent gene transcription (CRE-luciferase assay) in HEK-cells transiently expressing hMOPr-WT and hMOPr-A6V, and found similar potency and efficacy between both variants for all opioids

tested[125]. In CHO-KI cells expressing hMOPr-A6V, Knapman et al. (2015)[183] reported a decrease in opioid-mediated ERK1/2 phosphorylation, in addition to a significant reduction in adenylyl cyclase (AC) inhibition by DAMGO, morphine and β-endorphin; interestingly, only buprenorphine out of the 11 opioids tested had its ability to signal in both pathways abolished.

In contrast to A6V, a large number of clinical studies have analysed N40D polymorphism; however, no definitive functional consequences for this mutation has been ascertained. Previous reports showed an association of N40D polymorphism with pain sensitivity, drug addiction and social behaviour[180,248]. A reduced response to opioids is the most frequent finding of studies on this polymorphism, however no effect and a higher response have also been reported[248]. Many studies had investigated the correlation between N40D and drugs of abuse as alcohol and opioids, and once again contradictory data have been reported regarding use, dependence and dependence treatment (mainly with opioid antagonist naltrexone)[168,179,180,300]. Troisi et al. (2011)[343] for the first time reported a study in humans where N40D polymorphism was associated to social hedonic capacity and this result has been recently reproduced in a mouse model[45].

Furthermore, molecular studies of N40D polymorphism consequences have investigated regulation of receptor expression and signalling. A decrease in receptor number on cell surface was previously reported by some studies[156,373], and this could be linked to the loss of N-glycosylation site and/or introduction of a methylation to the gene[253]. Nevertheless, other studies did not find any difference in receptor expression in Neuro 2A cells[96] and CHO-KI cells[182]. Bond et al. (1998)[38] was the first to study signalling profile in this variant. They reported that out of many opioid agonists and one antagonist tested, only β-endorphin presented a significantly higher binding affinity in AV-12 cells stably transfected with wild-type or N40D hMOPr. Moreover ability to signal via GIRK channels was measured by electrophysiology in *Xenopus* oocytes transiently injected with variants mRNAs, and again only β-endorphin efficacy varied, being threefold higher in N40D compared with WT variant. Unfortunately, this result could not be reproduced by later studies[31,183,189] and many conflicting results for opioids efficacy and

potency in different pathways have been reported. Interestingly, we demonstrated that buprenorphine, an opioid rarely assessed but clinically important, has compromised signalling in three different pathways, inhibition of AC, phosphorylation of ERK1/2 and GIRK activation (GIRK work reproduced in this chapter)[182]. Beyer et al. (2004)[31] reported internalisation profile of N40D to be indistinguishable from that observed for WT hMOPr[31] and they also found similar cAMP inhibition desensitisation time course induced by morphine, morphine-6-glucoronide or β-endorphin in HEK293 expressing WT and N40D hMOPr.

Investigation on A6V and N40D hMOPr polymorphisms stably transfected in AtT20 cells is presented in this chapter. In addition to published work in efficacy and potency to opioids; desensitisation, receptor phosphorylation and loss of receptor surface were examined in cells with similar receptor expression. To the best of my knowledge this is the first report of hMOPr serine 377 (Ser377) residue phosphorylation, and desensitisation of GIRK pathway in both N-terminal variants.

5.2 Results

5.2.1 Human MOPr Expression in AtT20 Cells

hMOPr-WT, A6V and N40D were stably transfected in AtT20 cells using the Flp-In™ system. A large difference in receptor expression between variants can be misleading when assessing signalling pathways, therefore whole cell hMOPr expression was measured using [^{3}H]DAMGO. No significant difference between cell surface receptor number was observed for hMOPr-A6V or hMOPr-N40D when compared with hMOPr-WT (Figures 5.2**(A)** and 5.2**(B)**). B_{max} for AtT20-hMOPr-WT was 1393±84 fmol/mg total protein, 1772±151 fmol/mg for AtT20-hMOPr-A6V and 1321±55 fmol/mg for AtT20-hMOPr-N40D (Figure 5.2**(C)**, t-test, $p>0.05$). In addition, the affinity for [^{3}H]DAMGO was compared between variants and, as shown in Figure 5.2**(D)**, all three K_Ds were similar being approximately 3nM (t-test, $p>0.05$).

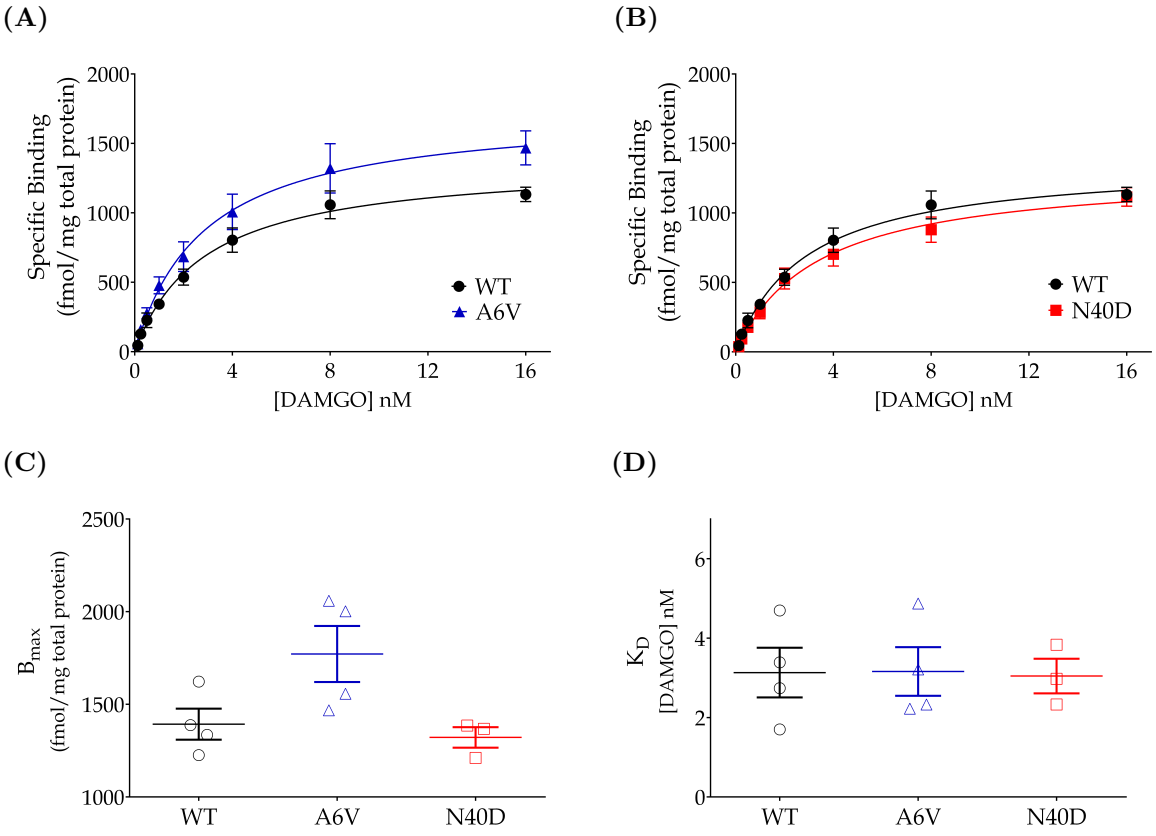

Figure 5.2. hMOPr-WT, hMOPr-A6V and hMOPr-N40D expression in AtT20 cells. **(A)** Saturation binding curve of [^{3}H]DAMGO in intact AtT20-hMOPr-WT and AtT20-hMOPr-A6V. **(B)**Saturation binding curve of [^{3}H]DAMGO in intact AtT20-hMOPr-WT and AtT20-hMOPr-N40D. **(C)** B_{max} results. **(D)** K_D results. No significant difference in B_{max} or K_D was observed between cells expressing hMOPr-WT and N-terminal variants (t-test, p>0.05). Data represent the mean ±SEM, n=3-4.

5.2.2 Human MOPr Signalling via GIRK Channel Activation

Many signalling pathways can be activated by opioid agonist induced conformational changes in the MOPr. GIRK activation by $\beta\gamma$ subunits produces cell hyperpolarisation which can be measured using FLIPR® membrane potential dye. AtT20 cells expressing WT, A6V or N40D hMOPr were treated with varying concentrations of opioid agonists and somatostatin, maximum hyperpolarisation was measured for each concentration (Figure 5.3) and concentration response curves (CRCs) plotted (Figures 5.4).

Figure 5.3 illustrates representative traces of data collected for DAMGO and buprenorphine CRCs in AtT20-hMOPr-N40D. All higher efficacy opioid agonists tested had a similar pattern to that shown for DAMGO where the rate of signal decay was fast for

low concentrations and slowed down as concentration increased. Uniquely, buprenorphine decay rate in the MOPr signal was fast even at high concentrations, and this signalling profile occurred for all variants assessed.

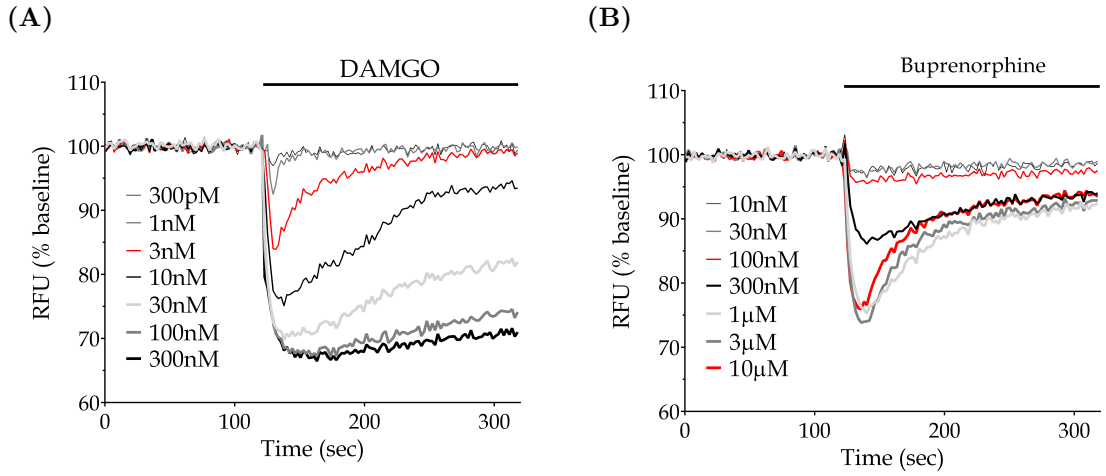

Figure 5.3. Representative traces showing decrease in fluorescence signal, corresponding to membrane hyperpolarisation, following application of varying concentrations of DAMGO and buprenorphine to AtT20-hMOPr-N40D. **(A)** DAMGO stimulated hyperpolarisation. **(B)** Buprenorphine stimulated hyperpolarisation. Note that signal recovery profile for buprenorphine was very different from DAMGO as high concentrations also caused fast signal decay. Data from one experiment in duplicate normalised to baseline.

A6V and N40D polymorphisms did not affect signalling by β-endorphin, DAMGO, methadone and endomorphin-2 (Figure 5.4, Table 5.1). Morphine ability to stimulate GIRK opening was also unaffected at hMOPr-N40D, while its efficacy was slightly reduced at hMOPr-A6V (t-test, p=0.0261), nevertheless this is unlikely to have any biological significance. Buprenorphine and pentazocine, which presented a low intrinsic activity at all hMOPr variants (Table 5.1), have unchanged efficacies and potencies in cells expressing A6V variant, however in AtT20-hMOPr-N40D cells buprenorphine was less potent, with $p\text{EC}_{50}$ of 6.7±0.1 compared with $p\text{EC}_{50}$ of 7.0±0.1 in AtT20-hMOP-WT cells (t-test, p=0.0140), but with similar efficacy (WT E_{max} of 22±1, N40D E_{max} of 19±2, t-test, p=0.1169). Pentazocine's ability to signal was also disrupted by N40D polymorphism, where a large decrease in the efficacy was observed (WT E_{max} of 7±1, N40D E_{max} of 4±1, t-test, p=0.0099), but had no effect on potency (WT $p\text{EC}_{50}$ of 7.2±0.1, N40D $p\text{EC}_{50}$ of 7.1±0.2, t-test, p=0.6389). Note that pentazocine E_{max} values

are significant when compared to basal signal (one-sample t-test, $p<0.05$).

To assess the ability of AtT20 cell populations to hyporpolarise across cell lines created, SST CRC was determined for all AtT20 cells expressing hMOPr variants. Somatostatin efficacy and potency were similar between all hMOPr variants (t-test, $p<0.05$), which is important to show that differences observed in CRCs were not related to hyperpolarisation variances in the cell lines.

Table 5.1. Summary of opioid and SST efficacy and potency of GIRK activation in AtT20 cells expressing WT, A6V or N40D hMOPr

GIRK activation	**E_{max}(%)**			**pEC_{50}**		
Opioid	WT	A6V	N40D	WT	A6V	N40D
β-Endorphin	35±1	33±2	34±1	7.1±0.2	7.0±0.1	7.0±0.1
DAMGO	34±1	31±1	32±1	8.4±0.1	8.5±0.1	8.4±0.1
Methadone	33±1	32±1	33±2	7.3±0.1	7.4±0.1	7.3±0.1
Endomorphin-2	32±1	30±1	31±1	8.1±0.1	8.1±0.1	7.9±0.1
Morphine	31±1	28±1*	30±1	7.6±0.1	7.6±0.1	7.4±0.1
Buprenorphine	**22±1**	**22±2**	**19±2**	7.0±0.1	7.2±0.1	6.7±0.1*
Pentazocine	**7±1**	**5±1**	**4±1***	7.2±0.1	7.0±0.2	7.1±0.2
SST	33±1	33±1	32±1	8.3±0.1	8.4±0.1	8.3±0.2

Opioids are listed in rank order of maximal effect at MOPr-WT. Opioids with E_{max} significantly lower than DAMGO are set in bold (one-way *ANOVA*, followed by t-test, corrected for multiple comparisons, $p<0.05$). Marked with * are results significantly different to hMOPr-WT (t-test, $p<0.05$).Values shown are mean ± SEM, n=5-11.

Figure 5.4.*(following page)*: Opioid agonists and SST concentration response curves in AtT20 expressing WT (black), A6V (blue) and N40D (red) hMOPr. **(A)** β-Endorphin, **(B)** DAMGO, **(C)** methadone and **(D)** endomorphin-2 signalling was not affected by polymorphisms. **(E)** Morphine efficacy at A6V variant was lower when compared to WT (t-test, $p<0.05$). **(F)** Buprenorphine was less potent while **(G)** pentazocine efficacy was reduced by almost 50% in N40D variant (t-test, $p<0.05$). Note that **(H)** SST signalling was similar between cell lines (t-test, $p>0.05$). Data represent the mean ± SEM of pooled data from 5-11 independent determinations performed in duplicate.

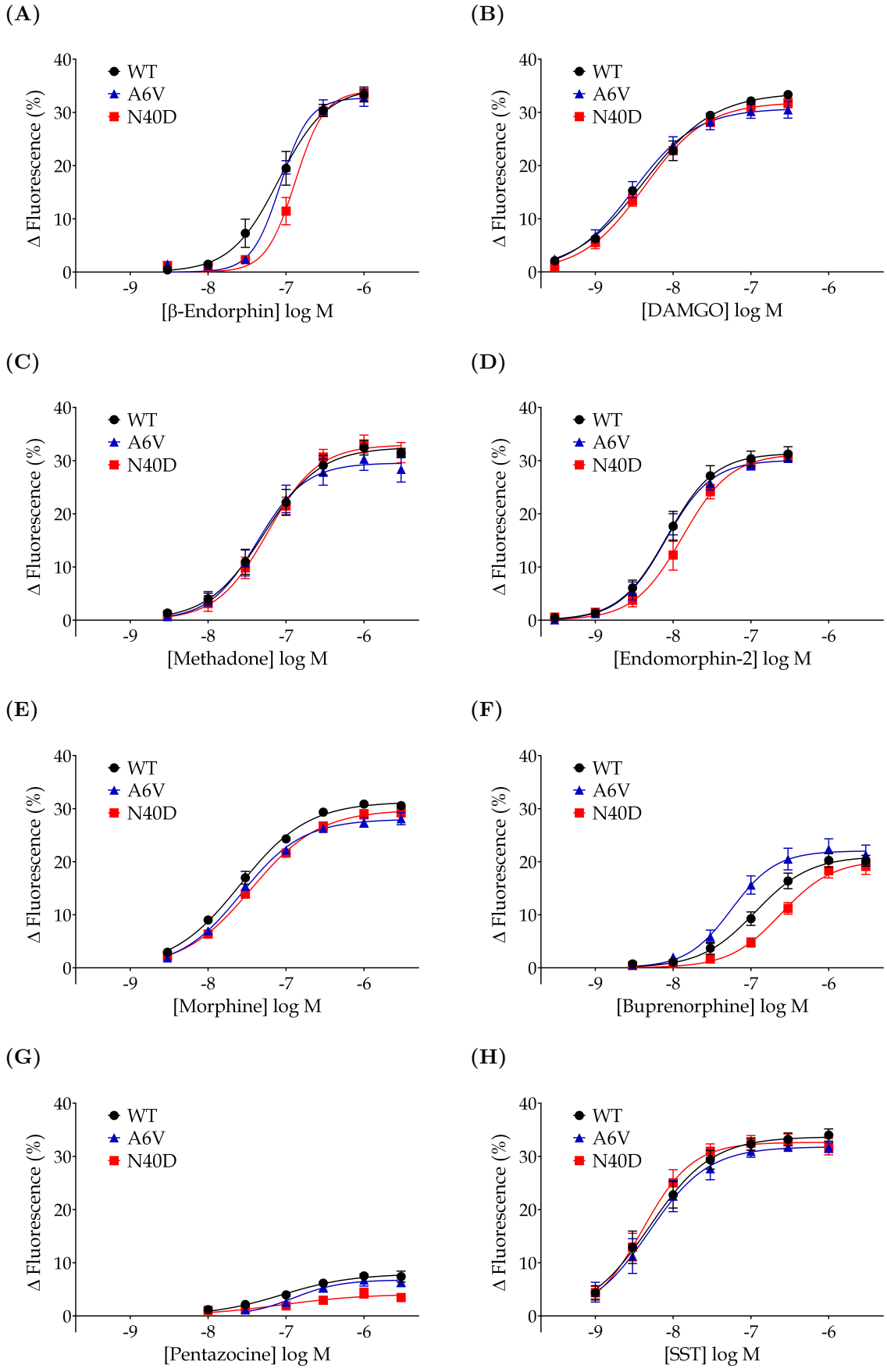
(A)
WT
A6V
N40D
Δ Fluorescence (%)
[β-Endorphin] log M
(B)
[DAMGO] log M
(C)
[Methadone] log M
(D)
[Endomorphin-2] log M
(E)
[Morphine] log M
(F)
[Buprenorphine] log M
(G)
[Pentazocine] log M
(H)
[SST] log M

5.2.3 Opioid-Mediated Signal Desensitisation in AtT20 cells

The effect of A6V and N40D polymorphisms on GIRK signal desensitisation was assessed using FLPR® membrane potential dye as described in methods (Section 3.5). Figure 5.5 shows representative traces for homologous and heterologous desensitisation in AtT20 expressing hMOPr-N40D.

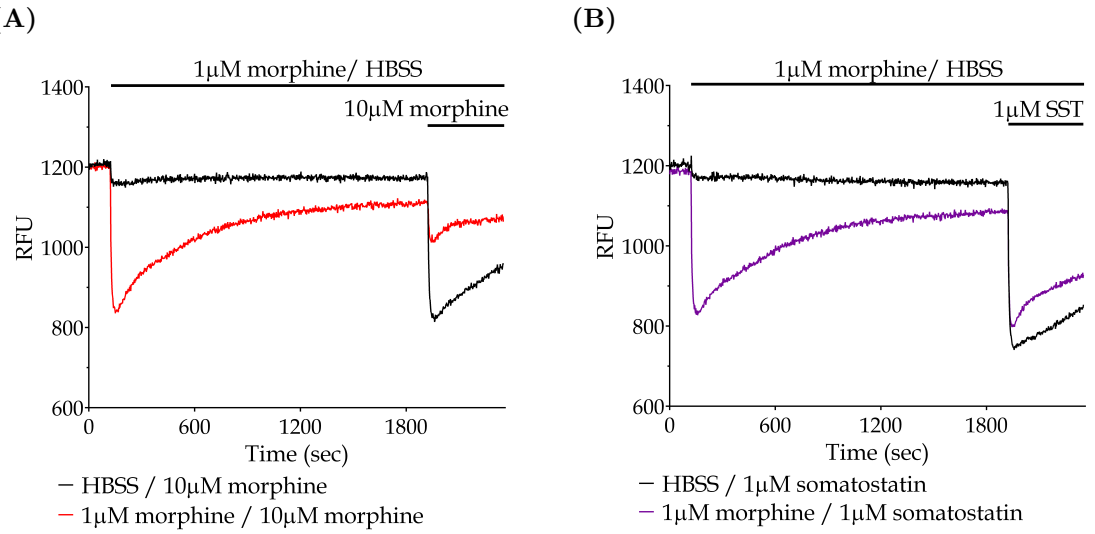

Figure 5.5. Raw traces of **(A)** homologous and **(B)** heterologous desensitisation in AtT20-hMOPr-N40D stimulated for 30 minutes with 1μM morphine before a high concentration of morphine (10μM) or SST (1μM) was added. Difference in maximum response was used to calculate desensitisation and plot a time course. Signal decay from 1μM morphine was fitted to a one-phase exponential association and time constant (τ) obtained.

In addition to morphine and DAMGO, the main opioids analysed in this project, buprenorphine and endomorphin-2 induced signal decay and desensitisation were examined. Signal desensitisation by opioid peptide endomorphin-2 was previously compared to DAMGO where it induced faster desensitisation of GIRK signalling in LC neurons[294]. Also considering the efficacy and potency results reported in the present work, it would be interesting to assess desensitisation of pentazocine and buprenorphine in AtT20-N40D; however pentazocine signal hyperpolarisation was too low to obtain reliable desensitisation data.

To assess signal decay after opioid stimulus (1μM DAMGO, 1μM morphine), 40 minutes traces were fitted to a one-phase exponential association, then hMOPr-A6V

and hMOPr-N40D time constant (τ) and maximum decay (Y_{max}) were compared to hMOPr-WT (Table 5.2). A slightly lower extent of decay was observed for DAMGO at A6V (WT R_{max} of 94±1, A6V R_{max} of 91±1, *t*-test, p=0.0332) and similar result was obtained for endomorphin-2 (WT R_{max} of 95±1, A6V R_{max} of 92±1, *t*-test, p=0.0396), however such a small difference could be related to tiny differences in receptor expression and is unlikely to have any biological relevance. In general signal decay was unaffected across variants (*t*-test, p>0.05).

The fastest rate of signal decay was observed for buprenorphine which also presented the higher extent of decay (one-way *ANOVA* corrected for multiple comparisons, p>0.05). In addition, DAMGO and endomorphin-2 had similar rate of decay (one-way *ANOVA* corrected for multiple comparisons, p>0.05).

Table 5.2. Summary of time constant (τ) and maximum decay (Y_{max}) of signal in AtT20 cells expressing WT, A6V or N40D hMOPr

	τ(sec)			Y_{max}(%)		
Opioid	WT	A6V	N40D	WT	A6V	N40D
DAMGO	898±131	1019±76	973±123	94±1	**91±1***	92±1
Morphine	612±76	725±52	664±74	96±1	94±1	95±1
Endomorphin-2	1044±185	1008 ±221	1260±404	95±1	**92±1***	94±1
Buprenorphine	239±36	154±44	232±57	98±1	97±1	98±1

Signal decay data were fitted to a one-phase exponential association and $t^1/_2$ and Y_{max} (plateau) obtained. Highlighted are results significantly different to hMOPr-WT (*t*-test , p<0.05). Values shown are mean ± SEM, n=4-6.

By using a challenge concentration of opioid or SST after 5, 10, 20, 30 or 40 minutes of opioid stimulus, homologous and heterologous signalling desensitisation time courses was examined. Morphine, DAMGO and endomorphin-2 time courses were not affected by A6V and N40D polymorphisms as shown in Figure 5.6 (two-way *ANOVA*, p>0.05). To further assess time course results, $t^1/_2$ and maximum desensitisation (D_{max}) was compared between variants and are summarised in table 5.3. D_{max} of morphine and endomorphin-2 was not influenced by polymorphisms (*t*-test, p>0.05), however a slightly lower homologous D_{max} by DAMGO was observed for A6V (58±2%)

and N40D (59±2%) compared with WT (66±1%), while only A6V affected heterologous DAMGO D_{max} (WT D_{max} of 55±2%, A6V D_{max} of 46±2%, *t*-test, $p<0.05$).

Buprenorphine homologous desensitisation data did not fit a one-phase exponential association; note that buprenorphine signal desensitised much faster when compared to other opioids tested and signal fluctuated in an uneven pattern. A6V polymorphism resulted in a decrease in homologous desensitisation (two-way *ANOVA*, $p<0.05$) and a faster rate of heterologous desensitisation ($t^1/_2$ of 2.4±0.7 min, *t*-test, $p=0.0439$) when compared with hMOPr-WT ($t^1/_2$ of 6.8±1.4 min), while N40D desensitisation was unaffected.

Figure 5.6.*(following page)*: Effect of N-terminal polymorphisms on homologous and heterologous signal desensitisation by DAMGO, morphine, endomorphin-2 and buprenorphine in AtT20 cells expressing hMOPr WT (black), A6V (blue) or N40D (red). **(A)** Homologous and **(B)** heterologous desensitisation after 1μM DAMGO stimulus. **(C)** Homologous and **(D)** heterologous desensitisation after 1μM morphine stimulus. **(E)** Homologous and **(F)** heterologous desensitisation after 1μM endo-2 stimulus. **(G)** Homologous and **(H)** heterologous desensitisation after 1μM buprenorphine stimulus, note that homologous data had a very distinct pattern not fitting a one-phase exponential curve. Polymorphisms did not affect homologous and heterologous signal desensitisation time course by DAMGO, morphine or endomorphin-2 (two-way *ANOVA*, $p>0.05$). Altered buprenorphine induced homologous desensitisation at hMOPr-A6V was observed (two-way *ANOVA*, $p=0.0043$), all other buprenorphine results were hMOPr-WT alike (two-way *ANOVA*, $p>0.05$). Data are expressed as percentage desensitisation from vehicle control, and represent the mean ± SEM of 4-6 independent determinations performed in duplicate.

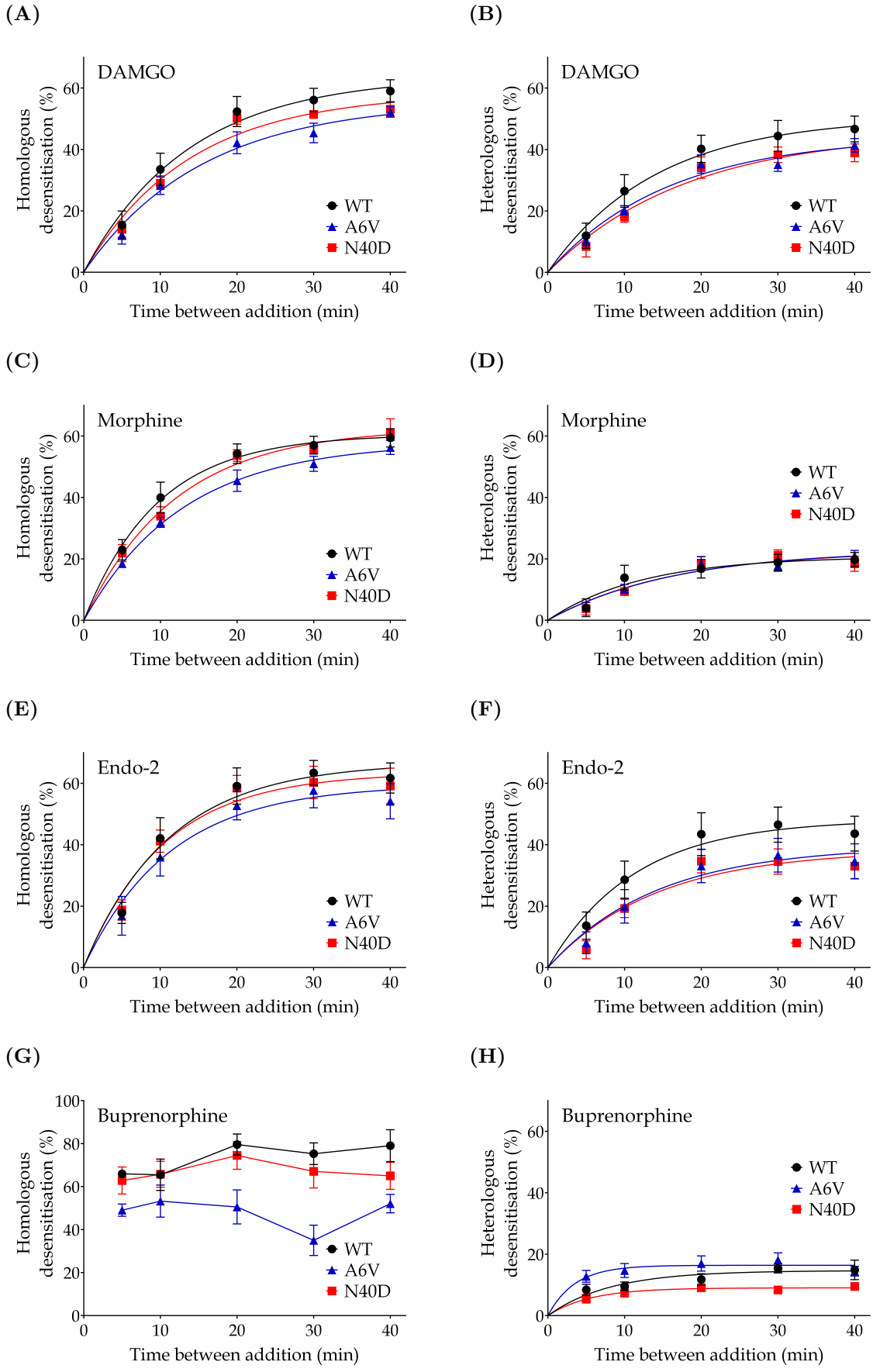
(A)
DAMGO
Homologous desensitisation (%)
Time between addition (min)
WT
A6V
N40D
(B)
DAMGO
Heterologous desensitisation (%)
Time between addition (min)
WT
A6V
N40D
(C)
Morphine
Homologous desensitisation (%)
Time between addition (min)
WT
A6V
N40D
(D)
Morphine
Heterologous desensitisation (%)
Time between addition (min)
WT
A6V
N40D
(E)
Endo-2
Homologous desensitisation (%)
Time between addition (min)
WT
A6V
N40D
(F)
Endo-2
Heterologous desensitisation (%)
Time between addition (min)
WT
A6V
N40D
(G)
Buprenorphine
Homologous desensitisation (%)
Time between addition (min)
WT
A6V
N40D
(H)
Buprenorphine
Heterologous desensitisation (%)
Time between addition (min)
WT
A6V
N40D

Table 5.3. Summary of desensitisation time course $t^1/_2$ and D_{max} in AtT20 cells expressing WT, A6V or N40D hMOPr

	$\mathbf{t^1/_2}$**(min)**			$\mathbf{D_{max}}$**(%)**		
Opioid	WT	A6V	N40D	WT	A6V	N40D
Homologous desensitisation						
DAMGO	12.4±2.9	12.5±2.6	9.8±1.0	66±1	**58±2***	**59±2***
Morphine	7.5±1.3	9.1±0.7	8.5±0.9	61±2	58±3	63±3
Endomorphin-2	8.6±1.2	8.5±1.2	7.2±1	68±4	61±5	64±6
Heterologous desensitisation						
DAMGO	14.2±4.1	12.1±1.8	15.2±4.2	55±2	**46±2***	49±3
Morphine	12.2±5.8	11.2±3	11.6±1	25±2	23±1	23±2
Endomorphin-2	9.4±1.5	12.4±2.7	10.5±1.4	49±5	42±6	38±4
Buprenorphine	6.8±1.4	**2.4±0.7***	8.5±4.9	16±3	16±2	11±2

Desensitisation data were fitted to a one-phase exponential association and $t^1/_2$ and D_{max} (plateau) obtained. Note that buprenorphine induced homologous desensitisation did not fit the curve. Highlighted are results significantly different to hMOPr-WT (t-test, $p<0.05$). Values shown are mean ± SEM, n=4-6.

Overall, besides some small variations in DAMGO and endomorphin-2 signal decay and desensitisation, the change in buprenorphine induced homologous desensitisation in AtT20-hMOPr-A6V is the only finding likely to have a biological relevance.

5.2.4 Opioid-Mediated Phosphorylation of hMOPr Ser377

Many studies showed that phosphorylation of Ser377 residue of hMOPr-WT, or Ser375 in mMOPr-WT, is agonist dependent and that the extent of phosphorylation by morphine is much less than by DAMGO[71,102,311]. To assess the effect of polymorphisms on hMOPr phosphorylation induced by 1μM morphine and 1μM DAMGO after 5 or 30 minutes treatment, the selective antibody to phosphorylation on Ser377 was used and data are presented in Figure 5.7. Note that this is the only selective antibody for MOPr phosphorylation available commercially.

As expected morphine induced phosphorylation of Ser377 to a lesser extent than DAMGO in hMOPR-WT, and no difference was observed between variants for both

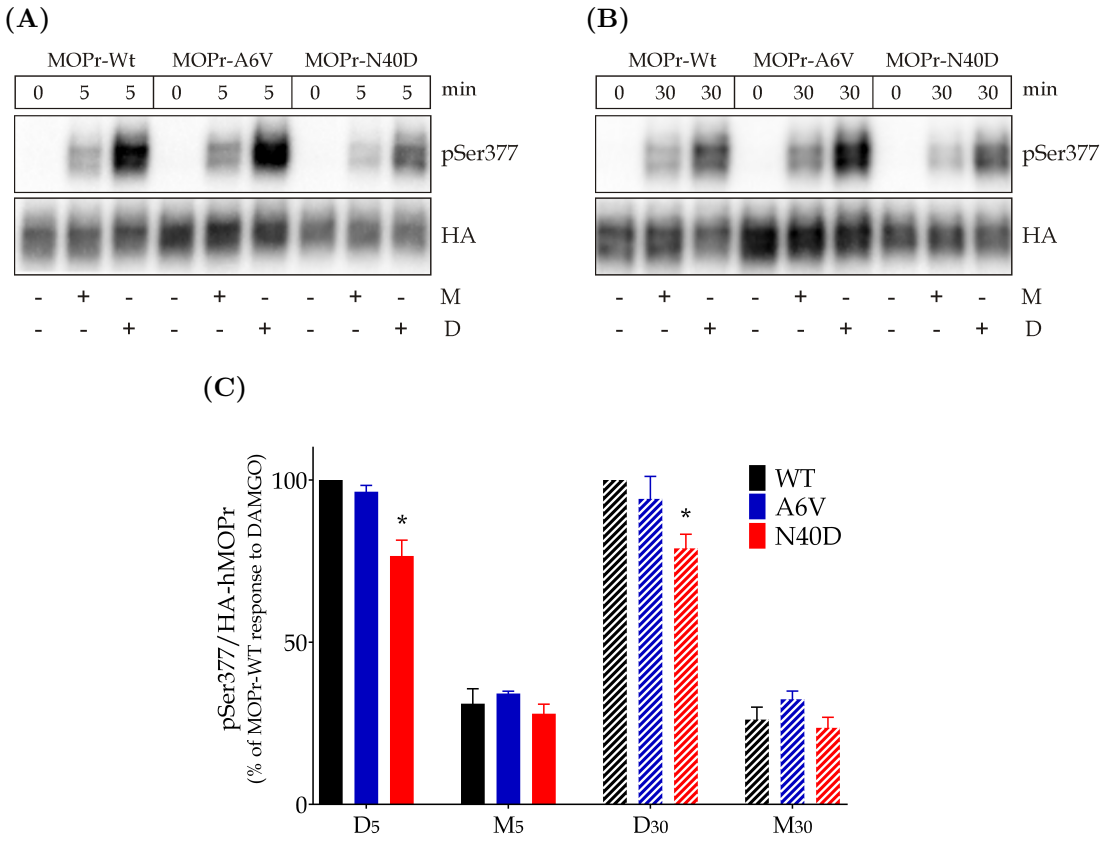

Figure 5.7. Morphine and DAMGO induced phosphorylation of hMOPr Ser377 residue in AtT20 expressing hMOPr variants. **(A)** and **(B)** are representative blots from one of five independent experiments of 5 or 30 minutes opioid treatment respectively . AtT20 cells stably transfected with hMOPr-WT, hMOPr-A6V or hMOPr-N40D were either not exposed (-) or exposed (+) to 1μM DAMGO (D) or 1μM morphine (M) for 5 or 30 minutes. The cells were lysed and immunoblotted with anti-pSer377 antibody (pSer377, upper panel), then blot was stripped and reprobed with anti-HA antibody to detect total hMOPr (HA, lower panel). Further methods details are described in Section 3.6 **(C)** Morphine and DAMGO incubated for 5 (no pattern) or 30 minutes (stripe pattern) induced similar extension of Ser377 residue phosphorylation in WT and A6V hMOPr (t-test, p>0.05). While hMOPr-N40D polymorphism also did not change Ser377 phosphorylation by morphine, DAMGO results was significantly different for both time points (one-sample t-test, p<0.05). Data are presented as % of DAMGO-induced Ser377 phosphorylation (pSer377) in AtT20-hMOPr-WT (100%) ± SEM; note that all results were corrected for total receptor number (pSer377/HA). Data quantified by densitometric analysis.

time points (t-test, p>0.05). All results were normalised to DAMGO induced phosphorylation on Ser377 of hMOPr-WT (100%), and after 5 minutes incubation with morphine, 31±5% phosphorylation was observed for hMOPr-WT, 34±1% for hMOPr-A6V and 28±3% for hMOPr-N40D. A similar data was obtained for 30 minutes incubation (WT 26±4%, A6V 32±3%, N40D 24±3; t-test, p>0.05, n= 5-6).

DAMGO mediated robust phosphorylation of Ser377 at 5 and 30 minutes time points. WT and A6V phosphorylation intensity were similar, however N40D polymorphism significantly decreased phosphorylation at both 5 (WT 100%, N40D 77±5%, one-sample t-test, p=0.0174) and 30 minutes treatment (WT 100%, N40D 79±4%, one-sample t-test, p=0.0084).

Considering the interesting results in GIRK activation and desensitisation with buprenorphine, hMOPr phosphorylation induced by this semisynthetic opioid was also assessed. Buprenorphine treatment led to a low extent of Ser377 phosphorylation in all hMOPr variants tested (t-test, p<0.05); for this reason morphine was used instead of DAMGO to normalise results since DAMGO band saturated before buprenorphine could develop. A6V polymorphism caused an increase of buprenorphine-induced Ser377 phosphorylation to 34±6% in 5 min and 41±3% in 30 minutes when compared with WT, 16±4% in 5 min and 24±4% in 30 min (t-test, p<0.05). The Ser377 phosphorylation for N40D variant was similar to WT (16±3% in 5 min and 24±8% in 30 min).

A decrease in protein glycosylation can affect protein migration leading to a lower molecular weight. Figures 5.7 and 5.8 representative blots illustrates the lack of significant change on hMOPr-N40D molecular weight, which indicated the possibility of low or absent glycosylated in N40 position of hMOPr expressed in AtT20 cells.

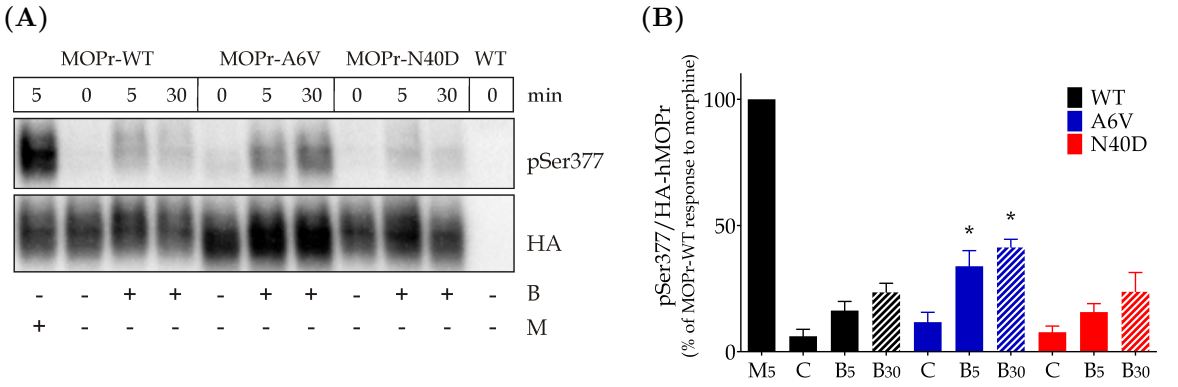

Figure 5.8. Buprenorphine induced phosphorylation of hMOPr Ser377 residue in AtT20 expressing hMOPr variants. **(A)** AtT20 cells stably transfected with hMOPr-WT, hMOPr-A6V or hMOPr-N40D were either not exposed (-) or exposed (+) to 1μM buprenorphine (B) for 5 or 30 minutes. The cells were lysed and immunoblotted with anti-pSer377 antibody (pSer377, upper panel), then blot was stripped and reprobed with anti-HA antibody to detect total hMOPr (HA, lower panel). Phosphorylation of hMOPr-WT induced by 1μM morphine (M) for 5 minutes was added to normalise results. Representative blot from one of five independent experiments is shown and methods are described in Section 3.6. **(B)** Buprenorphine induced similar extension of Ser377 residue phosphorylation in WT and N40D hMOPr, while phosphorylation of hMOPr-A6V was significantly increased for both 5 (no pattern) and 30 (stripe pattern) minutes time points(t-test, $p<0.05$). Data are presented as % of morphine-induced Ser377 phosphorylation in AtT20-hMOPr-WT (100%) ±SEM; note that all results were corrected for total receptor number (pSer377/HA). Data quantified by densitometric analysis.

5.2.5 Cell Surface Loss of hMOPr

To further assess the effect of N-terminal polymorphisms in hMOPr regulation in AtT20 cells expressing hMOPr variants, the amount of hMOPr WT, A6V and N40D membrane surface loss was quantified after morphine and DAMGO treatment for 5 and 30 minutes using a whole-cell ELISA technique.

Figure 5.9 shows the obtained results and as previously reported morphine did not mediate significant receptor loss from the surface for both concentrations tested (1μM and 10μM). 0.1μM DAMGO also did not induce a significant decrease in membrane receptor however DAMGO in higher concentrations (1μM and 10μM) produced a significant receptor internalisation which was much greater after 30 minutes when compared to 5 minutes for all variants (t-test, $p<0.05$).

Quantified hMOPr-A6V on cell surface was indistinguishable from hMOPr-WT,

however a significant lower amount of membrane hMOPr was observed when AtT20-hMOPr-N40D cells was incubated for 30 minutes with 1μM (WT 79±1%, N40D 67±2%, *t*-test, p=0.0006) or 10μM DAMGO (WT 63±2%; N40D 54±3%, *t*-test, p=0.0079). Therefore only N40D polymorphism affect hMOPr downregulation (two-way *ANOVA*, corrected for multiple comparisons, p<0.05).

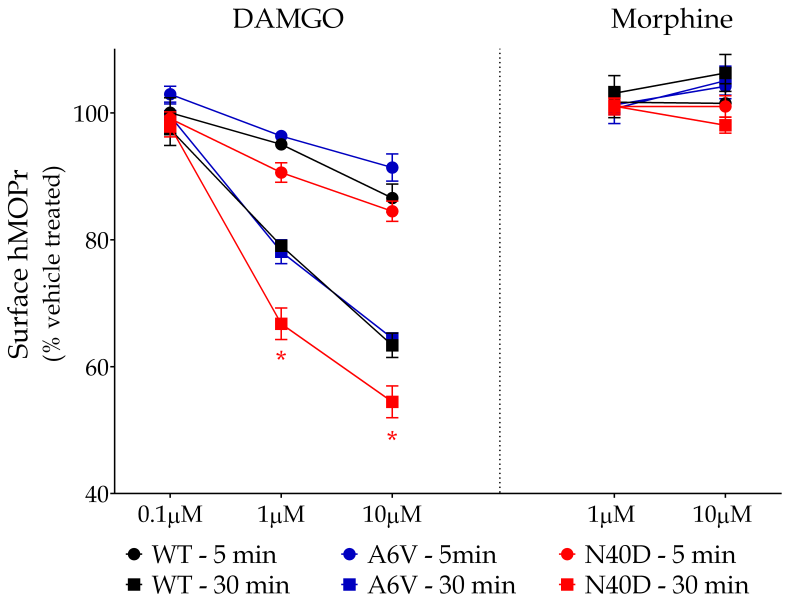

Figure 5.9. Loss of membrane hMOPr-WT, hMOPr-A6V and hMOPr-N40D after DAMGO or morphine incubation for 5 or 30 minutes. Data obtained as described in Section 3.8. The amount of hMOPr on membrane was reduced after 1μM and 10μM DAMGO treatment when compared to 0.1μM DAMGO for all variants (*t*-test, p<0.05). Morphine and 0.1μM DAMGO did not induce membrane receptor loss (one-sample *t*-test, p>0.05). When comparing N-terminal polymorphisms to hMOPr-WT, A6V did not affect receptor surface numbers while hMOPr-N40D surface loss was increased when incubated for 30 minutes with 1μM or 10μM DAMGO (two-way *ANOVA*, corrected for multiple comparisons, p<0.05 marked with *). Data represent the mean ± SEM of pooled data from 4-5 independent determinations performed in triplicate.

5.3 Discussion

OPRM1 gene codes for the hMOPr and it is well established that in some populations non-synonymous SNPs are present in the coding region. The allele prevalence of some polymorphisms can be high; for example N40D (A118G) can be prevalent in up to 48% of Asians, and A6V (C17T) up to 20% of Northern Indians. These two populations

alone account for a large portion of the planet's population, it follows that one can estimate the importance of studying these two N-terminal hMOPr polymorphisms.

In this chapter the effect of A6V and N40D polymorphisms were assessed by expressing hMOPr-WT, hMOPr-A6V or hMOPr-N40D in AtT20 cells using the Flp-In™ system. This system facilitated the production of isogenic cell lines, which is characterised by the integration of the receptor variants constructs at the same location in the genome[307]. This similar transcriptional environment between cell lines enables a better way of comparing differences amongst polymorphisms. A summary of this chapter findings is presented in Table 5.4.

Identifying and understanding protein post-translational modifications (PTMs) is critical in the study of GPCRs regulation. One very important PTM is glycosylation, where approximately 90% are N (asparagine) -linked glycosylations. hMOPr has five asparagine at the N-terminal, and NetNGlyc 1.0 Server predicts that three of them have a high potential of being glycosylated (Figure 5.1). The N40D polymorphism removes one of these likely glycosylated sites. However, in this study western blots showed molecular weight of hMOPr-N40D and hMOPr-WT to be similar, excluding the possibility of a highly glycosylated site in AtT20-hMOPr cells. In addition, glycosylation may increase protein stability, which in some studies reportedly increased protein expression. Nevertheless, the expression of both hMOPr variants were similar when quantified by radioligand binding; taken together these results suggest that N40 position of hMOPr-WT expressed in AtT20 cells may not be glycosylated. Similar findings for receptor expression were previously reported in CHO-KI and Neuro 2A cells expressing hMOPr-WT and hMOPr-N40D[96,182]. Huang et al. (2012)[156] reported a lower molecular weight of hMOPr-N40D in mutant mouse striatum and thalamus membrane, which was likely caused by lower receptor glycosylation[156]. They also showed similar results in HEK293 and CHO cells expressing hMOPr-N40D, and correlated this modification with the lower receptor half-life found in CHO cells. Zhang et al. (2005)[373] also observed a reduced protein expression in CHO cells expressing hMOPr-N40D. Interestingly even though the protein expression was more than ten-fold lower, the mRNA level was only 1.5-fold lower, and despite omitting protein glycosylation, N40D molecular

Table 5.4. Summary of N-terminal polymorphisms findings

hMOPr variant	Assay performed	Key observations
A6V	Radioligand binding	Similar expression and affinity
	GIRK activation	Morphine slightly lower efficacy*
	Desensitisation time course	DAMGO induced slightly lower maximum homologous and heterologous desensitisation*
		Buprenorphine induced decreased homologous desensitisation and faster heterologous desensitisation
	Signal decay	DAMGO and endomorphin-2 induced slightly lower extent of decay*
	Ser377 phosphorylation	Buprenorphine induce phosphorylation to a higher extent at 5 and 30 minutes
	Cell surface hMOPr loss	Similar regulation
N40D	Radioligand binding	Similar expression and affinity
	GIRK activation	Buprenorphine less potent and pentazocine almost two-fold decrease in efficacy
	Desensitisation time course	DAMGO induced slightly lower maximum homologous desensitisation*
	Signal decay	Similar rate and extent of decay for all opioid tested
	Ser377 phosphorylation	DAMGO induce phosphorylation to a lesser extent at 5 and 30 minutes
	Cell surface hMOPr loss	Higher DAMGO concentrations increased loss at 30 minutes

All results are in comparison with hMOPr-WT. Results different from hMOPr-WT marked with * are unlikely to have biological relevance

weight in the published blot did not appear to be different from hMOPr-WT.

One plausible explanation for the conflicting data presented is that although mammalian cell lines are a great tool due to their capacity to produce complex glycosylation of human proteins, they may present different pattern of protein glycosylation to human cells. Within the endoplasmic reticulum and Golgi apparatus of each cell line, the presence and/or level of enzymes (glycosidases and glycosyltransferases) involved in the glycosylation process vary; this is the main reason for different protein glycosylation and is extremely important since different cell lines should be able to produce proteins

with specific properties related to its function[137,231]. This change in glycosylation pattern may be a problem when using heterologous expression system as it could lead to different observations[68,193]. However, it is important to note that brain N-glycosylation of MOPr seems to have region-specific patterns[155]; thus, studying MOPr in different cell lines might give a better picture of possibilities in different areas of the nervous system.

Another possible explanation for lower MOPr expression found by some studies in brain tissue and cell lines (CHO and HEK293)[31,156,373] is that, in eukaryotes, DNA methylation is one of many epigenetic mechanism used to control gene expression. Methylation is most commonly introduced at cytosine-phosphate-guanine (CpG) sites, where a cytosine is directly followed by a guanine in the sequence, and this common epigenetic signalling tool can interfere with mRNA formation. Interestingly, a CpG site is introduced in the N40D polymorphism; therefore, N40D gene has an extra methylation site. Oertel et al. (2012)[253] reported an increase in methylation pattern in hMOPr-N40D gene. This could be responsible for the reduced levels of G118 mRNA found in chronic opioid users when compared to the wild-type genotype, where upregulation of hMOPr-WT was observed to compensate for a reduced signalling efficiency in heroin users. This epigenetic modification could also explain why such variability is found between clinical studies as methylation patterns vary according to many different factors such as sex, age and environmental exposures like diet, nutrition and air pollution[87]. Furthermore, gene-specific methylation/demethylation in human nasopharyngeal carcinoma KB cells can be induced by depletion of nutrients like folic acid[166]; thereby, different growth conditions in tissue culture in addition to diversity between the cell lines studied could also influence results, if epigenetic is truly involved in N40D polymorphism gene expression. It is important to note that hMOPr-WT and hMOPr-N40D were expressed in FlpIn™ AtT20 or CHO-KI[182] in similar levels; therefore, if this site is methylated in the conditions studied, it did not significantly alter receptor expression.

MOPr phosphorylation is another important post-translational modification. Schulz

et al. (2004)[311] reported that DAMGO induced a fast and robust MOPr phosphorylation while a lesser extent phosphorylation was induced by morphine in HEK293 cells expressing mMOPr. Using a phosphorylation mutant of Ser375 (Ser377 in hMOPR) it was shown that this residue is the primary phosphoacceptor site in mMOPr treated with morphine and DAMGO, and it is involved in receptor internalisation; latter shown to be the key step[171,236]. In this study how A6V and N40D polymorphisms affected internalisation and phosphorylation of this primary phosphorylation site was assessed. DAMGO and morphine had a similar Ser377 phosphorylation and membrane receptor loss in hMOPr-A6V compared to hMOPr-WT, this supports the hypothesis by Schulz et al. (2004)[311]. An intriguing result was obtained for N40D polymorphism, where DAMGO induced phosphorylation of Ser377 was reduced by approximately 21%, while, in contrast to expected, cell surface receptors after treatment also decreased. Note that in the assay performed only receptor numbers on cell surface was measured after opioid treatment; internalisation was not measured. If receptor internalisation was similar, as previously reported[31], there is likely to be a decrease in hMOr-N40D recycling or production compared to hMOPr-WT (maybe due to epigenetic modification or lower glycosylation). Further studies are necessary to better understand these findings.

In the present study GIRK activation and signalling desensitisation were also examined. In AtT20-hMOPr-WT, DAMGO and endomorphin-2 mediated signal had similar maximum hyperpolarisation and rate of decay. This findings differed from results reported by Rivero et al. (2012)[294] in rat LC neurons, where endomorphin-2 induced faster decay. This difference could be related to receptor reserve, as within the same study they observed a similar maximum response between these two agonists in LC neurons; however, in cells treated with β-FNA, the relative efficacy for endomorphin-2 was much lower than for DAMGO. This shows that to observe a decay in DAMGO signalling, a higher number of receptor would need to be 'removed' compared to endomorphin-2 thus explaining the faster signal decay by endomorphin-2 in this system.

A6V polymorphism did not significantly affect signalling via GIRK. This suggests

a pathway-dependent impact, taking into consideration that this polymorphism significantly diminished stimulation of ERK1/2 phosphorylation by all opioids tested, and also compromised adenylyl cyclase inhibition by DAMGO, morphine and β-endorphin in CHO-KI cells expressing hMOPr variants[183]. However, differences in cell lines need to be considered, for example glycosylation profile as mentioned above, and expression of proteins involved in signal transduction. Furthermore, buprenorphine signalling was completely abolished in both pathways in CHO cells expressing hMOPr-A6V, while in the present study buprenorphine induced phosphorylation and desensitisation differently in AtT20-hMOPr-A6V compared with AtT20-hMOPr-WT. The change in signal and receptor regulation following buprenorphine treatment at hMOPr-A6V further supports the hypothesis that buprenorphine signalling is altered by the A6V polymorphism. It is somewhat surprising that A6V amino acid change from valine to alanine at the very beginning of the N-terminal is able to alter receptor regulation. Valine and alanine are both hydrophobic amino acids. In comparison, alanine with a smaller side chain is less hydrophobic than valine, though valine is more bulky, restricting the conformation of the main chain. Buprenorphine is also a bulky and hydrophobic molecule, thus maybe these spatial and polarity change may somehow interfere with ligand-receptor interaction.

Beyer et al. (2004)[31] reported that in HEK293 cells morphine did not change N40D polymorphism desensitisation time course measure by cAMP accumulation. In the present study a similar result was obtained for desensitisation of hMOPr signalling via GIRK channels activation. The hMOPr-N40D effect on homologous signalling desensitisation was small and only observed with DAMGO. This data combined with the reduced phosphorylation of Ser377 would further support the idea that desensitisation and phosphorylation are correlated; however, similar reduction on desensitisation was observed for A6V variant without any phosphorylation change.

Membrane potential maximum hyperpolarisation mediated by buprenorphine and pentazocine was reduced at N40D variant, and this was unrelated to receptor expression. Note that compromised buprenorphine signalling was also observed in other pathways in CHO-KI cells[182]. Buprenorphine is used for pain management and opioid

dependence; therefore, it would be of clinical interest to determine if people presenting these polymorphisms respond differently to this commonly used opioid drug.

Compared to other opioid agonists, buprenorphine has unique properties: its analgesic dose response curve is bell-shaped and it has a ceiling effect for respiratory depression[92,362]. Buprenorphine has slow receptor association/dissociation kinetic, which can lead to observations such as those of Virk et al. (2009)[346] where naloxone was unable to reverse buprenorphine induced hyperpolarisation. This paper also showed that preincubation with 5nM buprenorphine blocked rat MOPr acute desensitisation by ME and etorphine in LC neurons; however, they measured desensitisation by signal depolarisation not rechallenge method, and in the same whole-cell recording assay change in membrane potential after buprenorphine exposure was undetectable even after using saturating concentrations. In the present study, rate and extent of desensitisation and signal decay of buprenorphine were analysed in AtT20-hMOPr-WT cells. Interestingly, signal decay was uniquely fast compared to other ligands tested and maximum decay was higher than for all other opioids, almost reaching resting membrane potential. Homologous desensitisation time course was also faster and maximum desensitisation, as a proportion of the original response, higher than any other opioid tested, however a low heterologous desensitisation was observed. This suggests that buprenorphine did not directly block GIRK channels, implying that homologous hMOPr desensitisation is not caused by GIRK desensitisation. A possible explanation is that RGS proteins may be involved in buprenorphine fast signal decay, just as previously mentioned for low concentration of morphine, however because of slow off rate dissociation of buprenorphine, hMOPr are not able to reengage G protein receptor signalling. Then a possible explanation for results obtained is that A6V amino acid change may cause a small decrease in buprenorphine affinity, and when a higher concentration of buprenorphine was added (challenge), it was still able to signal as blockage was slightly diminished; this could also explain higher Ser377 phosphorylation. The results obtained could somehow be related to RGS, however no information was found in the literature that could support the role of RGS in decreased desensitisation. It would be interesting to perform desensitisation assay by Virk et al. (2009)[346] comparing hMOPr-WT and

hMOPr-A6V.

Another approach to assess differences in hMOPr variants would be to look at hMOPr conformations; however this area remains largely unexplored. In 2012, Manglik et al.[220] published the first crystal structure of the mMOPr, but unfortunately the region of interest for us was deleted as a large part of the C and the N-terminal was removed to avoid crystallogenesis inhibition. Using conformation selective antibodies, Gupta et al.[139] demonstrated that conformational changes caused by receptor activation affect MOPr N-terminal, in special the midportion region of MOPr where the N40D polymorphism is located. These changes could be different between hMOPr-WT and N-terminal variants, and this may explain some of the results observed in this chapter.

The notion that polymorphisms to the N-terminal can affect GPCR signalling is supported by a number of publications. In 5-hydroxytryptamine 2B receptor N-terminal polymorphisms was shown to be involved in increased agonist signalling pathways and slowed desensitisation kinetics[28]. Another GPCR N-terminal polymorphism that had been linked to variations in drug response was found in human β2-adrenergic receptor, and a recent study had shown that this A16G variant affects ligands accessibility and binding pocket[316]. This last study used structural modelling and atomistic molecular dynamics simulation to analyse the conformations of the polymorphic receptor variant. It would be intriguing to apply a similar analysis to hMOPr N-terminal polymorphisms.

One important point to note in this study is that only polymorphic homozygous genotypes were used to investigate the full effect of A6V and N40D variants. However, the majority of the population that carries the polymorphic allele only presents a heterozygous genotype. The effects determined here may be modified if cells are transfected with both hMOPr-WT and polymorphism.

In conclusion, A6V and N40D polymorphisms affect receptor function differently in AtT20 cells expressing hMOPr variants. I have shown for the first time that hMOPr-A6V mainly interferes with desensitisation and phosphorylation by buprenorphine,

while pentazocine and buprenorphine signalling via GIRK is compromised at hMOPr-N40D. In addition, DAMGO phosphorylation and cell surface receptor loss in AtT20-hMOPr-N40D cells had an interesting profile and might bring some new mechanistic possibilities on how this variant can cause previously reported clinical differences in hMOPr-WT. More studies are necessary to further evaluate these findings and understand the molecular mechanisms behind them. It is also of great importance to determine if these findings can be translated to clinics in terms of opioid treatment.

6

Regulation of TM1 and ICL2 SNPs of hMOPr

The hMOPr SNPs reported in this chapter are rare, consequently they do not attract as much attention as polymorphisms of the N-terminal. However it is always interesting to understand how small changes in different parts of the receptor can change its regulation. Therefore, here we assessed L85I, a SNP of the first transmembrane (TM) region, and R181C, a second intracellular loop (ICL) SNP.

Contents

6.1 Introduction

Investigating rare polymorphisms of hMOPr may not be very interesting clinically. However it helps to better understand the molecular mechanisms underlying MOPr regulation, which is important for developing better analgesic opioids and that, in turn, would benefit a large percentage of the population.

Ravindranathan et al.[287], in 2009, described for the first time L85I and R181C variants by sequencing OPRM1 in 550 subjects participants in the San Diego Sibling Pair Study, where researches were looking for genes that may increase susceptibility to alcohol use disorders[67]. They reported an allelic frequency of 0.002 for both SNPs in that population. The non synonymous substitution C253A change the amino acid leucine to an isoleucine (L85I) and it is a polymorphism in the first transmembrane region of the hMOPr, while C541T is an alteration from amino acid arginine to cysteine (R181C) in the second intracellular loop (Figure 6.1).

The signalling profile of L85I variant is fairly similar to hMOPr-WT in HEK293 cells; however, this variant efficiently internalised with acute morphine treatment. This finding varies from the well established data in MOPr-WT[7,331,347]. Moreover, when HEK293 cells were co-transfected with both WT and L85I variants, morphine treatment could also induce hMOPr-WT internalisation, this data indicates a dimerisation between these variants[287]. They also showed that tolerance and up-regulation of cAMP (superactivation) induced by morphine was reduced at L85I variant *in vitro*. A recent study by Cooke et al. (2015)[81] of the rat homologue of the human L85I SNP (hence L83I) confirmed the previous finding regarding morphine induced internalisation and

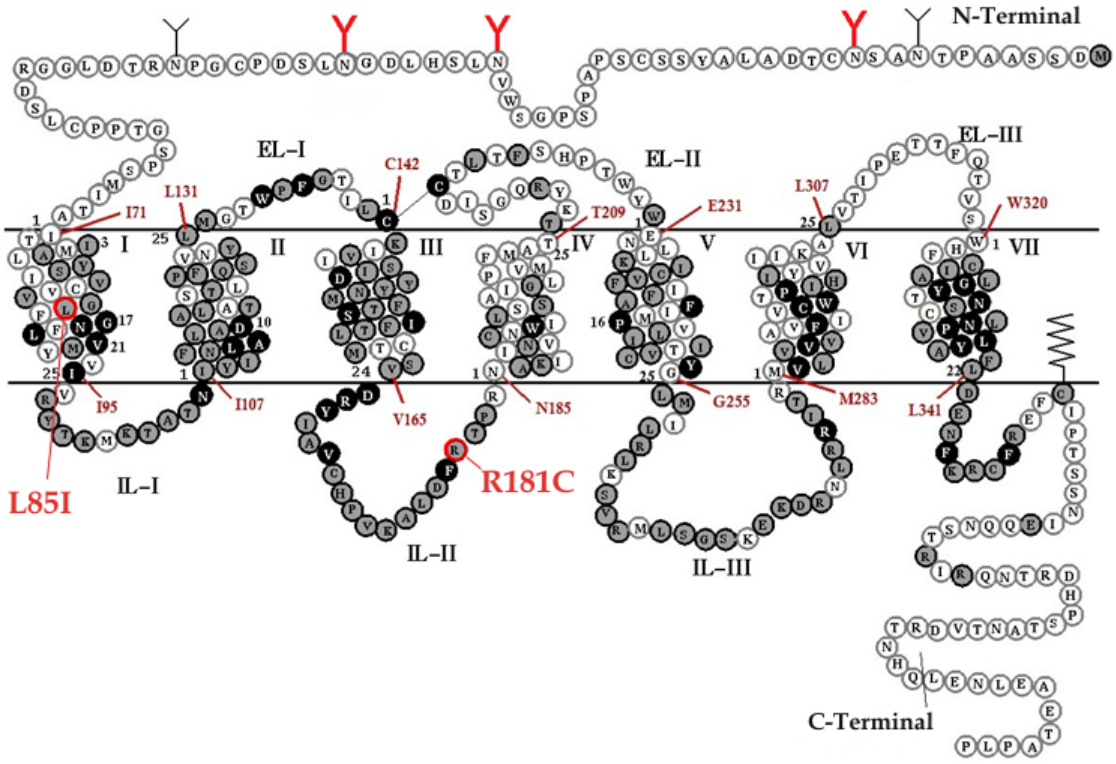

Figure 6.1. Serpentine structure and amino acid sequence of the human μ-opioid receptor wild-type. TM1 and ICL2 amino acids altered by SNPs L85I and R181C are highlighted in red. Adapted figure from Center for Opioid Research and Design (CORD)[83].

additionally added phosphorylation and β-arrestin recruitment studies. Interestingly, they showed L85I variant phosphorylation and β-arrestin binding not to be affected by this mutation; however, internalisation was dynasore sensitive and receptor constitutive internalisation was not significantly different between WT and L83I hMOPr. They also reported acute signalling differences between both variants, the maximum extent of cAMP inhibition by DAMGO at MOPr-WT was greater than for MOPr-L83I, and maximum ERK phosphorylation mediated by morphine and DAMGO was reduced by polymorphism. Nevertheless, no difference was observed in the ability of supramaximal concentrations of DAMGO and morphine to activate [^{35}S]-GTPγS binding.

The R181C variant was previously characterised as a total loss of function mutation in stably transfected HEK293[287]. Despite demonstrating a similar affinity to DAMGO when compared with WT variant, hMOPr-R181C was unable to cause DAMGO mediated receptor internalisation and efflux of intracellular calcium via an

assay where transiently-transfected with a chimeric G protein Δ6-$G_{qi4-myr}$ mutant was used. Residue R181 is in a similar region to the DRY motif, which is one of the most conserved sequences in class A GPCR. Previous reports had linked this motif and the ICL2 to G protein and β-arrestin interactions, and stabilisation of inactive conformation of receptor transmembrane domains in the absence of ligand[61,204,355]. Most importantly, crystal structure analysis of the mMOPr suggested a polar interaction between the aspartic acid (D) residue of the dry motif and the arginine mutated in R181C[220].

In this study hMOPr-L85I and hMOPr-R181C were expressed in AtT20 cells and assessed for receptor signalling and regulation. This is the first study to examine these polymorphisms ability to activate GIRK signalling and desensitisation, in addition to evaluate if previous reported results in HEK293 cells can be reproduced in a different cell type.

6.2 Results

6.2.1 Human MOPr Expression in AtT20 Cells

To enable a reliable comparison of receptor signalling it is important to assess receptor expression. The hMOPr-WT, L85I and R181C were stably transfected in AtT20 cells using the Flp-In™ system. Binding of [^{3}H]DAMGO to whole cells was determined as described in methods (Section 3.4), and K_D and B_{max} calculated.

No significant difference between cell surface receptor number was observed for hMOPr-L85I when compared with hMOPr-WT (Figure 6.2**(A)**). B_{max} for AtT20-hMOPr-WT was 1393±84 fmol/mg total protein and 1105±88 fmol/mg for AtT20-hMOPr-L85I (Figure 6.2**(C)**, *t*-test, $p>0.05$); L85I also did not affect K_D for [^{3}H]DAMGO as shown on Figure 6.2**(D)** (*t*-test, $p>0.05$).

In contrast to previous report where R181C K_D was not different from WT[287], in the present study R181C variant binding to DAMGO was diminished to the point that K_D and B_{max} could not be reliably calculated (Figure 6.2**(B)**).

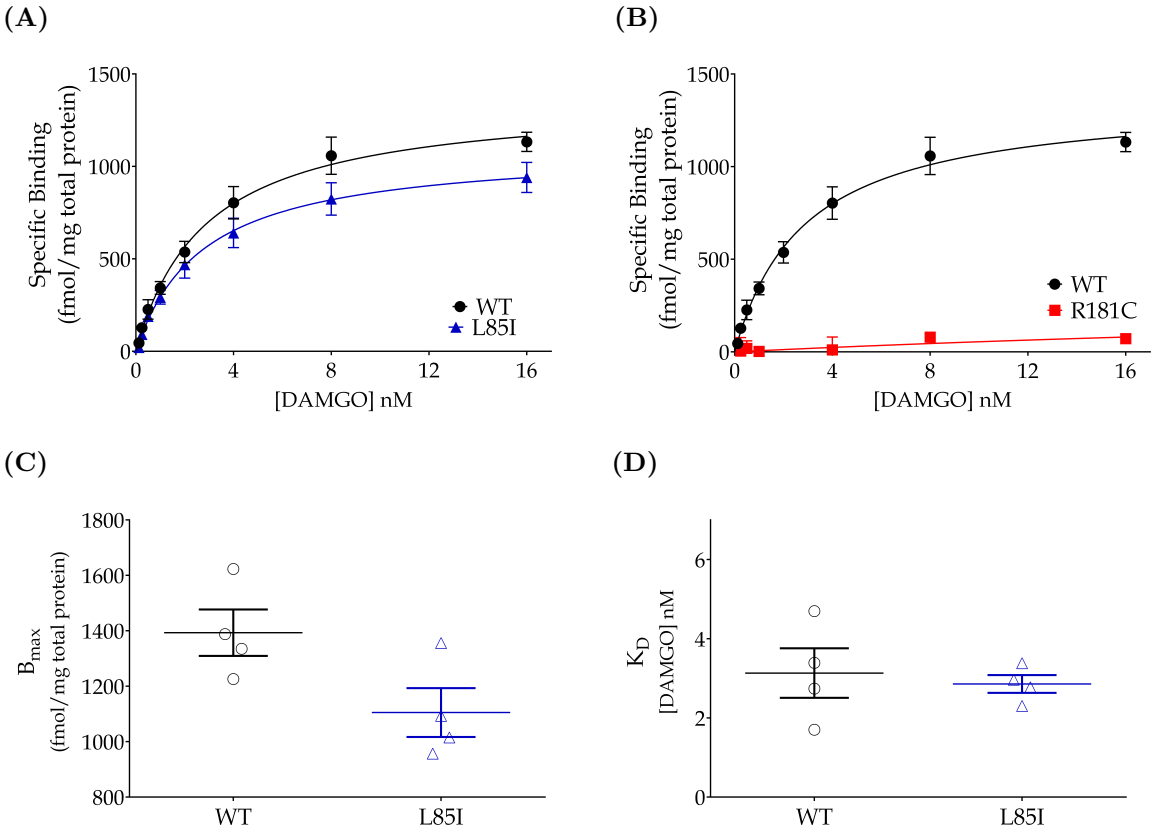

Figure 6.2. hMOPr-WT, hMOPr-L85I and hMOPr-R181C expression in AtT20 cells. **(A)** Saturation binding curve of [^{3}H]DAMGO in intact AtT20-hMOPr-WT and AtT20-hMOPr-L85I. **(B)** Saturation binding curve of [^{3}H]DAMGO in intact AtT20-hMOPr-WT and AtT20-hMOPr-R181C. This polymorphism deeply compromised receptor binding at concentrations tested. **(C)** B_{max} results. **(D)** K_D results. No significant difference in B_{max} or K_D was observed between cells expressing hMOPr-WT and hMOPr-L85I (t-test, p>0.05). Data represent the mean ± SEM, n=4.

Considering the binding result for AtT20-hMOPr-R181C, it was necessary to assess the presence of the receptor on the cell surface. Immunocytochemistry technique was performed as describe in methods (Section 3.7) without the permeabilisation step, and hMOPr-R181C are clearly present in the cell surface and no apparent difference was observed between AtT20 cells expressing hMOPr-R181C and hMOPr-WT as shown on Figure 6.3. Therefore R181C polymorphism severely compromised DAMGO ability to bind to receptor in AtT20 cells.

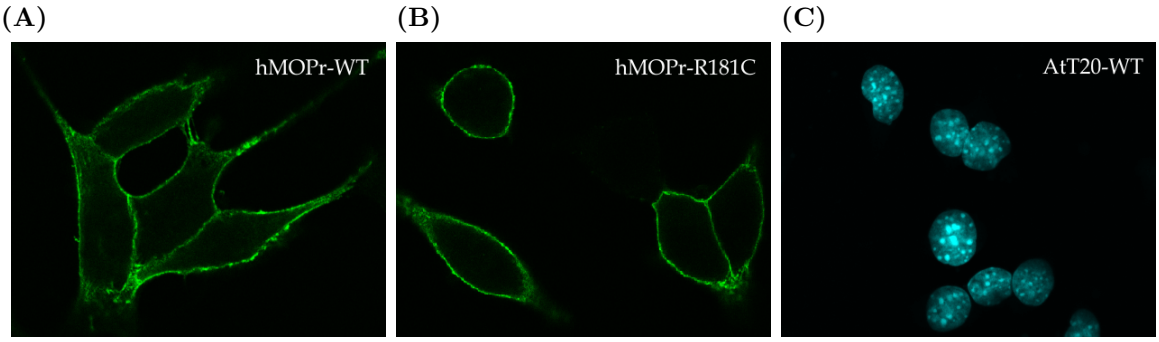

Figure 6.3. Evidence of hMOPr-R181C and hMOPr-WT expressed in AtT20 cells membrane. Fluorescence confocal images of non-treated **(A)** AtT20-hMOPr-WT, **(B)** AtT20-hMOPr-R181C and **(C)** AtT20-WT cells. HA-488 conjugated antibody was used to label hMOPr on cell surface. Image obtained under a 488nM laser excitation with fixed gain. AtT20-WT also showing merged UV channel with DAPI staining of the nucleus. Data are representative confocal images from three independent experiments.

6.2.2 Human MOPr Signalling via GIRK Channel Activation

Activation of GIRK channels by MOPr hyperpolarises neurons and inhibits nociceptive action potential transmission[250]. To assess the effect of L85I and R181C hMOPr polymorphism on this important pathway, changes in membrane potential in transfected populations of AtT20 cells after treatment with varying concentrations of opioids or SST were recorded using FLIPR® membrane potential dye.

Figures 6.4**(A)** and 6.4**(B)** illustrate representative traces of data collected for DAMGO and methadone concentration response curves (CRCs) in AtT20-hMOPr-R181C. Out of the six opioids tested (DAMGO, β-endophin, methadone, morphine, buprenorphine and pentazocine), DAMGO was the only tested opioid to mediate a clear response in this variant, however with a dramatically reduced efficacy, E_{max} of 11±1%, and potency, pEC50 of 6.3±0.1, when compared with hMOPr-WT E_{max} of 34±1% and pEC_{50} of 8.4±0.1 (Figure 6.5, Table 6.1). Methadone also appeared to elicit a response from 1μM concentration but higher concentrations produced a distinct membrane potential depolarisation, this could be as a result of GIRK channels blockage as previously reported for this opioid[232].

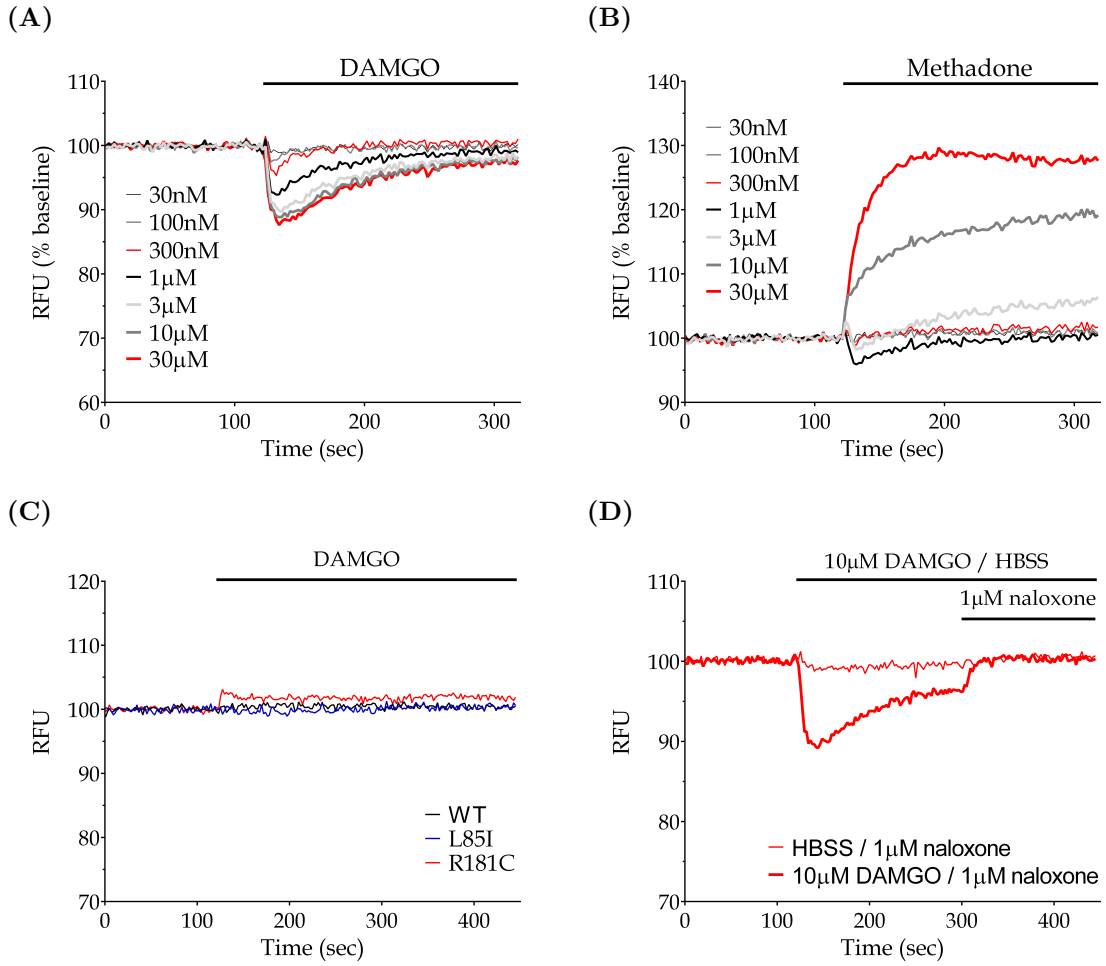

Figure 6.4. Representative traces showing change in fluorescence signal, corresponding to membrane hyperpolarisation/depolarisation, following application of varying concentrations of **(A)** DAMGO and **(B)** methadone to AtT20-hMOPr-R181C. R181C polymorphism compromised DAMGO and methadone stimulated hyperpolarisation. Methadone directly blocked GIRK channels at high concentrations as previously reported[232]. **(C)** Overnight treatment with 200ng/mL pertussis toxin (PTX) abolished DAMGO signalling at all variants as expected for $G_{i/o}$ mediated signalling. **(D)** Opioid antagonist naloxone can reverse DAMGO signal at R181C variant and it did not affect membrane potential baseline supporting that DAMGO signal was hMOPr-R181C specific and this variant was not constitutively activated. PTX and naloxone data from three experiments in duplicate normalised to baseline.

Overnight incubation with pertussis toxin (PTX) was able to block the response to DAMGO in both variants tested, showing that hyperpolarisation was $G_{i/o}$ mediated (Figure 6.4(C)); furthermore at R181C variant naloxone was able to restore membrane potential to baseline and did not affect basal membrane potential which confirms that DAMGO signal was evoked by activation of hMOPr-R181C, and suggests that this

receptor was not constitutively active (Figure 6.4**(D)**).

The L85I polymorphism did not affect signalling via GIRK channel in AtT20 cells, as shown in Figure 6.5 and Table 6.1, where potency (E_{max}) and efficacy (pEC_{50}) of a range of compounds are presented and compared to WT.

The ability of AtT20 cell populations to hyperpolarise across all different cell lines was assessed by determining SST CRCs. The differences observed in CRCs were not related to variances in the cell lines ability to hyperpolarise, as somatostatin efficacy and potency were similar between all hMOPr variants (t-test, $p<0.05$).

Table 6.1. Summary of opioid efficacy and potency of GIRK activation in AtT20 cells expressing WT, L85I or R181C hMOPr

GIRK activation	**E_{max}(%)**			**pEC_{50}**		
Opioid	WT	L85I	R181C	WT	L85I	R181C
β-Endorphin	35±1	32±2	N/A	7.1±0.2	7.0±0.1	N/A
DAMGO	34±1	32±2	11±1*	8.4±0.1	8.5±0.1	6.3±0.1*
Methadone	33±1	29±3	N/A	7.3±0.1	7.3±0.1	N/A
Morphine	**31±1**	**29±2**	N/A	7.6±0.1	7.6±0.1	N/A
Buprenorphine	**22±1**	**20±2**	N/A	7.0±0.1	7.1±0.1	N/A
Pentazocine	**7±1**	**7±1**	N/A	7.2±0.1	7.0±0.1	N/A
SST	33±1	32±1	34±2	8.3±0.1	8.3±0.1	8.3±0.2

Opioids are listed in rank order of maximal effect at MOPr-WT. Opioids with E_{max} significantly lower than DAMGO are set in bold (one-way *ANOVA*, followed by t-test, corrected for multiple comparisons, $p<0.05$). Marked with * are results significantly different to hMOPr-WT (t-test, $p<0.05$).Values shown are mean ± SEM, n=5-6.

Figure 6.5.*(following page)*: Opioid agonists and SST concentration response curves in AtT20 expressing WT (black), L85I (blue) and R181C (red) hMOPr. **(A)** DAMGO, **(B)** β-endorphin, **(C)** methadone, **(D)** morphine, **(E)** buprenorphine and **(F)** pentazocine signalling were not affect by L85I polymorphism. R181C variant abolished signalling from all opioids but DAMGO where efficacy and potency were dramatically reduced (t-test, $p<0.05$). Note that **(G)** SST signalling was similar between cell lines (t-test, $p>0.05$), thus inability of hMOPr-R181C to signal was receptor not cell related. Data represent the mean ± SEM of pooled data from 5-6 independent determinations performed in duplicate.

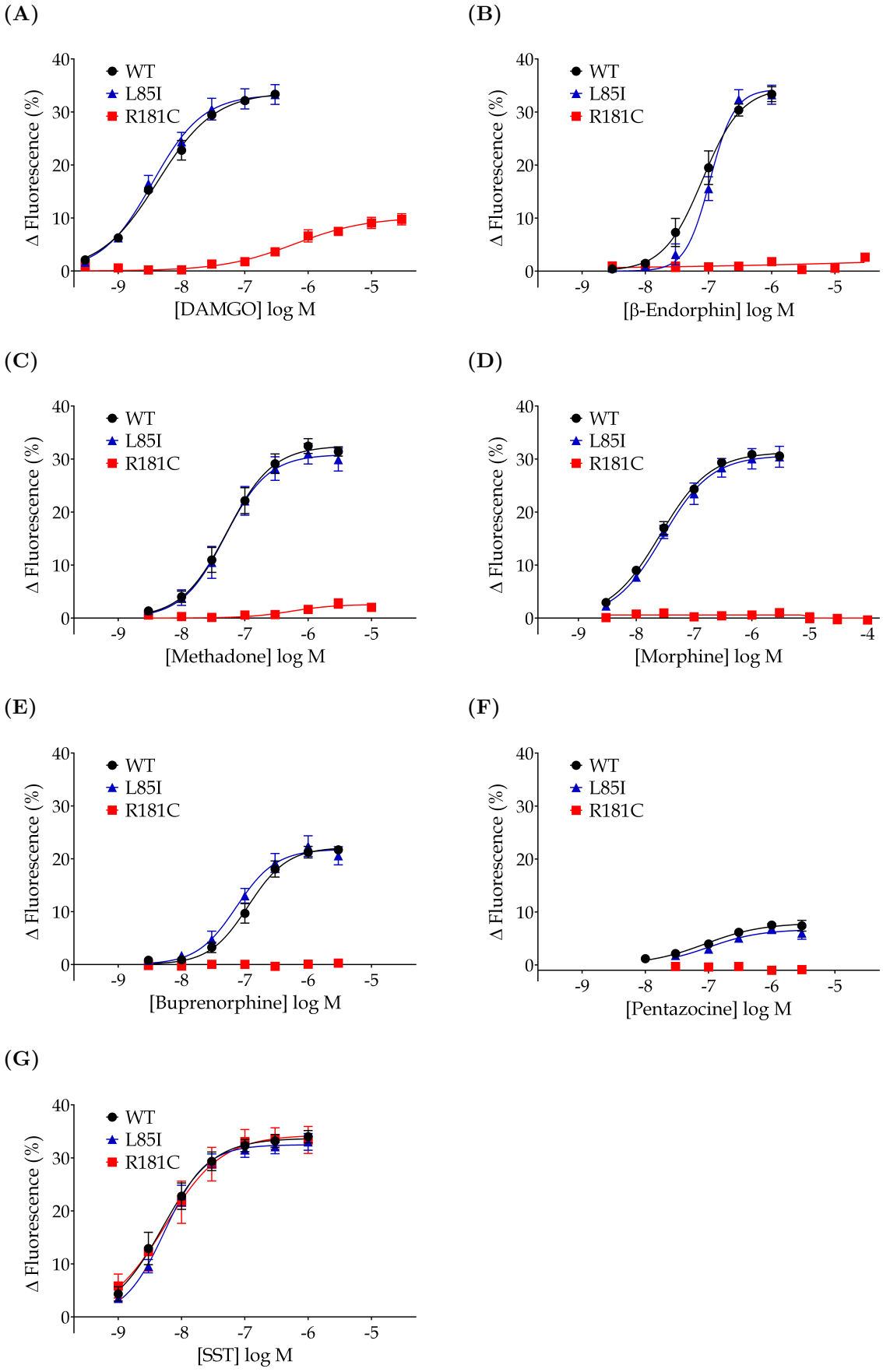
(A)
WT
L85I
R181C
Δ Fluorescence (%)
[DAMGO] log M
(B)
[β-Endorphin] log M
(C)
[Methadone] log M
(D)
[Morphine] log M
(E)
[Buprenorphine] log M
(F)
[Pentazocine] log M
(G)
[SST] log M

6.2.3 Opioid-Mediated Signal Desensitisation in AtT20 cells

AtT20-hMOPr-WT and AtT20-hMOPr-L85I were previously shown to be differently regulated by chronic exposure to morphine when examining cAMP levels and gene expression (CRE)[287]. In the present work, acute DAMGO and morphine induced desensitisation of hMOPr signalling via GIRK channel was assessed for these variants as previously described in the methodology chapter (Section 3.5). Desensitisation was also determined for R181C polymorphism; and considering how the signalling through this pathway was deeply affected, two different protocols were used. Firstly DAMGO concentrations were as regularly used for all variants, 1μM stimulus followed by 10μM challenge, but in the second protocol higher concentrations were used: 10μM DAMGO as stimulus and 30μM for challenge. Representative traces for this last protocol are presented in Figure 6.6. Note that after 10μM DAMGO stimulus adding 30μM DAMGO did not result in any signal hyperpolarisation and SST signal was barely altered.

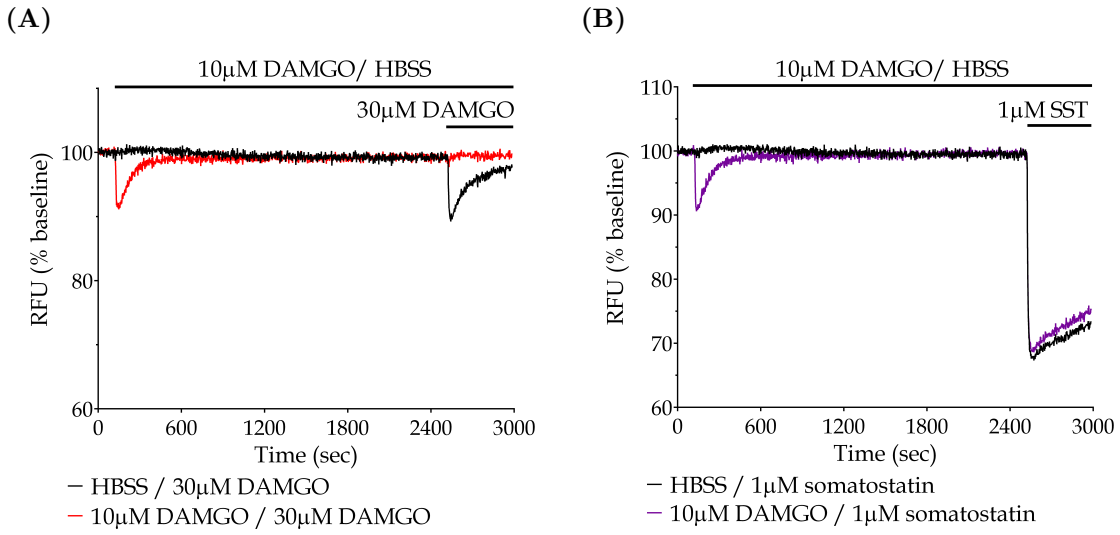

Figure 6.6. Representative traces of **(A)** homologous and **(B)** heterologous desensitisation in AtT20-hMOPr-R181C stimulated for 40 minutes with 10μM DAMGO before a challenge concentration of DAMGO (30μM) or SST (1μM) was added. Difference in maximum response was used to calculate desensitisation and plot a time course. Signal decay was fitted to a one-phase exponential association and time constant (τ) obtained.

Figure 6.7 and Table 6.2 show that L85I polymorphism did not affect signal desensitisation by DAMGO or morphine. In contrast, DAMGO induced homologous and heterologous desensitisation at hMOPr-R181C were significantly different to hMOPr-WT (two-way *ANOVA*, $p<0.05$). Homologous desensitisation by 10μM DAMGO stimulus resulted in a complete signalling desensitisation, while 1μM DAMGO caused a faster rate ($t^1/_2$ of 3.6±0.6 min) but a similar extent of desensitisation (D_{max} of 73±4%) of hMOPr-R181C evoked GIRK channel currents when compared with hMOPr-WT ($t^1/_2$ of 12.4±2.9 min and D_{max} of 66±1%). Somatostatin signalling after 1μM and 10μM DAMGO stimulus in AtT20-hMOPr-R181C was reduced by less than 10% compared with SST alone, which made heterologous desensitisation at this variant hard to quantify and likely to be biologically irrelevant. This is in stark contrast to hMOPr-WT which showed substantial heterologous desensitisation of somatostatin receptor signalling after DAMGO stimulus.

Table 6.2. Summary of desensitisation time course $t^1/_2$ and D_{max} in AtT20 cells expressing WT, L85I or R181C hMOPr

	$t^1/_2$(min)			**D_{max}(%)**		
Opioid	WT	L85I	R181C	WT	L85I	R181C
Homologous desensitisation						
DAMGO	12.4±2.9	7.8±1.3	**3.6±0.6***	66±1	63±4	73±4
Morphine	7.5±1.3	5.8±0.7	N/A	61±2	62±4	N/A
Heterologous desensitisation						
DAMGO	14.2±4.1	8.3±1.5	N/A	55±2	50±4	N/A
Morphine	12.2±5.8	4.4±1.0	N/A	25±2	20±4	N/A

Desensitisation data were fitted to a one-phase exponential association and $t^1/_2$ and D_{max} (plateau) obtained. Note that desensitisation at R181C variant was only obtained for DAMGO, and data presented are for 1μM stimulus since 10μM stimulus, in addition to both heterologous desensitisation data set, did not fit the exponential curve. Highlighted is the only result significantly different to hMOPr-WT (*t*-test, $p<0.05$). Values shown are mean ± SEM, n=4-6.

Signal decay after opioid stimulus was also assessed using time constant (τ) and maximum decay (Y_{max}) obtained from one-phase association fit into signal recorded (Table 6.3). L85I polymorphism did not change decline in signalling when compared

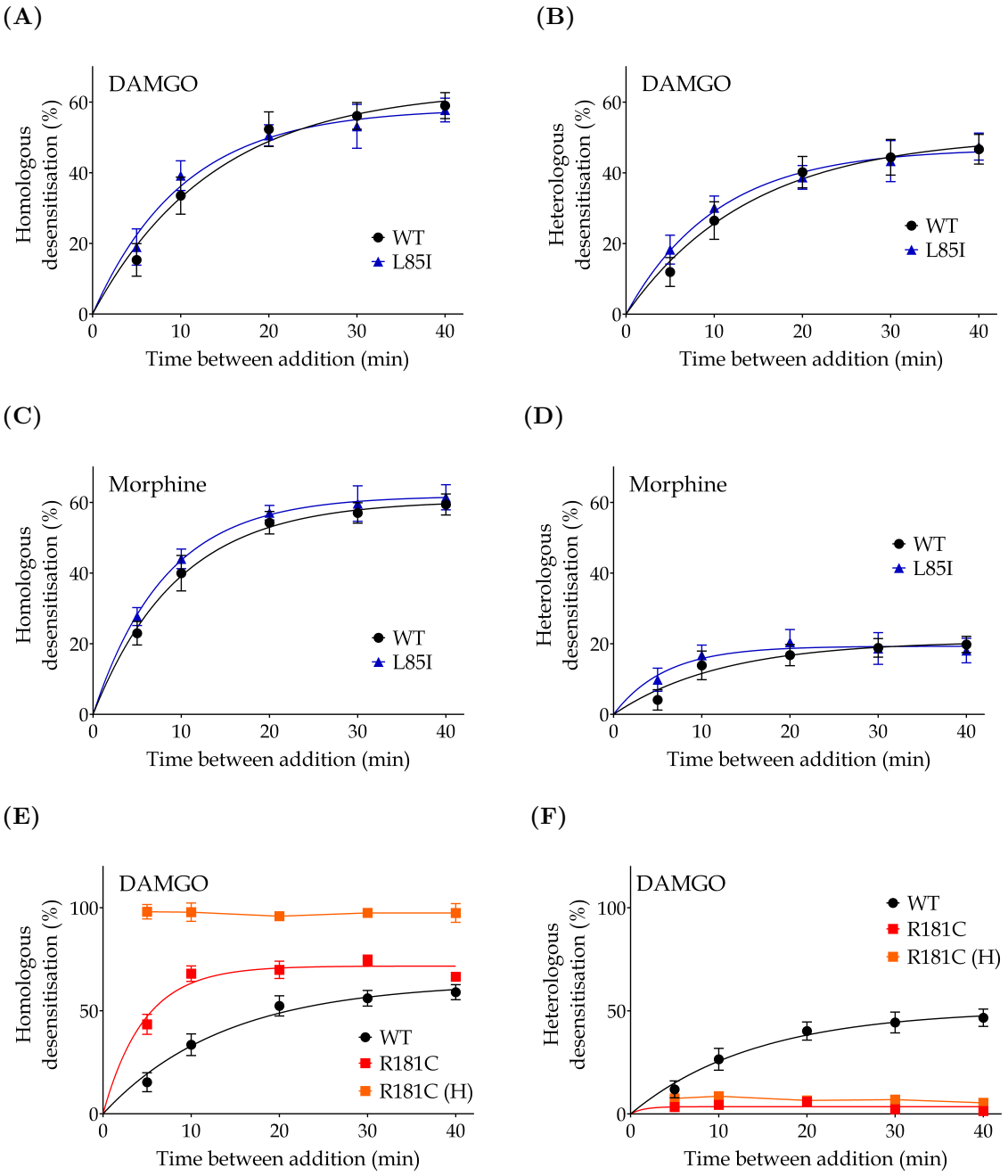

Figure 6.7. In AtT20 cells, homologous and heterologous desensitisation time courses were not affected by L85I polymorphism, in stark contrast to R181C variant (two-way *ANOVA*, $p<0.05$). **(A)** Homologous and **(B)** heterologous desensitisation after 1μM DAMGO stimulus, and **(C)** Homologous and **(D)** heterologous desensitisation after 1μM morphine stimulus in hMOPr-L85I (blue) and hMOPr-WT (black). **(E)** Homologous and **(F)** heterologous desensitisation after 1μM (red) or 10μM (orange) DAMGO stimulus. 10μM DAMGO produced a complete signal desensitisation at R181C variant and did not significantly affect SST signalling; a one-phase exponential curve could not be fitted to these data points. Data are expressed as percentage desensitisation from vehicle control, and represent the mean ± SEM of 4-6 independent determinations performed in duplicate.

to hMOPr-WT (t-test, p>0.005), while R181C variant had a much faster rate of decay for both DAMGO concentrations and most interestingly signal returned to resting membrane potential (Y_{max} of 100±1%), which was not observed for hMOPr-WT (Y_{max} of 94±1, t-test, p<0.0001).

Table 6.3. Summary of time constant (τ) and maximum decay (Y_{max}) of signal in AtT20 cells expressing WT, L85I or R181C hMOPr

	τ(sec)			Y_{max}(%)		
Opioid	WT	L85I	R181C	WT	L85I	R181C
DAMGO (1μM)	898±131	947±190	**129±79***	94±1	94±1	**100±1***
DAMGO (10μM)			**109±13***			**100±1***
Morphine	612±76	601±81	N/A	96±1	95±1	N/A

Signal decay data were fitted to a one-phase exponential association and $t^1/_2$ and Y_{max} (plateau) obtained. Highlighted are results significantly different to hMOPr-WT (t-test, p<0.05). Values shown are mean ± SEM, n=4-6.

6.2.4 Opioid-Mediated Phosphorylation of hMOPr Ser377

To better understand receptor regulation, the effect of L85I and R181C polymorphisms on phosphorylation of Ser377 residue of hMOPr was assessed after exposure to 1μM morphine and 1μM DAMGO for 5 or 30 minutes. The commercially available selective antibody to phosphorylation on Ser377 was used as described on methods (Section 3.6) and data are presented in Figure 6.8.

DAMGO mediated robust phosphorylation of Ser377 at 5 and 30 minutes time points in hMOPr-WT, thus all results were normalised to DAMGO induced phosphorylation on Ser377 of hMOPr-WT (100%). L85I polymorphism decreased DAMGO induced phosphorylation at both 5 (74±6%, one-sample t-test, p=0.0456) and 30 minutes treatment (77±3%, one-sample t-test, p=0.0215). Morphine mediated phosphorylation was similar after 5 and 30 minutes exposure in WT and L85I variants; at 5 minutes 29±4% phosphorylation was observed for hMOPr-WT and 33±10% for hMOPr-L85I; and at 30 minutes incubation 20±5% phosphorylation was observed for hMOPr-WT and 19±4%for hMOPr-L85I (t-test, p>0.05, n=3).

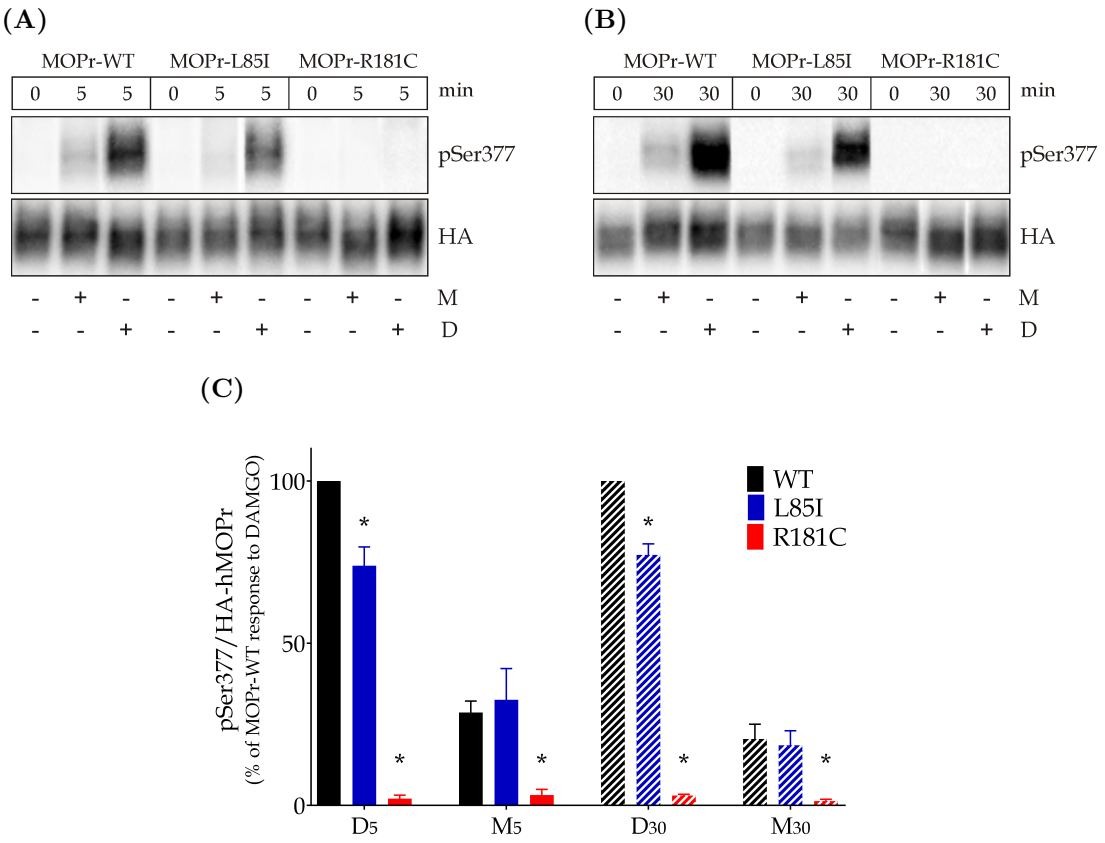

Figure 6.8. Morphine and DAMGO induced phosphorylation of hMOPr Ser377 residue in AtT20 expressing hMOPr variants. **(A)** and **(B)** are representative blots from one of three independent experiments of 5 or 30 minutes opioid treatment respectively . AtT20 cells stably transfected with hMOPr-WT, hMOPr-L85I or hMOPr-R181C were either not exposed (-) or exposed (+) to 1μM DAMGO (D) or 1μM morphine (M) for 5 or 30 minutes. The cells were lysed and immunoblotted with anti-pSer377 antibody (pSer377, upper panel), then blot was stripped and reprobed with anti-HA antibody to detect total hMOPr (HA, lower panel). Further methods details are described in Section 3.6 **(C)** Densitometric analysis of Ser377 residue phosphorylation induced by morphine and DAMGO exposure for 5 (no pattern) or 30 minutes (stripe pattern). Morphine stimulated a similar phosphorylation of Ser377 while DAMGO induced a slightly lower extent of phosphorylation of Ser377 in hMOPr-L85I when compared to hMOPr-WT (one-sample t-test, $p<0.05$). hMOPr-R181C polymorphism abolished Ser377 phosphorylation by morphine and DAMGO (t-test, $p<0.05$). Data are presented as % of DAMGO-induced Ser377 phosphorylation (pSer377) in AtT20-hMOPr-WT (100%) ± SEM; note that all results were corrected for total receptor number (pSer377/HA).

The hMOPr-R181C Ser377 residue was not phosphorylated by agonists tested. Furthermore, western blot results for total hMOPr (HA antibody) confirmed significant hMOPr-R181C expression.

6.2.5 Loss of Membrane hMOPr and internalisation

The effect of L85I and R181C polymorphisms in agonist-induced loss of cell surface receptor following 5 and 30 minutes stimulation with varying concentrations of DAMGO and morphine was assessed using a whole-cell ELISA technique (Section 3.8); results are presented in Figure 6.9.

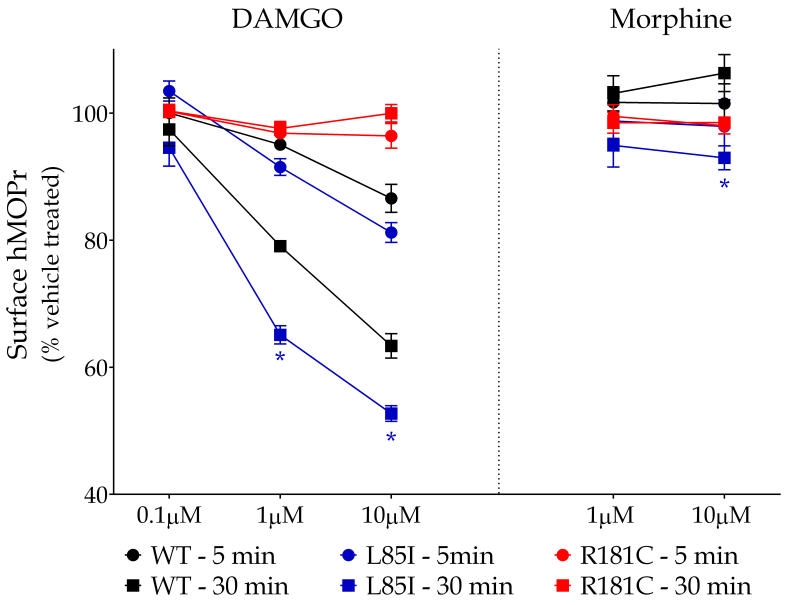

Figure 6.9. Loss of surface hMOPr-WT, hMOPr-L85I and hMOPr-R181C after DAMGO or morphine incubation for 5 or 30 minutes in AtT20 cells. 0.1μM DAMGO and 1μM morphine did not induce membrane hMOPr loss in WT and L85I variant, but a significant difference at 30 minutes time point with 10μM morphine at L85I variant was observed (one-sample t-test, $p>0.05$). A DAMGO induced concentration dependence of hMOPr-WT and hMOPr-L85I loss from the cell surface was observed, where the amount of hMOPr on membrane was reduced after 1μM and 10μM stimulus when compared with 0.1μM (t-test, $p<0.05$). When comparing polymorphisms with hMOPr-WT, R181C polymorphism deeply affected receptor moviment from the membrane, while hMOPr-L85I surface loss was increased when incubated for 30 minutes with 1μM or 10μM DAMGO (two-way *ANOVA*, corrected for multiple comparisons, $p<0.05$ marked with *). Interestingly a small but significant difference induced by 10μM morphine in L85I was detected (t-test, $p<0.05$ marked with *). Data obtained using whole cell ELISA technique as described in Section 3.8 and represent the mean ± SEM of pooled data from 4-5 independent determinations performed in triplicate.

A similar concentration dependent loss of hMOPr-WT and hMOPr-L85I was observed for DAMGO, however after 30 minutes incubation the decrease of L85I variant on surface was significantly higher for the 1μM (65±1%) and 10μM DAMGO (53±1%) when compared with hMOPr-WT (79±1% [1μM] and 63±2% [10μM], t-test, $p<0.05$).

Most interestingly, after 30 minutes incubation with 10μM morphine a small surface loss of hMOPr-L85I was observed (93±2, one-sample t-test, $p<0.05$), thus presenting a different regulation when compared to hMOPr-WT (106±2, t-test, $p<0.05$). Note that no significant increase in hMOPr-WT on cell surface after morphine treatment was observed (one-sample t-test, $p>0.05$).

No significant change in surface hMOPr-R181C quantity was observed after DAMGO or morphine exposure when compared to same cells without opioid stimulus (one-sample t-test, $p>0.05$); this is in agreement with phosphorylation results.

Therefore cell surface hMOPr loss was abolished at R181C polymorphism and increased at L85I variant when compared to hMOPr-WT.

6.3 Discussion

In this chapter two rare hMOPr polymorphisms with very different profiles were assessed. L85I polymorphism impact on the biological function of hMOPr was predicted by PROVEAN (Protein Variation Effect Analyser) software[325] to be neutral, while R181C amino acid substitution to be deleterious; according to the data obtained in this study these predictions were mostly right as shown in Table 6.4.

Examining the crystal structure of mMOPr published by Manglik et al. (2012)[220], it was possible to observe that the first transmembrane (TM) helix was not directly involved in the binding pocket, as no contact between this helix and the ligand used (β-FNA) was determined. However, the importance of this TM helix should not be underestimated as TM helices of GPCRs are very important for transmitting messages to the intracellular signalling domains, and residues in TM1 is predicted to be part of the sodium pocket, which plays a crucial role in receptor activation[115]. Despite crystal structure studies showing TM5 and TM6 as the main dimer interface, TM1, TM2

Table 6.4. Summary of L85I and R181C polymorphisms findings

hMOPr variant	Assay performed	Key observations
L85I	Radioligand binding	Similar expression and affinity
	GIRK activation	Similar efficacy and potency for all opioids tested
	Desensitisation time course	Similar homologous and heterologous desensitisation for morphine and DAMGO
	Signal decay	Similar rate and extent of decay for DAMGO and morphine
	Ser377 phosphorylation	DAMGO induce phosphorylation to a lesser extent at 5 and 30 minutes
	Cell surface hMOPr loss	Higher DAMGO and morphine concentrations increased loss at 30 minutes
R181C	Radioligand binding	No binding detected, however surface receptors confirmed by ICC
	GIRK activation	Only DAMGO evoked a clear response but with much lower potency and efficacy
	Desensitisation time course	1μM DAMGO induced faster but similar extent of homologous desensitisation 10μM DAMGO induced complete homologous desensitisation Low heterologous desensitisation
	Signal decay	Faster rate of decay and complete return to resting membrane potential
	Ser377 phosphorylation	Not phosphorylated
	Cell surface hMOPr loss	No surface receptor loss

All results are in comparison with hMOPr-WT.

and helix 8 was also associated to oligomerisation, probably of higher order. A recent study using molecular dynamics simulations showed that mMOPr forms homodimers mainly between interfaces TM5/TM5 and TM1-TM2/TM5-TM6[278]; hence, supporting the importance of TM1 for dimer formation. The change of leucine to isoleucine in L85I in the TM1 is not expected to dramatically alter receptor conformation and function, since these amino acids have similar hydrophobicity and size. However, a subtle change could disrupt the interface for oligomerisation; note that mutation of TM1 was previously reported to disrupt heterodimer between MOPr and δ-opioid receptor (DOPr)[148]. In the present study in AtT20 cells, L85I polymorphism when compared to

WT variant did not affect receptor signalling and desensitisation measured via membrane potential change. Nevertheless, alteration in DAMGO phosphorylation and total surface receptors was detected, and most interesting morphine was also able to induce a small loss in surface hMOPr-L85I. This last finding was already reported by two other studies in HEK293 cells[81,287], but they observed a much higher extent of surface receptor loss mediated by morphine but no change mediated by DAMGO. It is important to note that in one study[81], L83I rat orthologue was used and time of exposure to 10μM DAMGO was only 5 minutes, a time point where no difference was found here; and interestingly approximately two-fold higher receptor loss measured by ELISA was observed in HEK293 cells when compared to AtT20 cells. Morphine internalisation was much more prominent in HEK293 cells in both mentioned studies than in AtT20, this suggests a higher efficacy of HEK293 cells phosphorylation and/or endocytosis machinery which may be explained by different level of protein expression; notably Atwood et al. (2011)[15] reported that HEK293 cells expressed a much higher and larger variety of mRNA levels of GPCR related signalling proteins such as GRK than AtT20 cells.

Many studies have demonstrated that MOPr are present not only as a monomer but also as homodimers and homotetramers, in addition to forming heteromers with other GPCRs[129,345]. The co-internalisation of hMOPr-L85I and hMOPr-WT mediated by morphine was previously reported in HEK cells coexpressing both variants, this suggested dimerisation of these variants[287]. This does not necessarily contradict the hypothesis that L85I amino acid substitution disrupts dimer interface, if we consider that TM5-TM6 is the main interface, it actually could be only disrupting part of homodimers or formation of oligomers of higher order. The same investigation on co-internalisation assessed coexpression of WT and R181C variants in HEK293 cells and did not find co-internalisation induced by DAMGO with this polymorphism. Thus, in this case dimers were not formed between these two variants, or were not stable to remain dimerised when opioid agonist is present. This would highlight another possibility that L85I polymorphism could actually strengthen dimer interaction; however it still does not explain how morphine mediated internalisation.

While only a small number of published work is available regarding MOPr homodimers, a much larger number can be found on DOPr. The levels of DOPr homodimers are decreased with the increase of agonist, and the time course of internalisation is longer than monomerisation. This suggests that the formation of monomers precedes internalisation, where after separation receptor can recruit necessary machinery for internalisation. Morphine did not affect the levels of dimers or monomers, which was correlated with the inability of morphine to induce internalisation in CHO cells expressing mouse DOPr[91]. The sequences of DOPr and MOPr TM helices are quite similar, 76% homology, thereby it is quite surprising that in DOPr dimers are monomerised to be internalised whist in MOPr dimerisation was suggested to facilitate morphine internalisation[147]. MOPr expressed in HEK293 cells exposed to a subsaturating DAMGO concentration concurrently with a saturating morphine concentration was internalised, differently from both drugs individually. A different way of approaching this findings could be that a low concentration of DAMGO could destabilise the dimers and increase GRK recruitment, which then, as a monomer, morphine induced internalisation would be increased because of higher recruitment of endocytosis related proteins. However, hMOPr-L85I morphine induced internalisation was probably not related to well established regulatory processes for MOPr[236], as Cooke et al. (2015)[81] reported for L83I mutation β-arrestin and Ser377 phosphorylation was not increased compared to rMOPr-WT, but it still required GRK2 and dynamin to internalise. Therefore, it suggests that hMOPr-L85I endocytosis by morphine recruits an unknown pathway which could be similar to observed in another GPCR (leukotriene B_4 receptor 1), where GRK2 and dynamin are necessary but not βarrestin-2[64]. Moreover, this mechanism may be less efficient in AtT20 cells compared to HEK293 cells.

MOPr phosphorylation by GRK is a well established regulatory process efficiently performed by opioid agonist DAMGO, but not efficiently stimulated by morphine. In the present work, morphine did not induce higher Ser377 phosphorylation in hMOPr-L85I variant when compared to hMOPr-WT supporting previous findings by Cooke et al. (2015)[81], in contrast L85I DAMGO phosphorylation was slightly reduced. Taking into consideration that hMOPr can be phosphorylated in many different sites[63],

morphine may increases phosphorylation pattern in a different residue which was not assessed here. Moreover, this could explain DAMGO mediated decrease in Ser377 phosphorylation but increase receptor surface loss, as increased GRK2 affinity to another site could decrease GRK2 availability to phosphorylate Ser377. This could result in overall higher phosphorylation status which may more efficiently recruit endocytosis machinery through regular pathway, or maybe partially through an unknown pathway as mentioned for morphine. It would be interesting to determine not only total hMOPr-L85I phosphorylation but also check specific residues which were previously reported to be poorly phosphorylated by morphine[103].

With regard to hMOPr-L85I polymorphism signalling, our signalling findings via GIRK activation are supported by activation of [^{35}S]-GTPγS binding induced by submaximal concentrations of morphine and DAMGO in HEK293 cells expressing hMOPr-WT and hMOPr-L85I variants[81]. In contrast, the same work also showed that ERK phosphorylation by DAMGO and morphine were reduced in L85I variant; ERK was not studied in this work however it is possible that it could be activated by a G protein independent pathway which is recruited differently by protomers conformation. Furthermore, tolerance and cAMP superactivation mediated by chronic morphine treatment were reported to be reduced in HEK293 cells expressing hMOPr-L85I, when compared with same cells expressing hMOPr-WT. These results were correlated with morphine increasing the ability to drive receptor endocytosis[287]. In this work, morphine induced acute homologous and heterologous desensitisation in transfected AtT20 cells, and signal decay was not affected by L85I polymorphism. It is important to mention that not only differences in pathways but also differences in cell lines used and between chronic and acute processes need to be taken into consideration. Chronic opioid exposure can lead to adaptations in MOPr regulation; therefore, varying regulatory mechanisms between desensitisation and tolerance may be expected, this topic was reviewed by Williams et al. (2013)[356].

In contrast to hMOPr-L85I polymorphism, hMOPr-R181C signalling via GIRK channels activation was dramatically compromised. In contrast to a previous report which characterised this variant as a complete loss-of-function mutation[287], in the

present study DAMGO induced signalling was detected via GIRK activation, but with a threefold decline in maximum effect and over 100-fold decrease in potency. The decrease in DAMGO binding to hMOPr-R181C is definitely one of the factors involved in these results; however how this happen can be speculated by assessing GPCRs conformation and function studies of the ICL2 and surrounding regions. Li et al. (2001)[204] reported that the aspartic acid residue of the rMOPr DRY motif is important to stabilise the receptor in inactive conformation; while four mutants of this residue became constitutively active, one mutant had lower basal [^{35}S]GTPγS binding and reduced affinity for DAMGO. This less active mutant assumed a more stable conformation than the wild-type receptor. Possibly a similar conformation could be achieved by R181C mutation as cysteine can form disulfide bonds which has a well established role in the folding and stabilization of proteins; however, this bonds are commonly unstable in the cytosol as it is a strongly reducing environment. Another conceivable hypothesis is that the removal of the polar bridge between R181C, reported by Manglik et al. (2012)[220] for mMOPr, will cause a change in conformation that will affect the normal interaction between G proteins and the DRY motif.

Interestingly Wilbanks et al. (2002)[355] showed that a mutation in the aspatic acid residue of the DRY motif of two well studied GPCRs, α_{1b} adrenergic and angiotensin II type IA receptors, resulted in constitutive desensitisation and internalisation of the receptor coupled to β-arrestin. Another study supported the involvement of the second intracellular loop in ligand-activated receptor induced β-arrestin recruitment by showing the importance of a conserved proline on position 9 (starting from DRY motif) for β-arrestin binding and mediated internalisation[224]. In the present study, the R181C variant was probably not constitutively active and hMOPr signalling by DAMGO could still be desensitised even though DAMGO signal was strongly reduced. Ser377 was not phosphorylated and cell surface hMOPr-R181C loss was not significantly different between treated and non treated cells. It is important to point out that the lack of cell surface receptor loss and Ser377 phosphorylation could be related to MOPr-R181C not being well stabilised in an active form of the drug-bond receptor. This is supported by the low efficacy obtained, and assays not being sensitive enough to capture changes

in a small population of receptors. Following the same line of thought, the best explanation for low affinity would once again be related to receptor conformation. Using a simplistic ternary complex model probably the equilibrium between G protein uncoupled and coupled were dramatically shifted to the uncoupled side of the equation; in consequence of R181C polymorphism restraining the receptor in a conformation that is unlikely to couple to G proteins, the low affinity state.

A plausible explanation to the difference in affinity to DAMGO found between the present study and the previous reported could be related to the G proteins expressed in the cell lines tested. Out of the 5 G proteins preferentially stimulated by MOPr[75], AtT20 only express G_{i2} in significant mRNA levels, while HEK293 cells expressed G_{i2},G_{i3} and G_z according to Atwood et al. (2011)[15]. In cannabinoid receptor CB_1, the second intracellular loop plays a major role in the specificity of which G protein couples to the receptor, thus I could hypothesise that R181C variant may changed the second loop to conformation where affinity to G_i proteins are dramatically reduced while G_z could be maintained. That would explain why AtT20-hMOPr-R181C cells K_D for DAMGO is reduced as GPCR coupled to G proteins adopt a conformation with higher ligand affinity[334], and cells with more G_z protein such as HEK293 cells would bind with higher affinity to DAMGO. Furthermore Ravindranathan et al. (2009)[287] have used a mutated G_i protein to check for calcium release, if the affinity for this G protein is dramatically reduced, and HEK293 cells express another G protein with higher affinity to this polymorphic receptor, it would justify why they did not detect any signalling.

Little heterologous signal desensitisation was observed when R181C was exposed to high concentrations of DAMGO, thus GIRK channels were not desensitised and G proteins were available, however a fast but similar extent of homologous desensitisation was observed with 1μM DAMGO stimulus, and a complete desensitisation at 5 minutes with 10μM DAMGO stimulus. The data presented suggests that for 1μM DAMGO exposure in AtT20-hMOPr-R181C the absence of phosphorylation and surface loss of receptor could be related to a faster receptor desensitisation but not extension of it. Nevertheless, the complete desensitisation by a saturating DAMGO concentration

was probably related to receptor conformation, where we could speculate that after signalling receptors may be constrained to a non-active conformation. This would also explain the fast and complete decay of membrane potential to resting state after agonist stimulus. Birdsong et al. (2013)[32] corroborates with this speculation that agonist change in hMOPr conformation could change affinity and desensitisation, however in hMOPr-WT it would be long-lasting but reversible while interaction is strengthen in hMOPr-R181C then harder to reverse or irreversible.

Another plausible explanation to a higher desensitisation of hMOPr-R181C signalling by a saturating DAMGO concentration could be that because affinity is so radically affected by this polymorphism, effectively there is no DAMGO receptor reserve. As previously shown[79], if there is little receptor reserve, an increase in apparent rate of desensitisation can be anticipated.

It is important to note that polymorphic homozygous genotypes are highly unlikely with rare polymorphisms, with exception of highly inbred populations. Cells expressing heterozygous genotype signalling and regulation may show a different profile to data presented here, as one polymorphism can be dominant as previously reported for trafficking[287]. Especially in regards to R181C, which function is compromised, establishing the effect of this polymorphism in carriers would be interesting to determining if hMOPr-WT can dominate and neglect the R181C polymorphism, thus generating a irrelevant biological difference between WT homozygous and WT/R181C heterozygous genotype carriers. Also examining L85I polymorphism in the clinics may elucidate one of the major questions regarding the link between morphine internalisation and tolerance.

Overall, only small differences in AtT20-hMOPr-L85I signalling and regulation were observed. Although unlikely to be relevant clinically, these differences point to a mechanism of hMOPr regulation still not elucidated. In addition, taking into consideration the location of the amino acid change in L85I polymorphism, a possible involvement of receptor dimerisation need to be considered and further assessed. The hMOPr-R181C polymorphism signalling and regulation were deeply affected. Better understanding

this variant molecular mechanisms may help to answer some important questions regarding receptor conformation, regulation and G protein binding.

7

The 3rd Intracellular Loop: hMOPr SNPs and Phosphosite Mutants

The third intracellular loop is a highly conserved region across all opioid receptors and it has been linked with G protein coupling and signal transduction. In this chapter we investigate three rare naturally occurring single-nucleotide polymorphisms (SNPs) in addition to three phosphosite mutants of the third intracellular region. The focus is on the role of this region not only in hMOPr signalling, but also in receptor regulation.

Contents

7.1 Introduction

The importance of the third intracellular loop of GPCRs was shown by many studies which highlighted the crucial role this region plays not only in G protein coupling, but also in regulatory processes[130,333]. A single amino acid substitution in the intracellular region can result in a great change in the ability of the receptor to activate signalling pathways, as reported in the last chapter; in addition, it can help to elucidate how a receptor region is involved in signal transduction and regulation. Furthermore, better understanding the role of phosphorylation sites can contribute valuable information on molecular mechanisms underlying MOPr activity.

Three rare hMOPr SNPs in the third intracellular loop (ICL3) were part of this study (Figure 7.1). Out of the three missense mutations, two produced a substitution of an arginine to a histidine at positions 260 (R260H) and 265 (R265H), while one variant changed position 268 amino acid from serine to proline (S268P) thus deleting a potential phosphorylation site. R260H polymorphism was first identified by Bond et al. (1998)[38] in a study of opioid addiction where only one heterozygous individual of 152 subjects presented the allele G779A (R260H). Hoehe et al. (2000)[152] in another genetic study of opioid users described the other two ICL3 polymorphisms, G794A (R265H) and T802C (S268P), also with a low allele frequency of one in 172 African-Americans subjects each (<1%). Note that the allele frequency of these SNPs in the general population is unknown but assumed to be rare considering the low number of reports in the current literature. Aside from the description of the existence of variants in opioid dependence and addiction studies, the low number of subjects expressing these

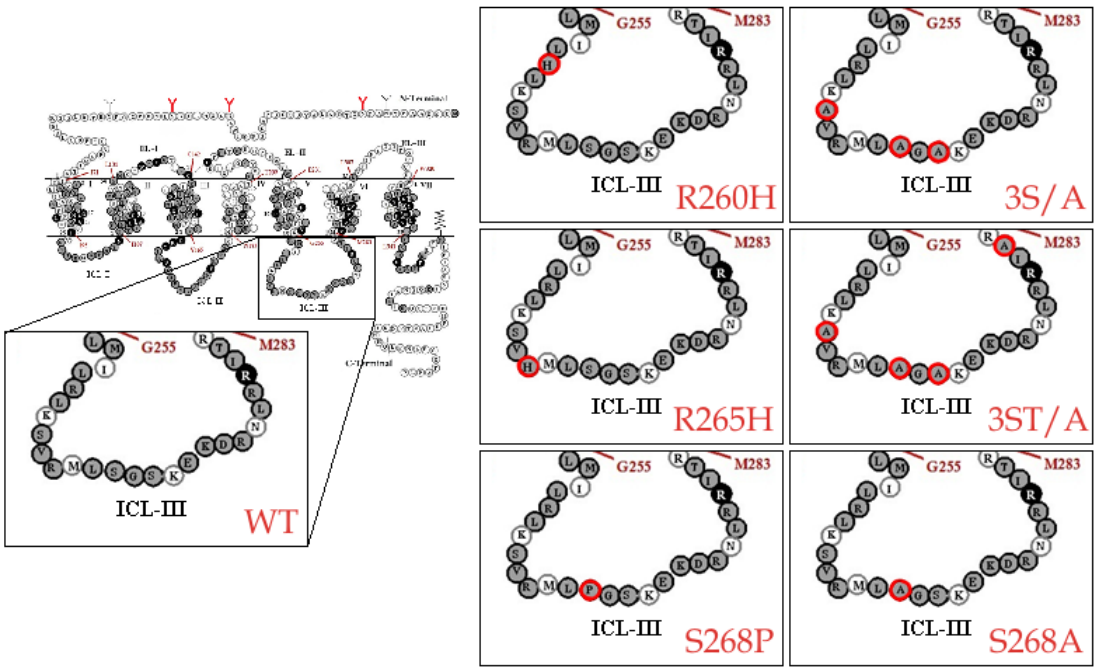

Figure 7.1. Serpentine structure of the human μ-opioid receptor with area enlarged showing third intracellular loop amino acid sequence for all seven variants studied. SNPs (left panel) and phosphosite mutations (right panel) altered amino acids are highlighted in red. Adapted figure from Center for Opioid Research and Design (CORD)[83].

variants has limited the correlation of these hMOPr polymorphisms with opioid abuse.

Only a few studies had investigated the effect of these ICL3 polymorphisms in receptor signalling and regulation. Overall, all three SNPs negatively affect hMOPr ability to signal measured via GTPγS binding and adenylyl cyclase inhibition (reviewed by Knapman and Connor in 2015[180]). An early study by Belfort et al. (2001)[27] researched the effect of R265H and S268P SNPs in GTPγS binding in COS cells and reported lower DAMGO efficacy for both variants and lower potency only at hMOPr-S268P. Since hMOPr-S268P signalling was deeply compromised, it was further assessed using a reporter gene responsive to cAMP levels in transiently transfected HEK293 cells, morphine, DAMGO and β-endorphin potency and efficacy were also reduced. Another study also using a reporter gene to determine adenylyl cyclase (AC) inhibition by MOPr corroborated the above findings by showing DAMGO and endomorphin-1 efficacy was reduced for S268P and R265H, while potency was also reduced for R260H[125]. R260H efficacy was only reported to be affected by Wang et al. (2001)[350]

in a GTPγS binding assay in HEK293 cell exposed to morphine. In the same study, R265H and S268P polymorphisms were reported to decrease calmodulin interaction with hMOPr and reduce tolerance measured using GTPγS binding assay. These could be related to interference on calcium/calmodulin-dependent protein kinase II (CaMKII) phosphorylation.

The ICL3 region of the hMOPr contains four potential phosphorylation sites: three serines (Ser263, Ser268 and Ser270) and one threonine (Thr281), note that rat and mouse MOPr N-terminal have two amino acids deleted, thus the amino acid position is always different by two (e.g. Ser263 in human is Ser261 in rat or mouse). Chen et al. (2013)[63]demonstrated the ability of CaMKII, PKC and GRK2 to phosphorylate the rat MOPr ICL3 peptide; however, they did not identify which residues were specifically phosphorylated by which kinase. ICL3 phosphorylation by CaMKII had been previously reported to modulate desensitisation of MOPr signalling using *Xenopus* oocytes and HEK293 expression systems[184,237]. Although initially two residues of the rat MOPr ICL3, Ser261 and Ser266, were identified as CaMKII phosphorylation sites, further studies confirmed Ser266 as the primary site[185]. Mutation of this residue to alanine decreased the DAMGO induced rate of acute signal desensitisation via GIRK activation measured using signal decay in *Xenopus laevis* oocytes when compared to the wild-type receptor; a similar result was observed for the hMOPr type when S268P variant was assessed.

Capeyrou et al. (1997)[54] investigated the effect of a hMOPr with all ICL3 and C-terminal serine and threonine mutated to alanine on affinity and cAMP accumulation in CHO-KI-hMOPr. This phosphosite mutant has a much lower expression than hMOPr-WT, while affinity and potency were similar, but efficacy was almost halved for all agonists tested which included morphine and DAMGO. Furthermore, both receptors after chronic exposure to morphine, DAMGO and etorphine caused tolerance and adenylyl cyclase (AC) superactivation, however whilst hMOPr-WT was downregulated with DAMGO the mutated receptor was upregulated. This last result is in agreement with the importance of the C-terminal phosphorylation for trafficking[171], however it is hard to separate the effect of the ICL3 and C-terminal in the results presented and the

difference in expression could have an impact in the results.

Therefore to better understand the consequence of deleting exclusively the ICL3 phosphorylation sites, here we substituted serine/threonine to alanine producing three phosphosite mutants of the hMOPr (Figure 7.1): single point mutation hMOPr-S268A (Ser268), all serine substitutions hMOPr-3S/A (Ser263, Ser268 and Ser270) and all phosphorylation sites of the ICL3 region mutation hMOPr-3ST/A (hMOPr-3S/A mutations and Thr281). The hMOPr-S268A was constructed to directly compare with hMOPr-S268P and determine the involvement of this potential phosphorylation site loss in signalling and regulation. mMOPr crystal structured study showed a polar interaction between threonine 279 and arginine 165 of the DRY motif, in addition this threonine residue is part of the 28 residues involved in the dimerisation of mMOPr via TM5-TM6 interface interaction[220]. Substitution of the Thr279 to lysine resulted in a constitutive active receptor, while change to aspartic acid did not affect basal [^{35}S]GTPγS binding and decreased DAMGO receptor activation also measured by [^{35}S]GTPγS binding[154]. Considering these studies we constructed hMOPr-3S/A and hMOPr-3ST/A, thus we could determine the consequences of deleting the serines without the influence of the predicted deleterious substitution of Thr281.

In the present study, the effect of three rare SNPs and three phosphorylation mutants of the hMOPr ICL3 expressed in AtT20 Flp-In cell on signalling and regulation was examined. The Flp-In™ system enables the construction of isogenic cell lines which provides a more comparable system to investigate difference between mutant and wild-type receptors than random mutagenesis. I aimed to re-examine and supplement current knowledge of hMOPr ICL3 variants signalling and desensitisation, in addition to determine Ser377 phosphorylation and acute surface receptor loss.

7.2 Results

7.2.1 Human MOPr Expression in AtT20 Cells

All hMOPr ICL3 SNPs and phosphosite mutants were stably transfected in AtT20 cells using the FlpIn™ system. To reliably assess and compare MOPr variants signalling it is essential to determine receptor density in each cell line to be used, for this purpose whole cell radioligand binding assay was performed using the radioactive opioid ligand [^{3}H]DAMGO. K_D and B_{max} presented in Table 7.1 were calculated based on saturation binding curves fitted to data collected as shown in Figure 7.2.

hMOPr expression measured at whole cell AtT20 was diminished to significantly lower levels only at hMOPr-3S/A and hMOPr-3ST/A. B_{max} of 508±42 fmol/mg total protein was determined for hMOPr-3S/A and 202±9 fmol/mg for hMOPr-3ST/A while a much higher B_{max} of 1393±84 fmol/mg for hMOPr-WT was obtained (*t*-test, $p<0.001$). AtT20-hMOPr-S268P had a slightly lower B_{max} while AtT20-hMOPr-R265H had a slightly higher B_{max} (Table 7.1), however these small differences are unlikely to be relevant. Noticeably affinity (K_D) values were not significantly affected in hMOPr ICL3 variants tested (Table 7.1).

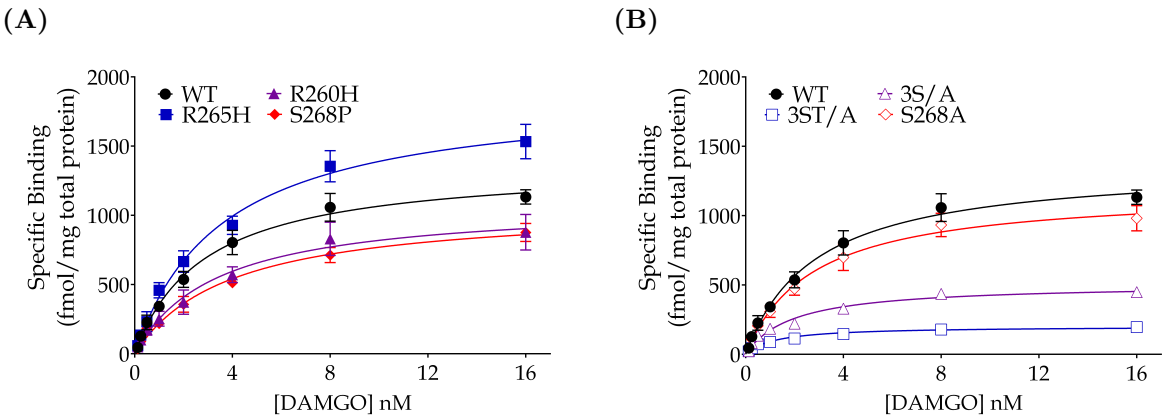

Figure 7.2. ICL3 SNPs and phosphosite mutants expression in AtT20 cells. **(A)** Saturation binding curve of [^{3}H]DAMGO in intact AtT20 expressing ICL3 SNPs. **(B)** Saturation binding curve of [^{3}H]DAMGO in intact AtT20 expressing ICL3 phosphosite mutants. Note that multiple mutations of serine and threonine to alanine in the ICL3 produce a lower receptor expression. Data represent the mean ± SEM, n=3-4.

Table 7.1. Summary of K_D and B_{max} in intact AtT20 cells expressing hMOPr ICL3 variants

		SNPs			Phosphomutants		
	WT	R260H	R265H	S268P	3S/A	3ST/A	S268A
B_{max}	1393±84	1104±146	1893±117*	1071±88*	**508±42***	**202±9***	1190±117
K_D	3.1±0.6	3.6±0.9	3.7±0.4	3.9±0.4	1.9±0.3	1.2±0.1	2.8±0.4

B_{max} in fmol/mg of total protein and K_D in nM. Marked with * are results significantly different to hMOPr-WT (t-test, $p<0.05$) however only results largely different from hMOPr-WT are set in bold (t-test, $p<0.001$).Values shown are mean ± SEM, n=3-4.

7.2.2 Human MOPr Signalling via GIRK Channel Activation

The hMOPr ICL3 region is thought to be involved in G protein coupling. The effect of ICL3 on G protein signalling can be measured in AtT20 cells expressing hMOPr via GIRK activation. To assess cell hyperpolarisation produced by opening of GIRK, FLIPR® membrane potential dye was used and real-time kinetics recorded. A decrease in fluorescence representing membrane hyperpolarisation was detected after opioid exposure (Figure 7.3) and the maximum hyperpolarisation reached for each opioid concentration was used to plot a concentration response curve (CRC) as shown in figures 7.4 and 7.5.

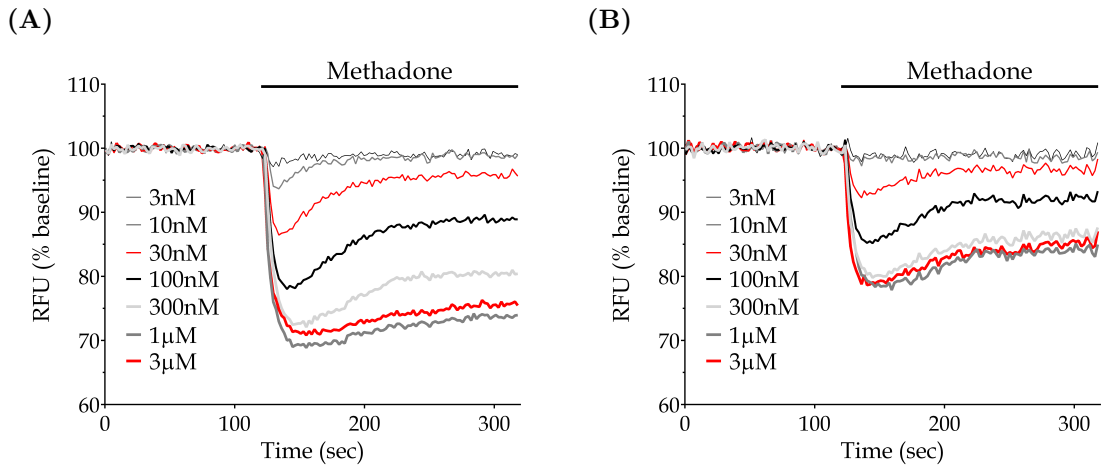

Figure 7.3. Representative traces of change in fluorescence signal, corresponding to membrane hyperpolarisation, induced by varying concentrations of methadone in **(A)** AtT20-hMOPr-WT and **(B)** AtT20-hMOPr-R265H. Methadone efficacy was compromised in R265H polymorphism, however potency was unchanged.

Opioid efficacy at hMOPr ICL3 SNPs was significantly compromised, with the exception of S268P polymorphism in which E_{max} of high efficacious agonists β-endorphin and DAMGO were unaffected (Figure 7.4, Table 7.2). Interestingly, morphine potency and efficacy were greatly reduced at all SNPs especially at R260H variant, where a two-fold decrease of E_{max} was observed (WT 31±1%, R260H 16±2%), in addition to a ten-fold reduction of $p\text{EC}_{50}$ (WT 7.6±0.1, R260H 6.5±0.1). Likewise, methadone signalling was greatly affected, only R265H variant potency was not compromised. Surprisingly, buprenorphine $p\text{EC}_{50}$s were not affected by hMOPr ICL3 SNPs; it was the only opioid tested whose potency was not reduced by R260H polymorphism. Pentazocine failed to promote GIRK activation in cells expressing hMOPr ICL3 SNPs.

Table 7.2. Summary of opioid and SST efficacy and potency of GIRK activation in AtT20 cells expressing hMOPr ICL3 SNPs

GIRK activation	**E_{max}(%)**				**$p\text{EC}_{50}$**			
Opioid	WT	R260H	R265H	S268P	WT	R260H	R265H	S268P
β-Endorphin	35±1	27±2*	26±2*	32±2	7.1±0.2	6.7±0.1*	6.9±0.1	6.7±0.1
DAMGO	34±1	28±2*	26±1*	32±1	8.4±0.1	**7.6±0.1***	8.3±0.1	**7.8±0.1***
Methadone	33±1	21±2*	**20±2***	24±2*	7.3±0.1	**6.3±0.1***	7.0±0.1	6.6±0.1*
Morphine	31±1	**16±2***	**22±1***	**23±1***	7.6±0.1	**6.5±0.1***	**7.3±0.1***	**6.9±0.1***
Buprenorphine	22±1	**7±2***	**14±1***	**10±1***	7.0±0.1	7.1±0.2	7.1±0.1	6.6±0.1
SST	33±1	32±2	34±2	32±1	8.3±0.1	8.1±0.1	8.3±0.1	8.1±0.1

Opioids are listed in rank order of maximal effect at MOPr-WT. Marked with * are results significantly different to hMOPr-WT (t-test, $p<0.05$), however only results largely different from hMOPr-WT are set in bold (t-test, $p<0.001$). Values shown are mean ± SEM, n=5-7.

Figure 7.4.*(following page)*: Opioid agonists and SST concentration response curves in AtT20 expressing WT (black), R260H (purple), R265H (blue) and S268P (red) hMOPr. **(A)** DAMGO, **(B)** β-endorphin, **(C)** methadone, **(D)** morphine and **(E)** buprenorphine signalling were affect by polymorphisms. **(F)** Pentazocine signalling was abolished at all hMOPr ICL3 SNPs. Note that **(G)** SST signalling was similar between cell lines (t-test, $p>0.05$). Data represent the mean ± SEM of pooled data from 5-7 independent determinations performed in duplicate.

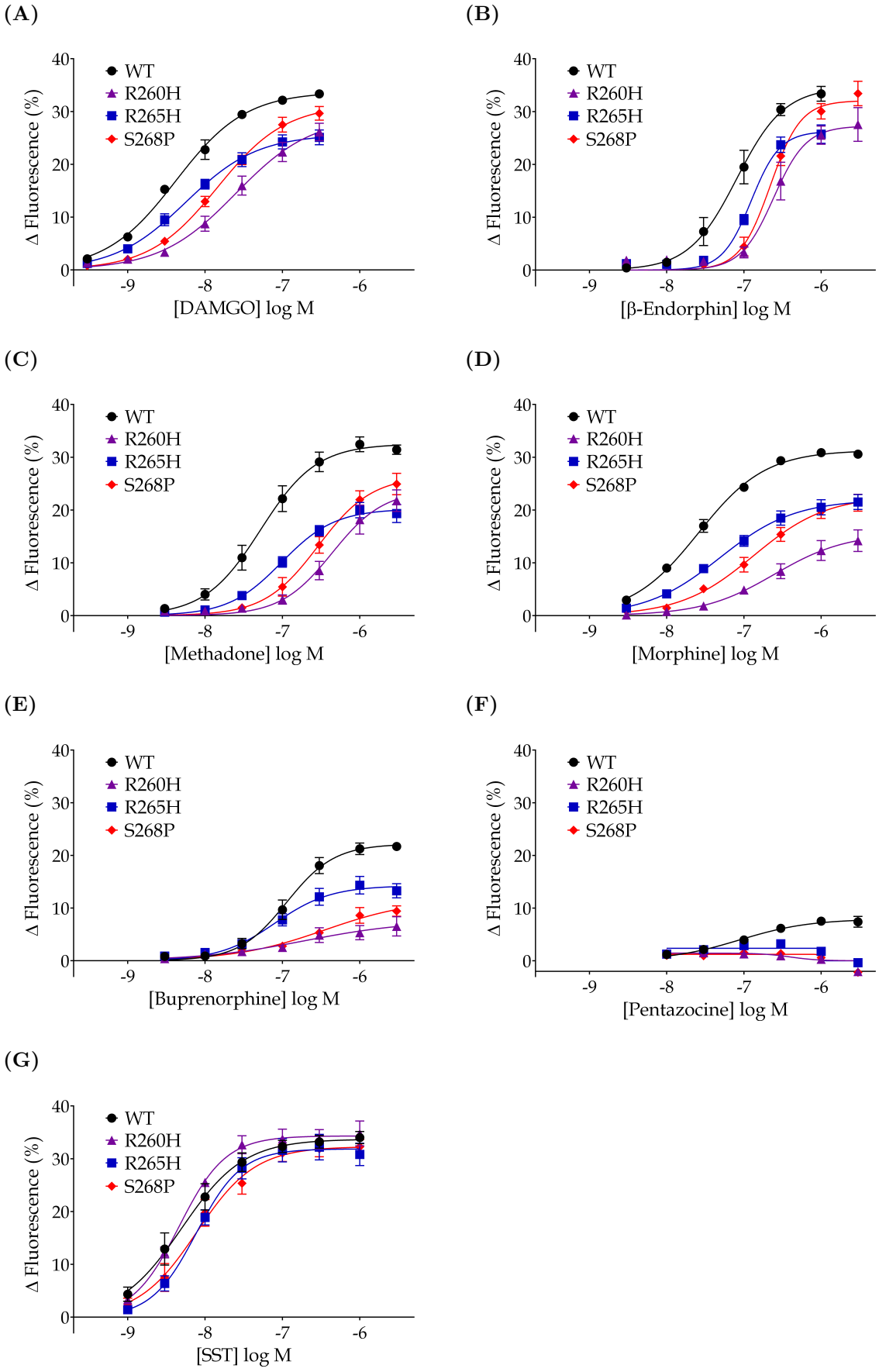
(A)
WT
R260H
R265H
S268P
Δ Fluorescence (%)
[DAMGO] log M
(B)
[β-Endorphin] log M
(C)
[Methadone] log M
(D)
[Morphine] log M
(E)
[Buprenorphine] log M
(F)
[Pentazocine] log M
(G)
[SST] log M

The effect of hMOPr ICL3 phosphosite mutations on GIRK activation is shown in Figure 7.5 and Table 7.3. The decrease in efficacy of all opioids at 3ST/A variant could be correlated to the sevenfold decrease in expression as it affected efficacy but not potency, with the exceptions of morphine and methadone. These two opioids efficacy and potency were also reduced in AtT20-hMOPr-3S/A that was unrelated to almost threefold decrease in expression as reduced potencies were also observed and further supported by unaffected buprenorphine efficacy. The difference in DAMGO induced $p\mathrm{EC}_{50}$ observed between WT and 3S/A variants is probably biologically unimportant, as 3ST/A and 3S/A potency was very similar and only slightly lower than WT and S268A.

In general S268A mutant signalling was similar to hMOPr-WT. Buprenorphine was slightly more potent in AtT20-hMOPr-S268A, with $p\mathrm{EC}_{50}$ of 7.4±0.1 compared with $p\mathrm{EC}_{50}$ of 7.0±0.1 in AtT20-hMOPr-WT (t-test, $p<0.05$). At the same mutant, buprenorphine efficacy was unaffected while pentazocine was slightly less efficacious, hMOPr-WT E_{max} was 7±1% and hMOPr-S268A E_{max} was 5±1%. This is in contrast to S268P polymorphism, where buprenorphine E_{max} was dramatically reduced to 10±1% while $p\mathrm{EC}_{50}$ was not significantly affected (6.6±0.1), in addition to abolished pentazocine signalling. This supports the hypothesis that alteration in signalling observed for S268P polymorphism is not related to the deletion of a phosphorylation site but the substitution of serine to proline, which is the most unflexible amino acid.

The ability of AtT20 cell populations to hyperpolarise across all different cell lines was assessed by determining SST CRCs. Differences observed in CRCs were not related to variances in the cell lines ability to hyperpolarise as somatostatin efficacy and

Figure 7.5.*(following page)*: Opioid agonists and SST concentration response curves in AtT20 expressing WT (black), 3S/A (purple), 3ST/A (blue) and S268A (red) hMOPr. **(A)** DAMGO, **(B)** Endomorphin-2, **(C)** methadone, **(D)** morphine, **(E)** buprenorphine and **(F)** pentazocine signalling at phosphosite mutants. The hMOPr-S268A signalling was similar to hMOPr-WT, only buprenorphine and pentazocine was slightly affected. All opioids efficacy was diminished at hMOPr-3ST/A while at hMOPr-3S/A only morphine, methadone and pentazocine efficacy was significantly reduced. Note that **(G)** SST signalling was similar between cell lines (t-test, $p>0.05$). Data represent the mean ± SEM of pooled data from 5-6 independent determinations performed in duplicate.

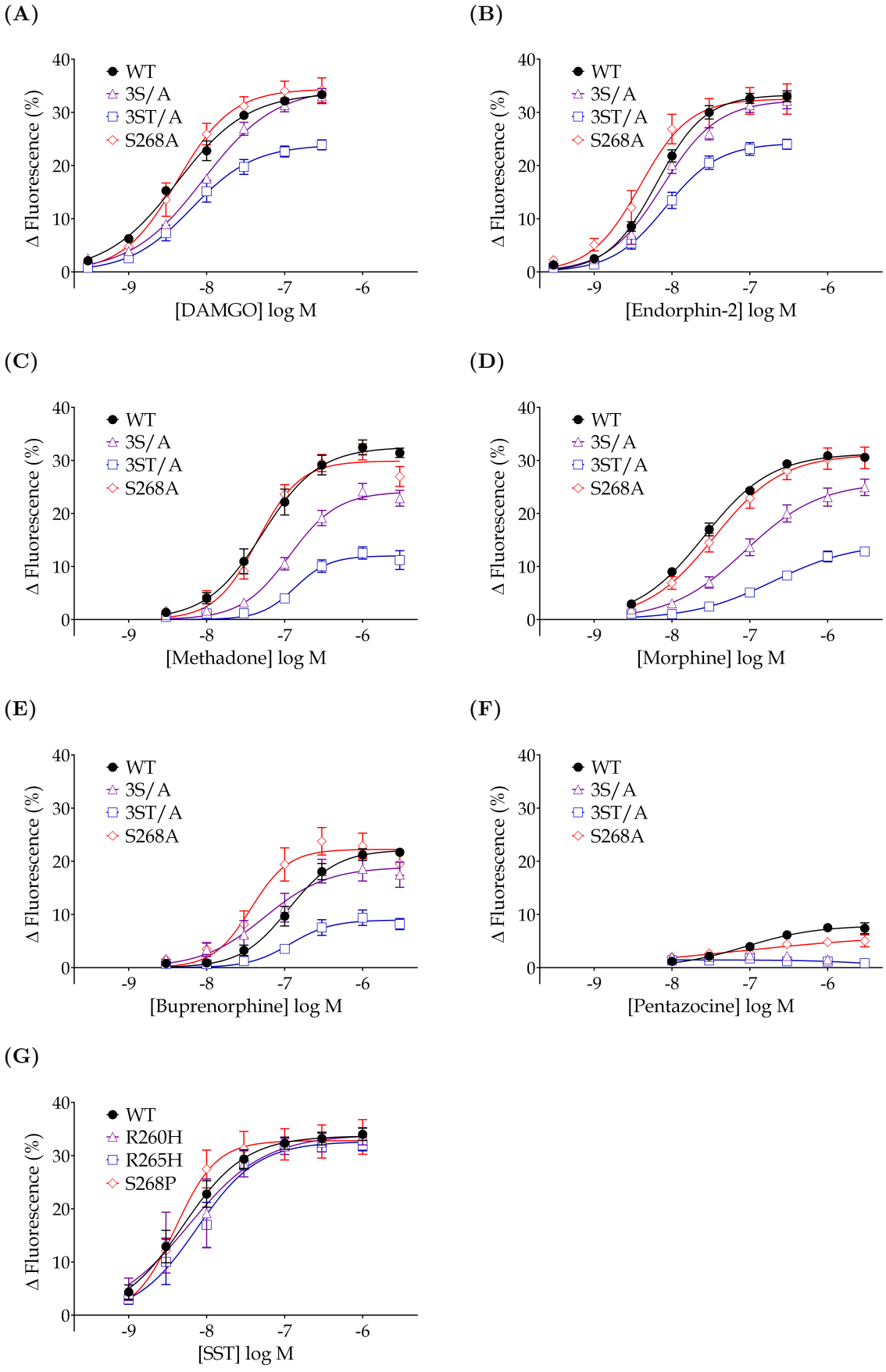
(A)
WT
3S/A
3ST/A
S268A
Δ Fluorescence (%)
[DAMGO] log M
(B)
[Endorphin-2] log M
(C)
[Methadone] log M
(D)
[Morphine] log M
(E)
[Buprenorphine] log M
(F)
[Pentazocine] log M
(G)
R260H
R265H
S268P
[SST] log M

Table 7.3. Summary of opioid and SST efficacy and potency of GIRK activation in AtT20 cells expressing hMOPr ICL3 phosphosite mutants

GIRK activation	**E_{max}(%)**				***p*EC$_{50}$**			
Opioid	WT	3S/A	3ST/A	S268A	WT	3S/A	3ST/A	S268A
DAMGO	34±1	34±1	**24±1***	34±2	8.4±0.1	8.1±0.1*	8.2±0.1	8.4±0.1
Methadone	33±1	25±2*	**12±2***	30±2	7.3±0.1	6.9±0.1*	6.9±0.1*	7.4±1
Endomorphin-2	33±1	32±1	**24±1***	32±3	8.2±0.1	8.2±0.1	8.1±0.1	8.3±0.1
Morphine	31±1	26±2*	**15±1***	31±2	7.6±0.1	**7.1±0.1***	**6.6±0.1***	7.5±0.1
Buprenorphine	22±1	19±2	**9±1***	22±2	7.0±0.1	7.3±0.2	6.9±0.1	7.4±0.1*
Pentazocine	7±1	N/A	N/A	5±1*	7.2±0.1	N/A	N/A	7.1±0.1
SST	33±1	32±1	32±2	33±3	8.3±0.1	8.2±0.2	8.3±0.3	8.4±0.1

Opioids are listed in rank order of maximal effect at MOPr-WT. Marked with * are results significantly different to hMOPr-WT (t-test, p<0.05), however only results largely different from hMOPr-WT are set in bold (t-test, p<0.001). Values shown are mean ± SEM, n=5-6.

potency were similar between all hMOPr variants (Tables 7.2 and 7.3, t-test, p<0.05).

In summary, morphine and methadone signalling was compromised and pentazocine response was abolished at all ICL3 variants with exception of S268A mutant. Buprenorphine efficacy was diminished at all ICL3 SNPs and 3ST/A mutant, however potency was not reduced but in contrast it was increased at S268A mutant. Overall, disregarding 3ST/A which decrease in signalling was probably largely related to lower expression, the SNPs had a much larger effect on signalling than phosphosite deletions which suggests conformation and structural importance over 'basal' phosphorylation state for the third intracellular loop involvement in G protein hMOPr signalling.

7.2.3 Opioid-Mediated Signal Desensitisation in AtT20 cells

Many regulatory processes are possibly involved in receptor signalling desensitisation as reviewed by Williams et al. (2013[356]). The effect of phosphosite mutants on signalling loss is of large interest as phosphorylation of the hMOPr has been frequently correlated to signalling desensitisation. Three hMOPr ICL3 SNPs in addition to the phosphosite mutations where assessed in the previously described desensitisation assay using FLIPR® membrane potential dye (Section 3.5).

Homologous and heterologous desensitisation were examined by stimulating cells

with 1μM morphine or 1μM DAMGO followed by a challenge concentration of 10μM morphine or 10μM DAMGO for homologous or 1μM SST for heterologous. Figure 7.6 demonstrates traces for heterologous desensitisation in AtT20-hMOPr-WT and AtT20-hMOPr-S268P, note that at S268P polymorphism heterologous desensitisation was deeply reduced. The difference in maximum hyperpolarisation for the challenge concentration was compared as previously described, and results plotted in a desensitisation time course according to the time gap between opioid exposures (5, 10, 20, 30 or 40 minutes).

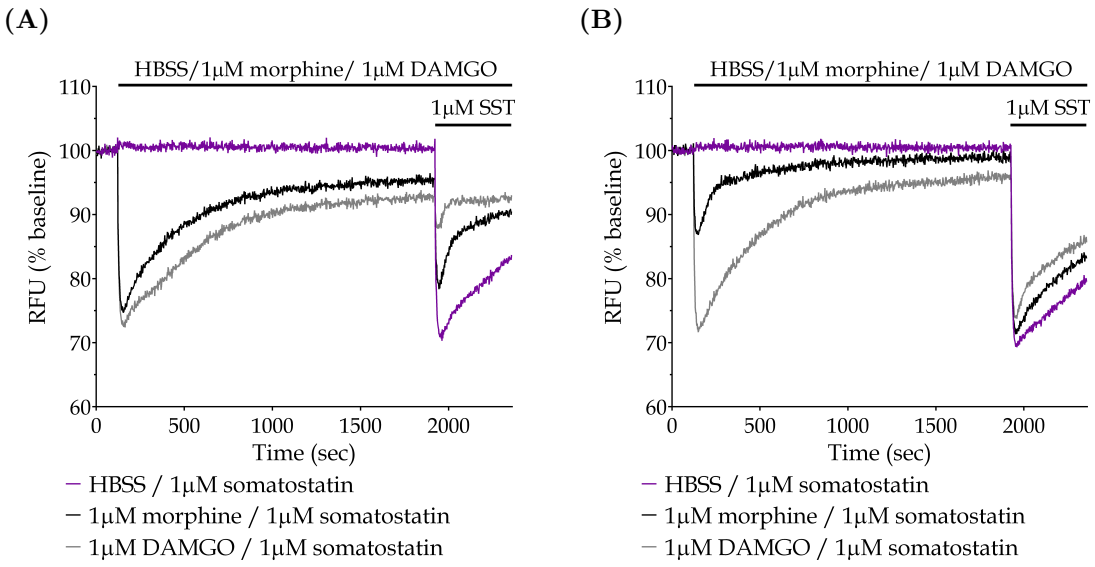

Figure 7.6. Representative traces of heterologous desensitisation mediated by 30 minutes 1μM DAMGO and 1μM morphine stimulus in **(A)** AtT20-hMOPr-WT and **(B)** AtT20-hMOPr-S268P. Difference in 1μM SST maximum response was used to calculate desensitisation and plot a time course. At hMOPr-S268P morphine signal decay was adjacent to baseline after 30 minutes exposure to morphine. In addition, hMOPr-S268P compromised heterologous desensitisation mediated by morphine and DAMGO.

Figure 7.7 shows desensitisation time courses mediated by morphine and DAMGO for hMOPr ICL3 SNPs. R260H variant was the only SNP to significantly affect DAMGO induced homologous desensitisation time course, while both R260H and S268P compromised heterologous desensitisation (two-way *ANOVA*, $p<0.05$). Homologous desensitisation time course by morphine was greatly affected at R260H polymorphism ($p<0.0001$), and a small change was also observed for the other two SNPs

($p<0.05$). To further assess time course results, $t^1/_2$ and maximum desensitisation (D_{max}) were compared between variants and are summarised on Table 7.4. Rate of homologous desensitisation was significantly faster at R260H for both agonists tested however only morphine had a increased D_{max} of 75±2% compared to 61±2% for hMOPr-WT (*t*-test, $p<0.001$). Interestingly, S268P variant had a slightly reduction in DAMGO induced D_{max} 55±2% while morphine not only increased extension of desensitisation (D_{max} 67±2%) but also rate (*t*-test, $p<0.05$).

All three ICL3 SNPs largely reduced heterologous D_{max} where hMOPr-R260H was the most affect variant with D_{max} of 14±2% for DAMGO and 5±1% for morphine compared to hMOPr-WT D_{max} of 55±2% for DAMGO and 25±2% for morphine.

Table 7.4. Summary of desensitisation time course $t^1/_2$ and D_{max} in AtT20 cells expressing hMOPr ICL3 SNPs

	$t^1/_2$(min)				**D_{max}(%)**			
Opioid	WT	R260H	R265H	S268P	WT	R260H	R265H	S268P
Homologous desensitisation								
DAMGO	12.4±2.9	4.3±0.4*	5.5±0.3	6.5±1.0	66±1	68±2	62±2	55±2*
Morphine	7.5±1.3	2.4±0.2*	4.5±0.4	3.9±0.4*	61±2	**75±2***	66±1	67±2*
Heterologous desensitisation								
DAMGO	14.2±4.1	7.5±2	4.5±0.9	8.0±2.6	55±2	**14±2***	**32±1***	**20±5***
Morphine	12.2±5.8	4.6±1	5.3±0.6	7.9±3.6	25±2	**5±1***	**16±1***	**6±1***

Desensitisation data were fitted to a one-phase exponential association and $t^1/_2$ and D_{max} (plateau) obtained. Marked with * are results significantly different to hMOPr-WT, (*t*-test, $p<0.05$) however only results largely different from hMOPr-WT are set in bold (*t*-test, $p<0.001$). Values shown are mean ± SEM, n=4-6.

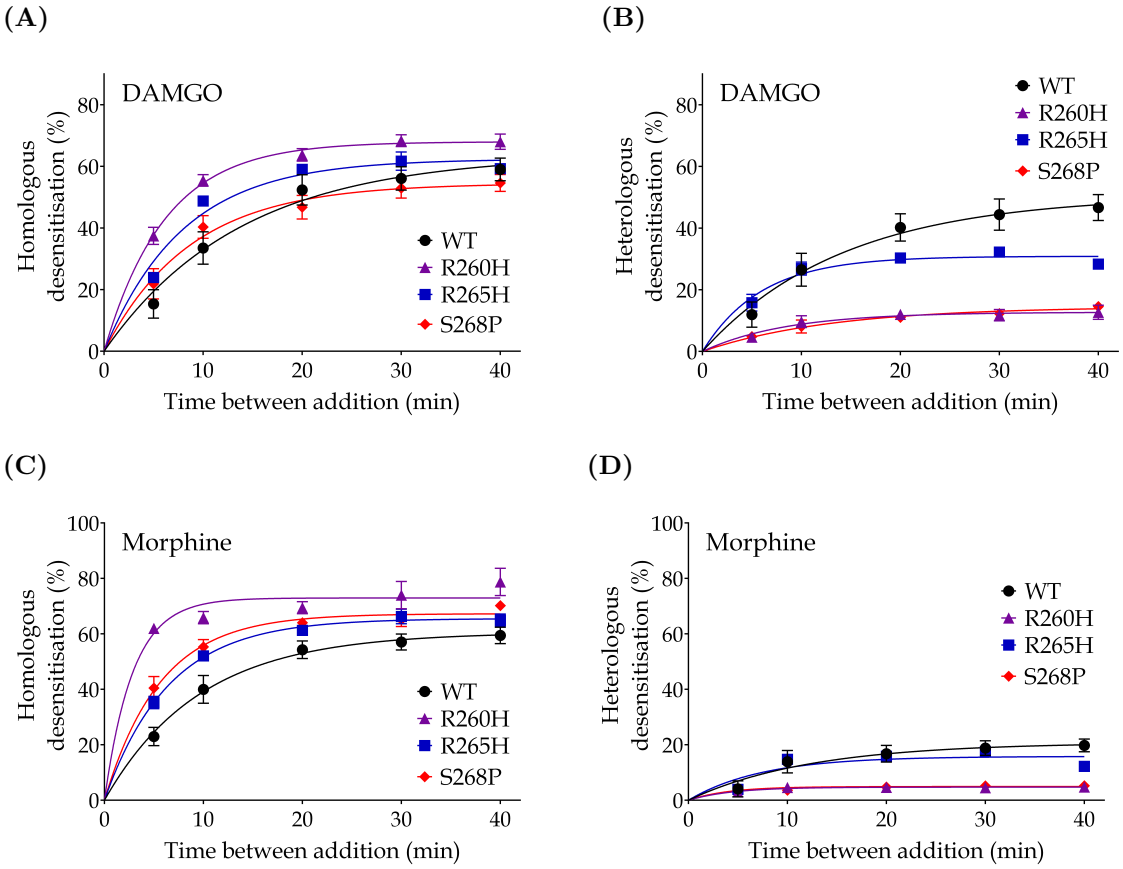

Figure 7.7. Effect of ICL3 SNPs on homologous and heterologous signal desensitisation by DAMGO and morphine in AtT20 cells expressing hMOPr WT (black), R260H (purple), R265H (blue) or S268P (red). **(A)** Homologous and **(B)** heterologous desensitisation after 1μM DAMGO stimulus. **(C)** Homologous and **(D)** heterologous desensitisation after 1μM morphine stimulus. Homologous desensitisation time course at hMOPr-R260H variant was significantly higher while heterologous desensitisation was dramatically reduced for both hMOPr-R260H and hMOPr-S268P (two-way *ANOVA*, $p<0.05$). S268P also slightly affected morphine induced homologous desensitisation. Likewise, R265H polymorphism produced a slightly higher homologous desensitisation, in addition to a lower maximum heterologous desensitisation by DAMGO (*t*-test, $p<0.05$). Data are expressed as percentage desensitisation from vehicle control, and represent the mean ± SEM of 5-6 independent determinations performed in duplicate.

Figure 7.8 shows desensitisation time courses mediated by morphine and DAMGO for hMOPr ICL3 phosphosite mutants. Analysis of variance (two-way *ANOVA, $p<0.05$*) between mutants and WT time courses indicated that hMOPr-3ST/A was the only mutant to affect both homologous and heterologous desensitisation while hMOPr-3S/A also significantly compromised DAMGO induced heterologous desensitisation.

Note that even with a very low receptor expression observed for AtT20-hMOPr-3ST/A, signal did not completely desensitise. Increased homologous D_{max} of 82±3 by DAMGO at hMOPr-3ST/A in comparison with hMOPr-WT of 66±1 was determined. DAMGO and morphine induced heterologous D_{max} was significantly diminished at both 3S/A and 3ST/A mutants. Furthermore, rate of homologous desensitisation was faster at 3ST/A.

Differently from S268P polymorphism, S268A did not affect homologous or heterologous desensitisation, thus desensitisation impact observed at S268P was not caused by phosphosite deletion.

Table 7.5. Summary of desensitisation time course $t^1/_2$ and D_{max} in AtT20 cells expressing hMOPr ICL3 phosphosite mutants

	$t^1/_2$(min)				**D_{max}(%)**			
Opioid	WT	3S/A	3ST/A	S268A	WT	3S/A	3ST/A	S268A
Homologous desensitisation								
DAMGO	12.4±2.9	4.8±0.9	1.7±0.2*	7.0±2.3	66±1	50±4*	**82±3***	60±4
Morphine	7.5±1.3	4.0±0.9	2.0±0.4*	5.2±0.8	61±2	64±4	76±3*	61±4
Heterologous desensitisation								
DAMGO	14.2±4.1	4.3±1.2	7.0±2.1	5.1±1.0	55±2	**20±3***	**6±1***	47±4
Morphine	12.2±5.8	3.7±0.7	3.6±0.5	4.4±1.2	25±2	12±3*	**5±1***	24±4

Desensitisation data were fitted to a one-phase exponential association and $t^1/_2$ and D_{max} (plateau) obtained. Marked with * are results significantly different to hMOPr-WT (*t*-test, ($p<0.05$), however only results largely different from hMOPr-WT are set in bold (*t*-test, $p<0.001$). Values shown are mean ± SEM, n=4-6.

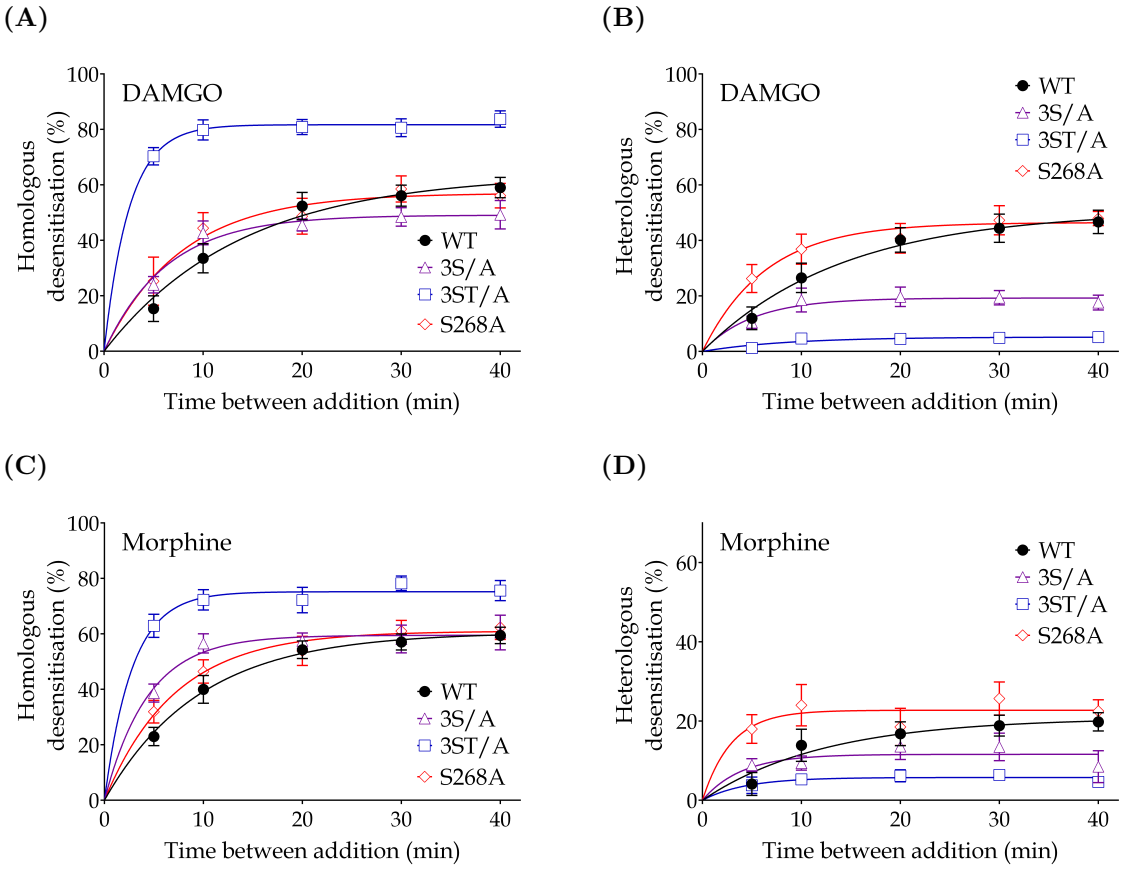

Figure 7.8. Effect of ICL3 phosphosite mutations on homologous and heterologous signal desensitisation by DAMGO and morphine in AtT20 cells expressing hMOPr WT (black), 3S/A (purple), 3ST/A (blue) or S268A (red). **(A)** Homologous and **(B)** heterologous desensitisation after 1μM DAMGO stimulus. **(C)** Homologous and **(D)** heterologous desensitisation after 1μM morphine stimulus. S268A mutation did not affect homologous and heterologous desensitisation (two-way *ANOVA*, $p>0.05$). Homologous desensitisation was also not changed at hMOPr-3S/A, however heterologous desensitisation was deeply compromised (two-way *ANOVA*, $p<0.05$). The phosphosite mutant hMOPr-ST/A had a severe effect on desensitisation, it increased homologous desensitisation while abolishing heterologous desensitisation (two-way *ANOVA*, $p<0.05$). Data are expressed as percentage desensitisation from vehicle control, and represent the mean ± SEM of 5-6 independent determinations performed in duplicate.

To determine if there was a correlation between desensitisation and receptor expression, a scatter plot of desensitisation (D_{max}) versus expression (B_{max}) was produced and is shown in Figure 7.9. Correlation analysis produced r^2, a p value and correlation coefficient (r), which indicated a positive correlation for the homologous desensitisation and a negative correlation for heterologous desensitisation. The value r^2 indicated how much of the variance was shared between desensitisation and expression. Homologous desensitization r^2 of 7% by DAMGO and 21% by morphine were determined, while heterologous desensitisation r^2 of 39% by DAMGO and 26% by morphine were found. No compelling evidence was present in the data analysed to conclude that the correlation was real ($p>0.05$). Therefore desensitisation measured was not a direct effect from receptor expression.

To complement desensitisation data presented above, signalling decay after opioid stimulus was examined by fitting 40 minutes stimulus traces to a one-phase exponential association. Time constant (τ) and maximum decay (Y_{max}) for SNPs and phosphosite mutants are presented in Table 7.6 and Table 7.7 respectively.

Rate and extent of decay stimulated by 1μM morphine and DAMGO was affected by R260H polymorphism and 3ST/A mutant, while R265H only slightly increased rate with no effect on maximum decay. A faster rate and higher decay was determined for morphine in AtT20-hMOPr-S268P, however the same was not observed for S268A mutant. Interestingly maximum decay at R260H, S268P and 3ST/A variants were significantly different from WT, where membrane potential virtually returned to resting potential.

Table 7.6. Summary of time constant (τ) and maximum decay (Y_{max}) of signal in AtT20 cells expressing hMOPr ICL3 SNPs

	τ**(sec)**				$\mathbf{Y}_{max}$**(%)**			
Opioid	WT	R260H	R265H	S268P	WT	R260H	R265H	S268P
DAMGO	898±131	437±47*	546±40*	578±74	94±1	96±1*	94±1	94±1
Morphine	612±76	**144±21***	331±20*	255±26*	96±1	**99±1***	96±1	98±1*

Signal decay data were fitted to a one-phase exponential association and $t^1/_2$ and Y_{max} (plateau) obtained. Marked with * are results significantly different to hMOPr-WT (t-test, $p<0.05$), however only results largely different from hMOPr-WT are set in bold (t-test, $p<0.001$). Values shown are mean ± SEM, n=5-6.

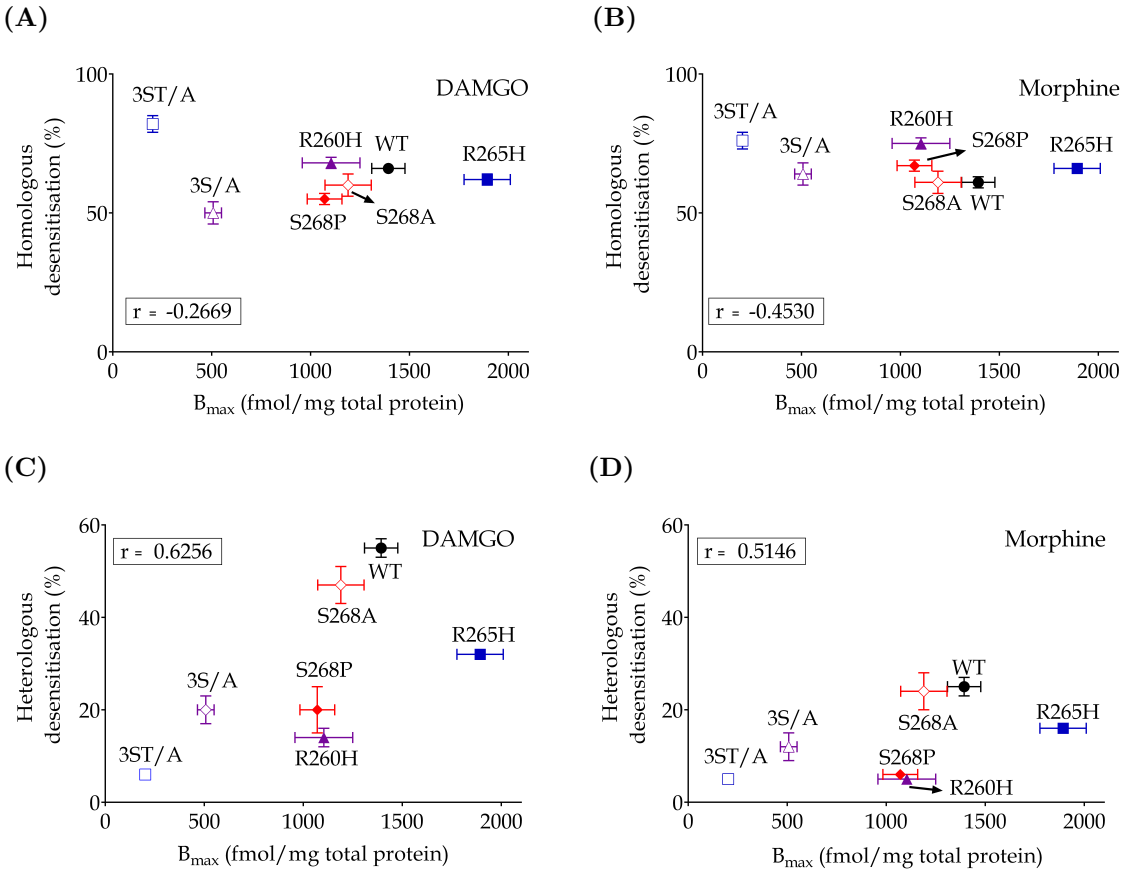

Figure 7.9. Correlation analysis of desensitisation (D_{max}) versus expression (B_{max}) in AtT20 expressing ICL3 variants. **(A)** DAMGO and **(B)** morphine induced homologous desensitisation. **(C)** DAMGO and **(D)** morphine induced heterologous desensitisation. No significant correlation was observed ($p<0.05$). The correlation coefficient (r) indicated a positive correlation between homologous desensitisation and expression while a negative correlation between heterologous desensitisation and expression.

Table 7.7. Summary of time constant (τ) and maximum decay (Y_{max}) of signal in AtT20 cells expressing hMOPr ICL3 SNPs

	τ(sec)				Y_{max}(%)			
Opioid	WT	3S/A	3ST/A	S268A	WT	3S/A	3ST/A	S268A
DAMGO	898±131	584±98	**265±31***	832±142	94±1	92±1	97±1*	91±2
Morphine	612±76	305±54*	**186±25***	459±111	96±1	96±1	99±1*	94±1

Signal decay data were fitted to a one-phase exponential association and $t^1/_2$ and Y_{max} (plateau) obtained. Marked with * are results significantly different to hMOPr-WT (*t*-test, $p<0.05$), however only results largely different from hMOPr-WT are set in bold (*t*-test, $p<0.001$). Values shown are mean ± SEM, n=5-6.

Overall, homologous desensitisation was largely affected by R260H and 3ST/A while

heterologous desensitisation was also affected by R265H, S268P and 3S/A. We also showed by correlation analysis that the differences in receptor expression were not the only factor involved in the results presented here for heterologous and homologous signalling desensitisation.

7.2.4 Opioid-Mediated Phosphorylation of hMOPr Ser377

The effect on agonist dependent phosphorylation of Ser377 residue was assessed for all hMOPr ICL3 variants using Western Blot technique as described in Methods Section 3.6. Cells were exposed to 1μM DAMGO and 1μM morphine stimulus in a similar way to performed in desensitisation assay, thus we could compare phosphorylation levels before opioid challenge at 5 and 30 minutes which are time points where desensitisation maximum are partially and totally reached.

Figure 7.10 shows representative blots for 5 and 30 minutes incubation and densitometric analysis results for ICL3 SNPs. Only R260H variant phosphorylation at Ser377 was significantly affected; DAMGO induced Ser377 phosphorylation was reduced from 100% (WT) to 39±4% at 5 minutes and from 100% (WT) to 37±2% at 30 minutes (one sample t-test, $p<0.05$).

Immunoblots and densitometric analysis for phosphorylation of Ser377 residues at hMOPr phosphosite mutants are shown in Figure 7.11. In agreement with expression results, 3ST/A variant anti-HA band was very faint at similar loading concentration to AtT20-hMOPr-WT (10μg total protein), while no phosphorylation band was observed before hMOPr-WT bands saturated. Therefore a threefold increase on loading concentration of AtT20-hMOPr-3ST/A was used to calculate results presented. Even after increasing concentration, phosphorylation band was not very clear which indicated a lesser phosphorylation at Ser377 than hMOPr-WT. At hMOPr-3S/A variant phosphorylation induced by DAMGO was also decreased; at 5 minutes only 34±14% was detected and at 30 minutes 63±1% compared to 100% phosphorylation of hMOPr-WT (one sample t-test, $p<0.05$). No significant differences between WT and S268A variants were observed.

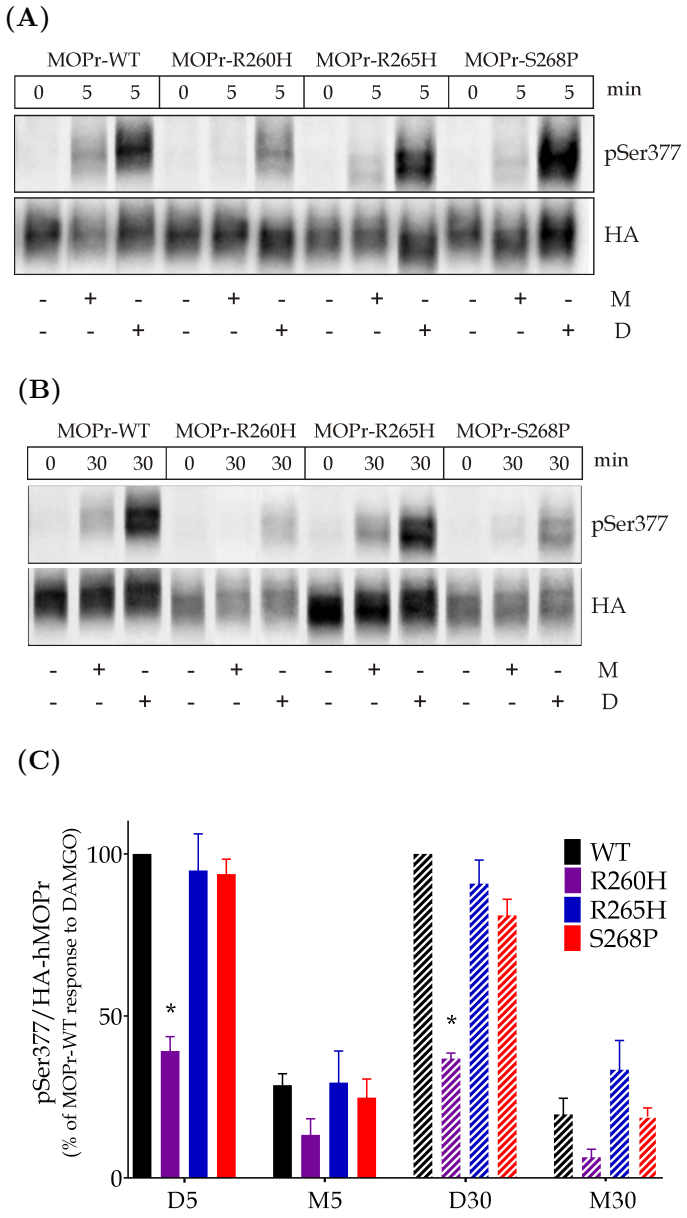

Figure 7.10. Morphine and DAMGO induced phosphorylation of hMOPr Ser377 residue in AtT20 expressing hMOPr ICL3 SNPs. **(A)** and **(B)** are representative blots from one of three independent experiments of 5 or 30 minutes opioid incubation respectively. AtT20 cells stably transfected with hMOPr-WT, hMOPr-R260H, hMOPr-R265H or hMOPr-S268P were either not exposed (-) or exposed (+) to 1μM DAMGO (D) or 1μM morphine (M) for 5 or 30 minutes. The cells were lysed and immunoblotted with anti-pSer377 antibody (pSer377, upper panel), then blot was stripped and reprobed with anti-HA antibody to detect total hMOPr (HA, lower panel). Further methods details are described in Section 3.6. **(C)** Quantified data by densitometric analysis. Morphine and DAMGO incubated for 5 (no pattern) or 30 minutes (stripe pattern) induced similar extension of Ser377 residue phosphorylation in hMOPr-R265H and hMOPr-S268P when compared to hMOPr-WT (*t*-test, p>0.05). DAMGO mediated phosphorylation at both time points were significantly reduced at hMOPr-R260H polymorphism (one-sample *t*-test, p<0.05). Data are presented as % of DAMGO-induced Ser377 phosphorylation (pSer377) in AtT20-hMOPr-WT (100%) ± SEM; note that all results were corrected for total receptor number (pSer377/HA).

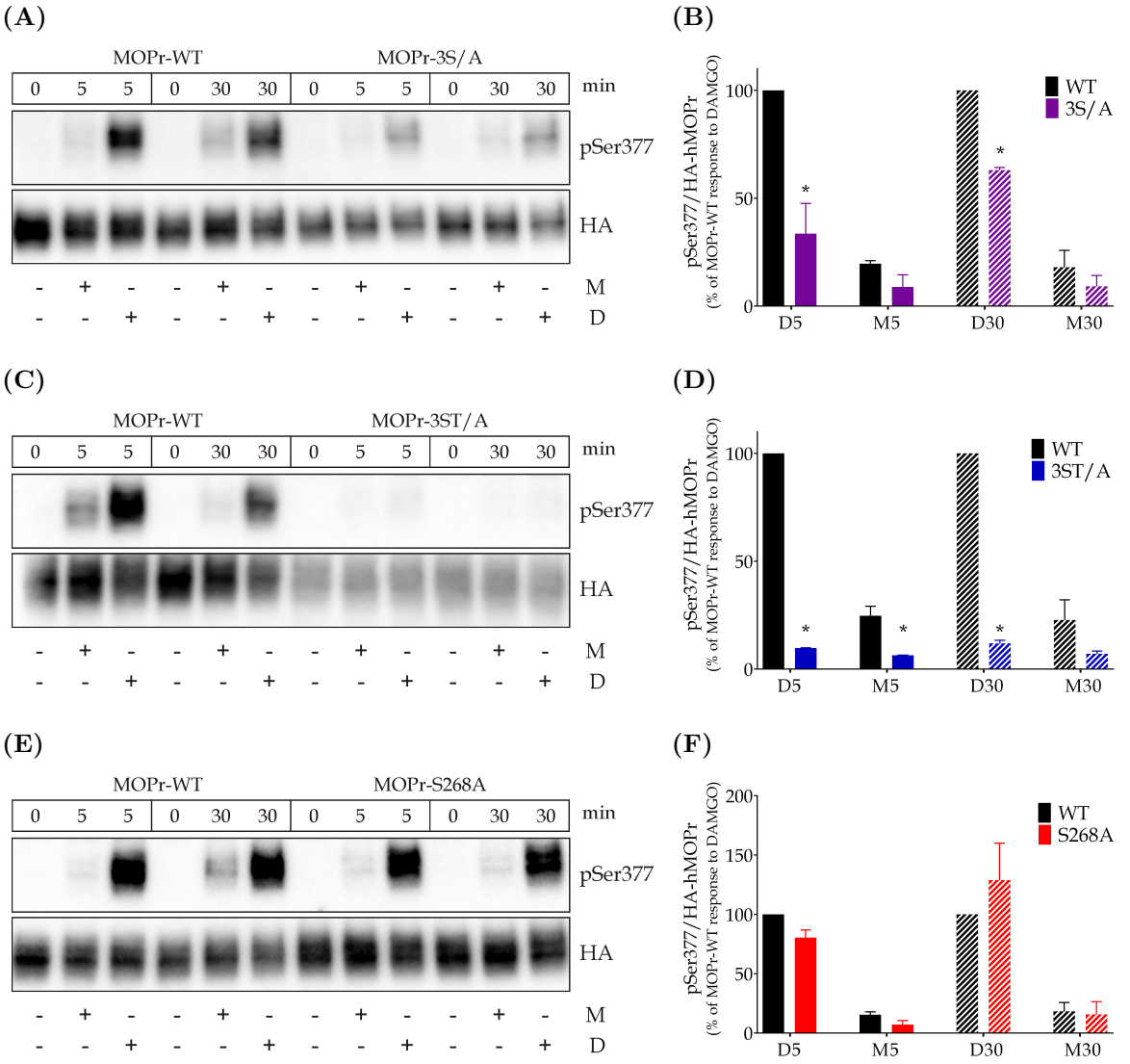

Figure 7.11. Morphine and DAMGO induced phosphorylation of hMOPr Ser377 residue in AtT20 expressing hMOPr phosphosite mutants. **(A)**, **(C)** and **(E)** are representative blots from one of three independent experiments. AtT20 cells stably transfected with hMOPr-WT or phosphosite mutants were either not exposed (-) or exposed (+) to 1μM DAMGO (D) or 1μM morphine (M) for 5 or 30 minutes. The cells were lysed and immunoblotted with anti-pSer377 antibody (pSer377, upper panel), then blot was stripped and reprobed with anti-HA antibody to detect total hMOPr (HA, lower panel). Further methods details are described in Section 3.6. **(B)**, **(D)** and **(F)** show Ser377 phosphorylation mediated by morphine and DAMGO incubated for 5 (no pattern) or 30 minutes (stripe pattern) quantified by densitometric analysis. Note that 30μg instead of 10μg of total protein was loaded for AtT20-hMOPr-3ST/A to be able to detect a band before AtT20-hMOPr-WT saturation. Data are presented as % of morphine-induced Ser377 phosphorylation in AtT20-hMOPr-WT (100%) ±SEM; note that all results were corrected for total receptor number (pSer377/HA).

An interesting finding when performing Western Blot analysis was that while hMOPr-WT only presented one intense band between 75-100 kD after immuno detection with HA antibody, hMOPr-3ST/A presented two fainter bands, the first one at regular molecular weight but the second one between 50-60 kD (Figure 7.12). An extremely faint band could also be determined for hMOPr-3S/A which indicated that this band could be present in all samples but in lower relative abundance. Therefore blots were exposed for longer and it was possible to detect the same band for all variants however only hMOPr-3ST/A band was clearly detected before hMOPr-WT HA band saturation, note that for this observation same total protein concentration was loaded for variants (10μg). Considering low surface expression and the presence of this low molecular weight second band we could speculate that at hMOPr-3ST/A mutant affect migration of receptor to membrane which alteration in post-translational modification such as glycosylation would explain faster electrophoretic shift and lower surface expression. An alternative explanation is that there is a faster internalisation of the 3ST/A receptor, and the band represents the receptor on the way to degradation. To support these hypotheses preliminary confocal images of AtT20 cells expressing hMOPr-WT, hMOPr-3S/A and hMOPr-ST/A not exposed to opioids were obtained as describe in Methods (Section 3.7). The difference in cell surface receptor expression was clear between the three variants, and as predicted 3ST/A presented a widespread distribution of hMOPr in the intracellular compartment which is not observed for the other clones (Figure 7.13). Interestingly all variants analysed presented a small receptor cluster in the cytoplasm.

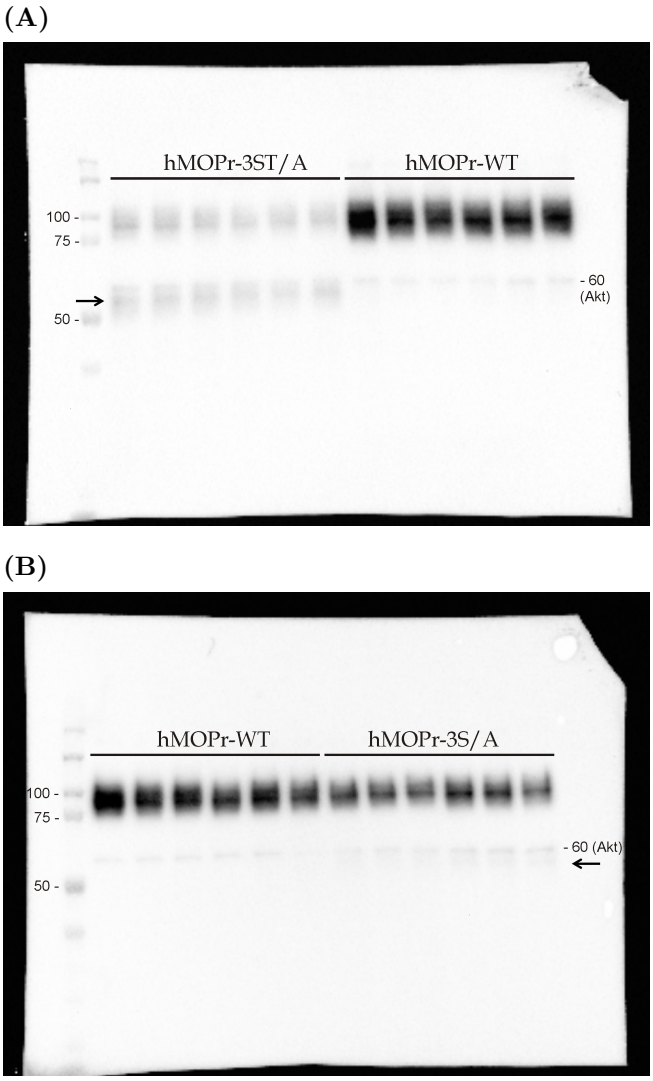

Figure 7.12. (A) At hMOPr-3ST/A The regular hMOPr band between 75-100kD was obtained in addition to a second band between 50-60kD (pointed by arrow). **(B)** In a lower extent, the same band was observed at hMOPr-3S/A. After increasing chemodetection exposure, it was possible to observe this band for all variants however only hMOPr-3ST/A had a higher concentration which could be clearly observed without saturating the main hMOPr-WT bands. Note that for these blots 10μg total protein was loaded per lane and anti-pan Akt antibody(60kD), which can be observed for all samples, was used to better determine molecular weight of second HA band.

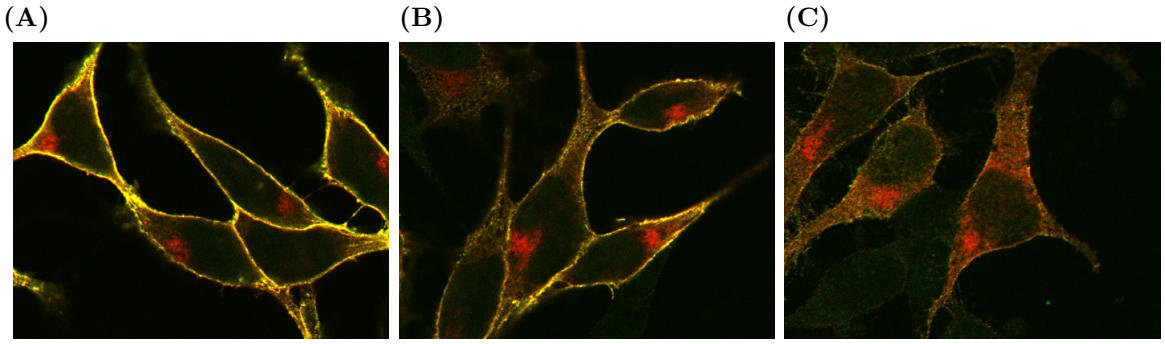

Figure 7.13. Fluorescence confocal images of non-treated **(A)** AtT20-hMOPr-WT, **(B)** AtT20-hMOPr-3S/A and **(C)** AtT20-hMOPr-3ST/A cells. HA-488 conjugated antibody was used to label hMOPr on cell surface before permeabilisation, then cells were permeabilised and immunostained with anti-HA followed by Alexa-fluor 594. Images were obtained under a 488nM (green) and 594nM (red) laser excitation with fixed gain then merged. Preliminary data show a large amount of hMOPr-3ST/A widespread in the intracellular compartment and almost undetectable amount on the surface membrane. Note that a localised receptor cluster was present in all variants.

7.2.5 Loss of Membrane hMOPr

Ser377 is a primary phosphorylation site at the C-terminal which is part of the STANT cluster which phosphorylation is crucial in MOPr internalisation[171,195]; therefore according to results described above, loss in membrane receptor would be expected to be affected at many ICL3 variants. hMOPr membrane surface loss was quantified after varying concentrations of morphine and DAMGO incubation for 5 and 30 minutes using a whole-cell ELISA technique (Figure 7.14).

Figures 7.14(A) and 7.14(B) show results for hMOPr-R260H, hMOPr-R265H, hMOPr-S268P and hMOPr-S268A. In agreement with Ser377 results, only R260H variant was affected comparing with hMOPr-WT, where the cell surface loss mediated by DAMGO was significantly decreased (two-way *ANOVA*). The greatest change was observed at 30 minutes incubation with 10μM DAMGO where opioid induced a surface loss of 85$\pm$2% for hMOPr-R260H and 63$\pm$2% for hMOPr-WT (t-test, p= 0.0005).

The low expressions of hMOPr-3S/A and hMOPr-3ST/A in AtT20 cells were confirmed by the low fluorescence readings obtained for total amount of surface receptors before opioid incubation. The low signal-noise ratio observed mainly for 3ST/A variant would reduce the precision of the analysis, however data obtained was very consistent.

3S/A variant presented a higher receptor loss for all DAMGO concentrations except 0.1μM DAMGO incubated for 5 minutes, whilst at hMOPr-3ST/A 0.1μM DAMGO concentration incubated for 30 minutes produced a 84% receptor loss compared to 97% for hMOPr-WT (t-test, p= 0.0022) and the other concentrations did not cause any further loss (Figure 7.14(C)). Note that at 5 minutes hMOPr-3ST/A was not significantly different from hMOPr-WT.

Morphine did not significantly affect quantity of any hMOPr ICL3 variants on the cell surface.

Figure 7.14.*(following page)*: Loss of membrane hMOPr ICL3 variants after varying concentrations of DAMGO and morphine incubation for 5 or 30 minutes. Data obtained as described in Methods Section 3.8. **(A)** After 1μM and 10μM DAMGO incubation the decrease of hMOPr-R260H on cell surface was not as prominent as for hMOPr-WT (t-test, p<0.05) while hMOPr-R265H had a similar effect to hMOPr-WT (t-test, p>0.05). **(B)** Both point mutations at Ser268 residue did not affect membrane receptor loss. **(C)** A significant lower hMOPr-3S/A amount were found at the membrane after incubation with high DAMGO concentrations at both time points when compared to hMOPr-WT. Only at 30 min incubation with DAMGO hMOPr-3ST/A was compromised, however interestingly 0.1μM DAMGO was enough to significantly decrease receptor numbers on surface (one-sample t-test, p>0.05) however no further significant decrease was observed with higher DAMGO concentrations. Data represent the mean ± SEM of pooled data from 4-5 independent determinations performed in triplicate.

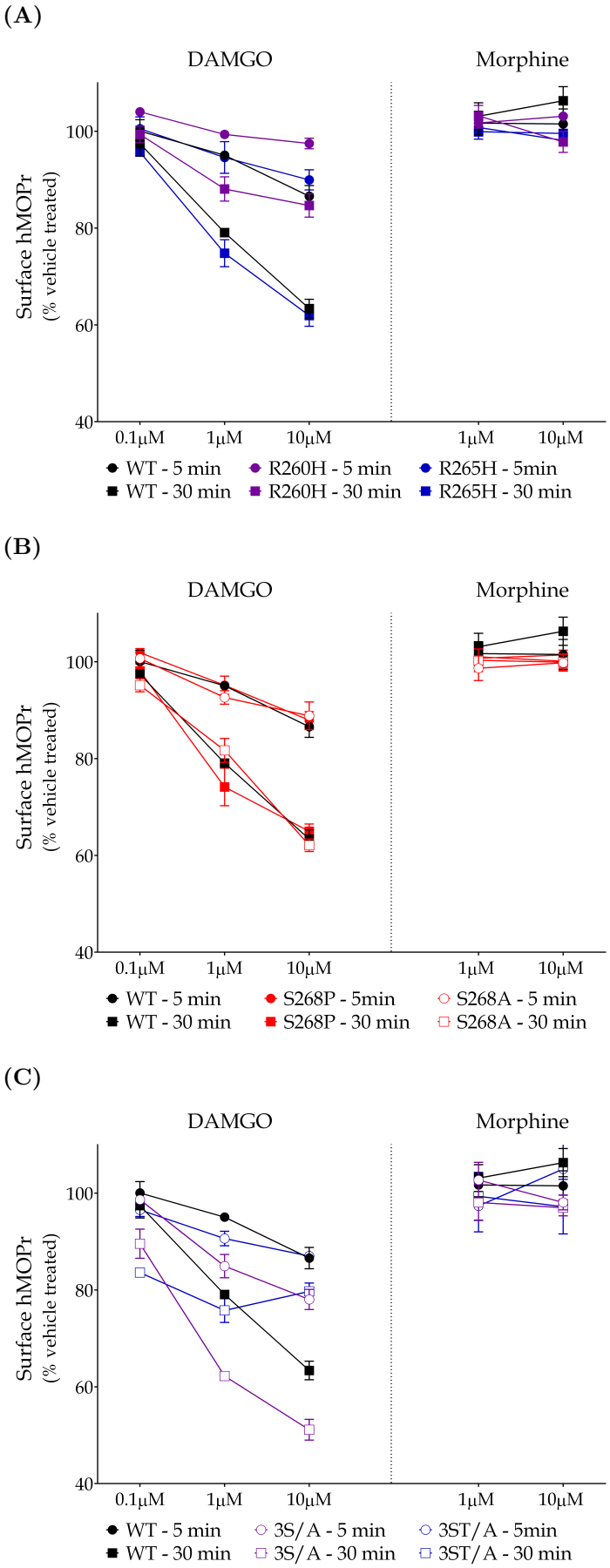
(A)
DAMGO
Morphine
Surface hMOPr (% vehicle treated)
100
80
60
40
0.1μM
1μM
10μM
1μM
10μM
WT - 5 min
R260H - 5 min
R265H - 5min
WT - 30 min
R260H - 30 min
R265H - 30 min
(B)
DAMGO
Morphine
Surface hMOPr (% vehicle treated)
100
80
60
40
0.1μM
1μM
10μM
1μM
10μM
WT - 5 min
S268P - 5min
S268A - 5 min
WT - 30 min
S268P - 30 min
S268A - 30 min
(C)
DAMGO
Morphine
Surface hMOPr (% vehicle treated)
100
80
60
40
0.1μM
1μM
10μM
1μM
10μM
WT - 5 min
3S/A - 5 min
3ST/A - 5min
WT - 30 min
3S/A - 30 min
3ST/A - 30 min

7.3 Discussion

The importance of the hMOPr ICL3 for G protein signalling was confirmed by the present study. More specifically changes in the N-terminal region of the ICL3 had a great effect on G protein coupling while multiple phosphosite mutations, especially when including the Thr281 in the distal region, greatly affected receptor expression. A summary of the results for hMOPr ICL3 variants are presented in Table 7.8 and Table 7.9.

The sevenfold decrease in surface hMOPr-3ST/A expression, detected by radioligand binding, was also reported by a previous study where all serine and threonine of ICL3 and C-terminal were mutated to alanine and expressed in CHO-KI cells[54]. Interestingly, this paper also measured affinity for DAMGO and morphine which was identical to the results observed for hMOPr-WT. Here K_D results was also not significantly different between mutants/polymorphisms and hMOPr-WT; therefore, despite ICL3 mutations having large effect on G protein activation, they did not affect DAMGO affinity.

In hMOPr ICL3 SNPs, an extensive reduction in opioid agonist efficacy was reported. Note that this was not correlated to low receptor expression, as R265H had a slightly higher expression than hMOPr-WT but still presented lower efficacy than WT receptor. In addition, these findings are supported by previous studies of these mutations which have been reviewed by Knapman and Connor (2015)[180]; with the exception of the greater loss of function for R260H polymorphism observed in the present study. This could be related to many factors such as the variation in heterologous systems used, the majority of previous studies used *Xenopus* oocytes and HEK cells, and also the difference in assays performed. Some of the published results used a gene reporter to determine cAMP inhibition[27,125], an indirect measure which could have the interference of downstream factors; others used membrane preparations and considerably invasive techniques where pH was manipulated. The importance of pH when assessing R260H and R265H needs to be emphasised because the amino acid substitute histidine has a pKa slightly lower than physiological pH. Therefore, depending of the pH of the

Table 7.8. Summary of hMOPr ICL3 SNPs findings

hMOPr variant	Assay performed	Key observations
R260H	Radioligand binding	Similar B_{max} and K_D
	GIRK activation	All opioids tested less potent (except buprenorphine) and less efficacious
	Desensitisation time course	Faster rate but higher extent of homologous desensitisation only for morphine Heterologous desensitisation largely compromised
	Signal decay	Higher rate and extent
	Ser377 phosphorylation	Less DAMGO induced phosphorylation
	Cell surface hMOPr loss	Decreased surface loss mediated by DAMGO
R265H	Radioligand binding	Slightly higher B_{max} and similar K_D
	GIRK activation	Lower efficacy for all opioids but only morphine less potent
	Desensitisation time course	Heterologous desensitisation largely compromised
	Signal decay	Faster rate of decay but no effect on extent
	Ser377 phosphorylation	Similar phosphorylation
	Cell surface hMOPr loss	Similar trafficking
S268P	Radioligand binding	Slightly lower B_{max} and similar K_D
	GIRK activation	Lower efficacy for morphine, methadone and buprenorphine while DAMGO methadone and morphine less potent
	Desensitisation time course	Homologous desensitisation faster rate and higher extent by morphine and lower extent by DAMGO Heterologous desensitisation largely compromised
	Signal decay	Morphine induced higher rate and extent of decay
	Ser377 phosphorylation	Similar phosphorylation
	Cell surface hMOPr loss	Similar trafficking

All results are in comparison with hMOPr-WT. Pentazocine did not signal in any of these variants

Table 7.9. Summary of hMOPr ICL3 SNPs findings

hMOPr variant	Assay performed	Key observations
3S/A	Radioligand binding	Lower B_{max} and similar K_D
	GIRK activation	Lower efficacy for methadone and morphine and lower potency for morphine, methadone and DAMGO
	Desensitisation time course	Lower extent of homologous desensitisation by DAMGO
		Heterologous desensitisation largely compromised
	Signal decay	Morphine induced faster rate of decay
	Ser377 phosphorylation	Less DAMGO induced phosphorylation
	Cell surface hMOPr loss	Increased receptor loss induced by DAMGO
3ST/A	Radioligand binding	Much lower B_{max} and similar K_D
	GIRK activation	Lower efficacy for all opioids and lower potency for methadone and morphine
	Desensitisation time course	Increased rate and extent of homologous desensitisation
		Heterologous desensitisation largely compromised
	Signal decay	Higher rate and extent of decay
	Ser377 phosphorylation	Less DAMGO and morphine induced phosphorylation
	Immunocytochemistry	Large amount of receptors in the cytoplasm region
	Cell surface hMOPr loss	Decreased receptor loss induced by high DAMGO concentrations at 30 minutes but increased at 1μM DAMGO
S268A	Radioligand binding	Similar B_{max} and K_D
	GIRK activation	Lower efficacy for pentazocine and higher potency for buprenorphine
	Desensitisation time course	Not affected
	Signal decay	Not affected
	Ser377 phosphorylation	Similar phosphorylation
	Cell surface hMOPr loss	Similar trafficking

All results are in comparison with hMOPr-WT. Pentazocine did not signal at hMOPr-3S/A and hMOPr-3ST/A

cell or of the assay performed histidine could be protonated or non-protonated which could differently affect loop conformation and G protein interaction around the amino acid region. It is noteworthy that the majority of the buffers used for biological assays are pH 7.4, while intracellular pH (pH_i) of an intact cell varies according to cell type, extracellular pH (pH_o) and stimuli such as osmotic pressure and temperature[295,303]. HEK293 cells and *Xenopus* oocytes pH_i under physiological conditions (pH_o=7.4) is 7.3[310,351], while AtT20 D16V is approximately 7.2[206], in addition, a large range of pH_i was reported by Chesler (2003)[66] in brain cell types.

Ghanouni et al. (2001)[132] demonstrated that the sequence of conformational changes in β_2-adrenergic receptor that happens after receptor activation stabilise more than one active conformation. Furthermore, the active conformation induced by a high efficacious agonist was significantly distinct from low efficacious agonists[132]. A recent investigation using crystal structure of active β_2-adrenergic receptor showed an interaction between the nanobody, which mimicked the G_s protein, and the receptor cytoplasmic ends of TM5 and TM6, which helped to stabilise the active conformation[285]. Considering that the information for β_2-adrenergic receptor could be translated to MOPr, we could speculate that mutations at the proximal and distal regions of the ICL3 could destabilise the described interaction between G protein and MOPr. This would explain the compromised signalling in some variants. Carefully examining the data obtained here, it is possible to observe that GIRK activation efficacy and potency by morphine and methadone are most frequently affected by variants. Therefore, we could propose that these two agonists stabilise conformations alike that activate G protein, and these conformations are highly dependent on stabilisation by the ICL3 region, differently from endogenous and synthetic peptides, and buprenorphine. This is further supported by S268P results which compromised GIRK activation was not observed for opioid peptides, however this effect was not supported by S268A which confirmed that difference in signalling obtained was probably a consequence of ICL3 deformation caused by proline, not the loss of a phosphorylation site. Proline is the only amino acid to have a cyclic side chain which severely restricts conformational flexibility, it

introduces kinks into alpha helix structures and are highly conserved in transmembrane 6 and 7 of GPCRs. The substitution of a small serine with a limited flexibility proline would restrict ICL3 conformation which could affect other residues interaction with G protein thus being less favourable for G protein coupling/activation, which, as mentioned, is especially important for morphine and methadone signalling.

The importance of the N-terminal, mid and C-terminal region of the ICL3 to DAMGO mediated G protein activation was also previously determined by using interfering peptides[130]. DAMGO stimulated GTPase activity was not affected when using a peptide for the mid-region of the ICL3 , which supports our S268A data. In contrast, the high resolution crystal structure of the hDOPr suggests many residues across the ICL3 are important for this opioid receptor to stabilise a 'close' conformation in the inactive state, by extensive hydrogen-bonding networking[115]. Interestingly, the residues involved in this network are also found in the hMOPr; therefore, speculating the same finding in hMOPr we could say that Arg278, the key residue which is in close proximity to Thr181, interacts directly with Leu261, Arg265 (R265H amino acid substitution) and Val264, and through a salt bridge with Asp274. Moreover, residues Leu267 and Val264, which are both next to amino acids changed in R265H and S268P polymorphisms, would be inserted back in the transmembrane pocket where hydrophobic clusters are formed with Val171 in the ICL2, Leu261 and Leu277. Finally, a supposed interaction between helix 8 (C-terminal) and Leu257, Val171 and Arg260 would be found, which Arg260 is the mutated residue at R260H and the only residue to deeply affect phosphorylation of C-terminal residue Ser377. Therefore, this work in hDOPr emphasises the importance of the amino acids mutated in the polymorphisms studied. The disruption of the water-mediated hydrogen bond between hMOPr-R260H and the C-terminal could be the main reason for decrease in phosphorylation observed, and maybe even the highlighted effect of R260H in desensitisation.

In stark contrast to morphine and methadone, buprenorphine potency was not reduced by ICL3 variants, and at S268A mutant buprenorphine potency was slightly increased. These are interesting findings as previously buprenorphine had been demonstrated to be the only opioid to compromise N-terminal polymorphism N40D signalling,

thus confirming the different intrinsic characteristics of this opioid related to receptor activation and signalling. Interestingly, molecular dynamics simulations of the MOPr active and inactive state supports the idea that buprenorphine engages a different conformation from other agonists such as morphine, Shim et al. (2013)[318] described 2D distribution of MOPr activated by buprenorphine as between those of the agonists and antagonists tested.

The motif '$X_1BBX_2X_3B$' at the C-terminal of the ICL3 (base of the TM6) is highly conserved across class A GPCRs and mutation of this region was reported to produce constitutive active receptors[2,112,293]. The largest change detected in crystal structure of β_2-adrenergic receptor between active and inactive conformation is the movement of the cytoplasmic face of TM6 outwards with the rupture of the ionic lock. However, in contrast to this adrenergic receptor, mMOPr crystal structure did not present an ionic bridge between the DRY motif and the cytoplasmic end of TM6 (ICL3 distal region), mMOPr have a polar interaction between arginine (DRY motif) and Threonine 279 (Thr281 in hMOPr)[220,285]. This interaction presumably can stabilise MOPr inactive state, as mutating threonine to lysine (T279Y) produced a constitutive active receptor, while substitution of threonine to aspartic acid (T279D) affected GTPγS binding without causing constitutive activation probably by strengthening polar interaction[154]. Similarly to hMOPr-3ST/A, rMOPr-T279Y expression was dramatically decreased and an intracellular pool of receptor was observed, thus hMOPr-3ST/A could be constitutively active which will be further evaluated by calcium channel activation, as acute naloxone or overnight pertussis toxin treatment were not able to detect a change in basal membrane potential in assay used (data not shown). Note that detecting constitutive activity via GIRK activation is more complicated than using calcium channels, as to detect an increase in basal signalling at GIRK assays a larger number of receptors are necessary because, while only one $\beta\gamma$ subunit is necessary to inhibit I_{Ca}, multiple subunits are necessary to activate GIRK[78].

Decreased MOPr expression and a greater intracellular pool of MOPr have been reported not only for mutations in the ICL3 distal region, but also ICL3 proximal region and C-terminal tail mutations[59,313]. In CHO-rMOPr-T279Y, the intracellular

pool of receptor was not significantly affected by naloxone treatment despite increase in surface expression. While in HEK293 expressing rMOPr with multiple deletions in the N-terminal of the ICL3 (which includes R260H) was also rescued by naloxone to membrane but cytoplamic receptor pool was not able to be detected after treatment. Despite successful naloxone rescue, this receptor was not constitutively active and even after rescue, DAMGO efficacy was lower which indicated lower efficiency in G protein activation that has been already discussed here for this ICL3 region[59]. A defective trafficking of GPCRs to the plasma membrane can cause accumulation of the receptors in the intracellular compartment. The above mentioned N-terminal ICL3 of rMOPr was found to be colocalised with calnexin, and it was proposed that this receptor was retained in the endoplasmic reticulum (ER) and naloxone acted as chaperones to support trafficking to the plasma membrane. Further studies are necessary to assess if naloxone could increase receptor expression of hMOPr ICL3 variants, especially 3S/A and 3ST/A, in addition it would be interesting to also determine if defective trafficking from ER to membrane is the main responsible for the low expression rate observed.

Dong et al. (2007)[105] reviewed the mechanisms involved in GPCR trafficking from the ER through the Golgi apparatus to the plasma membrane. Many ER exporting motifs have been identified in the C-terminal of GPCRs and the N-terminal region also plays a role in receptor migration, where N-glycosylation is involved in receptor surface expression in some GPCRs including MOPr and κ-opioid receptor[157,205]. ER retention motifs have also been identified and the amino acid arginine is regularly present; vasopressin V2 contains this motif at the ICL3 but its expression is not affected which is proposed to be related to region obstruction in normal conditions. Interestingly, next to Thr281 there is an arginine rich region, we could speculate that at regular conformation, this region is masked; however, with the Thr281 mutation and polar interaction disrupted, this region exposure could be increased and protein retained. Therefore, without reaching the Golgi apparatus where N-glycosylation is normally maturated, normal protein glycosylation pattern would be compromised which could explain hMOPr-3ST/A low molecular weight band detected in Western blot. This supports the idea that this mutation has a negative effect in receptor trafficking from ER to

membrane. Furthermore, considering that at any given time a small portion of receptor should be undergoing maturation in the ER, it is plausible that this low molecular weight band was identified in lower quantities in all variants tested. It is noteworthy that many regulation processes are involved in controlling receptor expression, therefore low expression observed for some clones could be a combination of lower amount of receptor reaching the membrane with increased receptor internalisation probably induced by receptor instability or constitutive activity.

Dimerisation has been linked to modulation in the membrane expression of GPCRs, where dimer formation in the ER can be negatively modulated by increasing receptor sequestration, or positively modulated by increasing transportation to the membrane as reviewed by Milligan (2010)[241]. hMOPr homodimer and heterodimer formation have been previously described[148,220,272]; however, it is not known if MOPr dimerisation is a random process of receptors colliding on cell surface or a process that starts at the ER. A study by Decaillot et al. (2008)[97] supports dimerisation before reaching plasma membrane as they reported the involvement of a Golgi chaperone, RTP4, in MOPr-DOPr heterodimers expression. In addition to the polar interaction between the DRY motif and Thr279 of the mMOPr, Thr279 was also one of the interaction points for TM5-TM6 dimerisation described by Manglik et al. (2012)[220] as the main dimer interface. Therefore, homodimer and heterodimer formation involving this phosphosite mutant could be reduced, which could negatively affect receptor trafficking from ER. Besides ER sequestration of hMOPr-3ST/A, epigenetics, which is another component of the complicated cellular process to regulate protein expression, can further decrease the amount of receptor which is delivered to the plasma membrane. RNA synthesis can be downregulated by methylation which is a common epigenetic modification introduced at cytosine-phosphate guanine (CpG)sites[253]. Note that one extra CpG site is added for the mutation of the T281A, which synergistically would work with the other regulation possibilities to decrease receptor expression.

According to Chen at al. (2013)[63], ICL3 peptide is phosphorylated by GRK2, PKC and CaMKII in vitro; however, the significance of this in receptor signalling and

regulation in intact cell is poorly understood. In this work, deletions of multiple phosphorylation sites at the ICL3 had a mixed effect in GIRK signalling and desensitisation. MOPr C-terminal tail phosphorylation and desensitisation have long been correlated, especially when phosphorylation efficient agonist DAMGO was used, while morphine desensitisation was previously shown to be phosphorylation and β-arrestins independent[71]. The reduced hMOPr-ST/A expression and a possible constitutive activity could have influenced this variant desensitisation; however, the dramatic effect on homologous desensitisation, which was not observed at also low expressed hMOP-3S/A, was probably related to intrinsic properties of this receptor. Interestingly, molecular dynamics simulation had suggested that the mechanism of constitutive activation of Thr279 produced by substitution of Thr to Lys is different from agonist bound receptor[318]. Therefore, a possible explanation is that this difference is a result of the receptor assuming different conformations, and agonist induced conformation changes would be different for hMOPr-3ST/A, which could be faster and highly desensitised. The present study showed for the first time that the triple serine deletions at hMOPr-3S/A did not deeply affect desensitisation which is in contrast with previous point mutations[185].

The Ser268 residue was previously reported to be the primary site for CaMKII phosphorylation. This is involved in receptor desensitisation as phosphosite deletion (rMOPr-S268A, rMOPr-S268P and hMOPr-268P) decreased receptor signalling decay induced by DAMGO in *X. laevis* oocytes directly injected with CaMKII[185]. These results were not confirmed here, AtT20-hMOPr-S268P signal decay after DAMGO exposure was not affected by polymorphism and similar result was observed for hMOPr-S268A. It is important to note that homologous desensitisation measured by opioid challenge after stimulus was slightly decreased by DAMGO at hMOPr-S268P. In contrast, morphine mediated homologous desensitisation and signal decay rate and extent were higher, which support the higher interference of S268P polymorphism in morphine induced signalling and regulation. In spite of analysing activation of the same pathway, comparing responses between two completely different systems is always difficult. AtT20 is a mammalian cell which natively expresses GIRK channels and CaMKII

while *Xenopus* oocytes were injected with GIRKs and pre-activated CaMKII. Moreover, CaMKII is not necessarily activated in native conditions; therefore, even though the potential exists for Ser268 phosphorylation, it does not necessarily occur in AtT20 cells. Further studies assessing inhibition of CaMKII with KN-93 in desensitisation would supplement the presented findings.

Wang et al. (2001)[350] studied calmodulin interaction in HEK293 cells expressing ICL3 SNPs. They reported that the interaction with G protein and calmodulin binding was deficient for variants 265H and S268P, suggesting a possible partial overlap of binding domains in this protein. Diminished morphine tolerance after chronic treatment at R265H and S268P was measured using GTPγS binding assay which was proposed to be related to interference in CaMKII phosphorylation. In the present, work maximum acute homologous desensitisation induced by morphine and DAMGO was mainly affected at R260H which was the only ICL3 SNP to have Ser377 phosphorylation and surface receptor loss induced by DAMGO dramatically decreased. This supports the hypothesis that phosphorylation and β-arrestin recruitment may not be necessary for receptor desensitisation.

Signalling through β-arrestin has also been demonstrated for GPCRs in addition to its role in desensitisation and involvement in receptor internalisation[187,367].β-arrestins can bind to rMOPr ICL3 peptide[63]; however, this does not necessarily translate to intact cells. A similar finding was reported by Cen et al. (2001)[58], they demonstrated the ability of β-arrestins to bind the ICL3 peptide of DOPr, which is largely similar to the ICL3 of the MOPr. Noticeably, the region tested for β-arrestin binding did not include amino acid corresponding to Thr281 in DOPr, and pre-bound C-terminal β-arrestin 1 was still able to bind ICL3 which indicated a different site of interaction in the β-arrestin molecule. Considering the canonical recruitment of β-arrestin by GRK phosphorylation of serine/threonine residues, phosphorylation of at least two of the four serines available at DOPr ICL3 would be expected; however, deleting all the four phosphorylation sites did not affect [D-Pen^{2,5}]Enkephalin (DPDPE) induced G protein coupling and homologous desensitisation measured by signal decay in *Xenopus* oocytes[187]. Note that recent studies had reported a phosphorylation independent

β-arrestin 2 recruitment[133]. In this work phosphosite mutation of the three available serines at the ICL3 affected receptor signalling and regulation; one of the interesting findings was that although Ser377 phosphorylation was reduced by 1μM DAMGO, receptor loss from the membrane was increased while maximum homologous desensitisation was decreased. The meaning of these findings still need to be further investigated however we could speculate that the decrease in DAMGO induced Ser377 phosphorylation may be related to lower GRK2 activation. Dominant negative GRK2 mutant was demonstrated to decrease DAMGO but not morphine maximum homologous desensitisation in HEK293 cells[22,167]. These raise the possibility of the involvement of the serine residues of the ICL3 in GRK2 activation, but it still does not explain the increase in receptor loss. The increase in surface receptor loss induced by 0.1μM DAMGO could indicate that less drug is necessary to be able to detect receptor internalisation because of reduced total receptor number. Maybe at saturating concentration they would have similar maximum loss, pointing to a saturation of the internalisation machinery which would restrict the rate of hMOPr-WT internalisation. Note that this is not supported by data presented for other hMOPr region mutations. A more plausible explanation is that there is also the possibility of a hMOPr-3S/A being less stable thereby it is removed from the membrane in a faster rate than hMOPr-WT which would explain lower expression in an isogenic system (FlpIn™ system).

Heterologous desensitisation was affected by all ICL3 variants with the only exception hMOPr-S268A. A negative correlation between receptor expression and heterologous desensitisation was determined however no perfect correlation was observed. R265H expression was higher but maximum heterologous desensitisation was lower, while R260H and S268P, which receptor expression was similar to WT and S268A variants, had a much lower maximum heterologous desensitisation. This clearly indicates that ICL3 is directly involved in heterologous desensitisation and considering Ser377 phosphorylation pattern of these receptors, the role of phosphorylation was not evident. However, we should not disregard phosphorylation as previous study has shown that MOPr activation by DAMGO produced SST receptor phosphorylation[272], and many other phosphosites could be involved in addition to other kinases, as Ser377

phosphorylation reflects GRK activation[221], while CaMKII and PKC could also be involved. Raveh et al. (2010)[286] reported a phosphorylation independent mechanism where GRK2 accelerated desensitisation by sequestration of $G_{\beta\gamma}$ subunits which could also affect heterologous desensitisation as SST receptor activate GIRK by the same pathway. Therefore, it is possible that heterologous desensitisation decreases as a consequence of reduced GRK2 activation by ICL3 variants. Nevertheless, this sounds unlikely as homologous desensitisation was not affected, and there was an increase at some variants; moreover, hMOPr-S268P Ser377 phosphorylation was not compromised indicating GRK2 recruitment. A weak link between MOPr surface loss and desensitisation data was also observed in the present work which refutes the possibility of cointernalisation of both receptors. Pfeiffer et al. (2002)[272] study supports these findings as DAMGO activation of MOPr-SST receptor dimers caused desensitisation of both receptors but not internalisation of SST receptor. It is noteworthy that heterologous desensitisation is probably a result of combined factors; therefore, looking for a combination of factors instead of individual ones may help to elucidate its complex mechanisms. The deleterious effect of ICL3 in G protein dependent pathways and the deeply compromised heterologous desensitisation of ICL3 clones point to G protein involvement. However, we should not discount that heterologous desensitisation could be evoked by G protein dependent and independent pathways, in addition to involvement of conformational changes and heterodimerisation which is still poorly understood.

In conclusion, MOPr ICL3 is a highly dynamic region which is clearly involved in G protein activation. Modifications in this loop, especially the proximal and distal region, not only can affect signalling but also receptor expression and regulation which indicate the importance of this highly conserved region. Further studies are needed to determine the role of phosphorylation in the ICL3, however from this study I have demonstrated that multiple phosphosite deletions in the ICL3 affect receptor expression and supply evidence that ICL3 and Ser377 phosphorylation are not necessary for receptor desensitisation.

8

Regulation of C-terminal Phosphosite Mutant of hMOPr

A large body of evidence supports the role of the μ-opioid receptor (MOPr) C-terminal tail in receptor regulation. The primary question addressed in this chapter is the relevance of C-tail phosphorylation to MOPr signalling and desensitisation. This was assessed with one phosphorylation mutant of the MOPr where all serine and threonine sites were deleted (hMOPr-CST/A).

Contents

8.1 Introduction

The intracellular regions of GPCRs interact with proteins such as G proteins and arrestins, responsible for receptor signalling and regulation. Besides a well established role for MOPr C-terminal phosphorylation in β-arrestin recruitment and receptor endocytosis, the significance for this regulatory process in terms of receptor signalling and desensitisation is still not well understood[356].

While the three intracellular loops of the hMOPr are highly conserved across opioid receptors, the C-terminal tail of the MOPr, excluding the proximal region, is relatively unique to this receptor. This clearly indicates the important role this receptor region plays in differential signalling and regulation compared to the other opioid receptors. The hMOPr C-terminal domain contains 11 potential serine/threonine phosphorylation sites, all of which were deleted in the present study (hMOPr-CST/A, Figure 8.1). Interestingly, the rat and mouse MOPr have one threonine which is part of the well studied TSS**T** cluster that is not present in hMOPr. In addition, one Tyrosine (Tyr338), which is part of a highly conserved motif (NPXXY) in the base of the TM7 region, was not deleted in this study, as we focused on serine/threonine phosphorylation sites.

Phosphorylation of C-terminal tail serine/threonine residues of MOPr has been extensively investigated and it is established that some agonists such as DAMGO induce a robust and widespread phosphorylation of this region while other agonists, such as morphine, does not mediate phosphorylation as efficiently[99,311,365]. In HEK293 cells expressing MOPr, the rate and extent of Ser377 phosphorylation induced by DAMGO are higher than morphine, however interestingly, after agonist removal, dephosphorylation

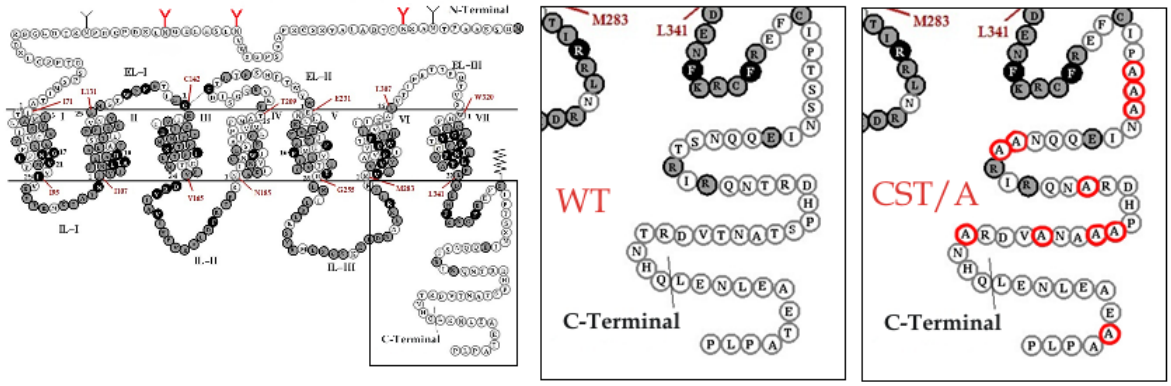

Figure 8.1. Serpentine structure of the human μ-opioid receptor with area enlarged showing hMOPr-WT and hMOPr-CST/A C-terminal amino acid sequence. The eleven point mutations from serine and threonine to alanine are highlighted in red in the hMOPr-CST/A C-terminal tail. Adapted figure from Center for Opioid Research and Design (CORD)[83].

of DAMGO induced phosphorylation was fast and complete while morphine phosphorylation was sustained[311]. The correlation between internalisation and cessation of receptor signalling with reduced tolerance and dependence was reported by Finn and Whistler (2001)[122]. The inability of morphine to effectively phosphorylate and internalise the MOPr followed by inefficient dephosphorylation at the plasma membrane was previously correlated with faster development of tolerance[311]; however, new evidence had ascertained that MOPr can be adequately dephosphorylated at the membrane level and that the receptor can be recovered[95,102].

In 2011, Doll et al.[102] reported for the first time the agonist-selective patterns of mMOPr induced by morphine and DAMGO by using three phosphosite specific antibodies for Ser363, Thr370 and Ser375 (in hMOPr Ser365, Thr372 and Ser377 respectively). A constitutive phosphorylation of Ser363 was established while Thr370 and Ser375 were only phosphorylated after agonist exposure. While DAMGO induced a robust phosphorylation of both sites, morphine did not induce phosphorylation of Thr370 and phosphorylation of Ser375 was much less than that produced by DAMGO. Interestingly, Ser375, which is part of the STANT cluster, was shown to be the primary site for DAMGO phosphorylation; this hierarchical phosphorylation starting at Ser375 was later confirmed by Just et al. (2013)[171]. Of note early studies determined that substitution of Thr394 affected desensitisation and downregulation which suggested

phosphorylation of this residue[259,260,357], however more recent studies using highly sensitive techniques could not confirm phosphorylation of this threonine[63,195,247].

Mass spectrometric studies were able to confirm and further complement immunological findings[63,195]. Residue Ser363 was confirmed as a constitutive phosphorylation site while Thr370 also appears to be phosphorylated at basal conditions however it is further phosphorylated by agonist stimulus. The STANT cluster is the main phosphorylation region that largely differentiates DAMGO and morphine phosphorylation levels, and it is a crucial region for β-arrestin recruitment and endocytosis. The TSST cluster is also phosphorylated by agonists, the last two residues being the phosphate acceptors according to Chen et al. (2013)[63]. The mass spectrometric analysis was complemented by examining the differential phosphorylation of the above residues by calcium/calmodulin-dependent protein kinase II(CaMKII), protein kinase C (PKC) and G protein kinase 2 (GRK2) *in vitro*, where Ser363 is mainly phosphorylated by PKC but also by CaMKII, TSST by PKC, Thr370 by CaMKII and Ser375 by GRK2[63]. Overall, these kinase and residue correlations were similar to that found in other studies[221] with the exception of Thr370 which has been reported to be phosphorylated by GRK2/3 and PKCα[103,163]. In addition, DAMGO phosphorylation of Ser375 is largely dependent on GRK2/3 while morphine recruits GRK5[103,167], which could explain why overexpression of a GRK2 dominant negative mutant reduced desensitisation induced by DAMGO but not morphine[23,167]. Interestingly, the importance of PKCα in morphine induced desensitisation was reported by Bailey et al.(2009)[23], where inhibiting or knocking out this isoform clearly affected the expected desensitisation response by morphine.

β-arrestin binding to the MOPr is enhanced by phosphorylation of the C-terminal tail which is related to GRK2 activation and mainly mMOPr Ser375 residue phosphorylation[63]. In a study by Chu et al.(2008)[71] in HEK293 cells expressing MOPr C-terminal phosphosite mutants, MOPr induced intracellular Ca^{2+} ($[Ca^{2+}]_i$) release was monitored after opioid exposure and they concluded that morphine but not DAMGO acute desensitisation was phosphorylation and β-arrestin independent. In contrast, a desensitisation study in LC neurons of β-arrestin knockout mice surprisingly demonstrated that

absence of β-arrestin 2 did not affect desensitisation induced by met-enkephalin (ME) compared to wild-type (WT) counterpart[95]. A recent study by Yousuf et al. (2015)[364] in AtT20-mMOPr demonstrated that phosphosite deletion by alanine substitution of Ser363, Thr370 and Thr375 or these residues plus Thr376, Thr379 and Thr383 did not affect morphine and ME desensitisation; however, if all serine and threonine sites were deleted, similar to the clone used in the present study but in mMOPr, desensitisation by ME was abolished while morphine desensitisation was unaffected. The later study also examined at heterologous desensitisation which was unchanged for all variants, but interestingly the PKC inhibitor, calphostin-C, deeply compromised heterologous desensitisation mediated by morphine at the C-terminal total phosphosite deleted variant.

An interesting new role for the hMOPr C-terminal tail phosphorylation in agonist binding was recently described by Birdsong et al. (2015)[33]. Prolonged agonist exposure by morphine or ME slowed the dissociation of DermA594, which with ME but not morphine was partially affected by TSST and STANT cluster phosphorylation. This indicates an allosteric modulation of ligand binding by the C-terminal phosphorylation produced by some agonists, most likely those which can efficiently phosphorylate the C-terminal sites.

Many studies had provided evidence of agonist-dependent MOPr phosphorylation and β-arrestin recruitment (reviewed by Williams et al. [2013][356]), however how these regulatory processes correlate to signalling and acute receptor desensitisation are still not well understood. In the present work, an isogenic cell system and a novel non-invasive real-time kinetic assay were used to assess GIRK activation and acute signalling desensitisation induced by DAMGO and morphine of AtT20-hMOPr-CST/A, a complete C-terminal serine and threonine deleted receptor.

8.2 Results

8.2.1 Human MOPr Expression in AtT20 Cells

Constructs hMOPr-WT and hMOPr-CST/A were stably transfected into AtT20 cells using the Flp-In™ system and varying concentrations of radioligand [^{3}H]DAMGO used to measure receptor expression. Saturation binding curves, obtained as shown in Figure 8.2**(A)**, and B_{max} and K_D were not significantly affected (t-test, p>0.05). B_{max} for AtT20-hMOPr-WT was 1393±84 fmol/mg total protein and 1473±80 fmol/mg for AtT20-hMOPr-CST/A (Figure 8.2**(B)**), and K_D was 3.1±0.6nM for WT and 1.4±0.1 for CST/A (Figure 8.2**(C)**).

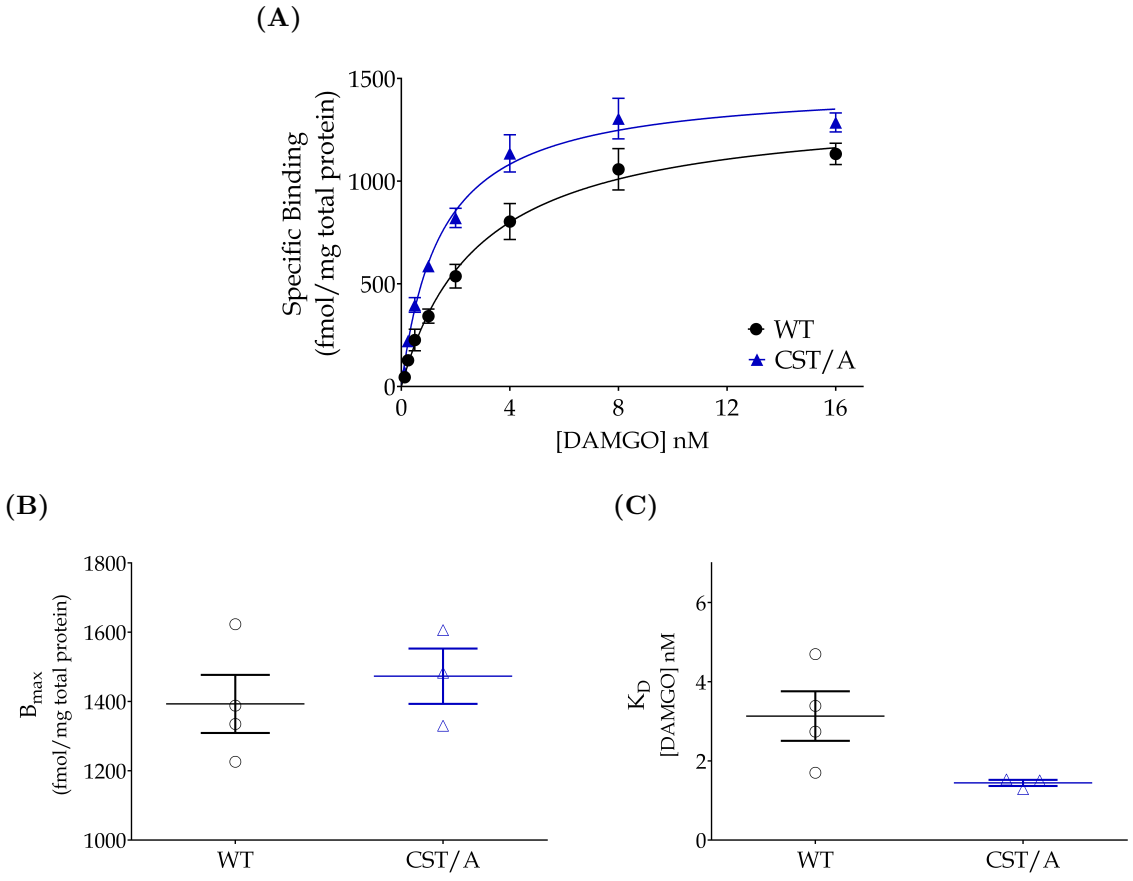

Figure 8.2. hMOPr-WT and hMOPr-CST/A expression in AtT20 cells. **(A)** Saturation binding curve of [^{3}H]DAMGO in intact AtT20-hMOPr-WT and AtT20-hMOPr-CST/A. **(B)** B_{max} results. **(C)** K_D results. No significant difference in B_{max} or K_D was observed between cells expressing hMOPr-WT and hMOPr-CST/A (t-test, p>0.05). Data represent the mean ±SEM, n=3-4.

8.2.2 Human MOPr Signalling via GIRK Channel Activation

The effect of complete phosphorylation site deletion of the C-terminal tail on hMOPr signalling is still not well characterised. FLIPR® membrane potential dye was used as previously described to examine hyperpolarisation induced by varying concentrations of opioids and somatostatin (SST) in populations of AtT20-hMOPr-WT and AtT20-hMOPr-CST/A. Representative traces of endomorphin-2 mediated hyperpolarisation are presented in Figure 8.3 and concentration response curves for SST and all opioids tested are shown in Figure 8.4.

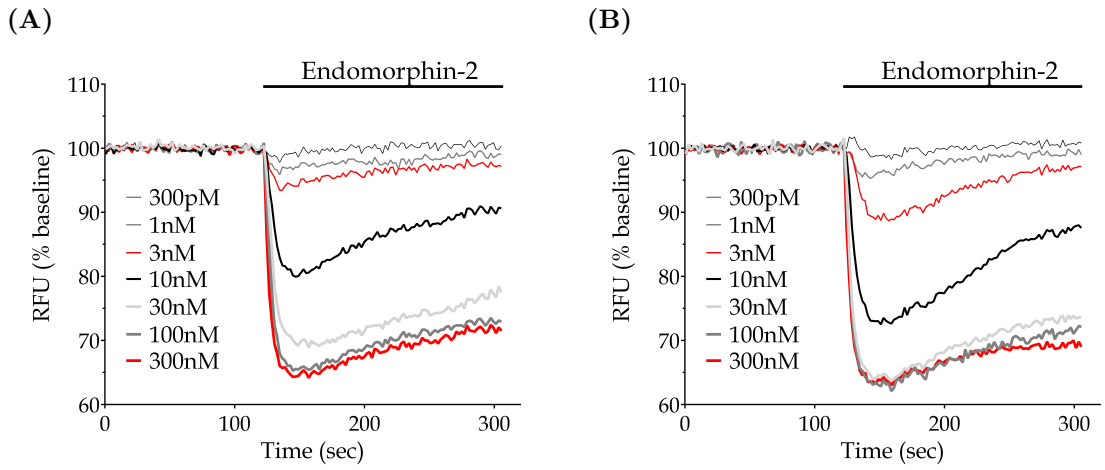

Figure 8.3. Representative traces showing decrease in fluorescence signal, corresponding to membrane hyperpolarisation, following application of varying concentrations of endomorphin-2 to **(A)** AtT20-hMOPr-WT and **(B)** AtT20-hMOPr-CST/A. Note that higher potency at hMOPr-CST/A can be observed.

The CST/A mutation did not affect the efficacy of the opioids tested as shown in Table 8.1; however, the low efficacy agonist buprenorphine was more potent in AtT20-hMOPr-CST/A cells, with pEC_{50} of 7.3±1 compared with pEC_{50} of 7.0±0.1 in AtT20-hMOPr-WT (t-test, $p<0.05$). Interestingly, the high efficacy agonist endomorphin-2 also presented a slightly higher potency at hMOPr-CST/A with pEC_{50} of 8.4±0.1 differently from hMOPr-WT (pEC_{50} of 8.1±0.1).

Somatostatin eficacy and potency was similar between hMOPr variants (t-test, $p<0.05$), which is important to show that differences observed in CRCs were not related to variances in cell lines ability to hyperpolarise.

Table 8.1. Summary of opioid and SST efficacy and potency of GIRK activation in AtT20 cells expressing WT or CST/A hMOPr

GIRK activation	$\mathbf{E}_{max}$**(%)**		$\boldsymbol{p}\mathbf{EC}_{50}$	
Opioid	WT	CST/A	WT	CST/A
DAMGO	34±1	33±2	8.4±0.1	8.5±0.1
Methadone	33±1	29±2	7.3±0.1	7.5±0.1
Endomorphin-2	32±1	33±2	8.2±0.1	8.4±0.1*
Morphine	**31±1**	**29±2**	7.6±0.1	7.6±0.1
Buprenorphine	**22±1**	**22±1**	7.0±0.1	7.3±0.1*
Pentazocine	**7±1**	**6±2**	7.2±0.1	7.3±0.1
SST	33±1	31±2	8.3±0.1	8.2±0.2

Opioids are listed in rank order of maximal effect at MOPr-WT. Opioids with E_{max} significantly lower than DAMGO are set in bold (one-way *ANOVA*, followed by *t*-test, corrected for multiple comparisons, $p<0.05$). Marked with * are results significantly different to hMOPr-WT (*t*-test, $p<0.05$).Values shown are mean ± SEM, n=5-6.

Figure 8.4.*(following page)*: Opioid agonists and SST concentration response curves in AtT20 expressing WT (black) and CST/A (blue) hMOPr. **(A)** Endomorphin-2 and **(B)** buprenorphine are more potent in the CST/A mutant (t-test, $p<0.05$). **(C)** DAMGO, **(D)** methadone, **(E)** morphine and **(F)** pentazocine signalling was not affected in the phosphosite mutant. Note that **(G)** SST signalling was similar between cell lines (*t*-test, $p>0.05$). Data represent the mean ± SEM of pooled data from 5-6 independent determinations performed in duplicate.

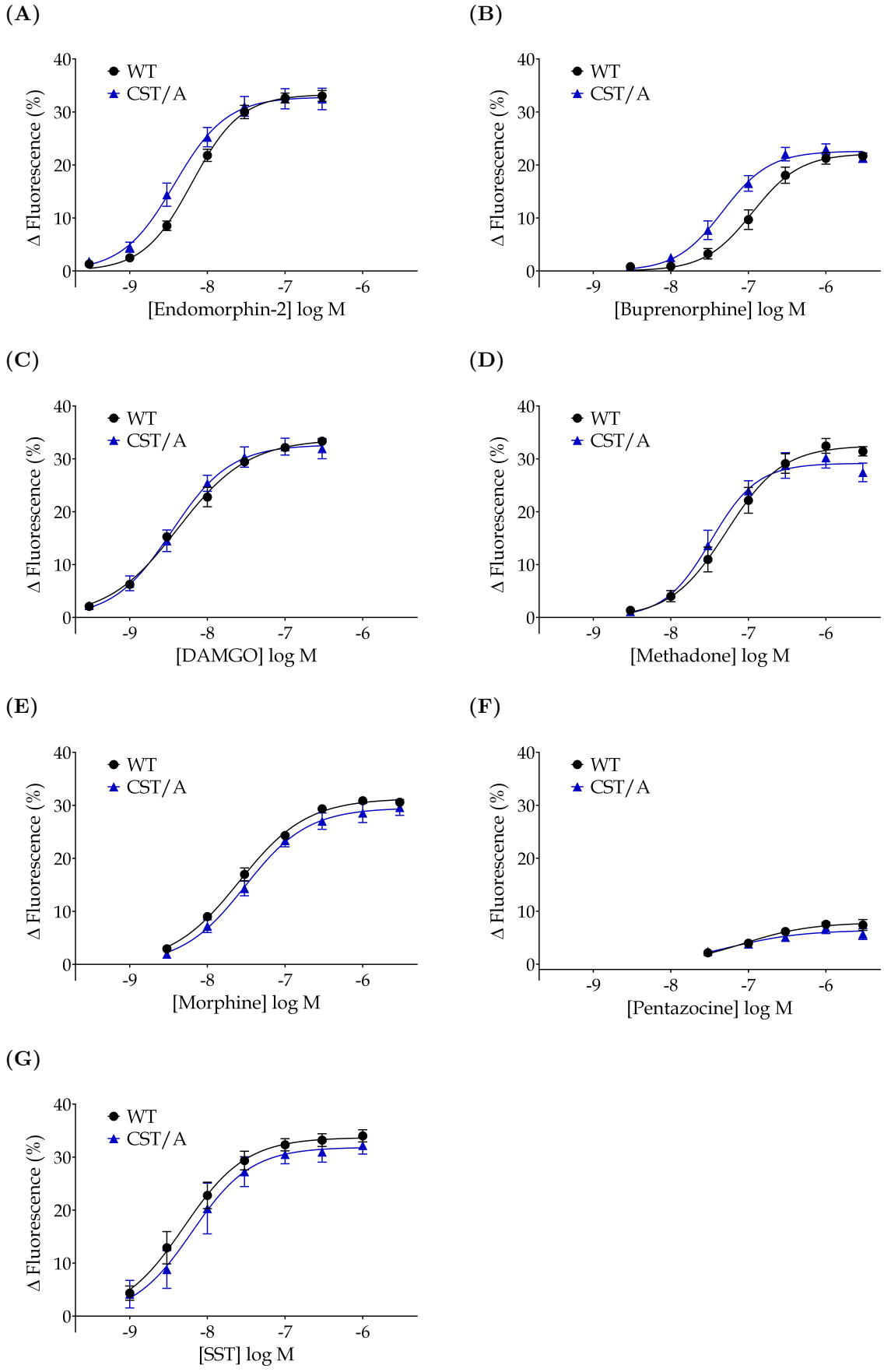
(A)
WT
CST/A
Δ Fluorescence (%)
[Endomorphin-2] log M
(B)
WT
CST/A
Δ Fluorescence (%)
[Buprenorphine] log M
(C)
WT
CST/A
Δ Fluorescence (%)
[DAMGO] log M
(D)
WT
CST/A
Δ Fluorescence (%)
[Methadone] log M
(E)
WT
CST/A
Δ Fluorescence (%)
[Morphine] log M
(F)
WT
CST/A
Δ Fluorescence (%)
[Pentazocine] log M
(G)
WT
CST/A
Δ Fluorescence (%)
[SST] log M

8.2.3 Opioid-Mediated Signal Desensitisation in AtT20 cells

To assess the importance of hMOPr C-terminal phosphorylation in agonist induced acute signalling desensitisation, AtT20-hMOPr-CST/A cells were exposed to a stimulus opioid concentration then challenged with a saturating concentration. Using FLPR® membrane potential dye as previously described (Section 3.5), hyperpolarisation recorded after challenge concentration was compared to the response obtained from cells not exposed to stimulus opioid concentration. Desensitisation was then compared to the results obtained with AtT20-hMOPr-WT results. In addition, heterologous desensitisation was also examined by challenging cells with SST after opioid stimulus as shown in representative traces in Figure 8.5.

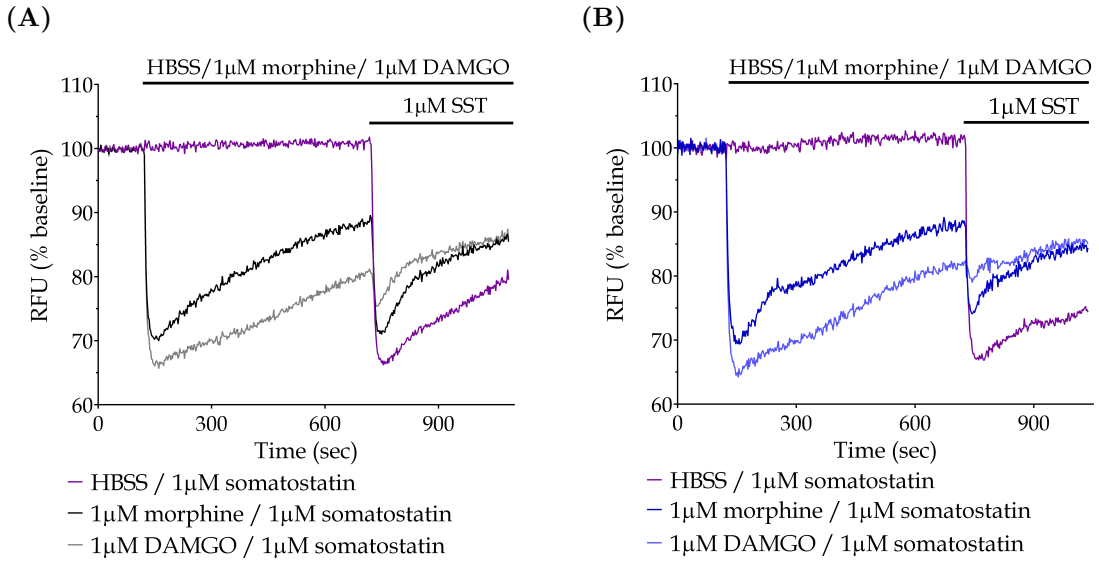

Figure 8.5. Representative traces of heterologous desensitisation mediated by 10 minutes DAMGO and morphine stimulus in **(A)** AtT20-hMOPr-WT and **(B)** AtT20-hMOPr-CST/A. Difference in maximum response was used to calculate desensitisation and plot a time course. Note that the difference in SST hyperpolarisation especially after morphine stimulus was lower in hMOPr-CST/A when compared with hMOPr-WT.

Varying interval times between stimulus and challenge addition were used to obtain homologous and heterologous desensitisation time courses (Figure 8.6). Interestingly the analysis of variance between time courses of both hMOPr variants only identified significant differences between heterologous desensitisation data (two-way *ANOVA*, $p<0.05$), where the higher variance was observed at 10 minutes for DAMGO and 20

minutes for morphine (multiple *t*-test, p<0.01). To further assess time course results, $t^1/_2$ and maximum desensitisation (D_{max}) was compared between variants and are summarised in Table 8.2. Since phosphorylation has been linked to hMOPr regulation it was surprising that homologous D_{max} of morphine and DAMGO was not influenced by phosphosite deletions (*t*-test, p>0.05), however a slightly higher morphine induced heterologous D_{max} was observed for CST/A (36±4%) compared with WT (25±2%, *t*-test, p>0.05).

Despite the lack of difference in extent of homologous desensitisation, it was apparent from the time course that the rate of desensitisation was faster in the phosphorylation deficient receptor. A $t^1/_2$ of 4.8±0.6 min was obtained with DAMGO for the CST/A mutant compared with 12.4±2.9 min for the hMOPr-WT; a similar rate reduction of almost twofold was also determined for morphine homologous and DAMGO heterologous desensitisation time course derived $t^1/_2$, as shown in Table 8.2.

Table 8.2. Summary of desensitisation time course $t^1/_2$ and D_{max} in AtT20 cells expressing WT and CST/A hMOPr

	$t^1/_2$(min)		**D_{max}(%)**	
Opioid	WT	CST/A	WT	CST/A
Homologous desensitisation				
DAMGO	12.4±2.9	**4.8±0.6***	66±1	61±4
Morphine	7.5±1.3	**3.8±0.2***	61±2	59±4
Heterologous desensitisation				
DAMGO	10.5±2.1	**4.9±0.6***	55±2	58±4
Morphine	12.2±5.8	4.4±1.6	25±2	**36±4***

Desensitisation data were fitted to a one-phase exponential association and $t^1/_2$ and D_{max} (plateau) obtained. Highlighted are results significantly different to hMOPr-WT (*t*-test, p<0.05). Values shown are mean ± SEM, n=5-6.

To complement the data obtained, signal decay during 40 minutes stimulus was also assessed for the CST/A mutant (Table 8.3). Corroborating the homologous desensitisation time course data, the maximum decay observed for DAMGO was similar between variants and only a slightly decrease with morphine was found with the CST/A mutant (*t*-test, p=0.0426). In contrast to the rate of desensitisation reported, the time

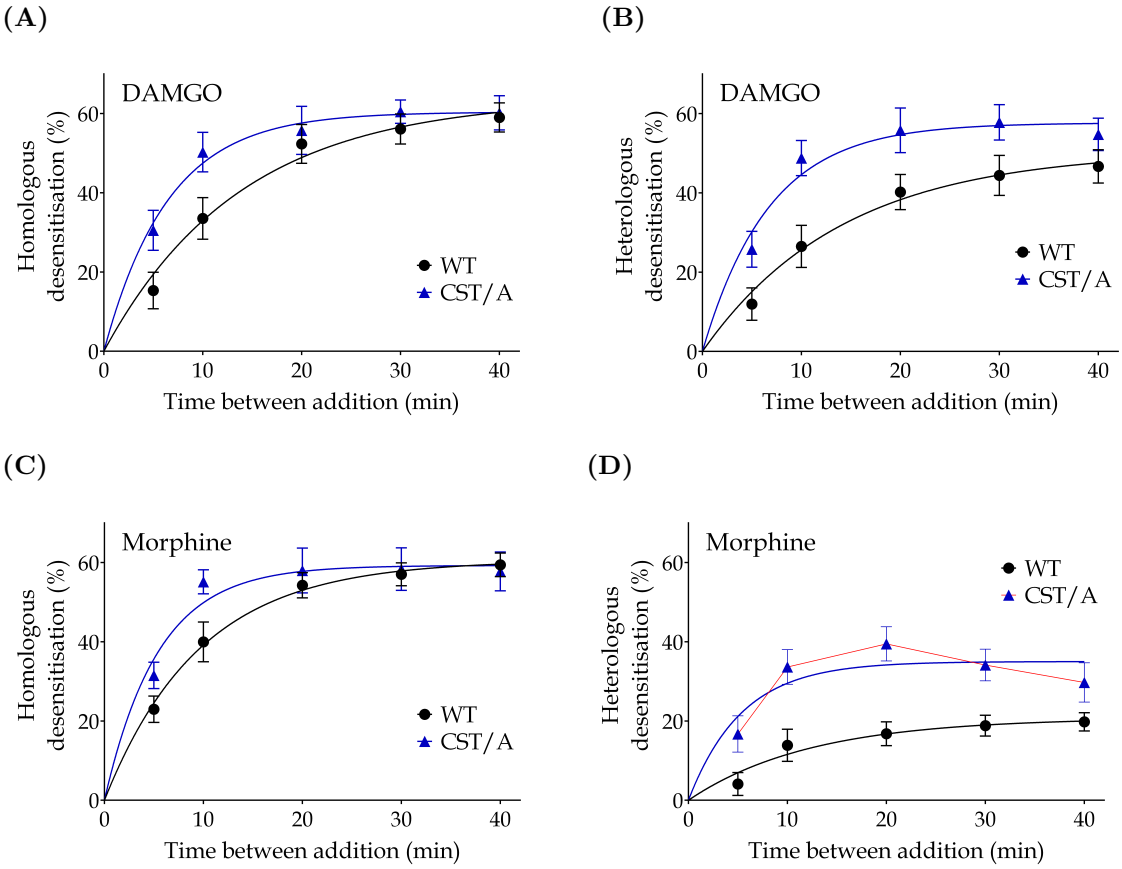

Figure 8.6. Effect of C-terminal total phosphosite deletion on homologous and heterologous signal desensitisation by DAMGO and morphine. AtT20 cells expressing hMOPr-WT (black) or hMOPr-CST/A (blue) were assessed using FLPR® membrane potential dye as described in the methods chapter. **(A)** Homologous and **(B)** heterologous desensitisation after 1μM DAMGO stimulus. **(C)** Homologous and **(D)** heterologous desensitisation after 1μM morphine stimulus. Note that heterologous data had a bell shape pattern (red). CST/A mutation did not significantly change the homologous signal desensitisation time course by DAMGO and morphine, however the heterologous desensitisation time course mediated by both opioids were affected (two-way *ANOVA*, $p<0.05$). Data are expressed as percentage desensitisation from vehicle control, and represent the mean ± SEM of 5-6 independent determinations performed in duplicate.

constant of signal decay was not affected by C-terminal phosphosite deletion (*t*-test, $p>0.05$).

Overall, it was astonishing to uncover that deletion of all C-terminal tail phosphorylation sites of the hMOPr only caused a relatively small change in the homologous desensitisation rate and mainly affected the heterologous desensitisation time course.

Table 8.3. Summary of time constant (τ) and maximum decay (Y_{max}) of signal in AtT20 cells expressing WT or CST/A hMOPr

	τ(sec)		$\mathbf{Y}_{max}$(%)	
Opioid	WT	CST/A	WT	CST/A
DAMGO	898±131	721±165	94±1	91±2
Morphine	612±76	479±96	96±1	**92±1***

Signal decay data were fitted to a one-phase exponential association and $t^1/_2$ and Y_{max} (plateau) obtained. Highlighted are results significantly different to hMOPr-WT (t-test, $p<0.05$). Values shown are mean ± SEM, n=5-6.

8.2.4 Opioid-Mediated Phosphorylation of hMOPr Ser377

Considering the surprising results obtained for signalling and desensitisation, an assay to examine phosphorylation of Ser377, therefore validate phosphorylation deletion, was performed.

Figures 8.7**(A)** and 8.7**(B)** show western blot results for hMOPr-WT and hMOPr-CST/A which confirm the phosphorylation deletion. Note that AtT20-hMOPr-WT was always carried in parallel in the same blot as a control. Further analysing the western blot data obtained, it was possible to determine that the total amount of hMOPr in AtT20-hMOPr-WT and AtT20-hMOPr-CST/A was similar after correcting HA data using GAPDH (Figure 8.7**(C)**, (t-test, $p>0.05$).

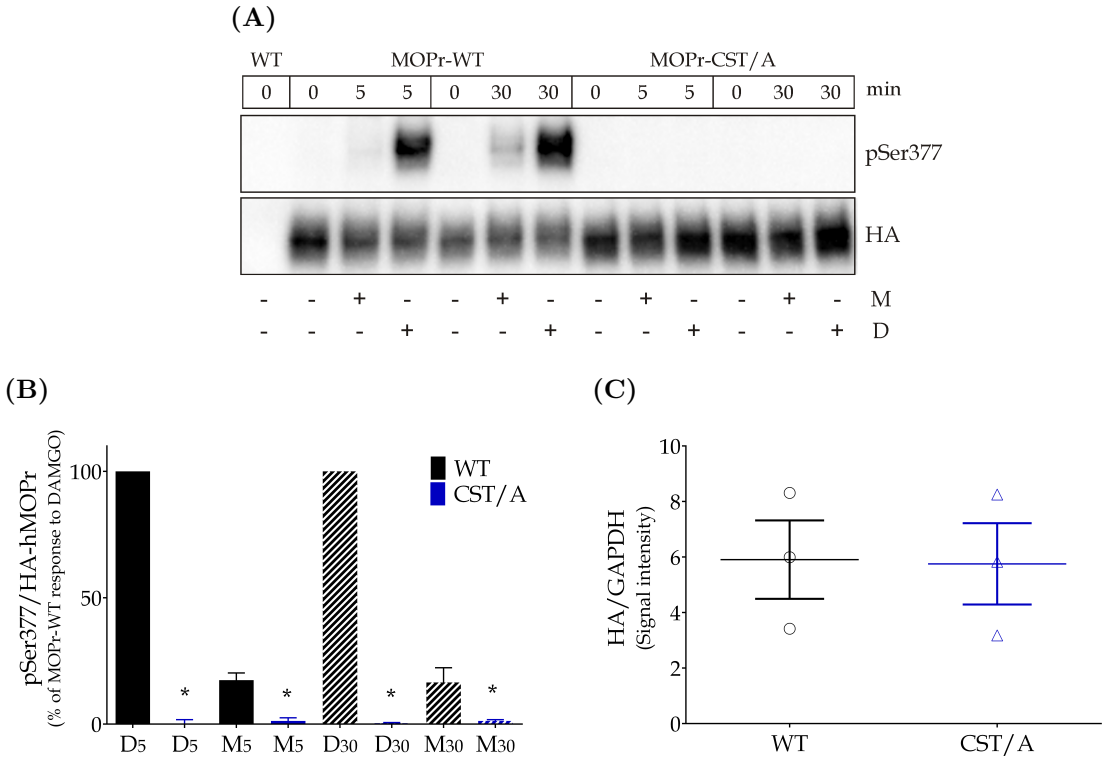

Figure 8.7. Morphine and DAMGO induced phosphorylation of hMOPr Ser377 residue in AtT20-hMOPr-WT but not AtT20-hMOPr-CST/A as expected for a phosphosite deleted mutant. **(A)** Representative blot from one of three independent experiments of 5 and 30 minutes opioid treatment. AtT20 cells stably transfected with hMOPr-WT or hMOPr-CST/A were either not exposed (-) or exposed (+) to 1μM DAMGO (D) or 1μM morphine (M) for 5 or 30 minutes. The cells were lysed and immunoblotted with anti-pSer377 antibody (pSer377, upper panel), then the blot was stripped and reprobed with anti-HA antibody to detect total hMOPr (HA, lower panel). Further methods details are described in Section 3.6 **(B)** pSer377 quantified by densitometric analysis after morphine and DAMGO incubation for 5 (no pattern) or 30 minutes (stripe pattern). Data are presented as % of DAMGO-induced Ser377 phosphorylation (pSer377) in AtT20-hMOPr-WT (100%) ± SEM; note that results were corrected for total receptor number (pSer377/HA). **(C)** AtT20-hMOPr-WT and AtT20-hMOPr-CST/A presented similar quantities of total receptor measured using HA corrected with loading control GAPDH (t-test, p>0.05, n=3)

8.2.5 Loss of Membrane hMOPr

Just et al. (2013)[171] reported that deletion of phosphorylation sites in the mMOPr abolished opioid induced receptor internalisation. To confirm that the CST/A mutant does not leave the cell surface given the absence of phosphorylation sites on C-terminal, using a whole-cell ELISA technique the amount of hMOPr WT and hMOPr-CST/A membrane surface loss was quantified after morphine and DAMGO treatment for 5

and 30 minutes.

Figure 8.8 shows the results obtained. As expected the amount of hMOPr-CST/A on the membrane did not significantly change after opioid treatment (one-sample t-test, p>0.05), while DAMGO mediated a significant receptor endocytosis at hMOPr-WT which was much higher after 30 minutes when compared to 5 minutes (t-test, p<0.05).

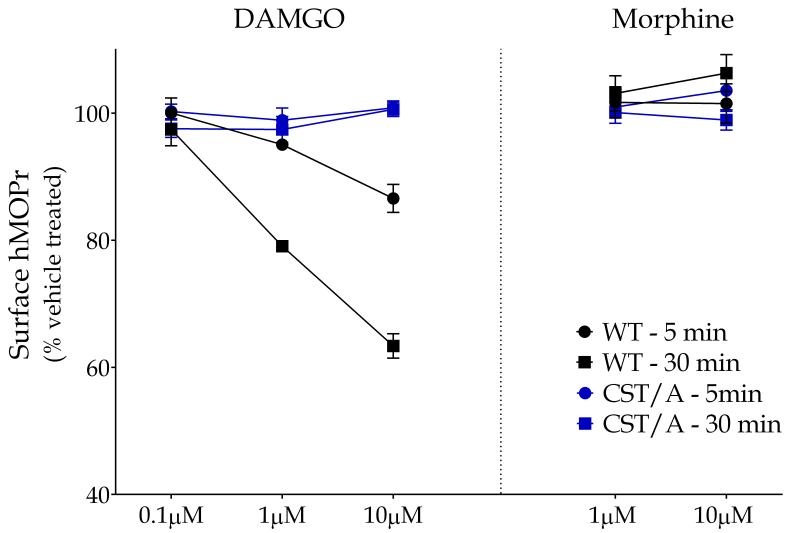

Figure 8.8. Loss of membrane hMOPr-WT and hMOPr-CST/A after DAMGO or morphine incubation for 5 or 30 minutes. As expected, the amount of hMOPr-CST/A at the cell surface did not change after DAMGO and morphine incubation (one-sample t-test, p>0.05), while receptor levels on the surface were reduced in the AtT20-hMOPr-WT cells after 1μM and 10μM DAMGO incubation when compared to 0.1μM DAMGO (t-test, p<0.05). Data obtained as described in Section 3.8 represent mean ± SEM of pooled data from 4-5 independent determinations performed in triplicate.

8.3 Discussion

The MOPr C-terminal tail is phosphorylated at many residues and the role of this phosphorylation on β-arrestin recruitment and receptor internalisation has been previously established[171,236]. However, the involvement of phosphorylation in receptor signalling and desensitisation is still to be elucidated and considering the studies available it is clear that complex mechanisms are in play. The present work, has now confirmed that a complete deletion of the C-terminal phosphorylation sites produces a receptor that can signal via GIRK activation in a similar manner to the wild-type receptor, while

the effect on desensitisation is not as dramatic as might be predicted. A summary of this chapter's findings are presented in Table 8.4.

Table 8.4. Summary of C-terminal total phosphosite deletion findings

hMOPr variant	Assay performed	Key observations
CST/A	Radioligand binding	Similar B_{max} and K_D
	GIRK activation	Endomorphin-2 and buprenorphine more potent
	Desensitisation time course	Faster rate but same extent of homologous desensitisation
		Heterologous desensitisation affected by both opioids. DAMGO faster rate while morphine higher extent of desensitisation (bell curve)
	Signal decay	Morphine induced slightly lower extent of decay
	Ser377 phosphorylation	Not phosphorylated
	Cell surface hMOPr loss	No receptor loss

All results are in comparison with hMOPr-WT

The C-terminal tail amino acid sequence of the MOPr is very different from other GPCRs. Little homology is observed when compared to opioid receptors, which emphasises the different role it plays across this family. Georgoussi et al. (2006)[131] demonstrated *in vitro* that the MOPr C-tail peptide was unable to bind to any form of Gα, in contrast to the DOPr C-tail where interaction was detected. Yet the G$\beta\gamma$ subunit interacted with both tails. In another study by the same group[130], the C-terminal tail was identified as a critical MOPr region for receptor signalling as it is involved in the interaction between receptor and G proteins. The present study demonstrated that alanine substitution of serine and threonine sites did not significantly affect GIRK activation, therefore if the C-terminal is involved in G protein coupling or activation, it was definitely not disturbed by the mutation induced conformational change and the lack of phosphorylation, even of constitutive phosphorylated residues (Ser365 and Thr372)[63].

For a long time, GPCRs were thought to signal exclusively via G proteins while GRKs and arrestins were regulatory proteins whose roles were limited to controlling

processes such as receptor phosphorylation, internalisation and recycling. Recent evidence has changed our understanding of GPCR signalling, with new emerging information supporting GRKs and arrestins as G protein independent signal transducers[291].

A good correlation between β-arrestin 2 recruitment and MOPr Ser377 phosphorylation has been shown previously[236]. If MOPr can signal through β-arrestin pathways, compromised signalling would be expected in hMOPr-CST/A mutant. It is important to highlight that different phosphorylation patterns can produce a different arrestin conformation which can be related to signalling or to activation of the endocytosis machinery alone. At the β_2-adrenergic receptor, while GRK5/6 phosphorylation was G protein-independent and activation of ERK was mediated by β-arrestin, GRK2/3 phosphorylation was G protein-dependent and was primarily responsible for receptor internalisation[292]. Importantly, both kinases were involved in desensitisation. Therefore, MOPr studies which assessed β-arrestin interaction with MOPr or recruitment[236,243], are not necessarily determining the bias in signalling, as β-arrestin can be recruited but restrained in a conformation that favours endocytosis, not signalling pathways like ERK activation. Unfortunately we were unable to reliably measure ERK pathway activation because basal ERK phosphorylation in AtT20 cells was too high; further studies will be conducted in HEK293 or CHO cells for this purpose.

Rivero et al. (2012)[294] reported that endomorphin-2 is an arrestin-biased agonist at MOPr-WT, where arrestin FRET analysis was performed in HEK293 cells and electrophysiology in LC neurons. The authors correlated this finding to an endomorphin-2 ability to promote a robust phosphorylation of Ser375 on MOPr. Based on the later study, it can be speculated that the inability of endomorphin-2 to mediate phosphorylation of hMOPr-CTST and recruit β-arrestin could be correlated to the slightly higher potency observed for this agonist in the present work. However, considering the time frame of GIRK activation versus phosphorylation and arrestin-binding[171,236], β-arrestin recruitment might be too delayed to be involved. In contrast, kinase activation is definitely an early enough process to be implicated as DAMGO phosphorylation of mMOPr Ser375 is almost complete at 20 seconds.

Buprenorphine did not significantly recruit β-arrestin 2[236], which is in agreement to

the very inefficient phosphorylation of Ser377 presented in Chapter 5. The significant increase in buprenorphine potency at hMOPr-CST/A in the present study is probably related to the distinct conformations that buprenorphine stabilises this receptor. According to Shim et al. (2013)[318] MOPr 2D distribution with this agonist was between agonist and antagonist in molecular dynamics simulations.

Acute desensitisation and internalisation are both regulatory processes however these regulatory mechanisms are temporally separated. The development of more precise techniques have made it clear that acute desensitisation is a much faster process than receptor internalisation[356]. The present study not only supports the temporal separation, but also the lack of correlation between internalisation and desensitisation as the hMOPr-CST/A mutant did not internalise yet homologous desensitisation was relatively similar to the hMOPr-WT. It is important to point out that the role of opioid receptor trafficking in the clinical response to agonists is controversial, for example both morphine and methadone are effective analgesics to which tolerance develops but they have contrasting effect in receptor trafficking.

Surprisingly, DAMGO and morphine homologous desensitisation in AtT20-hMOPr-CST/A was only slightly faster than WT, in the present study, however both showed similar maximum desensitisation at 40 minutes. Birdsong et al. (2015)[33] assessed desensitisation in brain slices of MOPr knockout mice injected with mMOPr-WT or phosphosite mutants. They measure desensitisation as decay after 30μM ME or sustained desensitisation where neurons were challenged with 100nM ME before and after 5 minutes stimulus with 30μM ME, with a wash between addition of different concentrations. The decay of ME signal was similar between all variants tested in the mediodorsal thalamus neurons but slightly different in LC neurons. Sustained desensitisation was significantly decreased when both STANT and TSST were mutated to alanine, with apparently a larger contribution from STANT; however both clusters individually had a non significant decrease. A recent study by Yousuf et al. (2015)[364] also examined desensitisation in phosphosite mutants but in AtT20 cells. Similarly to the above study they used a submaximal ME concentration (10nM) before and after 10μM ME or 10μM morphine with a 1 minute wash between additions to measure

sustained desensitisation. Interestingly, they found that desensitisation induced by morphine was not affected in all variants, while ME mediated desensitisation was abolished when all phosphosites were deleted; nevertheless deleting STANT in addition to Thr370, Ser363 and Thr383 did not affect desensitisation, which indicated that desensitisation could be related to TSST and/or Thr394. In addition, they completed their analysis by showing that sustained desensitisation with morphine can be abolished by a PKC inhibitor. These studies are quite conflicting. While one study highlights the role of STANT phosphorylation the other study dismisses it, however it is clear that when both STANT and TSST residues are mutated, ME sustained desensitisation is deeply compromised. Acute desensitisation measured using signal decay is in agreement with the DAMGO result presented here; however desensitisation after opioid challenge, called sustained desensitisation, is contradictory. The differences in the assays performed need to be taken into consideration, as not only were different opioid concentrations used but a wash step was also performed before opioid challenge. In this current study, the assay was wash-free, which meant no recovery time was given between stimulus and challenge and the desensitisation is determined using a saturating not a submaximal concentration. ME is a high efficacy agonist, therefore only a small portion of the receptors need to be occupied to produce a response. Moreover receptor reserve could be misleading when assessing desensitisation[79,294]. In cells with a large number of receptor reserve, receptor desensitisation may not be detected even when using submaximal probe concentration. In the present study, desensitisation was observed for both hMOPr variants therefore the cells used are likely to have none to low receptor reserve. In addition, Arttamangkul et al. (2015)[13] highlighted how different measurements can actually report distinct results, and clearly the present study is an example.

Previous studies have demonstrated the importance of phosphorylation in desensitisation by manipulating kinase activity. Decrease of morphine induced desensitisation has been demonstrated by inhibiting PKC[167] or more specifically its isoform PKCα[23], while the opposite was shown to be true when activating PKC heterologously via another receptor or using phorbol esters[13,21]. Differently from morphine,

DAMGO desensitisation was not affected by PKC modulation however GRK2 dominant negative mutant over-expression reduced DAMGO but not morphine induced desensitisation[23,167]. PKCϵ was also correlated to mMOPr desensitisation measured by intracellular calcium. This kinase mediated morphine desensitisation however only when Ser363, Thr370 and Ser375 were mutated to alanine it was also able to mediate DAMGO desensitisation[374].

Correlating the above kinase and phosphosite mutant desensitisation results is a complicated task. Phosphorylation of the STANT is accepted to be mediated by GRK2/3 by DAMGO and GRK5 by morphine, while PKC phosphorylates TSST, Ser363 and Thr370[63,221]. Thus the effect of STANT mutation by ME observed by Birdsong et al. (2015)[33] could correspond to the same decrease in desensitisation observed for GRK2 dominant negative mutation, however the synergism with TSST would be thought to involve PKC but it would be surprising as inhibiting PKC did not affect ME desensitisation in mMOPr-WT[364]. Nevertheless, as previously described, inhibiting phosphorylation by phosphosite mutation can convert DAMGO desensitisation to PKCϵ dependent[374], which may phosphorylate TSST and affect desensitisation which then supports the data reported. Considering the mutants used by Yousuf et al. (2015)[364], the PKC phosphorylation site, TSST, is the last one deleted which completely abolished ME desensitisation. This is conflicting considering PKC inhibition did not affect ME desensitisation in the same study, however again the proposed involvement of PKCϵ needs to be considered. It is also surprising that PKC affected morphine desensitisation but deleting all phosphorylation sites of the C-terminal did not affect morphine induced desensitisation. It could be speculated that a different region of the receptor is phosphorylated by PKC or PKC sterically affecting desensitisation and not the phosphorylation directly, as it may be recruited independently of phosphorylation sites being available. This is supported by the aforementioned study where use of a PKC inhibitor in the total C-terminal phosphosite deleted mutant abolished homologous and heterologous desensitisation by morphine; however, it is also possible that PKC affects the receptor indirectly by phosphorylating another protein which is responsible for morphine induced MOPr signalling desensitisation and also

SST receptor desensitisation.

Interestingly, DAMGO and morphine stimulation of hMOPr-CST/A produced a higher heterologous desensitisation than observed for hMOPr-WT at 10 minutes and 20 minutes respectively. Differences in heterologous desensitisation between relatively mature and immature rats were reported in LC neurons[211]; and it was not correlated with PKC activity but with a decrease in GRK2 expression with age which abolished heterologous desensitisation. Therefore, hMOPr may recruit GRK2, however because it is not able to phosphorylate hMOPr-CST/A it would cross phosphorylate SST receptor(s). This would be more plausible if these receptors are heterodimers as previously described[272]. In hMOPr-CST/A, because signalling via GIRK activation is similar to hMOPr-WT, it would be unlikely that the increase in heterologous desensitisation be related to effector unavailability. In addition, the bell shaped response to morphine stimulus and the faster rate of homologous desensitisation suggests that hMOPr-CST/A activates a mechanism which is faster than that activated by hMOPr-WT. It is possible that the increase in GRK2 activation by this receptor, without having the regular role to phosphorylate C-terminal residues, competes with GIRK for the G$\beta\gamma$ subunits, as previously reported[286], which is a fast process and would explain the increased rate in desensitisation. To further support this hypothesis, G$\beta\gamma$ subunits have been described to bind with the C-terminal tail[131], which would make the interaction even faster and highly probable.

In conclusion, substituting threonine and serine to alanine at the C-terminal tail of the hMOPr extinguished internalisation induced by DAMGO as previously reported by Just et al. (2013), while efficacy of GIRK activation by a range of opioids was not affected and potency was only slightly increased by buprenorphine and endomorphin-2. Interestingly, using a wash-free protocol to analyse desensitisation by a saturating concentration challenge after submaximal stimulus, the only difference observed for homologous desensitisation was an increase in desensitisation rate while the effect on heterologous desensitisation was much more evident. The results here presented support the hypothesis that phosphorylation of the C-terminal may affect the rate of homologous desensitisation but not maximum desensitisation; however, it is likely that

the lack of phosphorylation site, not phosphorylation per se, is the main factor responsible for the results obtained.

9

Summary and Prospects

In this study from the N to the C-terminal of the hMOPr, SNPs and phosphorylation deleted mutants expressed in FlpIn™ AtT20 cells were assessed with the aim to better understand signalling and regulation of the μ-opioid receptor. Starting with the development of a new technique to generate real-time kinetics of homologous and heterologous desensitisation data and combining with assays to examine receptor signalling and regulation (GIRK activation, Ser377 phosphorylation and receptor loss from the surface). This work is the first study to assess a large number of human MOPr variants in AtT20 cells, which are excitable cells like neurons.

Contents

9.1 General Discussion

The μ-Opioid receptor (MOPr) has a crucial role in opioid induced analgesia, nevertheless it is also involved in undesirable effects including tolerance and dependence[233]. In the present study we demonstrated that the consequence of altering one amino acid can be dramatic at the molecular level; this not only highlights the importance of certain receptor regions for signalling and regulation but also the significance of genetic variability on interpersonal variation in opioid response. Moreover we showed that hMOPr phosphorylation at the C-terminal and the third intracellular loop (ICL3) is not essential for acute desensitisation. The overview of the individual remarks are summarised in Table 9.1.

Amino acids substitution in the N-terminal, first transmembrane domain (TM1), second intracellular loop (ICL2), third intracellular loop (ICL3) and C-terminal of the hMOPr were studied. Only changes at ICL2 and ICL3 were profoundly detrimental to hMOPr signalling via GIRK activation and this confirms previous studies that support these 2 regions as crucial to G protein activation[130,224,315]. It is important to note that the C-terminal has also been linked to G protein signalling; however, in this instance the amino acid substitution was aimed to disrupt phosphorylation with minimal conformational change. Note that the region thought to be involved in G protein activation is the one close to TM7, now denominated helix 8, where a conserved sequence is observed[42,208].

The importance of the N-terminal region in signalling and regulation was confirmed by using hMOPr-A6V and hMOPr-N40D SNPs. N-terminal role in G protein activation is not as crucial as ICL2 and ICL3, these regions being in direct interaction with the G proteins; however, it is interesting to observe a change in signalling, desensitisation, phosphorylation and internalisation coming from a 'distant' region. Gupta et al. (2008)[139] had previously demonstrated that activation of MOPr produced a change in the N-terminal conformation. Here we demonstrated that a single amino acid change in the N-terminal can also affect agonist induced conformational change, considering changes in signalling and regulatory processes reported.

Table 9.1. Overview of findings. Similar (−) and different (+) results to hMOPr-WT according to data presented.

hMOPr variant	DAMGO Affinity (K_D)	GIRK activation	Homologous Desensitisation	Heterologous Desensitisation	Signal decay	Ser377 phosphorylation	Cell surface hMOPr loss
A6V	−	+ (M*)	+ (D*,B)	+ (D*,B)	+ (D*,E*)	+ (B)	−
N40D	−	+ (B,P)	+ (D*)	−	−	+ (D)	+ (D)
L85I	−	−	−	−	−	+ (D)	+ (D,M)
R181C	+	+ (A)	+ (D)	+ (D)	+ (D)	+ (D)	+ (D)
R260H	−	+ (A)	+ (M)	+ (D,M)	+ (D,M)	+ (D)	+ (D)
R265H	−	+ (A)	−	+ (D,M)	+ (D,M)	−	−
S268P	−	+ (M,Mt,B,D)	+ (M,D)	+ (M,D)	+ (M)	−	−
S268A	−	+ (B,P)	−	−	−	−	−
3S/A	−	+ (M,Mt,D)	+ (D)	+ (M,D)	+ (M)	+ (D)	+ (D)
3ST/A	−	+ (A)	+ (M,D)	+ (M,D)	+ (M,D)	+ (M,D)	+ (D)
CST/A	−	+ (E,B)	+ (M,D)	+ (D,M)	+ (M)	+ (M,D)	+ (D)

The letters in brackets indicate the opioid tested which presented a different response to hMOPr-WT. Results of drugs marked with * are unlikely to have biological relevance. DAMGO (D), morphine (M), methadone (Mt), buprenorphine (B), endomorphin-2 (E), pentazocine (P), all opioids tested (A)

The present work highlighted the different profile of buprenorphine compared with other opioids tested. It is well established that compared with other commonly used opioids buprenorphine has a slow dissociation rate and a low intrinsic activity, although how this opioid affected specific regions of the receptor is not well understood. To the best of my knowledge this is the first work to demonstrate that modification in the N and C-terminal structure affected buprenorphine signalling via GIRK activation, while changes in the ICL3 did not change buprenorphine potency as expected in line with other opioids response. This unexpected result could be related to the different conformations this agonist stabilise the receptor. According to molecular dynamics simulations buprenorphine 2D distribution is between those of agonists and antagonists[318].

Another interesting finding was the higher ICL3 'dependence' of morphine and methadone to activate G protein. While changes in membrane potential induced by morphine and methadone were similar in the N and C-terminal variants compared with hMOPr-WT, the decrease in efficacy and potency at ICL3 variants were markedly pronounced for these two opioids, when compared to the other opioids tested including buprenorphine. This is of great importance not only for ICL3 SNPs carriers who may have a lower response to these commonly prescribed opioids, but also points to a considerable difference in conformations stabilised by peptide opioids versus morphine and methadone.

Out of the eleven tested variants, L85I SNP at the first transmembrane domain was the only variant where signalling was identical to hMOPr-WT after exposure to a range of opioids; this supports that this region plays a minimal role in G protein coupling. However, regulation of this polymorphism is quite unique as it was the only receptor variant to slightly increase surface receptor loss after exposure to both DAMGO and morphine. Considering the hierarchical phosphorylation of the C-terminal STANT cluster and the importance of this cluster to β-arrestin recruitment and engaging endocytosis machinery, it is unlikely that phosphorylation is the main cause of increased receptor loss. According to structural studies of the MOPr this region is involved in dimerisation[220,278]; therefore, a possible explanation is that endocytosis is facilitated

by the formation of dimers, but this is merely speculative.

DAMGO affinity was only affected at the ICL2 variant. This supports the notion that at least for DAMGO, ICL3 is not involved in affinity but in signalling transduction. According to previous reports, GPCR-G protein are precoupled and ligand affinity is higher for G protein bound conformation[16,17,334]. I could speculate that the interaction between ICL2 and G protein stabilises the receptor in a higher affinity state, while ICL3 interaction is necessary to stabilise agonist bound active conformations which then activate G proteins; thus, ICL2 and ICL3 would be crucial for signalling.

In this project an isogenic system was used to obtain similar expression of the hMOPr variants across the different cell lines produced. Interestingly, the ICL3 with multiple phosphosite deletion presented a considerably lower receptor expression which was previously reported for mutation of the threonine[154]. We demonstrated for the first time the presence of hMOPr-3ST/A with lower molecular weight. This supports the possibility of a deficiency in receptor maturation and accumulation of this receptor in the ER. In addition, the lack of phosphorylation sites at the ICL3 could also be related to increase in down-regulation which needs to be further investigated.

In the present work mutation at the hMOPr incapacitating phosphorylation of the C-terminal not only caused an increase in the rate of homologous desensitisation, with no effect in the extent, but also increased heterologous desensitisation. This was the only variant tested that increased heterologous desensitisation, therefore it points to activation of a new mechanism or the 'overactivation' of the same mechanism observed for hMOPr-WT. Therefore, I demonstrated that phosphorylation sites at the C-terminal are not essential for acute desensitisation. The absence of phosphorylation sites affected heterologous desensitisation, and we hypothesised that kinases such as GRK2 would still be efficiently recruited but in the absence of the site to phosphorylate, it promiscuously and directly phosphorylate somatostatin receptors. Considering the fast kinetics observed, the sequestration of the $\beta\gamma$ subunits, as previously reported by Raveh et al. (2010)[286], would also explain the results obtained; recruited GRK2 without a place to phosphorylate would have more units to compete with GIRK for the $\beta\gamma$ subunits. In contrast to the C-terminal, multiple phosphosite deletions at

ICL3 compromised heterologous desensitisation which could inversely be related to a decrease in GRK2 recruitment, consequently, decrease in $\beta\gamma$ subunits sequestration which is supported by decreased phosphorylation. Nevertheless, this mechanism is not supported by S268P SNP regulation, where DAMGO induced phosphorylation was not affected, but heterologous desensitisation was deeply compromised. Therefore, this variant may hold the key to determine an even more complex mechanism involving heterologous desensitisation.

In this study desensitisation results obtained were often slightly different from previously reported[33,364]. This could be related to the use of different cell lines as we only used AtT20 while other groups mainly use HEK293 cells and LC neurons. AtT20 and HEK293 cells have different G proteins and varying amounts of kinases as previously demonstrated by Atwood et al. (2011)[15]. Therefore, the lower levels of GRK proteins observed in AtT20 cells could increase the possibility of activation of a desensitisation mechanism that is GRK independent. In addition, AtT20 cells presented a very high basal phosphoERK levels, which could also be relevant in terms of mechanism of desensitisation in these cells. The possibility of other mechanisms of desensitisation that is not phosphorylation and/or β-arrestin involved had been mentioned in some parts of this work. One interesting possibility is the role of RGS proteins which was reported by Garzon et al (2005)[127] in the central nervous system to desensitise MOPr under certain circumstances.

In conclusion, phosphorylation of the C-terminal and the ICL3 can slightly affect homologous desensitisation, but it is not the main regulatory process underlying hMOPr acute homologous desensitisation by DAMGO and morphine. In contrast, mechanisms involved in heterologous desensitisation are likely to be more dependent on phosphorylation; however, it is possible that the consequence of conformational changes post mutagenesis is the real cause of differential desensitisation regulation.

9.2 Limitations and Further Directions

A translational study is necessary to determine if findings observed here, such as the selective loss of buprenorphine effect at N40D, have the same impact in clinical setting. In Australia buprenorphine is not only widely used for chronic pain in malignant and non-malignant conditions but also in treatment of opioid addiction. Despite uncertainty regards association between N40D polymorphism and opioid addiction, the prevalence of the common polymorphism N40D is high among opioid addicts[9,173,249]. Therefore, it can be expected that many carriers of N40D allele are treated with buprenorphine. If the work presented by our group in Knapman et al. (2014)[182], where in many pathways compromised buprenorphine signalling was found for this variant, is proven to be clinically relevant, consideration should be taken when prescribing opioids for patients carrying this allele, as it would be less effective analgesic and potentially less effective maintenance therapy for opioid addicts. Despite a low prevalence of ICL2 and ICL3 SNPs allele, it would still be important to determine if these patients have a low response to opioids, as widely used opioids, such as morphine, had its signalling dramatically compromised at these variants. In fact, finding carriers of R181C SNPs may help to determine the importance of the MOPr in a manner never before studied.

It is noteworthy that in this study we only worked with polymorphic homozygous genotypes to investigate the full effect of the single-nucleotide polymorphisms. The majority of the polymorphic carriers present a heterozygous genotype. Therefore, the effect in these individuals may not be as noticeable as in individuals homozygous for the variant allele; note that for common SNPs homozygous genotype has been reported[88]. To address this limitation, in future studies we aim to use bicistronic vectors[198] to develop cell lines expressing both wild-type and polymorphic hMOPr. In theory this system would allow expression of equivalent amounts of both receptors; however, the final protein amount could be different as polymorphism can affect post-translational modifications and ER sequestration, in addition to mRNA expression by epigenetics modifications[105,253]. In the present study small differences were detected in some of the SNPs expression levels compared with hMOPr-WT, even though we used an isogenic

system; thus, it is likely that in a bicistronic system, WT and polymorphism expression will be different.

Studying post-translations modifications (PTM) of GPCRs may also help to understand receptor regulation. One PTM addressed in this thesis is the potential glycosylation deletion at the N40D polymorphism, which may not have been glycosylated at AtT20 cells. The importance of glycosylation will be further researched at a number of mutants within the potential glycosylation sites, and signalling and regulation assays similar to the ones performed in this work will be used. We also intend to determine if glycosylation of the potential sites are different between cell lines which has the potential to affect results obtained, and further influence comparisons between cell lines. It would also raise the possibility that differential glycosylation across different brain regions may be a role in regulation of MOPr function.

The hMOPr-R181C is a loss of function mutation that dramatically affected DAMGO binding. I hypothesised that this could be related to the inability of achieving a higher affinity state, where conformation is stabilised with the pre-assembled of the complex hMOPr-G protein. According to Atwood et al. (2011)[15], AtT20 only express one Gα protein isoform that preferentially binds to MOPr[75], and G_{i2} is pertussis toxin (PTX) sensitive; therefore, to support this hypothesis it would be interesting to compare binding of PTX treated AtT20-hMOPr-WT cells with AtT20-hMOPr-R181C. It is noteworthy that a similar assay has been performed to assess somatostatin receptor binding in AtT20 cells, and was found to dramatically reduced agonist binding[219].

In the present study, the information supplied by the crystal structure of the mMOPr was used to discuss many findings. It is important to highlight that even though the crystal structure is a great tool to better understand the MOPr, we need to take into consideration that it is an inactive conformation of the receptor, as it was bound to an antagonist. Furthermore, the N-terminal and the C-terminal tail were truncated and part of the third intracellular loop was substituted with a T4 lysozyme to facilitate crystallisation. Therefore, a crystal structure of one active state of MOPr would definitely increase our understanding of the present results. However, a G protein or a substitute (like nanobody used for β_2-adrenergic receptor[285]) would be necessary

to be bound to the receptor, and determining if the receptor used was able to signal would be important. The truncated receptor with the lysozyme at ICL3 would probably interfere with the active conformation(s) as observed for the much smaller change S268P.

Another limitation of the present work is regarding the interference of the triple-HA tag in hMOPr conformation and ability to signal. A single amino acid substitution at position 6 (A6V) can subtly affect receptor signalling and regulation; it follows that adding 39 amino acids to the N-terminal would have some deleterious effect. Nevertheless, it is important to acknowledge that previous studies did compare signalling between MOPr with and without an epitope-tag attached to the N-terminal, and no significant difference was observed for binding and cAMP inhibition[7]. Furthermore, all clones had the triple HA-tag, thus besides the N-terminal SNPs where close proximity could have a larger effect, it is unlikely that the tag interfered with transmembrane or intracellular variants differently from hMOPr-WT.

We focused on studying the effect of hMOPr variants in isogenic hMOPr expressed in AtT20 cells, thereby eliminating possible interference factors when comparing signalling and regulation between different cell lines. These cells were chosen because it is excitable and we aimed to evaluate membrane potential changes in cells natively expressing GIRK. However, it is important to note that AtT20 cells not only have quite a different mRNA profile for GPCR related signalling proteins compared with the widely used HEK293 cells, as published by Atwood et al. (2011)[15], but we also detected a high level of basal ERK phosphorylation, which unfortunately made it impossible to determine signalling through this pathway. Therefore for future studies in G protein dependent and independent pathways in the phosphorylation mutants, ERK activation will be studied in CHOKI FlpIn™ cells as previously described by our group for the bias signalling study of hMOPr SNPs[182,183]. In addition, we are seeking collaboration with experts in β-arrestin recruitment and signalling to determine the effect of phosphosite deletions in this still under characterised pathway for hMOPr.

MOPr desensitisation has been largely studied and may be involved in the development of opioid tolerance[356]. A vast number of studies have reported MOPr desensitisation. There is, however, a substantial variation in techniques to measure desensitisation. Note that Arttamangkul et al. (2015)[13] highlighted the importance of differentiating desensitisation results according to the methods of measurement used. In addition, the effectors involved in the measurement should always be taken into consideration, because although the majority of pathways measured are G protein dependent, different effectors may have different time courses after activation. Therefore, reliably comparing desensitisation results is difficult due to all the variations in the literature. At the present study we developed a novel real-time kinetics wash-free assay to measure MOPr desensitisation. This assay offered the advantages of non-invasiveness and high reproducibility[181]. Unfortunately, it added to the complicated field of comparing different assays measured under different conditions. The fact that we are measuring population response of whole cells instead of perforated single cells in electrophysiology, could already cause a small difference, however the largest difference observed and undoubtedly the biggest limitation of the assay performed, is that we cannot wash off the drugs before challenge. This is definitely a point to consider, especially if we take into consideration that many regulatory processes as dephosphorylation are extremely fast[102] and would definitely take place in short wash cycles. Therefore, without getting into the discussion of which assay would be the most appropriate, as every assay is indeed adding to the whole picture, the results reported here are highly reproducible and present an interesting addition to previously published desensitisation results of C-terminal phosphosite mutations.

The majority of the MOPr molecular studies utilises rat, mouse or human receptors. The percentage identity of human versus mouse and human versus rat is 94.22% each (Clustal Omega Software[256]) where most differences are in the C-terminal and the N-terminal region; however one change is in the first extracellular loop and one, exclusively in mMOPr, in the third transmembrane domain. Furthermore, in the C-terminal the last threonine of the TSST cluster is changed to asparagine in human while mMOPr doesn't have a threonine after the constitutively phosphorylated residue Ser363. In the

N-terminal of the rMOPr, a predicted N-glycosylation site in the proximal region is deleted, but another arginine is added at the distal region of this receptor. The present work supports the notion that a point mutation can affect receptor signalling and regulation, thereby when comparing interspecies MOPr results, consideration should be given to the possible signal and regulatory variation these amino acids changes can bring. One example was reported by Koch et al. (2000)[185] where the desensitisation rate of rMOPr cAMP inhibition at one hour was 50%, whilst hMOPr was nearly unchanged despite similar expression in HEK293 cells. Therefore, in addition to the difference in assays and heterologous system used, variations according to species used can be expected; thus further limiting comparison of results between studies.

Lastly, the allosteric binding influence of sodium was not discussed in this work. Sodium is a well established negative allosteric modulator that stabilises the inactive conformation of opioid receptors. Despite maintaining the same concentration of sodium across assays, it is likely that variants studied here, especially ICL2 and ICL3, affected sodium binding pocket if DOPr crystal structure can be translated to MOPr[115]. Therefore the functional effect of this allosteric pocket in MOPr variants will be assessed in later work, in addition to examining the effect of the newly described MOPr positive allosteric modulator[210].

In conclusion, this work supports the hypothesis that MOPr SNPs, especially from the ICL2 and ICL3, in the molecular level can affect receptor function. However, translational work is necessary to determine if this contributes to the inter-individual variability in opioid analgesic response. Furthermore, using a wash-free method to measure acute desensitisation, we determined that phosphorylation may not be an important component for acute desensitisation.

Appendices

A

Recipes, Materials and Equipment

A large amount of materials and equipment were used to perform the experiments required for this project. This appendix contains recipes, product codes/suppliers and equipment information listed.

A.1 Recipes

A.1.1 Hank's Balanced Salt Solution with HEPES (HBSS)

A.1.1.1 High Potassium HBSS

For FLPR® calcium 5 assays (see Appendix D.2.1)

Components	MW	Final Concentration (mM)	Amount
NaCl	58.44	137.93	4.0g
HEPES	238.31	22	2.6g
Na_2HPO_4	141.96	0.338	24mg
$NaHCO_3$	84.01	4.17	175mg
KH_2PO_4	136.09	0.441	30mg
$MgSO_4$	120.37	0.407	24.5mg
$MgCl_2$	95.21	0.493	123μL of 2M solution
KCl	74.55	5.33	198.7mg
Glucose	180.2	5.55	500mg
$CaCl_2$	110.98	1.26	630μL of 1M solution
Milli-Q water			To 500mL

Adjust pH to 7.4 and osmolarity to 300-330
Filter solution through a 0.22μm filter, for sterilisation and store at 4 ^{o}C

A.1.1.2 Low Potassium HBSS

For FLPR® membrane potential assays (see subsection 3.5)

Components	MW	Final Concentration (mM)	Amount
NaCl	58.44	145	4.2g
HEPES	238.31	22	2.6g
Na_2HPO_4	141.96	0.338	24mg
$NaHCO_3$	84.01	4.17	175mg
KH_2PO_4	136.09	0.441	30mg
$MgSO_4$	120.37	0.407	24.5mg
$MgCl_2$	95.21	0.493	123μL of 2M solution
Glucose	180.2	5.55	500mg
$CaCl_2$	110.98	1.26	630μL of 1M solution
Milli-Q water			To 500mL

Adjust pH to 7.4 and osmolarity to 300-330
Filter solution through a 0.22μm filter, for sterilisation and store at 4 ^{o}C

A.1.2 4% Paraformaldehyde Solution

Fixative for immunocytochemistry techniques (see sections 3.7 and 3.8).

Components	Final Concentration	Amount
Paraformaldehyde	4%	4g
Phosphate-buffered saline (PBS)		To 100mL

Warm PBS to 60 ^{o}C before adding PFA, then add $\sim$50μL of 10M NaOH
Adjust pH to $\sim$7.4 using pH strips then store at 4 ^{o}C or freeze

A.1.3 RIPA Lysis Buffer

Strong lysis buffer for protein extraction (see sections 3.4 and 3.6).

Components	MW	Final Concentration	Amount
Tris-HCl	157.60	50mM	788mg
NaCl	58.44	150mM	876.6mg
EDTA	292.24	5mM	146.12mg
NaF	42	10mM	42mg
Sodium pyrophosphate	446.1	10mM	446.1mg
IGEPAL® CA-630 (substitute for Nonidet P-40)		1%	1mL
Sodium deoxycholate	414.55	0.5%	500mg
SDS	288.38	0.1%	100mg
Milli-Q water			to 100mL

Ph Tris-HCl to 7.4 before adding extra igredients. Store at 4 ^{o}C in the dark
Filter solution through a 0.22μm filter for long term storage

Complete RIPA buffer contains the following additions:

- Protease inhibitor cocktail (Sigma) - 10μL/ml of buffer
- Phosphatase inhibitor cocktail (Roche) - 1 tablet in 10ml of buffer

Phosphatase inhibitor cocktail mix can be previously prepared and aliquots kept frozen; while protease inhibitor cocktail is only added immediately prior to experiment.

A.1.4 Phosphate-Buffered Saline with Tween-20 (PBST)

For immunocytochemistry experiments (see section 3.7).

Components	Final Concentration	Amount
Tween-20	0.01%	1mL
Phosphate-buffered saline		to 1L

Store at 4 ^{o}C

A.1.5 Tris-Buffered Saline (TBS)

A.1.5.1 Concentrated Tris-Buffered Saline (10X TBS)

For preparation of TBST.

Components	MW	Final Concentration	Amount
Tris base	121.14	0.5M	60.57g
NaCl	58.44	1.5M	87.66g
Milli-Q water			to 1L

Adjust pH to 7.4 before completing water (∼42mL of 32% HCl necessary)
Autoclave if long-term storage and store at 4 ^{o}C

A.1.5.2 Tris-Buffered Saline with Tween-20 (TBST)

For western blot experiments (see subsection 3.6.2).

Components	MW	Final Concentration	Amount
Tris base	121.14	0.05M	6.057g
NaCl	58.44	0.15M	8.766g
Tween-20		0.1%	1mL
Milli-Q water			to 1L

Adjust pH to 7.4 before completing water
100mL 10XTBS can be used instead of the salts

A.2 Materials

Cell Signalling and Radioligand Binding		
DAMGO,[tyrosyl-3-5-^{3}H(N)]-, 49.2 Ci/mmol	NET902250UC	PerkinElmer®
FLIPR® Calcium 5 Assay Kit	R8172	Molecular Devices
FLIPR® Membrane Potential Blue Assay kit	R8034	Molecular Devices
Probenecid	P8761	Sigma-Aldrich®
Optiphase Supermix Scintillation Fluid	1200-439	PerkinElmer®
96well plate (black wall, clear bottom)	3603	Costar

Drugs		
β-endorphin, human	RP11344	GenScript
Buprenorphine	D932	NMI
DAMGO (DAGO)	2283	Auspep
Endomorphin-2	2781	Auspep
Fentanyl		***
Methadone		***
Morphine		***
Naloxone Hydrochloride	ab120074	Abcam®
Pentazocine		***
Pertussis Toxin	3097	Tocris Bioscience
Pertussis Toxin	181	List Biol. Lab.
Phorbol-12-myristate-13-acetate (PMA)	P8139	Sigma-Aldrich®
Somatostatin (14)	2076	Auspep
Staurosporine	APN06113-1	Ascent
Staurosporine	ALX-380-014	Enzo Life Sciences

*** Kind gift from the Department of Pharmacology, University of Sydney

General Chemicals		
Calcium Chloride ($CaCl_2$)	190464K	AUS Tritium (VWR)
Dimethyl Sulfoxide (DMSO)	D45040	Sigma-Aldrich®
Di-sodium Hydrogen Orthophosphate (Na_2HPO_4)	SA026	Chem-Supply
D-(+)-Glucose	G7021	Sigma-Aldrich®
Ethanol	EA043	Chem-Supply
Ethylenediaminetetraacetic Acid (EDTA)	10093.5	AnalaR
HEPES	H4034	Sigma-Aldrich®
Hydrochloric Acid 32% (HCl)	A256-2.5L	Univar
IGEPAL® CA-630	I8896	Sigma-Aldrich®
Isopropanol	AL03232500	Chem-Supply
Magnesium Chloride ($MgCl_2$)	M8266	Sigma-Aldrich®
Magnesium Sulphate ($MgSO_4$)	M7506	Sigma-Aldrich®
Paraformaldehyde 96% (PFA)	416785000	Acros Organics
Phosphate-Buffered Saline (PBS) tablets	09-8912	Medicago
Potassium Chloride (KCl)	PA054	Chem-Supply
Potassium Dihydrogen Phosphate (KH_2PO_4)	26936.260	AnalaR Normapur
Sodium Bicarbonate ($NaHCO_3$)	S6297	Sigma-Aldrich®
Sodium Chloride (NaCl)	27810-362	AnalaR Normapur
Sodium Chloride (NaCl)	SA046	Chem-Supply
Sodium Deoxycholate	D6750	Sigma-Aldrich®
Sodium Dodecyl Sulphate (SDS)	L4390	Sigma-Aldrich®
Sodium Fluoride (NaF)	S1504	Sigma-Aldrich®
Sodium Hydroxide (NaOH)	221465	Sigma-Aldrich®
Sodium Pyrophosphate	S6422	Sigma-Aldrich®
Tris Base	103157P	AnalaR Normapur
Tris Base	1.08387	Merck
Tris-HCl	1.08219	Merck
Triton-X	30632	BDH Chem. (VWR)
Tween-20	0777	Amaresco

Tissue Culture		
Coverslip Round 12mm	GG-12	neuVitro
Dimethyl Sulfoxide (DMSO) for tissue culture	D2650	Sigma-Aldrich®
Dubelcco's Modified Eagle Medium (DMEM)	D6429	Sigma-Aldrich®
Fetal Bovine Serum (FBS)	12003C	Sigma®/SAFC
Leibovitz's L-15 Medium	11415-064	Gibco®
Penicillin(10,000U/mL)- Streptomycin(10,000μg/mL)	15140-122	Gibco®
Poly-D-Lysine	P6407/P0899	Sigma-Aldrich®
Phosphate-Buffered Saline (PBS)	20012-027	Gibco®
Tetracycline Hydrochloride	T9823	Sigma-Aldrich®
Trypan Blue Solution 0.4%	T8154	Sigma-Aldrich®
Trypsin-EDTA Solution 0.25%	T4049	Sigma-Aldrich®

Transfection		
Beta-Glo® Assay System	E4720	Promega
Fugene HD	E2311	Promega
G418 Sulfate 100mg/ml	ant-gn-5	InvivoGen
Hygromycin B 100mg/ml	ant-hm-5	InvivoGen
pFRT/lacZeo2 Vector	V6022-20	Life Technology™
pOG44 Flp-Recombinase Expression Vector	V6005-20	Life Technology™
ScaI 1000U restriction enzyme	R6211	Promega
Zeocin™ 100mg/mL	ant-zn-1	InvivoGen

Transformation		
Agarose, LE, Analytical Grade	V3125	Promega
Agar Bacteriological	LP0011	Oxoid
Alpha-Select Gold Efficiency Competent Cells	BIO-85027	Bioline
Ampicillin Sodium Salt	A0166	Sigma-Aldrich®
Bam HI Restriction Enzyme	R0260	Sigma-Aldrich®
Blue/Orange 6X Loading Dye	G190A	Promega
GelRed™	41002	Biotium
Hind III Restriction Enzyme	R1137	Sigma-Aldrich®
Hyperladder III	BIO-33055	Bioline
LB Broth (Lennox)	L3022	Sigma-Aldrich®
PureLink® Quick Plasmid Miniprep Kit	K2100-10	Life Technologies ™
1 kB DNA Ladder	G5711	Promega
Tris/Acetic acid/EDTA (TAE) Buffer (50X)	161-0743	Bio-Rad

Western Blot, Immunocytochemistry and Internalisation		
Anti-GAPDH - Loading Control Rb	Ab9485	Abcam®
Anti-HA 488 Conjugated (Clone 16B12)	A488-101-L	Covance
Anti-HA.11 Clone 16B12 Mouse	MMS-101P	Covance
Anti-Akt (pan)(40D4) Mouse	2920	Cell Signalling
Anti-phospho-μ-opioid receptor (Ser375)† Rb	3451	Cell Signalling
Anti-mouse IgG, HRP-linked	7076	Cell Signalling
Anti-rabbit IgG, HRP-linked	7074	Cell Signalling
Anti-mouse Alexa Fluor 594 IgG (H+L)	A11032	Life technologies ™
Bovine Serum Albumin (BSA)	A7906	Sigma-Aldrich®
4',6-Diamidino-2-Phenylindole (DAPI)	D3571	Life technologies ™
Clarity Western ECL Substract	170-5061	Bio-Rad
Diploma Skim Milk Powder	n/a	Coles
Mini-PROTEAN® SFX, 10% gel, 15 wells	456-8036	Bio-Rad
NuPAGE® Sample Reducing Agent (10X)	NP0009	Life technologies™
NuPAGE® LDS Sample Buffer (4X)	NP0007	Life Technologies ™
Perfect Western Blot Container	B101S	Bio Scientific
PhosSTOP Phosphatase Inhibitor Cocktail	04906837001	Roche
Pierce™ BCA Protein Assay Kit	23227	Thermo Scientific
Precision Plus Western C Standards	161-0376	Bio-Rad
Precision Plus Dual Color Standards	161-0374	Bio-Rad
Prolong® Gold Antifade Mountant with DAPI	P36941	Life technologies ™
Protease Inhibitor Cocktail	P8340	Sigma-Aldrich®
ReBlot Plus Strong Antibody Stripping Solution	2504	Merck Millipore
TransBlot Turbo RTA Transfer Kit, PVDF Mini	170-4272	Bio-Rad
Tris/Glycine/SDS Running Buffer (10X)	161-0772	Bio-Rad

†This product is called Ser375 as this is the position on mMOPr, yet for this thesis purposes Ser377 will be used as it is the correct residue position in hMOPr.

A.3 Equipment

General Laboratories	
Analytical Balance ED2245	Sartorius
Autoclave HICLAVE HV-110	Hirayama
ChemiDoc™ MP System	Bio-Rad
Docu-pHmeter	Sartorius
FlexStation® 3 Multi-Mode Microplate Reader	Molecular Devices
Fume Cupboard	Conditionaire Intern.
Gel Doc™ EZ System	Bio-Rad
Horizontal Electrophoresis Mini-Sub®Cell GT Cell	Bio-Rad
Incubator Shaker Innova® 42	Eppendorf
Magnetic Stirrer with Heating MR Hei-Standard	Heidolph
Microcentrifuge 5415R	Eppendorf
Mini-PROTEAN® Vertical Electrophoresis System	Bio-Rad
Mixer Reax Top	Heidolph
NanoDrop™ 2000 Spectrophotometer	Thermo Fisher Scientific
PHERAstar FS	BMG LABTECH
Pipettes (including automated multi-channel)	Gilson® and Eppendorf
Oven with Natural Convection ED115/ED240	Binder
Platform Rocker 8040	Biolone Global
PowerPac™ Universal Power Supply	Bio-Rad
Precision Balance EK-610i	A&D
Rotatory Suspension Mixer	Bacto Laboratories
Trans-Blot® Turbo™ Transfer System	Bio-Rad

Tissue Culture Laboratory	
Benchtop 314 Incubator (Ambient CO_2)	Lab-Line
Centrifuge 5430	Eppendorf
Countess® Automated Cell Counter	Life Technologies ™
Herasafe™ KS, ClassII Biological Safety Cabinet	Thermo Scientific™
HeraCell™ 150i CO_2 Incubators	Thermo Scientific™
Microscope Olympus CKX41	Olympus
Mr. Frosty™ Freezing Container	Thermo Scientific™
Water Bath - Constant temperature (NBCT2)	Labec

Microscopy Laboratory	
Confocal Laser Scanning Microscope System Leica TCS SP5X fitted with a variety of lasers, mercury/neon lamps and halogen lamps , camera Leica DFC 360FX	Leica Microsystems

Dept. of Pharmacology, University of Sydney	
MicroBeta® Plate Counter	PerkinElmer®

B

List of Suppliers

Abcam®	Melbourne, Victoria, Australia
Auspep	Tullamarine, Victoria, Australia
A&D	Thebarton, South Australia, Australia
Bacto Laboratories	Mt Pritchard, New South Wales, Australia
BD Biosciences	Macquarie Park, New South Wales, Australia
Binder	Tuttlingen, Germany
Bioline	Alexandria, New South Wales, Australia
Bioline Global	Smeaton Grange, New South Wales, Australia
Bio-Rad	Gladesville, New South Wales, Australia
BioScientific	Kirrawee, New South Wales, Australia
Bio-Strategy	Broadmeadows, Victoria, Australia
Biotium	Hayward, California, USA
BMG LABTECH	Mornington, Victoria, Australia
Cell Signalling Technology®	Danvers, Massachusetts, USA
Chem-Supply	Gillman, South Australia, Australia
Conditionaire International	Marrickville, New South Wales, Australia
Corning Life Sciences	Clayton, Victoria, Australia
Covance®	Macquarie Park, New South Wales, Australia
Enzo Life Sciences	Farmingdale, New York, USA
Eppendorf	North Ryde, New South Wales, Australia
Fisher Biotec	Wembley, Western Australia, Australia
Genesearch	Arundel, Queensland, Australia
GenScript	Piscataway, New Jersey, USA
Gibco® (Life Technologies™)	Mulgrave, Victoria, Australia
Gilson®	Middleton, Wisconsin, USA
GraphPad Software	La Jolla, California, USA
Heidolph	Schwabach, Germany
Integrated Sciences	Chatswood, New South Wales, Australia
Invitrogen™ (Life Technologies™)	Mulgrave, Victoria, Australia
InvivoGen	San Diego, California, USA
John Morris Scientific	Chatswood, New South Wales, Australia

Jomar Life Research	Stepney, South Australia, Australia
Labec	Marrickville, New South Wales, Australia
Leica Microsystems	North Ryde, New South Wales, Australia
Life technologies™(Thermo Fisher Scientific)	Mulgrave,Victoria, Australia
Merck Millipore	Bayswater, Victoria, Australia
Microsoft®	North Ryde, New South Wales, Australia
Molecular Devices	Sunnyvale, California, USA
Molecular Probes(Life Tech™)	Mulgrave, Victoria, Australia
List Biological Laboratories	Campbell, California, USA
National Measurement Institute	Lindfield, New South Wales, Australia
NeuVitro	Vancouver, Washington, USA
New England Biolabs	Ipswich, Massachusetts, USA
Olympus Life Science	Notting Hill, Victoria, Australia
Oxoid (Thermo Fisher Scientific)	Scoresby, Victoria, Australia
PerkinElmer®	Waltham, Massachusetts, USA
Promega	Alexandria, New South Wales, Australia
Pierce® (Thermo Fisher Scientific)	Scoresby, Victoria, Australia
Roche	Castle Hill, New South Wales, Australia
Sapphire Bioscience	Waterloo, New South Wales, Australia
Sartorius	Dandenong South, Victoria, Australia
Sigma-Aldrich®	Castle Hill, New South Wales, Australia
Thermo Fisher Scientific	Scoresby, Victoria, Australia
Tocris Bioscience	Bristol, United Kingdom
Univar	Ingleburn, New South Wales, Australia
VWR®	Murarrie, Queensland, Australia

C

Vectors and Transfection Related Results

C.1 Flp-In™ System Vectors

The information present in this section was obtained from Life Technologies™ manuals.

C.1.1 FRT/*lac*Zeo2 Vector

pFRT/*lac*Zeo2 is a 6.5kbp vector that expresses a fusion protein containing β-galactosidase and the Zeocin™ resistance marker under the control of a truncated SV40 early promoter ($P_{SV40\Delta}$). This vector is shown on Figure C.1, where it is possible to observe that neither the *lac*Z gene nor the Zeocin™ resistance gene contains its native ATG codon. The ATG initiation codon is placed directly upstream of a FRT site, also known as the FlpIn site. Therefore, before transfecting the gene of interest into the cells, the LacZ-Zeocin™ fusion genes are expressed, however after transfection they lose the initiation codon and the cells become Zeocin™ sensitive.

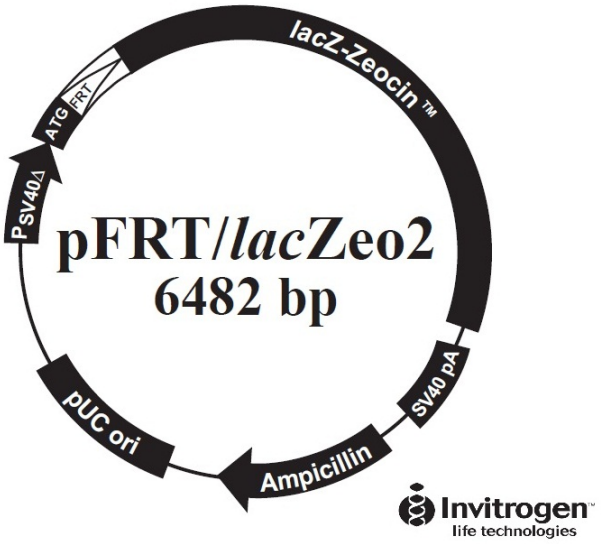

Figure C.1. pFRT/*lac*Zeo2 vector map. Reproduced with permission from Life Technologies™/Thermo Fisher Scientific.

C.1.2 pOG44 Vector

pOG44 is a 5.8kb Flp recombinase expression vector designed for use with the Flp-In™ System (see subsection 3.3.2). This vector expresses a temperature-sensitive Flp

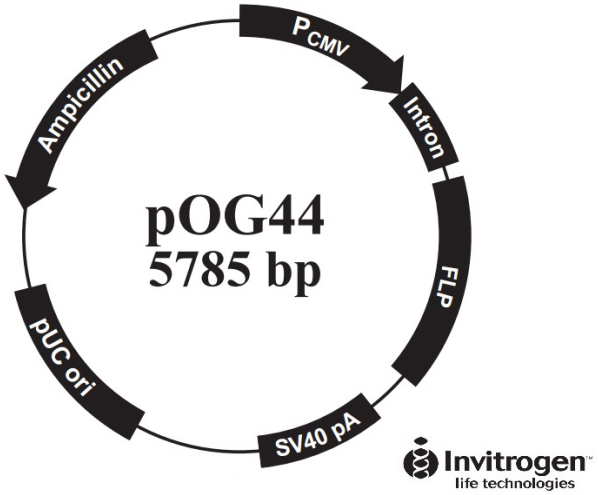

Figure C.2. pOG44 vector map. Reproduced with permission from Life Technologies™/Thermo Fisher Scientific.

recombinase (flp-F70L) under the control of the human CMV promoter as previously described[254].

The expression of the FLP gene is enhanced by a synthetic intron, and it is important to point out that this vector does not contain an antibiotic resistance marker, thus its transfection is transient. The vector map for this construct is shown in Figure C.2.

C.1.3 pcDNA™5/FRT/TO Vector

pcDNA™5/FRT/TO Vector is a inducible expression vector designed for use with Flp-In™ T-REx™ System, but can also be used with Flp-In™ System.

Note that transfection of this plasmid alone into mammalian cells, not in a Flp recombinase-dependent manner, will not confer hygromycin resistance to the cells because hygromycin resistance gene lacks a promoter and its native ATG start codon.

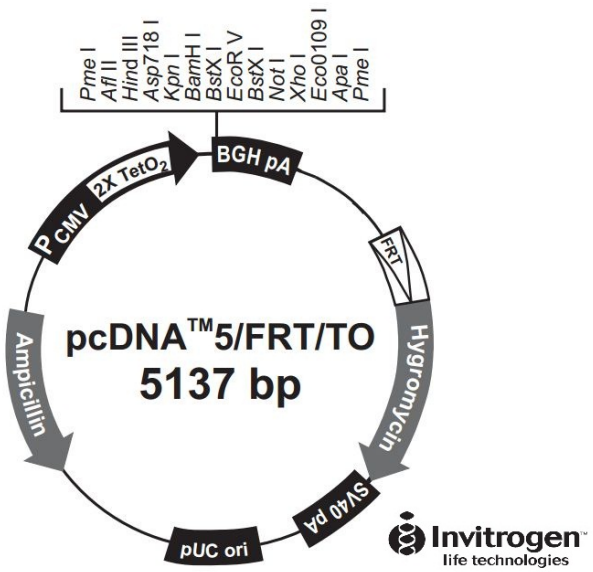

Figure C.3. pcDNA™5/FRT/TO vector map. Reproduced with permission from Life Technologies™/Thermo Fisher Scientific.

C.2 Transfection related results

Zeocin™ and hygromycin kill curves were performed to determine antibiotic concentration to select FRT/*lac*Zeo and hMOPr transfected clones respectively. Kill curves are shown in Figure C.4

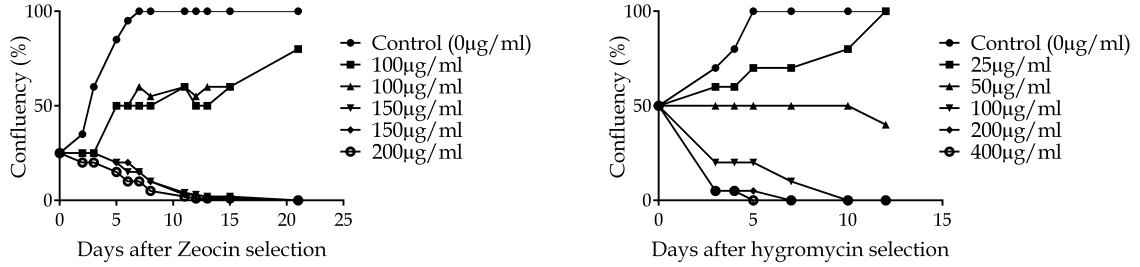

(A) Zeocin™ selection curve

(B) Hygromycin selection cruve

Figure C.4. Antibiotics kill curves

Beta-galactosidase activity were determined after FRT/*lac*Zeo transfection and results for all isolated clones, positive and negative controls are presented in Figure C.5. Beta-Glo® Assay Kit manufacture's instructions were followed and FlexStation 3 was used to measure luminescence.

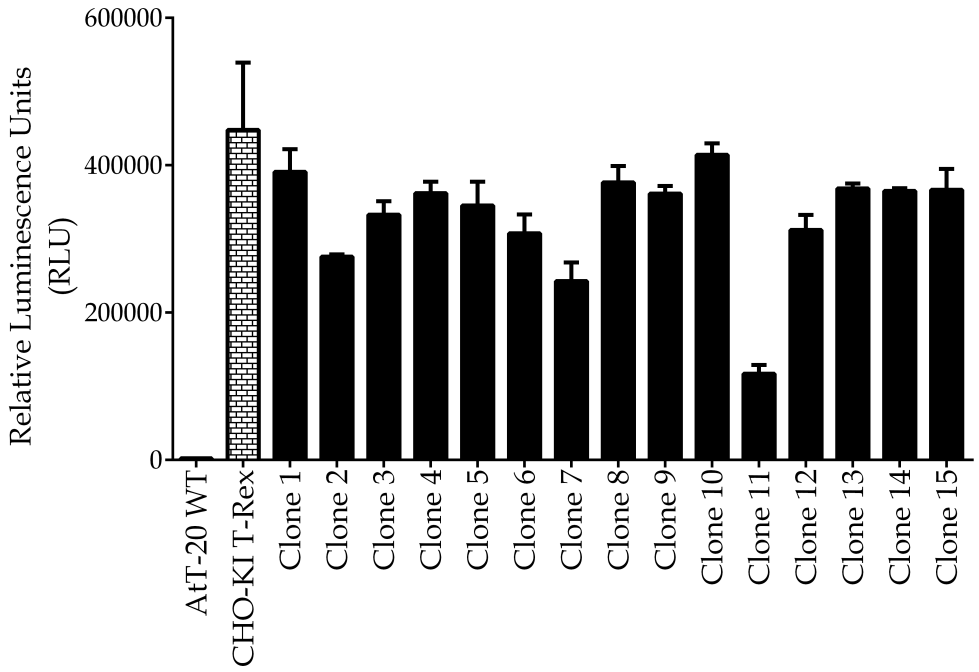

Figure C.5. β-Galactosidase Assay results. AtT-20 WT is the negative control and CHO-K1 Flp-In™ T-Rex™ WT is the positive control (n=2, ±SEM).

D

Kinase Modulator Controls

D.1 Introduction

In this project, MOPr signalling and desensitisation in the presence of a phorbol ester PKC activator, phorbol-12-myristate-13-acetate (PMA), and a kinase inhibitor, staurosporine, were analysed with the FLPR® Membrane Potential Assay (MPA) Kit. Considering that a small change was observed with these treatments, it was essential to have positive controls to ensure the activity of the kinase modulators.

Therefore to validate the assays performed on Chapter 4, activity of PMA and staurosporine was assessed using Transient Receptor Potential Vanilloid 1 ($TRPV_1$) transfected in HEK-293 Flp-In™ T-REx™ cells. This receptor is a calcium permeable non-selective cation channel that transmits pain signals induced by noxious stimuli. This receptor is activated by vanilloid ligands as capsaicin[55] and activation of PKC

has also been reported to independently induce this channel activity[277].

D.2 Experimental Methods

HEK-293 Flp-In™ T-REx™ expressing $TRPV_1$ was a kind gift from Prof. Peter McIntyre from RMIT University (Melbourne, Australia).

HEK-293 Flp-In™ T-REx™ $TRPV_1$ cells[†], in addition to all Flp-In™ advantages, also exhibit tetracycline-inducible expression of $TRPV_1$. Therefore these cells only express this receptor when treated with tetracycline, which is important for cell viability.

D.2.1 FLIPR®Calcium 5 assay

The FLPR® Calcium 5 Assay (CA) Kit allows for the detection of intracellular calcium changes in a simple and reliable assay. This kit utilises a calcium sensitive dye that is absorbed into the cell's cytoplasm during incubation. When intracellular calcium is increased by ligand-receptor binding, the dye binds to the extra calcium and fluorescence signal increase. This dye also contains an extracellular masking technology that decreases background interference and increase assay signal window (see Figure D.1).

Calcium 5 dye was purchased in bulk, reconstituted using 10mL of high-potassium HBSS (recipe in Appendix A) per vial, aliquoted and frozen at -80 ^{o}C. Before use, the dye was thawed, diluted 10X with high-potassium HBSS, mixed with probenecid to final concentration of 2.5mM and solution pH adjusted to 7.4. Probenecid, an anion-exchange protein inhibitor, is used to retain the calcium indicator since HEK-293 cells contain an anion-exchange protein.

FlexStation® 3 Microplate reader can simultaneously read and pipet therefore is uniquely suited to capture the fast kinetics associated with this assay. SoftMax Pro 5.4 microplate reader software was used to run FlexStation® 3.

[†]This is a stable cell line selected with hygromycin as previously described for the Flp-In™ system and blasticidin S for the Tet repressor expression plasmid.

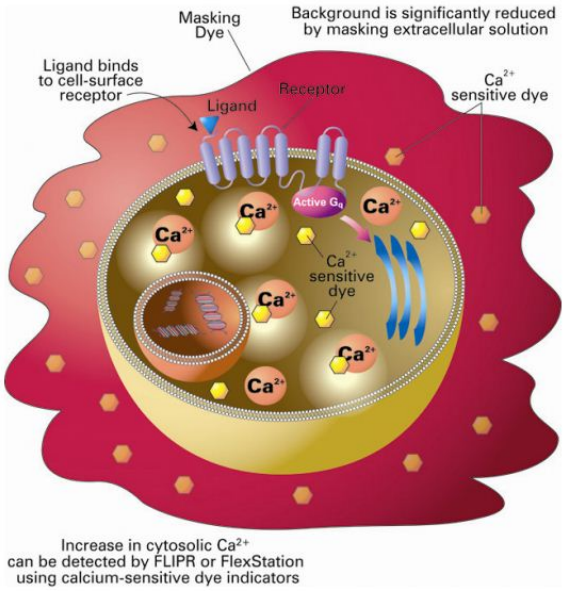

Figure D.1. FLPR® Calcium 5 assay principle. Reproduced from Molecular Devices.

D.2.1.1 Experimental Procedure

On the day before assay, cells are detached from each flask and resuspended in supplemented L15 as described on Section 3.1. Using an automated multi-channel pipette, 80μL of cells was loaded per well of a sterile, black wall, clear bottom 96-well plate previously coated with poly-D-lysine , and incubated at 37 ^{o}C overnight. Approximately 4 hours before loading dye, cells were induced by adding 20μL of tetracycline (final concentration 2μg/ml) to wells. 100μL of dye was loaded per well (200μL total) and incubated for 1 hour inside FlexStation® 3 set to 37 ^{o}C. During incubation, the dye passes through the cell membrane and esterases in the cytoplasm cleave the AM portion of the molecule. PMA, staurosporine and capsaicin (positive control) dilutions in HBSS were prepared and loaded to a V-shape 96-well drug plate according to experimental protocol.

After a 1 hour incubation, the experiment was run on a FlexStation® 3 using the experimental software setup parameters for CA which are shown on Table D.1.

First transfer was Staurosporine or HBSS, second transfer PMA or HBSS and third transfer capsaicin or HBSS. Incubation for 10 minutes occured between first and second, and also second and third addition. At least three technical and three biological

Table D.1. Calcium 5 assay experimental setup parameters

Read Mode	Fluorescence (RFUs) Bottom Read
Wavelength (nm)	485 (Ex) 525 (Em) 515 (Cutoff)
Sensitivity	Reading: 6 (normal) PMT sensitivity: Medium
Timing	Interval: 2 sec Time: 1620 sec
Assay Plate Type	96 well Costar blk/clrbtm
Compound Transfer - T1	Pipette Height: 190μL Volume: 20μL Rate: 2 ($\sim$31μL/sec) Time Point: 120 sec
Triturate Assay Plate - T1	Volume: 20μL Cycles: 2 Height: 190μL
Compound Transfer - T2	Pipette Height: 210μL Volume: 20μL Rate: 2 ($\sim$31μL/sec) Time Point: 720 sec
Triturate Assay Plate - T2	Volume: 20μL Cycles: 2 Height: 210μL
Compound Transfer - T3	Pipette Height: 230μL Volume: 20μL Rate: 2 ($\sim$31μL/sec) Time Point: 1320 sec
Triturate Assay Plate - T3	Volume: 20μL Cycles: 2 Height: 230μL
Compound Source	Greiner 96 Vbtm plate
Auto Calibrate	On
Auto Read	Off

replicates were done when collecting signalling data for this thesis using CA Kit.

D.2.1.2 Data Analysis

Raw data collected in RFUs was exported in .txt format and analysed using Microsoft® Excel. First, baseline average was calculated for each sample using the last 30 seconds previous to drug addition. Then results were normalised to baseline and corrected for the addition of the vehicle. Results were pasted in GraphPad Prism software and plotted.

No statistical analysis was done as for the purpose of this experiment only visual confirmation was required.

D.3 Results

PMA treatment of tetracycline induced HEK-293 Flp-In™ T-REx™ $TRPV_1$ cells led to a small increase on intracellular calcium concentration, indicating PKC activity. To determine staurosporine activity, this kinase inhibitor was added before PMA, and as expected PMA calcium release was inhibited. Capsaicin response was much faster and larger than PMA. Representative traces of results are presented in Figure D.2.

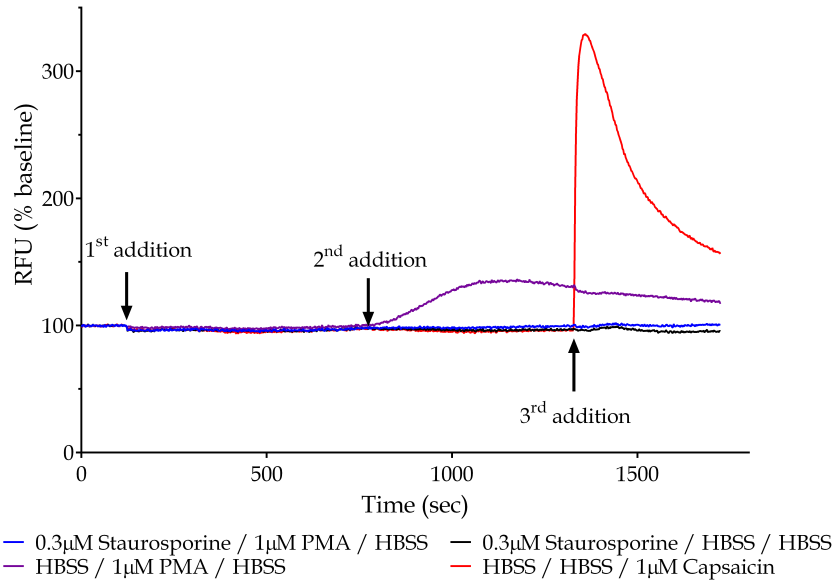

Figure D.2. Traces showing changes in intracellular calcium in the presence of kinase modulators and capsaicin. First addition was 0.3μM staurosporine or HBSS at 2 minutes point, then 1μM PMA or HBSS at 12 minutes followed by 1μM Capsaicin or HBSS at 22 minutes. Note that PMA leads to calcium increase (purple trace) which is inhibited by staurosporine (blue trace).

D.4 Discussion and Conclusion

Premkumar and Ahern (2000)[277] reported that treatment with the phorbol ester 12-O-tetradecanoylphorbol-13-acetate (TPA) evokes a slowly developing current on $TRPV_1$ transfected oocytes. In this project, a similar current was observed with PMA, another phosrbol ester, using CA kit, confirming this kinase activator activity. In addition, staurosporine inhibited PMA induced intracellular calcium increase, hence supporting the kinase inhibitor activity (Figure D.2).

Therefore based on results from this appendix both kinase modulators were active and behaved as expected.

E

Biosafety Approvals

Approval from the Institution Biosafety Committee was obtained to create and work with cell lines expressing the human μ-opioid receptor variants. These genetically modified organisms are classified as exempt dealings by the Office of Gene Technology Regulator. Biosafety approval numbers are IBC REF: 5201200023, 5201500367

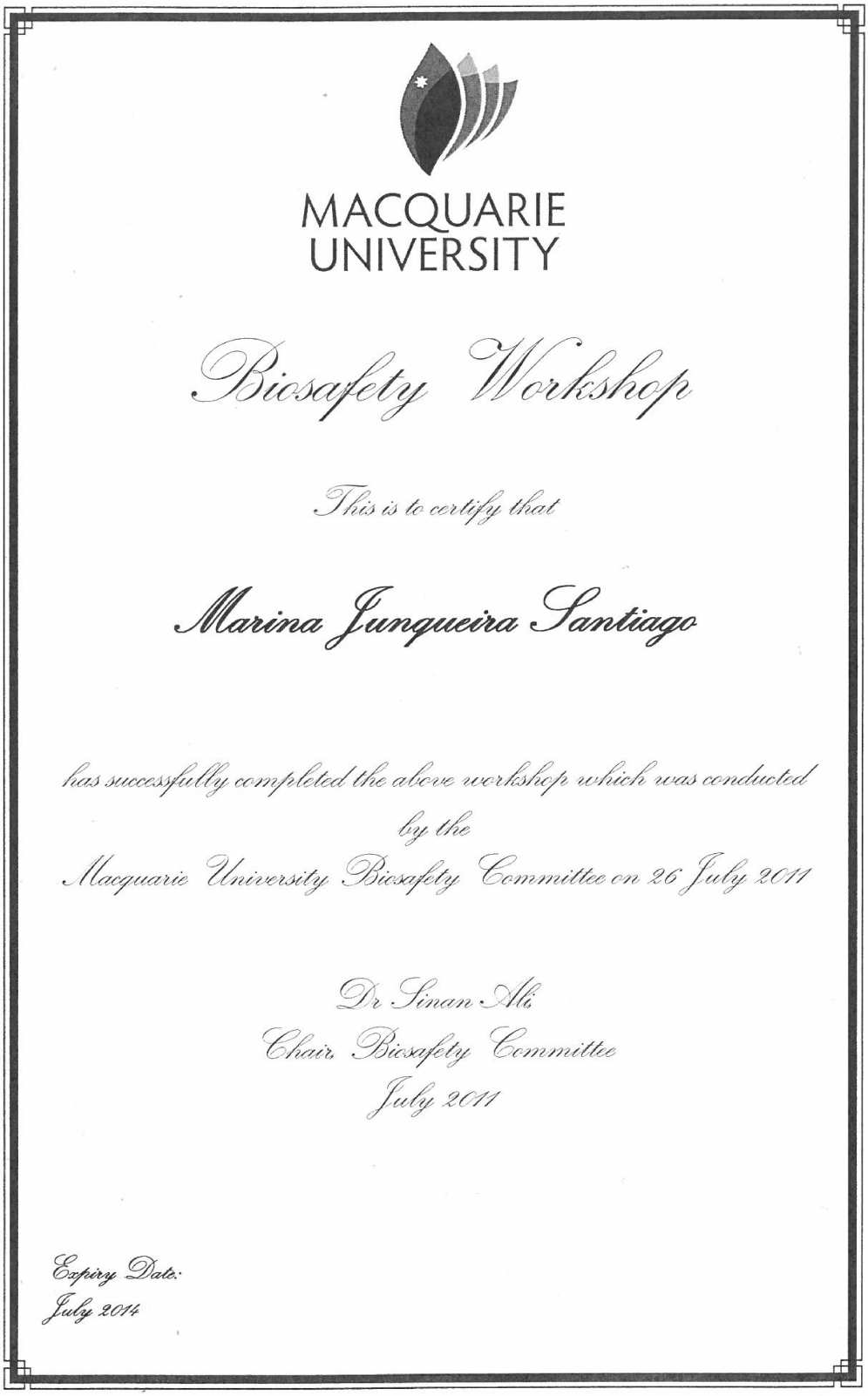

MACQUARIE UNIVERSITY

Biosafety Workshop

This is to certify that

Marina Junqueira Santiago

has successfully completed the above workshop which was conducted by the Macquarie University Biosafety Committee on 26 July 2011

Dr Sinan Ali
Chair, Biosafety Committee
July 2011

Expiry Date:
July 2014

F

Radiation Safety Certificate

In order to work with radioisotopes, it was necessary to complete a radiation safety course, which was completed in Sydney University where radioligand binding assays were carried out. This course covers the safe use of unsealed isotopes in research laboratories. The content includes:

- Radiation basics
- Safety with unsealed sources
- Regulatory requirements
- Local responsibilities

THE UNIVERSITY OF SYDNEY

Certificate of Attendance

This is to certify that

Marina Junqueira Santiago

has completed a training session on

Radiation safety

Provider: Work Health and Safety

Date: April 3, 2013

List of Figures

List of Tables

References

[1] CBS prediction servers website NetNGlyc 1.0. Available from: http://www.cbs.dtu.dk/services/netnglyc/, 2015 (Cited May 2015).
(Cited on page 22.)

[2] V. Abadji, J. M. Lucas-Lenard, C. Chin, and D. A. Kendall. Involvement of the carboxyl terminus of the third intracellular loop of the cannabinoid CB1 receptor in constitutive activation of Gs. *J Neurochem*, 72(5):2032–8, 1999.
(Cited on page 181.)

[3] H. Akil, D. J. Mayer, and J. C. Liebeskind. Antagonism of stimulation-produced analgesia by naloxone, a narcotic antagonist. *Science*, 191(4230):961–2, 1976.
(Cited on page 7.)

[4] S. P. Alexander, H. E. Benson, E. Faccenda, A. J. Pawson, J. L. Sharman, M. Spedding, J. A. Peters, A. J. Harmar, and Cgtp Collaborators. The concise guide to pharmacology 2013/14: G protein-coupled receptors. *Br J Pharmacol*, 170(8):1459–581, 2013.
(Cited on page 7.)

[5] V. A. Alvarez, S. Arttamangkul, V. Dang, A. Salem, J. L. Whistler, M. Von Zastrow, D. K. Grandy, and J. T. Williams. μ-opioid receptors: Ligand-dependent activation of potassium conductance, desensitization, and internalization. *J Neurosci*, 22(13):5769–76, 2002.
(Cited on page 35.)

[6] M. S. Angst. Intraoperative use of remifentanil for TIVA: Postoperative pain, acute tolerance, and opioid-induced hyperalgesia. *J Cardiothorac Vasc Anesth*, 29 Suppl 1:S16–S22, 2015.
(Cited on page 14.)

[7] J. R. Arden, V. Segredo, Z. Wang, J. Lameh, and W. Sadee. Phosphorylation and agonist-specific intracellular trafficking of an epitope-tagged mu-opioid receptor expressed in HEK 293 cells. *J Neurochem*, 65(4):1636–45, 1995.
(Cited on pages 126 and 219.)

[8] B. J. Arey. *The Role of Glycosylation in Receptor Signaling.* Glycosylation. 2012.
(Cited on page 22.)

[9] A. Arias, R. Feinn, and H. R. Kranzler. Association of an Asn40Asp (A118G) polymorphism in the μ-opioid receptor gene with substance dependence: a meta-analysis. *Drug Alcohol Depend*, 83(3):262–8, 2006.
(Cited on page 217.)

[10] S. Arner and B. A. Meyerson. Lack of analgesic effect of opioids on neuropathic and idiopathic forms of pain. *Pain*, 33(1):11–23, 1988.
(Cited on page 11.)

[11] S. Arttamangkul, M. Torrecilla, K. Kobayashi, H. Okano, and J. T. Williams. Separation of μ-opioid receptor desensitization and internalization: endogenous receptors in primary neuronal cultures. *J Neurosci*, 26(15):4118–25, 2006.
(Cited on pages 41 and 42.)

[12] S. Arttamangkul, E. K. Lau, H. W. Lu, and J. T. Williams. Desensitization and trafficking of μ-opioid receptors in locus ceruleus neurons: modulation by kinases. *Mol Pharmacol*, 81(3): 348–55, 2012.
(Cited on page 97.)

[13] S. Arttamangkul, W. Birdsong, and J. T. Williams. Does PKC activation increase the homologous desensitization of μ opioid receptors? *Br J Pharmacol*, 172(2):583–92, 2015.
(Cited on pages 36, 38, 78, 95, 207, and 220.)

[14] T. K. Attwood and J. B. Findlay. Fingerprinting G-protein-coupled receptors. *Protein Eng*, 7 (2):195–203, 1994.
(Cited on page 16.)

[15] B. K. Atwood, J. Lopez, J. Wager-Miller, K. Mackie, and A. Straiker. Expression of G protein-coupled receptors and related proteins in HEK293, AtT20, BV2, and N18 cell lines as revealed by microarray analysis. *BMC Genomics*, 12:14, 2011.
(Cited on pages 38, 93, 95, 97, 142, 146, 216, 218, and 219.)

[16] N. Audet, C. Gales, E. Archer-Lahlou, M. Vallieres, P. W. Schiller, M. Bouvier, and G. Pineyro. Bioluminescence resonance energy transfer assays reveal ligand-specific conformational changes within preformed signaling complexes containing δ-opioid receptors and heterotrimeric G proteins. *J Biol Chem*, 283(22):15078–88, 2008.
(Cited on page 215.)

[17] M. A. Ayoub, A. Al-Senaidy, and J. P. Pin. Receptor-G protein interaction studied by bioluminescence resonance energy transfer: lessons from protease-activated receptor 1. *Front Endocrinol (Lausanne)*, 3:82, 2012.

(Cited on page 215.)

[18] Misha-Miroslav Backonja. Opioids, clinical opioid tolerance. In GeraldF Gebhart and RobertF Schmidt, editors, *Encyclopedia of Pain*, pages 2520–2522. Springer Berlin Heidelberg, 2013.
(Cited on page 14.)

[19] C. P. Bailey and M. Connor. Opioids: cellular mechanisms of tolerance and physical dependence. *Curr Opin Pharmacol*, 5(1):60–8, 2005.
(Cited on pages 30 and 32.)

[20] C. P. Bailey, D. Couch, E. Johnson, K. Griffiths, E. Kelly, and G. Henderson. μ-opioid receptor desensitization in mature rat neurons: lack of interaction between DAMGO and morphine. *J Neurosci*, 23(33):10515–20, 2003.
(Cited on pages 35, 37, 41, 80, 94, and 95.)

[21] C. P. Bailey, E. Kelly, and G. Henderson. Protein kinase C activation enhances morphine-induced rapid desensitization of μ-opioid receptors in mature rat locus ceruleus neurons. *Mol Pharmacol*, 66(6):1592–8, 2004.
(Cited on pages 37, 78, 94, 95, and 207.)

[22] C. P. Bailey, J. Llorente, B. H. Gabra, F. L. Smith, W. L. Dewey, E. Kelly, and G. Henderson. Role of protein kinase C and μ-opioid receptor (MOPr) desensitization in tolerance to morphine in rat locus coeruleus neurons. *Eur J Neurosci*, 29(2):307–18, 2009.
(Cited on pages 78 and 186.)

[23] C. P. Bailey, S. Oldfield, J. Llorente, C. J. Caunt, A. G. Teschemacher, L. Roberts, C. A. McArdle, F. L. Smith, W. L. Dewey, E. Kelly, and G. Henderson. Involvement of PKCα and G-protein-coupled receptor kinase 2 in agonist-selective desensitization of μ-opioid receptors in mature brain neurons. *Br J Pharmacol*, 158(1):157–64, 2009.
(Cited on pages 36, 37, 95, 192, 207, and 208.)

[24] F. A. Baltoumas, M. C. Theodoropoulou, and S. J. Hamodrakas. Interactions of the α-subunits of heterotrimeric G-proteins with GPCRs, effectors and RGS proteins: a critical review and analysis of interacting surfaces, conformational shifts, structural diversity and electrostatic potentials. *J Struct Biol*, 182(3):209–18, 2013.
(Cited on page 16.)

[25] C. Bantel, S. Shah, and I. Nagy. Painful to describe, painful to diagnose: opioid-induced hyperalgesia. *Br J Anaesth*, 114(5):850–1, 2015.
(Cited on page 14.)

[26] A. H. Beckett and A. F. Casy. Synthetic analgesics: stereochemical considerations. *J Pharm Pharmacol*, 6(12):986–1001, 1954.
(Cited on page 7.)

[27] K. Befort, D. Filliol, F. M. Decaillot, C. Gaveriaux-Ruff, M. R. Hoehe, and B. L. Kieffer. A single nucleotide polymorphic mutation in the human μ-opioid receptor severely impairs receptor signaling. *J Biol Chem*, 276(5):3130–7, 2001.
(Cited on pages 151 and 176.)

[28] A. Belmer, S. Doly, V. Setola, S. M. Banas, I. Moutkine, K. Boutourlinsky, T. Kenakin, and L. Maroteaux. Role of the N-terminal region in G protein-coupled receptor functions: negative modulation revealed by 5-HT2B receptor polymorphisms. *Mol Pharmacol*, 85(1):127–38, 2014.
(Cited on page 123.)

[29] E. E. Benarroch. Endogenous opioid systems: current concepts and clinical correlations. *Neurology*, 79(8):807–14, 2012.
(Cited on page 11.)

[30] J. L. Benovic, H. Kuhn, I. Weyand, J. Codina, M. G. Caron, and R. J. Lefkowitz. Functional desensitization of the isolated β-adrenergic receptor by the β-adrenergic receptor kinase: potential role of an analog of the retinal protein arrestin (48-kda protein). *Proc Natl Acad Sci U S A*, 84(24):8879–82, 1987.
(Cited on page 34.)

[31] A. Beyer, T. Koch, H. Schroder, S. Schulz, and V. Hollt. Effect of the A118G polymorphism on binding affinity, potency and agonist-mediated endocytosis, desensitization, and resensitization of the human mu-opioid receptor. *J Neurochem*, 89(3):553–60, 2004.
(Cited on pages 102, 103, 119, 120, and 121.)

[32] W. T. Birdsong, S. Arttamangkul, M. J. Clark, K. Cheng, K. C. Rice, J. R. Traynor, and J. T. Williams. Increased agonist affinity at the μ-opioid receptor induced by prolonged agonist exposure. *J Neurosci*, 33(9):4118–27, 2013.
(Cited on pages 20, 21, and 147.)

[33] W. T. Birdsong, S. Arttamangkul, J. R. Bunzow, and J. T. Williams. Agonist binding and desensitization of the μ-opioid receptor is modulated by phosphorylation of the C-terminal tail domain. *Mol Pharmacol*, 2015.
(Cited on pages 21, 25, 36, 193, 206, 208, and 216.)

[34] T. K. Bjarnadottir, D. E. Gloriam, S. H. Hellstrand, H. Kristiansson, R. Fredriksson, and H. B. Schioth. Comprehensive repertoire and phylogenetic analysis of the G protein-coupled receptors in human and mouse. *Genomics*, 88(3):263–73, 2006.
(Cited on page 16.)

[35] C. Blanchet and C. Luscher. Desensitization of μ-opioid receptor-evoked potassium currents: initiation at the receptor, expression at the effector. *Proc Natl Acad Sci U S A*, 99(7):4674–9, 2002.

(Cited on page 35.)

[36] L. M. Bohn, R. R. Gainetdinov, F. T. Lin, R. J. Lefkowitz, and M. G. Caron. μ-Opioid receptor desensitization by β-arrestin-2 determines morphine tolerance but not dependence. *Nature*, 408 (6813):720–3, 2000.
(Cited on page 39.)

[37] L. M. Bohn, R. J. Lefkowitz, and M. G. Caron. Differential mechanisms of morphine antinociceptive tolerance revealed in βarrestin-2 knock-out mice. *J Neurosci*, 22(23):10494–500, 2002.
(Cited on page 37.)

[38] C. Bond, K. S. LaForge, M. Tian, D. Melia, S. Zhang, L. Borg, J. Gong, J. Schluger, J. A. Strong, S. M. Leal, J. A. Tischfield, M. J. Kreek, and L. Yu. Single-nucleotide polymorphism in the human mu opioid receptor gene alters β-endorphin binding and activity: possible implications for opiate addiction. *Proc Natl Acad Sci U S A*, 95(16):9608–13, 1998.
(Cited on pages 102 and 150.)

[39] G. Bonner, F. Meng, and H. Akil. Selectivity of μ-opioid receptor determined by interfacial residues near third extracellular loop. *Eur J Pharmacol*, 403(1-2):37–44, 2000.
(Cited on page 18.)

[40] M. Boom, M. Niesters, E. Sarton, L. Aarts, T. W. Smith, and A. Dahan. Non-analgesic effects of opioids: opioid-induced respiratory depression. *Curr Pharm Des*, 18(37):5994–6004, 2012.
(Cited on page 12.)

[41] S. L. Borgland, M. Connor, P. B. Osborne, J. B. Furness, and M. J. Christie. Opioid agonists have different efficacy profiles for G protein activation, rapid desensitization, and endocytosis of mu-opioid receptors. *J Biol Chem*, 278(21):18776–84, 2003.
(Cited on pages 31, 35, 41, 76, and 94.)

[42] D. O. Borroto-Escuela, W. Romero-Fernandez, G. Garcia-Negredo, P. A. Correia, P. Garriga, K. Fuxe, and F. Ciruela. Dissecting the conserved NPxxY motif of the M_3 muscarinic acetylcholine receptor: critical role of Asp-7.49 for receptor signaling and multiprotein complex formation. *Cell Physiol Biochem*, 28(5):1009–22, 2011.
(Cited on page 212.)

[43] S. L. Bowman, A. L. Soohoo, D. J. Shiwarski, S. Schulz, A. A. Pradhan, and M. A. Puthenveedu. Cell-autonomous regulation of μ-opioid receptor recycling by substance P. *Cell Rep*, 2015.
(Cited on pages 42 and 77.)

[44] J. D. Brederson and C. N. Honda. Primary afferent neurons express functional delta opioid receptors in inflamed skin. *Brain Res*, 2015.
(Cited on page 12.)

[45] L. A. Briand, M. Hilario, H. C. Dow, E. S. Brodkin, J. A. Blendy, and O. Berton. Mouse model of *OPRM1* (A118G) polymorphism increases sociability and dominance and confers resilience to social defeat. *J Neurosci*, 35(8):3582–90, 2015.
(Cited on page 102.)

[46] C. Brock, S. S. Olesen, A. E. Olesen, J. B. Frokjaer, T. Andresen, and A. M. Drewes. Opioid-induced bowel dysfunction: pathophysiology and management. *Drugs*, 72(14):1847–65, 2012.
(Cited on page 12.)

[47] M. J. Brownstein. A brief history of opiates, opioid peptides, and opioid receptors. *Proc Natl Acad Sci U S A*, 90(12):5391–3, 1993.
(Cited on pages 6, 7, and 13.)

[48] J. R. Bunzow, C. Saez, M. Mortrud, C. Bouvier, J. T. Williams, M. Low, and D. K. Grandy. Molecular cloning and tissue distribution of a putative member of the rat opioid receptor gene family that is not a mu, delta or kappa opioid receptor type. *FEBS Lett*, 347(2-3):284–8, 1994.
(Cited on page 7.)

[49] C. B. Burness and G. M. Keating. Oxycodone/naloxone prolonged-release: a review of its use in the management of chronic pain while counteracting opioid-induced constipation. *Drugs*, 74 (3):353–75, 2014.
(Cited on page 11.)

[50] D. L. Burns. Subunit structure and enzymic activity of pertussis toxin. *Microbiol Sci*, 5(9): 285–7, 1988.
(Cited on page 28.)

[51] D. B. Bylund, J. D. Deupree, and M. L. Toews. Radioligand-binding methods for membrane preparations and intact cells. *Methods Mol Biol*, 259:1–28, 2004.
(Cited on page 61.)

[52] C. M. Cahill, K. A. McClellan, A. Morinville, C. Hoffert, D. Hubatsch, D. O'Donnell, and A. Beaudet. Immunohistochemical distribution of delta opioid receptors in the rat central nervous system: evidence for somatodendritic labeling and antigen-specific cellular compartmentalization. *J Comp Neurol*, 440(1):65–84, 2001.
(Cited on page 12.)

[53] C. M. Cahill, A. M. Taylor, C. Cook, E. Ong, J. A. Moron, and C. J. Evans. Does the kappa opioid receptor system contribute to pain aversion? *Front Pharmacol*, 5:253, 2014.
(Cited on page 13.)

[54] R. Capeyrou, J. Riond, M. Corbani, J. F. Lepage, B. Bertin, and L. J. Emorine. Agonist-induced signaling and trafficking of the μ-opioid receptor: role of serine and threonine residues in the third cytoplasmic loop and C-terminal domain. *FEBS Lett*, 415(2):200–5, 1997.

(Cited on pages 152 and 176.)

[55] M. J. Caterina, M. A. Schumacher, M. Tominaga, T. A. Rosen, J. D. Levine, and D. Julius. The capsaicin receptor: a heat-activated ion channel in the pain pathway. *Nature*, 389(6653): 816–24, 1997.
(Cited on page 247.)

[56] J. Celver, M. Xu, W. Jin, J. Lowe, and C. Chavkin. Distinct domains of the μ-opioid receptor control uncoupling and internalization. *Mol Pharmacol*, 65(3):528–37, 2004.
(Cited on page 36.)

[57] J. P. Celver, J. Lowe, A. Kovoor, V. V. Gurevich, and C. Chavkin. Threonine 180 is required for G-protein-coupled receptor kinase 3- and β-arrestin 2-mediated desensitization of the mu-opioid receptor in *Xenopus* oocytes. *J Biol Chem*, 276(7):4894–900, 2001.
(Cited on pages 26 and 36.)

[58] B. Cen, Q. Yu, J. Guo, Y. Wu, K. Ling, Z. Cheng, L. Ma, and G. Pei. Direct binding of β-arrestins to two distinct intracellular domains of the δ opioid receptor. *J Neurochem*, 76(6): 1887–94, 2001.
(Cited on page 185.)

[59] V. Chaipatikul, L. J. Erickson-Herbrandson, H. H. Loh, and P. Y. Law. Rescuing the traffic-deficient mutants of rat μ-opioid receptors with hydrophobic ligands. *Mol Pharmacol*, 64(1): 32–41, 2003.
(Cited on pages 181 and 182.)

[60] C. Chen, V. Shahabi, W. Xu, and L. Y. Liu-Chen. Palmitoylation of the rat μ opioid receptor. *FEBS Lett*, 441(1):148–52, 1998.
(Cited on page 23.)

[61] X. P. Chen, W. Yang, Y. Fan, J. S. Luo, K. Hong, Z. Wang, J. F. Yan, X. Chen, J. X. Lu, J. L. Benovic, and N. M. Zhou. Structural determinants in the second intracellular loop of the human cannabinoid CB1 receptor mediate selective coupling to G(s) and G(i). *Br J Pharmacol*, 161(8):1817–34, 2010.
(Cited on page 128.)

[62] Y. Chen, A. Mestek, J. Liu, J. A. Hurley, and L. Yu. Molecular cloning and functional expression of a μ-opioid receptor from rat brain. *Mol Pharmacol*, 44(1):8–12, 1993.
(Cited on page 7.)

[63] Y. J. Chen, S. Oldfield, A. J. Butcher, A. B. Tobin, K. Saxena, V. V. Gurevich, J. L. Benovic, G. Henderson, and E. Kelly. Identification of phosphorylation sites in the COOH-terminal tail of the μ-opioid receptor. *J Neurochem*, 124(2):189–99, 2013.
(Cited on pages 23, 24, 25, 26, 27, 38, 143, 152, 183, 185, 192, 204, and 208.)

[64] Z. Chen, R. Gaudreau, C. Le Gouill, M. Rola-Pleszczynski, and J. Stankova. Agonist-induced internalization of leukotriene B_4 receptor 1 requires G-protein-coupled receptor kinase 2 but not arrestins. *Mol Pharmacol*, 66(3):377–86, 2004.
(Cited on page 143.)

[65] V. Cherezov, D. M. Rosenbaum, M. A. Hanson, S. G. Rasmussen, F. S. Thian, T. S. Kobilka, H. J. Choi, P. Kuhn, W. I. Weis, B. K. Kobilka, and R. C. Stevens. High-resolution crystal structure of an engineered human β2-adrenergic G protein-coupled receptor. *Science*, 318(5854): 1258–65, 2007.
(Cited on pages 18 and 23.)

[66] M. Chesler. *Regulation and Modulation of pH in the Brain*, volume 83. 2003.
(Cited on page 179.)

[67] H. Choquet, G. Joslyn, A. Lee, J. Kasberger, M. Robertson, G. Brush, M. A. Schuckit, R. White, and E. Jorgenson. Examination of rare missense variants in the chrna5-a3-b4 gene cluster to level of response to alcohol in the san diego sibling pair study. *Alcohol Clin Exp Res*, 37(8): 1311–6, 2013.
(Cited on page 126.)

[68] M. N. Christiansen, J. Chik, L. Lee, M. Anugraham, J. L. Abrahams, and N. H. Packer. Cell surface protein glycosylation in cancer. *Proteomics*, 14(4-5):525–46, 2014.
(Cited on page 119.)

[69] M. J. Christie. Cellular neuroadaptations to chronic opioids: tolerance, withdrawal and addiction. *Br J Pharmacol*, 154(2):384–96, 2008.
(Cited on pages 30, 32, 35, and 42.)

[70] M. J. Christie, J. T. Williams, and R. A. North. Cellular mechanisms of opioid tolerance: studies in single brain neurons. *Mol Pharmacol*, 32(5):633–8, 1987.
(Cited on page 93.)

[71] J. Chu, H. Zheng, H. H. Loh, and P. Y. Law. Morphine-induced μ-opioid receptor rapid desensitization is independent of receptor phosphorylation and beta-arrestins. *Cell Signal*, 20(9): 1616–24, 2008.
(Cited on pages 35, 38, 112, 184, and 192.)

[72] P. Chu Sin Chung and B. L. Kieffer. Delta opioid receptors in brain function and diseases. *Pharmacol Ther*, 140(1):112–20, 2013.
(Cited on page 13.)

[73] K. Y. Chung. Structural aspects of GPCR-G protein coupling. *Toxicol Res*, 29(3):149–55, 2013.
(Cited on page 16.)

[74] P. A. Claude, D. R. Wotta, X. H. Zhang, P. L. Prather, T. M. McGinn, L. J. Erickson, H. H. Loh, and P. Y. Law. Mutation of a conserved serine in TM4 of opioid receptors confers full agonistic properties to classical antagonists. *Proc Natl Acad Sci U S A*, 93(12):5715–9, 1996.
(Cited on pages 21 and 28.)

[75] M. Connor and M. D. Christie. Opioid receptor signalling mechanisms. *Clin Exp Pharmacol Physiol*, 26(7):493–9, 1999.
(Cited on pages 28, 97, 146, and 218.)

[76] M. Connor and G. Henderson. δ- and μ-opioid receptor mobilization of intracellular calcium in SH-SY5Y human neuroblastoma cells. *Br J Pharmacol*, 117(2):333–40, 1996.
(Cited on page 28.)

[77] M. Connor and I. Kitchen. Has the sun set on κ_3-opioid receptors? *Br J Pharmacol*, 147(4): 349–50, 2006.
(Cited on page 7.)

[78] M. Connor and J. Traynor. Constitutively active μ-opioid receptors. *Methods Enzymol*, 484: 445–69, 2010.
(Cited on pages 30 and 181.)

[79] M. Connor, P. B. Osborne, and M. J. Christie. μ-opioid receptor desensitization: is morphine different? *Br J Pharmacol*, 143(6):685–96, 2004.
(Cited on pages 38, 40, 94, 147, and 207.)

[80] M. Connor, E. E. Bagley, B. C. Chieng, and M. J. Christie. β-Arrestin-2 knockout prevents development of cellular μ-opioid receptor tolerance but does not affect opioid-withdrawal-related adaptations in single PAG neurons. *Br J Pharmacol*, 172(2):492–500, 2015.
(Cited on pages 31, 39, and 43.)

[81] A. E. Cooke, S. Oldfield, C. Krasel, S. J. Mundell, G. Henderson, and E. Kelly. Morphine-induced internalization of the L83I mutant of the rat μ-opioid receptor. *Br J Pharmacol*, 172 (2):593–605, 2015.
(Cited on pages 126, 142, 143, and 144.)

[82] A. D. Corbett, G. Henderson, A. T. McKnight, and S. J. Paterson. 75 years of opioid research: the exciting but vain quest for the Holy Grail. *Br J Pharmacol*, 147 Suppl 1:S153–62, 2006.
(Cited on page 8.)

[83] Center for Opioid Research (CORD) and Design. Available from: http://www.opioid.umn.edu/, 2015 (Cited April 2015).
(Cited on pages 17, 24, 127, 151, and 191.)

[84] C. M. Costantino, I. Gomes, S. D. Stockton, M. P. Lim, and L. A. Devi. Opioid receptor heteromers in analgesia. *Expert Rev Mol Med*, 14:e9, 2012.
(Cited on page 22.)

[85] B. M. Cox, A. Goldstein, and C. H. Hi. Opioid activity of a peptide, β-lipotropin-(61-91), derived from β-lipotropin. *Proc Natl Acad Sci U S A*, 73(6):1821–3, 1976.
(Cited on page 8.)

[86] B. M. Cox, M. J. Christie, L. Devi, L. Toll, and J. R. Traynor. Challenges for opioid receptor nomenclature: IUPHAR Review 9. *Br J Pharmacol*, 172(2):317–23, 2015.
(Cited on page 7.)

[87] K. S. Crider, T. P. Yang, R. J. Berry, and L. B. Bailey. Folate and dna methylation: a review of molecular mechanisms and the evidence for folate's role. *Adv Nutr*, 3(1):21–38, 2012.
(Cited on page 119.)

[88] J. J. Crowley, D. W. Oslin, A. A. Patkar, E. Gottheil, Jr. DeMaria, P. A., C. P. O'Brien, W. H. Berrettini, and D. E. Grice. A genetic association study of the mu opioid receptor and severe opioid dependence. *Psychiatr Genet*, 13(3):169–73, 2003.
(Cited on pages 101 and 217.)

[89] N. A. Crowley and T. L. Kash. Kappa opioid receptor signaling in the brain: Circuitry and implications for treatment. *Prog Neuropsychopharmacol Biol Psychiatry*, 2015.
(Cited on page 13.)

[90] H. A. Crystal, S. Hamon, M. Randesi, J. Cook, K. Anastos, J. Lazar, C. Liu, L. Pearce, E. Golub, V. Valcour, K. M. Weber, S. Holman, A. Ho, and M. J. Kreek. A C17T polymorphism in the mu opiate receptor is associated with quantitative measures of drug use in African American women. *Addict Biol*, 17(1):181–91, 2012.
(Cited on page 101.)

[91] S. Cvejic and L. A. Devi. Dimerization of the δ opioid receptor: implication for a role in receptor internalization. *J Biol Chem*, 272(43):26959–64, 1997.
(Cited on page 143.)

[92] A. Dahan. Opioid-induced respiratory effects: new data on buprenorphine. *Palliat Med*, 20 Suppl 1:s3–8, 2006.
(Cited on page 122.)

[93] V. C. Dang and M. J. Christie. Mechanisms of rapid opioid receptor desensitization, resensitization and tolerance in brain neurons. *Br J Pharmacol*, 165(6):1704–16, 2012.
(Cited on page 76.)

[94] V. C. Dang, I. A. Napier, and M. J. Christie. Two distinct mechanisms mediate acute μ-opioid receptor desensitization in native neurons. *J Neurosci*, 29(10):3322–7, 2009.
(Cited on page 36.)

[95] V. C. Dang, B. Chieng, Y. Azriel, and M. J. Christie. Cellular morphine tolerance produced by βarrestin-2-dependent impairment of μ-opioid receptor resensitization. *J Neurosci*, 31(19): 7122–30, 2011.
(Cited on pages 38, 41, 191, and 193.)

[96] I. Deb, J. Chakraborty, P. K. Gangopadhyay, S. R. Choudhury, and S. Das. Single-nucleotide polymorphism (A118G) in exon 1 of *OPRM1* gene causes alteration in downstream signaling by mu-opioid receptor and may contribute to the genetic risk for addiction. *J Neurochem*, 112 (2):486–96, 2010.
(Cited on pages 102 and 117.)

[97] F. M. Decaillot, R. Rozenfeld, A. Gupta, and L. A. Devi. Cell surface targeting of μ-δ opioid receptor heterodimers by RTP4. *Proc Natl Acad Sci U S A*, 105(41):16045–50, 2008.
(Cited on page 183.)

[98] F. Delom and D. Fessart. Role of phosphorylation in the control of clathrin-mediated internalization of GPCR. *Int J Cell Biol*, 2011:246954, 2011.
(Cited on page 77.)

[99] H. B. Deng, Y. Yu, H. Wang, W. Guang, and J. B. Wang. Agonist-induced μ opioid receptor phosphorylation and functional desensitization in rat thalamus. *Brain Res*, 898(2):204–14, 2001.
(Cited on page 190.)

[100] J. Desmeules, M. P. Gascon, P. Dayer, and M. Magistris. Impact of environmental and genetic factors on codeine analgesia. *Eur J Clin Pharmacol*, 41(1):23–6, 1991.
(Cited on page 100.)

[101] S. M. DeWire, D. S. Yamashita, D. H. Rominger, G. Liu, C. L. Cowan, T. M. Graczyk, X. T. Chen, P. M. Pitis, D. Gotchev, C. Yuan, M. Koblish, M. W. Lark, and J. D. Violin. A G protein-biased ligand at the μ-opioid receptor is potently analgesic with reduced gastrointestinal and respiratory dysfunction compared with morphine. *J Pharmacol Exp Ther*, 344(3):708–17, 2013.
(Cited on page 43.)

[102] C. Doll, J. Konietzko, F. Poll, T. Koch, V. Hollt, and S. Schulz. Agonist-selective patterns of μ-opioid receptor phosphorylation revealed by phosphosite-specific antibodies. *Br J Pharmacol*, 164(2):298–307, 2011.
(Cited on pages 23, 24, 25, 26, 27, 41, 77, 112, 191, and 220.)

[103] C. Doll, F. Poll, K. Peuker, A. Loktev, L. Gluck, and S. Schulz. Deciphering μ-opioid receptor phosphorylation and dephosphorylation in HEK293 cells. *Br J Pharmacol*, 167(6):1259–70, 2012.
(Cited on pages 27, 96, 144, and 192.)

[104] A. C. Dolphin. G protein modulation of voltage-gated calcium channels. *Pharmacol Rev*, 55(4): 607–27, 2003.
(Cited on page 31.)

[105] C. Dong, C. M. Filipeanu, M. T. Duvernay, and G. Wu. Regulation of G protein-coupled receptor export trafficking. *Biochim Biophys Acta*, 1768(4):853–70, 2007.
(Cited on pages 182 and 217.)

[106] E. Drews and A. Zimmer. Modulation of alcohol and nicotine responses through the endogenous opioid system. *Prog Neurobiol*, 90(1):1–15, 2010.
(Cited on page 15.)

[107] J. Droney, J. Ross, S. Gretton, K. Welsh, H. Sato, and J. Riley. Constipation in cancer patients on morphine. *Support Care Cancer*, 16(5):453–9, 2008.
(Cited on page 14.)

[108] R. O. Dror, D. H. Arlow, P. Maragakis, T. J. Mildorf, A. C. Pan, H. Xu, D. W. Borhani, and D. E. Shaw. Activation mechanism of the β_2-adrenergic receptor. *Proc Natl Acad Sci U S A*, 108(46):18684–9, 2011.
(Cited on pages 20 and 21.)

[109] R. M. Duhmke, D. D. Cornblath, and J. R. Hollingshead. Tramadol for neuropathic pain. *Cochrane Database Syst Rev*, (2):CD003726, 2004.
(Cited on page 11.)

[110] E. O. Dumas and G. M. Pollack. Opioid tolerance development: a pharmacokinetic/pharmacodynamic perspective. *AAPS J*, 10(4):537–51, 2008.
(Cited on page 14.)

[111] R. H. Dworkin, M. Backonja, M. C. Rowbotham, R. R. Allen, C. R. Argoff, G. J. Bennett, M. C. Bushnell, J. T. Farrar, B. S. Galer, J. A. Haythornthwaite, D. J. Hewitt, J. D. Loeser, M. B. Max, M. Saltarelli, K. E. Schmader, C. Stein, D. Thompson, D. C. Turk, M. S. Wallace, L. R. Watkins, and S. M. Weinstein. Advances in neuropathic pain: diagnosis, mechanisms, and treatment recommendations. *Arch Neurol*, 60(11):1524–34, 2003.
(Cited on page 11.)

[112] C. Egan, K. Herrick-Davis, and M. Teitler. Creation of a constitutively activated state of the 5-HT2A receptor by site-directed mutagenesis: revelation of inverse agonist activity of antagonists. *Ann N Y Acad Sci*, 861:136–9, 1998.

(Cited on page 181.)

[113] E. Erbs, L. Faget, G. Scherrer, A. Matifas, D. Filliol, J. L. Vonesch, M. Koch, P. Kessler, D. Hentsch, M. C. Birling, M. Koutsourakis, L. Vasseur, P. Veinante, B. L. Kieffer, and D. Massotte. A mu-delta opioid receptor brain atlas reveals neuronal co-occurrence in subcortical networks. *Brain Struct Funct*, 220(2):677–702, 2015.
(Cited on page 22.)

[114] C. J. Evans, Jr. Keith, D. E., H. Morrison, K. Magendzo, and R. H. Edwards. Cloning of a delta opioid receptor by functional expression. *Science*, 258(5090):1952–5, 1992.
(Cited on page 7.)

[115] G. Fenalti, P. M. Giguere, V. Katritch, X. P. Huang, A. A. Thompson, V. Cherezov, B. L. Roth, and R. C. Stevens. Molecular control of δ-opioid receptor signalling. *Nature*, 506(7487):191–6, 2014.
(Cited on pages 19, 140, 180, and 221.)

[116] B. Feng, Z. Li, and J. B. Wang. Protein kinase C-mediated phosphorylation of the mu-opioid receptor and its effects on receptor signaling. *Mol Pharmacol*, 79(4):768–75, 2011.
(Cited on pages 26 and 77.)

[117] S. S. Ferguson. Evolving concepts in G protein-coupled receptor endocytosis: the role in receptor desensitization and signaling. *Pharmacol Rev*, 53(1):1–24, 2001.
(Cited on page 40.)

[118] S. S. Ferguson and M. G. Caron. G protein-coupled receptor adaptation mechanisms. *Semin Cell Dev Biol*, 9(2):119–27, 1998.
(Cited on page 77.)

[119] S. S. Ferguson, 3rd Downey, W. E., A. M. Colapietro, L. S. Barak, L. Menard, and M. G. Caron. Role of β-arrestin in mediating agonist-promoted G protein-coupled receptor internalization. *Science*, 271(5247):363–6, 1996.
(Cited on page 77.)

[120] S. S. Ferguson, J. Zhang, L. S. Barak, and M. G. Caron. Molecular mechanisms of G protein-coupled receptor desensitization and resensitization. *Life Sci*, 62(17-18):1561–5, 1998.
(Cited on page 77.)

[121] H. L. Fields and E. B. Margolis. Understanding opioid reward. *Trends Neurosci*, 38(4):217–25, 2015.
(Cited on page 15.)

[122] A. K. Finn and J. L. Whistler. Endocytosis of the mu opioid receptor reduces tolerance and a cellular hallmark of opiate withdrawal. *Neuron*, 32(5):829–39, 2001.
(Cited on pages 41 and 191.)

[123] D. Fletcher and V. Martinez. Opioid-induced hyperalgesia in patients after surgery: a systematic review and a meta-analysis. *Br J Anaesth*, 112(6):991–1004, 2014.
(Cited on page 14.)

[124] S. M. Foord, T. I. Bonner, R. R. Neubig, E. M. Rosser, J. P. Pin, A. P. Davenport, M. Spedding, and A. J. Harmar. International union of pharmacology. XLVI. G protein-coupled receptor list. *Pharmacol Rev*, 57(2):279–88, 2005.
(Cited on page 16.)

[125] J. P. Fortin, L. Ci, J. Schroeder, C. Goldstein, M. C. Montefusco, I. Peter, S. E. Reis, G. S. Huggins, M. Beinborn, and A. S. Kopin. Theμ-opioid receptor variant N190K is unresponsive to peptide agonists yet can be rescued by small-molecule drugs. *Mol Pharmacol*, 78(5):837–45, 2010.
(Cited on pages 102, 151, and 176.)

[126] P. N. Fuchs, C. Roza, I. Sora, G. Uhl, and S. N. Raja. Characterization of mechanical withdrawal responses and effects of μ-, δ- and κ-opioid agonists in normal and mu-opioid receptor knockout mice. *Brain Res*, 821(2):480–6, 1999.
(Cited on page 13.)

[127] J. Garzon, M. Rodriguez-Munoz, E. de la Torre-Madrid, and P. Sanchez-Blazquez. Effector antagonism by the regulators of G protein signalling (RGS) proteins causes desensitization of mu-opioid receptors in the CNS. *Psychopharmacology (Berl)*, 180(1):1–11, 2005.
(Cited on pages 93 and 216.)

[128] J. Garzon, M. Rodriguez-Munoz, A. Lopez-Fando, and P. Sanchez-Blazquez. The RGSZ2 protein exists in a complex with μ-opioid receptors and regulates the desensitizing capacity of Gz proteins. *Neuropsychopharmacology*, 30(9):1632–48, 2005.
(Cited on page 93.)

[129] S. R. George, T. Fan, Z. Xie, R. Tse, V. Tam, G. Varghese, and B. F. O'Dowd. Oligomerization of μ- and δ-opioid receptors. generation of novel functional properties. *J Biol Chem*, 275(34): 26128–35, 2000.
(Cited on page 142.)

[130] Z. Georgoussi, M. Merkouris, I. Mullaney, G. Megaritis, C. Carr, C. Zioudrou, and G. Milligan. Selective interactions of μ-opioid receptors with pertussis toxin-sensitive G proteins: involvement of the third intracellular loop and the c-terminal tail in coupling. *Biochim Biophys Acta*, 1359 (3):263–74, 1997.
(Cited on pages 150, 180, 204, and 212.)

[131] Z. Georgoussi, L. Leontiadis, G. Mazarakou, M. Merkouris, K. Hyde, and H. Hamm. Selective interactions between G protein subunits and RGS4 with the C-terminal domains of the μ- and δ-opioid receptors regulate opioid receptor signaling. *Cell Signal*, 18(6):771–82, 2006.
(Cited on pages 204 and 209.)

[132] P. Ghanouni, Z. Gryczynski, J. J. Steenhuis, T. W. Lee, D. L. Farrens, J. R. Lakowicz, and B. K. Kobilka. Functionally different agonists induce distinct conformations in the G protein coupling domain of the β_2 adrenergic receptor. *J Biol Chem*, 276(27):24433–6, 2001.
(Cited on pages 21 and 179.)

[133] L. E. Gimenez, S. Kook, S. A. Vishnivetskiy, M. R. Ahmed, E. V. Gurevich, and V. V. Gurevich. Role of receptor-attached phosphates in binding of visual and non-visual arrestins to G protein-coupled receptors. *J Biol Chem*, 287(12):9028–40, 2012.
(Cited on pages 34 and 186.)

[134] L. Gluck, A. Loktev, L. Mouledous, C. Mollereau, P. Y. Law, and S. Schulz. Loss of morphine reward and dependence in mice lacking G protein-coupled receptor kinase 5. *Biol Psychiatry*, 76(10):767–74, 2014.
(Cited on page 96.)

[135] A. Goldstein, S. Tachibana, L. I. Lowney, M. Hunkapiller, and L. Hood. Dynorphin-(1-13), an extraordinarily potent opioid peptide. *Proc Natl Acad Sci U S A*, 76(12):6666–70, 1979.
(Cited on page 8.)

[136] J. Gonzalez-Barboteo, X. G. Alentorn, F. A. Manuel, V. A. Candel, M. A. Eito, I. Sanchez-Magro, M. N. Alvarez, F. J. Martin, and J. Porta-Sales. Effectiveness of opioid rotation in the control of cancer pain: the ROTODOL study. *J Opioid Manag*, 10(6):395–403, 2014.
(Cited on page 14.)

[137] M. Goto, K. Akai, A. Murakami, C. Hashimoto, E. Tsuda, M. Ueda, G. Kawanishi, N. Takahashi, A. Ishimoto, H. Chiba, and R. Sasaki. Production of recombinant human erythropoietin in mammalian cells: Host-cell dependency of the biological activity of the cloned glycoprotein. *Nat Biotech*, 6(1):67–71, 1988.
(Cited on page 119.)

[138] S. Granier, A. Manglik, A. C. Kruse, T. S. Kobilka, F. S. Thian, W. I. Weis, and B. K. Kobilka. Structure of the δ-opioid receptor bound to naltrindole. *Nature*, 485(7398):400–4, 2012.
(Cited on page 23.)

[139] A. Gupta, R. Rozenfeld, I. Gomes, K. M. Raehal, F. M. Decaillot, L. M. Bohn, and L. A. Devi. Post-activation-mediated changes in opioid receptors detected by N-terminal antibodies. *J Biol Chem*, 283(16):10735–44, 2008.
(Cited on pages 123 and 212.)

[140] H. Haberstock-Debic, M. Wein, M. Barrot, E. E. Colago, Z. Rahman, R. L. Neve, V. M. Pickel, E. J. Nestler, M. von Zastrow, and A. L. Svingos. Morphine acutely regulates opioid receptor trafficking selectively in dendrites of nucleus accumbens neurons. *J Neurosci*, 23(10):4324–32, 2003.
(Cited on page 42.)

[141] H. Haberstock-Debic, K. A. Kim, Y. J. Yu, and M. von Zastrow. Morphine promotes rapid, arrestin-dependent endocytosis of μ-opioid receptors in striatal neurons. *J Neurosci*, 25(34): 7847–57, 2005.
(Cited on page 42.)

[142] W. D. Hall and M. P. Farrell. Minimising the misuse of oxycodone and other pharmaceutical opioids in Australia. *Med J Aust*, 195(5):248–9, 2011.
(Cited on page 15.)

[143] J. M. Hambrook, B. A. Morgan, M. J. Rance, and C. F. Smith. Mode of deactivation of the enkephalins by rat and human plasma and rat brain homogenates. *Nature*, 262(5571):782–3, 1976.
(Cited on page 8.)

[144] B. K. Handa, A. C. Land, J. A. Lord, B. A. Morgan, M. J. Rance, and C. F. Smith. Analogues of beta-LPH61-64 possessing selective agonist activity at μ-opiate receptors. *Eur J Pharmacol*, 70(4):531–40, 1981.
(Cited on page 8.)

[145] W. Hauser, F. Bock, P. Engeser, G. Hege-Scheuing, M. Huppe, G. Lindena, C. Maier, H. Norda, L. Radbruch, R. Sabatowski, M. Schafer, M. Schiltenwolf, M. Schuler, H. Sorgatz, T. Tolle, A. Willweber-Strumpf, and F. Petzke. Recommendations of the updated LONTS guidelines. long-term opioid therapy for chronic noncancer pain. *Schmerz*, 29(1):109–30, 2015.
(Cited on page 10.)

[146] J. R. Havens, C. G. Leukefeld, A. M. DeVeaugh-Geiss, P. Coplan, and H. D. Chilcoat. The impact of a reformulation of extended-release oxycodone designed to deter abuse in a sample of prescription opioid abusers. *Drug Alcohol Depend*, 139:9–17, 2014.
(Cited on page 15.)

[147] L. He, J. Fong, M. von Zastrow, and J. L. Whistler. Regulation of opioid receptor trafficking and morphine tolerance by receptor oligomerization. *Cell*, 108(2):271–82, 2002.
(Cited on page 143.)

[148] S. Q. He, Z. N. Zhang, J. S. Guan, H. R. Liu, B. Zhao, H. B. Wang, Q. Li, H. Yang, J. Luo, Z. Y. Li, Q. Wang, Y. J. Lu, L. Bao, and X. Zhang. Facilitation of μ-opioid receptor activity by preventing δ-opioid receptor-mediated codegradation. *Neuron*, 69(1):120–31, 2011.

(Cited on pages 141 and 183.)

[149] J. V. Henderson, C. M. Harrison, H.C. Britt, C. F. Bayram, and G. C. Miller. Prevalence, causes, severity, impact, and management of chronic pain in Australian general practice patients. *Pain Medicine*, 14(9):1346–1361, 2013.
(Cited on page 11.)

[150] J. S. Heyman, J. L. Vaught, R. B. Raffa, and F. Porreca. Can supraspinal δ-opioid receptors mediate antinociception? *Trends Pharmacol Sci*, 9(4):134–8, 1988.
(Cited on page 13.)

[151] L. D. Hirning, H. I. Mosberg, R. Hurst, V. J. Hruby, T. F. Burks, and F. Porreca. Studies in vitro with ICI 174,864, [D-Pen2, D-Pen5]-enkephalin (DPDPE) and [D-Ala2, NMePhe4, Gly-ol]-enkephalin (DAGO). *Neuropeptides*, 5(4-6):383–6, 1985.
(Cited on page 8.)

[152] M. R. Hoehe, K. Kopke, B. Wendel, K. Rohde, C. Flachmeier, K. K. Kidd, W. H. Berrettini, and G. M. Church. Sequence variability and candidate gene analysis in complex disease: association of μ opioid receptor gene variation with substance dependence. *Hum Mol Genet*, 9(19):2895–908, 2000.
(Cited on page 150.)

[153] X. Y. Hua, A. Moore, S. Malkmus, S. F. Murray, N. Dean, T. L. Yaksh, and M. Butler. Inhibition of spinal protein kinase cα expression by an antisense oligonucleotide attenuates morphine infusion-induced tolerance. *Neuroscience*, 113(1):99–107, 2002.
(Cited on page 37.)

[154] P. Huang, J. Li, C. Chen, I. Visiers, H. Weinstein, and L. Y. Liu-Chen. Functional role of a conserved motif in TM6 of the rat μ opioid receptor: constitutively active and inactive receptors result from substitutions of Thr6.34(279) with Lys and Asp. *Biochemistry*, 40(45):13501–9, 2001.
(Cited on pages 19, 153, 181, and 215.)

[155] P. Huang, C. Chen, W. Xu, S. I. Yoon, E. M. Unterwald, J. E. Pintar, Y. Wang, P. L. Chong, and L. Y. Liu-Chen. Brain region-specific N-glycosylation and lipid rafts association of the rat mu opioid receptor. *Biochem Biophys Res Commun*, 365(1):82–8, 2008.
(Cited on pages 23 and 119.)

[156] P. Huang, C. Chen, S. D. Mague, J. A. Blendy, and L. Y. Liu-Chen. A common single nucleotide polymorphism A118G of the mu opioid receptor alters its N-glycosylation and protein stability. *Biochem J*, 441(1):379–86, 2012.
(Cited on pages 23, 102, 117, and 119.)

[157] P. Huang, C. Chen, and L. Y. Liu-Chen. Detection of μ opioid receptor (MOPR) and its glycosylation in rat and mouse brains by western blot with anti-muC, an affinity-purified polyclonal anti-MOPR antibody. *Methods Mol Biol*, 1230:141–54, 2015.
(Cited on page 182.)

[158] T. Hucho and J. D. Levine. Signaling pathways in sensitization: toward a nociceptor cell biology. *Neuron*, 55(3):365–76, 2007.
(Cited on page 29.)

[159] J. Hughes, T. W. Smith, H. W. Kosterlitz, L. A. Fothergill, B. A. Morgan, and H. R. Morris. Identification of two related pentapeptides from the brain with potent opiate agonist activity. *Nature*, 258(5536):577–80, 1975.
(Cited on page 8.)

[160] O. Iegorova, A. Fisyunov, and O. Krishtal. G-protein-independent modulation of P-type calcium channels by μ-opioids in Purkinje neurons of rat. *Neurosci Lett*, 480(2):106–11, 2010.
(Cited on page 32.)

[161] T. Iiri, Z. Farfel, and H. R. Bourne. G-protein diseases furnish a model for the turn-on switch. *Nature*, 394(6688):35–8, 1998.
(Cited on page 16.)

[162] K. Ikeda, T. Kobayashi, T. Kumanishi, H. Niki, and R. Yano. Involvement of G-protein-activated inwardly rectifying K (GIRK) channels in opioid-induced analgesia. *Neurosci Res*, 38(1):113–6, 2000.
(Cited on page 30.)

[163] S. Illing, A. Mann, and S. Schulz. Heterologous regulation of agonist-independent μ-opioid receptor phosphorylation by protein kinase C. *Br J Pharmacol*, 171(5):1330–40, 2014.
(Cited on pages 25, 26, 27, 77, 95, and 192.)

[164] S. Ingram, T. J. Wilding, E. W. McCleskey, and J. T. Williams. Efficacy and kinetics of opioid action on acutely dissociated neurons. *Mol Pharmacol*, 52(1):136–43, 1997.
(Cited on pages 31 and 93.)

[165] S. L. Ingram and J. T. Williams. Opioid inhibition of ih via adenylyl cyclase. *Neuron*, 13(1): 179–86, 1994.
(Cited on page 29.)

[166] M. S. Jhaveri, C. Wagner, and J. B. Trepel. Impact of extracellular folate levels on global gene expression. *Mol Pharmacol*, 60(6):1288–95, 2001.
(Cited on page 119.)

[167] E. A. Johnson, S. Oldfield, E. Braksator, A. Gonzalez-Cuello, D. Couch, K. J. Hall, S. J. Mundell, C. P. Bailey, E. Kelly, and G. Henderson. Agonist-selective mechanisms of μ-opioid receptor desensitization in human embryonic kidney 293 cells. *Mol Pharmacol*, 70(2):676–85, 2006.
(Cited on pages 35, 36, 37, 41, 78, 94, 95, 97, 186, 192, 207, and 208.)

[168] D. E. Jonas, H. R. Amick, C. Feltner, R. Wines, E. Shanahan, C. J. Rowe, and J. C. Garbutt. Genetic polymorphisms and response to medications for alcohol use disorders: a systematic review and meta-analysis. *Pharmacogenomics*, 15(13):1687–1700, 2014.
(Cited on page 102.)

[169] P. Joost and A. Methner. Phylogenetic analysis of 277 human G-protein-coupled receptors as a tool for the prediction of orphan receptor ligands. *Genome Biol*, 3(11):RESEARCH0063, 2002.
(Cited on page 16.)

[170] H. Joseph, S. Stancliff, and J. Langrod. Methadone maintenance treatment (mmt): a review of historical and clinical issues. *Mt Sinai J Med*, 67(5-6):347–64, 2000.
(Cited on page 15.)

[171] S. Just, S. Illing, M. Trester-Zedlitz, E. K. Lau, S. J. Kotowski, E. Miess, A. Mann, C. Doll, J. C. Trinidad, A. L. Burlingame, M. von Zastrow, and S. Schulz. Differentiation of opioid drug effects by hierarchical multi-site phosphorylation. *Mol Pharmacol*, 83(3):633–9, 2013.
(Cited on pages 25, 27, 38, 40, 96, 120, 152, 173, 191, 202, 203, and 205.)

[172] Jeong-Hun Kang. Protein kinase C (PKC) isozymes and cancer. *New Journal of Science*, 2014: 36, 2014.
(Cited on page 97.)

[173] S. Kapur, S. Sharad, R. A. Singh, and A. K. Gupta. A118G polymorphism in mu opioid receptor gene (*OPRM1*): association with opiate addiction in subjects of indian origin. *J Integr Neurosci*, 6(4):511–22, 2007.
(Cited on page 217.)

[174] M. W. Karaman, S. Herrgard, D. K. Treiber, P. Gallant, C. E. Atteridge, B. T. Campbell, K. W. Chan, P. Ciceri, M. I. Davis, P. T. Edeen, R. Faraoni, M. Floyd, J. P. Hunt, D. J. Lockhart, Z. V. Milanov, M. J. Morrison, G. Pallares, H. K. Patel, S. Pritchard, L. M. Wodicka, and P. P. Zarrinkar. A quantitative analysis of kinase inhibitor selectivity. *Nat Biotechnol*, 26(1):127–32, 2008.
(Cited on page 96.)

[175] E. Kelly, C. P. Bailey, and G. Henderson. Agonist-selective mechanisms of GPCR desensitization. *Br J Pharmacol*, 153 Suppl 1:S379–88, 2008.
(Cited on pages 34 and 42.)

[176] B. L. Kieffer. Recent advances in molecular recognition and signal transduction of active peptides: receptors for opioid peptides. *Cell Mol Neurobiol*, 15(6):615–35, 1995.
(Cited on page 7.)

[177] B. L. Kieffer, K. Befort, C. Gaveriaux-Ruff, and C. G. Hirth. The δ-opioid receptor: isolation of a cDNA by expression cloning and pharmacological characterization. *Proc Natl Acad Sci U S A*, 89(24):12048–52, 1992.
(Cited on page 7.)

[178] S. H. Kim, N. Stoicea, S. Soghomonyan, and S. D. Bergese. Remifentanil-acute opioid tolerance and opioid-induced hyperalgesia: a systematic review. *Am J Ther*, 22(3):e62–74, 2015.
(Cited on page 14.)

[179] M. Kleinjan, M. Rozing, R. C. Engels, and M. Verhagen. Co-development of early adolescent alcohol use and depressive feelings: The role of the mu-opioid receptor A118G polymorphism. *Dev Psychopathol*, pages 1–11, 2014.
(Cited on page 102.)

[180] A. Knapman and M. Connor. Cellular signalling of non-synonymous single-nucleotide polymorphisms of the human μ-opioid receptor (*OPRM1*). *Br J Pharmacol*, 172(2):349–63, 2015.
(Cited on pages 2, 21, 44, 101, 102, 151, and 176.)

[181] A. Knapman, M. Santiago, Y. P. Du, P. R. Bennallack, M. J. Christie, and M. Connor. A continuous, fluorescence-based assay of μ-opioid receptor activation in AtT-20 cells. *J Biomol Screen*, 18(3):269–76, 2013.
(Cited on pages ix, 62, 75, 78, 93, and 220.)

[182] A. Knapman, M. Santiago, and M. Connor. Buprenorphine signalling is compromised at the N40D polymorphism of the human μ opioid receptor *in vitro*. *Br J Pharmacol*, 171(18):4273–88, 2014.
(Cited on pages ix, 28, 99, 102, 103, 117, 119, 121, 217, and 219.)

[183] A. Knapman, M. Santiago, and M. Connor. A6V polymorphism of the human μ-opioid receptor decreases signalling of morphine and endogenous opioids *in vitro*. *British Journal of Pharmacology*, 172(9):2258–2272, 2015.
(Cited on pages ix, 99, 101, 102, 121, and 219.)

[184] T. Koch, T. Kroslak, P. Mayer, E. Raulf, and V. Hollt. Site mutation in the rat μ-opioid receptor demonstrates the involvement of calcium/calmodulin-dependent protein kinase ii in agonist-mediated desensitization. *J Neurochem*, 69(4):1767–70, 1997.
(Cited on pages 26 and 152.)

[185] T. Koch, T. Kroslak, M. Averbeck, P. Mayer, H. Schroder, E. Raulf, and V. Hollt. Allelic variation S268P of the human μ-opioid receptor affects both desensitization and G protein coupling. *Mol Pharmacol*, 58(2):328–34, 2000.
(Cited on pages 26, 36, 152, 184, and 221.)

[186] T. R. Kosten and T. P. George. The neurobiology of opioid dependence: implications for treatment. *Sci Pract Perspect*, 1(1):13–20, 2002.
(Cited on page 14.)

[187] A. Kovoor, V. Nappey, B. L. Kieffer, and C. Chavkin. μ and δ opioid receptors are differentially desensitized by the coexpression of β-adrenergic receptor kinase 2 and β-arrestin 2 in *Xenopus* oocytes. *J Biol Chem*, 272(44):27605–11, 1997.
(Cited on page 185.)

[188] W. Kromer. Endogenous opioids, the enteric nervous system and gut motility. *Dig Dis*, 8(6): 361–73, 1990.
(Cited on page 12.)

[189] T. Kroslak, K. S. Laforge, R. J. Gianotti, A. Ho, D. A. Nielsen, and M. J. Kreek. The single nucleotide polymorphism A118G alters functional properties of the human mu opioid receptor. *J Neurochem*, 103(1):77–87, 2007.
(Cited on page 102.)

[190] J. G. Krupnick and J. L. Benovic. The role of receptor kinases and arrestins in G protein-coupled receptor regulation. *Annu Rev Pharmacol Toxicol*, 38:289–319, 1998.
(Cited on pages 34 and 77.)

[191] M. J. Kuhar, C. B. Pert, and S. H. Snyder. Regional distribution of opiate receptor binding in monkey and human brain. *Nature*, 245(5426):447–50, 1973.
(Cited on page 12.)

[192] A. J. Kuszak, S. Pitchiaya, J. P. Anand, H. I. Mosberg, N. G. Walter, and R. K. Sunahara. Purification and functional reconstitution of monomeric μ-opioid receptors: allosteric modulation of agonist binding by Gi2. *J Biol Chem*, 284(39):26732–41, 2009.
(Cited on page 22.)

[193] P. M. Lanctot, P. C. Leclerc, M. Clement, M. Auger-Messier, E. Escher, R. Leduc, and G. Guillemette. Importance of N-glycosylation positioning for cell-surface expression, targeting, affinity and quality control of the human AT1 receptor. *Biochem J*, 390(Pt 1):367–76, 2005.
(Cited on page 119.)

[194] S. A. Laporte, R. H. Oakley, J. Zhang, J. A. Holt, S. S. Ferguson, M. G. Caron, and L. S. Barak. The β_2-adrenergic receptor/βarrestin complex recruits the clathrin adaptor AP-2 during endocytosis. *Proc Natl Acad Sci U S A*, 96(7):3712–7, 1999.

(Cited on page 39.)

[195] E. K. Lau, M. Trester-Zedlitz, J. C. Trinidad, S. J. Kotowski, A. N. Krutchinsky, A. L. Burlingame, and M. von Zastrow. Quantitative encoding of the effect of a partial agonist on individual opioid receptors by multisite phosphorylation and threshold detection. *Sci Signal*, 4(185):ra52, 2011.
(Cited on pages 24, 26, 27, 40, 173, and 192.)

[196] P. Y. Law, L. J. Erickson, R. El-Kouhen, L. Dicker, J. Solberg, W. Wang, E. Miller, A. L. Burd, and H. H. Loh. Receptor density and recycling affect the rate of agonist-induced desensitization of μ-opioid receptor. *Mol Pharmacol*, 58(2):388–98, 2000.
(Cited on pages 31 and 40.)

[197] P. Y. Law, Y. H. Wong, and H. H. Loh. Molecular mechanisms and regulation of opioid receptor signaling. *Annu Rev Pharmacol Toxicol*, 40:389–430, 2000.
(Cited on page 28.)

[198] J. Leandro, P. Leandro, and T. Flatmark. Heterotetrameric forms of human phenylalanine hydroxylase: co-expression of wild-type and mutant forms in a bicistronic system. *Biochim Biophys Acta*, 1812(5):602–12, 2011.
(Cited on page 217.)

[199] R. J. Lefkowitz. G protein-coupled receptors. III. new roles for receptor kinases and β-arrestins in receptor signaling and desensitization. *J Biol Chem*, 273(30):18677–80, 1998.
(Cited on page 32.)

[200] R. J. Lefkowitz. Seven transmembrane receptors: a brief personal retrospective. *Biochim Biophys Acta*, 1768(4):748–55, 2007.
(Cited on page 28.)

[201] R. J. Lefkowitz. A brief history of G-protein coupled receptors (Nobel Lecture). *Angew Chem Int Ed Engl*, 52(25):6366–78, 2013.
(Cited on page 33.)

[202] R. J. Lefkowitz and S. K. Shenoy. Transduction of receptor signals by β-arrestins. *Science*, 308 (5721):512–7, 2005.
(Cited on page 31.)

[203] E. S. Levitt and J. T. Williams. Morphine desensitization and cellular tolerance are distinguished in rat locus ceruleus neurons. *Mol Pharmacol*, 82(5):983–92, 2012.
(Cited on page 35.)

[204] J. Li, P. Huang, C. Chen, J. K. de Riel, H. Weinstein, and L. Y. Liu-Chen. Constitutive activation of the μ opioid receptor by mutation of D3.49(164), but not D3.32(147): d3.49(164) is

critical for stabilization of the inactive form of the receptor and for its expression. *Biochemistry*, 40(40):12039–50, 2001.
(Cited on pages 128 and 145.)

[205] J. G. Li, C. Chen, and L. Y. Liu-Chen. N-Glycosylation of the human κ opioid receptor enhances its stability but slows its trafficking along the biosynthesis pathway. *Biochemistry*, 46 (38):10960–70, 2007.
(Cited on page 182.)

[206] A. Lisi, M. Ledda, E. Rosola, D. Pozzi, E. D Emilia, L. Giuliani, A. Foletti, A. Modesti, S. Morris, and S. Grimaldi. Extremely low frequency electromagnetic field exposure promotes differentiation of pituitary corticotrope-derived AtT20 D16V cells. *Bioelectromagnetics*, 27(8): 641–651, 2006.
(Cited on page 179.)

[207] Q. Liu, M. S. Bee, and A. Schonbrunn. Site specificity of agonist and second messenger-activated kinases for somatostatin receptor subtype 2A (Sst2A) phosphorylation. *Mol Pharmacol*, 76(1): 68–80, 2009.
(Cited on page 96.)

[208] R. Liu, D. Nahon, B. le Roy, E. B. Lenselink, and I. Jzerman AP. Scanning mutagenesis in a yeast system delineates the role of the NPxxY(x)F motif and helix 8 of the adenosine A receptor in G protein coupling. *Biochem Pharmacol*, 2015.
(Cited on page 212.)

[209] W. Liu, E. Chun, A. A. Thompson, P. Chubukov, F. Xu, V. Katritch, G. W. Han, C. B. Roth, L. H. Heitman, I. Jzerman AP, V. Cherezov, and R. C. Stevens. Structural basis for allosteric regulation of GPCRs by sodium ions. *Science*, 337(6091):232–6, 2012.
(Cited on page 19.)

[210] K. Livingston and J. Traynor. Allosteric modulation of the μ-opioid receptor: Probe dependence and role of Na^+ ions. *The FASEB Journal*, 29(1 Supplement), 2015.
(Cited on page 221.)

[211] J. Llorente, J. D. Lowe, H. S. Sanderson, E. Tsisanova, E. Kelly, G. Henderson, and C. P. Bailey. μ-opioid receptor desensitization: homologous or heterologous? *Eur J Neurosci*, 36(12): 3636–42, 2012.
(Cited on pages 35, 76, and 209.)

[212] J. A. Lord, A. A. Waterfield, J. Hughes, and H. W. Kosterlitz. Endogenous opioid peptides: multiple agonists and receptors. *Nature*, 267(5611):495–9, 1977.
(Cited on page 7.)

[213] G. E. Loseth, D. M. Ellingsen, and S. Leknes. State-dependent μ-opioid modulation of social motivation. *Front Behav Neurosci*, 8:430, 2014.
(Cited on page 12.)

[214] J. D. Lowe and C. P. Bailey. Functional selectivity and time-dependence of μ-opioid receptor desensitization at nerve terminals in the mouse ventral tegmental area. *Br J Pharmacol*, 172 (2):469–81, 2015.
(Cited on page 94.)

[215] K. Lutfy and A. Cowan. Buprenorphine: a unique drug with complex pharmacology. *Curr Neuropharmacol*, 2(4):395–402, 2004.
(Cited on page 10.)

[216] L. M. Luttrell and R. J. Lefkowitz. The role of β-arrestins in the termination and transduction of G-protein-coupled receptor signals. *J Cell Sci*, 115(Pt 3):455–65, 2002.
(Cited on page 39.)

[217] T. A. Macey, J. D. Lowe, and C. Chavkin. Mu opioid receptor activation of ERK1/2 is GRK3 and arrestin dependent in striatal neurons. *J Biol Chem*, 281(45):34515–24, 2006.
(Cited on page 32.)

[218] S. Madishetti, N. Schneble, C. Konig, E. Hirsch, S. Schulz, J. P. Muller, and R. Wetzker. PI3Kγ integrates cAMP and Akt signalling of the μ-opioid receptor. *Br J Pharmacol*, 171(13):3328–37, 2014.
(Cited on page 28.)

[219] N. Mahy, M. Woolkalis, K. Thermos, K. Carlson, D. Manning, and T. Reisine. Pertussis toxin modifies the characteristics of both the inhibitory GTP binding proteins and the somatostatin receptor in anterior pituitary tumor cells. *J Pharmacol Exp Ther*, 246(2):779–85, 1988.
(Cited on page 218.)

[220] A. Manglik, A. C. Kruse, T. S. Kobilka, F. S. Thian, J. M. Mathiesen, R. K. Sunahara, L. Pardo, W. I. Weis, B. K. Kobilka, and S. Granier. Crystal structure of the μ-opioid receptor bound to a morphinan antagonist. *Nature*, 485(7398):321–6, 2012.
(Cited on pages 17, 18, 19, 21, 23, 26, 123, 128, 140, 145, 153, 181, 183, and 214.)

[221] A. Mann, S. Illing, E. Miess, and S. Schulz. Different mechanisms of homologous and heterologous μ-opioid receptor phosphorylation. *Br J Pharmacol*, 172(2):311–6, 2015.
(Cited on pages 23, 77, 187, 192, and 208.)

[222] A. Mansour, C. A. Fox, S. Burke, F. Meng, R. C. Thompson, H. Akil, and S. J. Watson. Mu, delta, and kappa opioid receptor mRNA expression in the rat CNS: an in situ hybridization study. *J Comp Neurol*, 350(3):412–38, 1994.
(Cited on page 12.)

[223] A. Mansour, C. A. Fox, H. Akil, and S. J. Watson. Opioid-receptor mRNA expression in the rat CNS: anatomical and functional implications. *Trends Neurosci*, 18(1):22–9, 1995.
(Cited on page 12.)

[224] S. Marion, R. H. Oakley, K. M. Kim, M. G. Caron, and L. S. Barak. A β-arrestin binding determinant common to the second intracellular loops of rhodopsin family G protein-coupled receptors. *J Biol Chem*, 281(5):2932–8, 2006.
(Cited on pages 145 and 212.)

[225] C. L. Marker, M. Stoffel, and K. Wickman. Spinal G-protein-gated K^+ channels formed by GIRK1 and GIRK2 subunits modulate thermal nociception and contribute to morphine analgesia. *J Neurosci*, 24(11):2806–12, 2004.
(Cited on page 30.)

[226] M. Martin, A. Matifas, R. Maldonado, and B. L. Kieffer. Acute antinociceptive responses in single and combinatorial opioid receptor knockout mice: distinct mu, delta and kappa tones. *Eur J Neurosci*, 17(4):701–8, 2003.
(Cited on pages 12 and 13.)

[227] W. R. Martin. Opioid antagonists. *Pharmacol Rev*, 19(4):463–521, 1967.
(Cited on page 7.)

[228] W. R. Martin, C. G. Eades, J. A. Thompson, R. E. Huppler, and P. E. Gilbert. The effects of morphine- and nalorphine- like drugs in the nondependent and morphine-dependent chronic spinal dog. *J Pharmacol Exp Ther*, 197(3):517–32, 1976.
(Cited on page 7.)

[229] L. Martini and J. L. Whistler. The role of mu opioid receptor desensitization and endocytosis in morphine tolerance and dependence. *Curr Opin Neurobiol*, 17(5):556–64, 2007.
(Cited on page 42.)

[230] J. C. Marvizon, W. Chen, and N. Murphy. Enkephalins, dynorphins, and β-endorphin in the rat dorsal horn: an immunofluorescence colocalization study. *J Comp Neurol*, 517(1):51–68, 2009.
(Cited on page 12.)

[231] H. Matsuhashi, Y. Horii, and K. Kato. Region-specific and epileptogenic-dependent expression of six subtypes of α2,3-sialyltransferase in the adult mouse brain. *J Neurochem*, 84(1):53–66, 2003.
(Cited on page 119.)

[232] A. Matsui and J. T. Williams. Activation of μ-opioid receptors and block of Kir3 potassium channels and NMDA receptor conductance by L- and D-methadone in rat locus coeruleus. *Br J Pharmacol*, 161(6):1403–13, 2010.
(Cited on pages 130 and 131.)

[233] H. W. Matthes, R. Maldonado, F. Simonin, O. Valverde, S. Slowe, I. Kitchen, K. Befort, A. Dierich, M. Le Meur, P. Dolle, E. Tzavara, J. Hanoune, B. P. Roques, and B. L. Kieffer. Loss of morphine-induced analgesia, reward effect and withdrawal symptoms in mice lacking the μ-opioid-receptor gene. *Nature*, 383(6603):819–23, 1996.
(Cited on pages 1, 13, 30, 32, and 212.)

[234] R. P. Mattick, J. Kimber, C. Breen, and M. Davoli. Buprenorphine maintenance versus placebo or methadone maintenance for opioid dependence. *Cochrane Database Syst Rev*, (2):CD002207, 2008.
(Cited on page 15.)

[235] J. P. McLaughlin and C. Chavkin. Tyrosine phosphorylation of the μ-opioid receptor regulates agonist intrinsic efficacy. *Mol Pharmacol*, 59(6):1360–8, 2001.
(Cited on page 26.)

[236] J. McPherson, G. Rivero, M. Baptist, J. Llorente, S. Al-Sabah, C. Krasel, W. L. Dewey, C. P. Bailey, E. M. Rosethorne, S. J. Charlton, G. Henderson, and E. Kelly. μ-Opioid receptors: correlation of agonist efficacy for signalling with ability to activate internalization. *Mol Pharmacol*, 78(4):756–66, 2010.
(Cited on pages 25, 40, 43, 120, 143, 203, and 205.)

[237] A. Mestek, J. H. Hurley, L. S. Bye, A. D. Campbell, Y. Chen, M. Tian, J. Liu, H. Schulman, and L. Yu. The human μ opioid receptor: modulation of functional desensitization by calcium/calmodulin-dependent protein kinase and protein kinase C. *J Neurosci*, 15(3 Pt 2): 2396–406, 1995.
(Cited on page 152.)

[238] T. G. Metzger and D. M. Ferguson. On the role of extracellular loops of opioid receptors in conferring ligand selectivity. *FEBS Lett*, 375(1-2):1–4, 1995.
(Cited on page 19.)

[239] J. C. Meunier, C. Mollereau, L. Toll, C. Suaudeau, C. Moisand, P. Alvinerie, J. L. Butour, J. C. Guillemot, P. Ferrara, B. Monsarrat, and et al. Isolation and structure of the endogenous agonist of opioid receptor-like ORL1 receptor. *Nature*, 377(6549):532–5, 1995.
(Cited on page 8.)

[240] W. E. Miller, S. Maudsley, S. Ahn, K. D. Khan, L. M. Luttrell, and R. J. Lefkowitz. β-arrestin1 interacts with the catalytic domain of the tyrosine kinase c-SRC. role of β-arrestin1-dependent targeting of c-SRC in receptor endocytosis. *J Biol Chem*, 275(15):11312–9, 2000.
(Cited on page 39.)

[241] G. Milligan. The role of dimerisation in the cellular trafficking of G-protein-coupled receptors. *Curr Opin Pharmacol*, 10(1):23–9, 2010.

(Cited on page 183.)

[242] M. Miyatake, T. J. Rubinstein, G. P. McLennan, M. M. Belcheva, and C. J. Coscia. Inhibition of EGF-induced ERK/MAP kinase-mediated astrocyte proliferation by μ opioids: integration of G protein and β-arrestin 2-dependent pathways. *J Neurochem*, 110(2):662–74, 2009.
(Cited on page 32.)

[243] P. Molinari, V. Vezzi, M. Sbraccia, C. Gro, D. Riitano, C. Ambrosio, I. Casella, and T. Costa. Morphine-like opiates selectively antagonize receptor-arrestin interactions. *J Biol Chem*, 285 (17):12522–35, 2010.
(Cited on page 205.)

[244] C. Mollereau, M. Parmentier, P. Mailleux, J. L. Butour, C. Moisand, P. Chalon, D. Caput, G. Vassart, and J. C. Meunier. ORL1, a novel member of the opioid receptor family. cloning, functional expression and localization. *FEBS Lett*, 341(1):33–8, 1994.
(Cited on page 7.)

[245] R. Moorman-Li, C. A. Motycka, L. D. Inge, J. M. Congdon, S. Hobson, and B. Pokropski. A review of abuse-deterrent opioids for chronic nonmalignant pain. *P T*, 37(7):412–8, 2012.
(Cited on page 11.)

[246] P. J. Moughan, M. F. Fuller, K. S. Han, A. K. Kies, and W. Miner-Williams. Food-derived bioactive peptides influence gut function. *Int J Sport Nutr Exerc Metab*, 17 Suppl:S5–22, 2007.
(Cited on page 9.)

[247] L. Mouledous, C. Froment, S. Dauvillier, O. Burlet-Schiltz, J. M. Zajac, and C. Mollereau. GRK2 protein-mediated transphosphorylation contributes to loss of function of μ-opioid receptors induced by neuropeptide FF (NPFF2) receptors. *J Biol Chem*, 287(16):12736–49, 2012.
(Cited on pages 24, 25, 26, 27, and 192.)

[248] E. Mura, S. Govoni, M. Racchi, V. Carossa, G. N. Ranzani, M. Allegri, and R. H. van Schaik. Consequences of the 118A>G polymorphism in the *OPRM1* gene: translation from bench to bedside? *J Pain Res*, 6:331–53, 2013.
(Cited on pages 15, 44, 101, and 102.)

[249] D. Nagaya, S. Ramanathan, M. Ravichandran, and V. Navaratnam. A118G mu opioid receptor polymorphism among drug addicts in Malaysia. *J Integr Neurosci*, 11(1):117–22, 2012.
(Cited on pages 15 and 217.)

[250] D. Nockemann, M. Rouault, D. Labuz, P. Hublitz, K. McKnelly, F. C. Reis, C. Stein, and P. A. Heppenstall. The K^+ channel GIRK2 is both necessary and sufficient for peripheral opioid-mediated analgesia. *EMBO Mol Med*, 5(8):1263–77, 2013.
(Cited on pages 30 and 130.)

[251] R. H. Oakley, S. A. Laporte, J. A. Holt, L. S. Barak, and M. G. Caron. Molecular determinants underlying the formation of stable intracellular G protein-coupled receptor-β-arrestin complexes after receptor endocytosis*. *J Biol Chem*, 276(22):19452–60, 2001.
(Cited on page 39.)

[252] Analgesics (revised October2012). eTG complete(internet). Melbourne, Australia. Therapeutic Guidelines Limited, 2015 March.
(Cited on pages 10 and 11.)

[253] B. G. Oertel, A. Doehring, B. Roskam, M. Kettner, N. Hackmann, N. Ferreiros, P. H. Schmidt, and J. Lotsch. Genetic-epigenetic interaction modulates μ-opioid receptor regulation. *Hum Mol Genet*, 21(21):4751–60, 2012.
(Cited on pages 102, 119, 183, and 217.)

[254] S. O'Gorman, D. T. Fox, and G. M. Wahl. Recombinase-mediated gene activation and site-specific integration in mammalian cells. *Science*, 251(4999):1351–5, 1991.
(Cited on pages 59 and 243.)

[255] W. M. Oldham and H. E. Hamm. Heterotrimeric G protein activation by G-protein-coupled receptors. *Nat Rev Mol Cell Biol*, 9(1):60–71, 2008.
(Cited on page 16.)

[256] EMBL-EBI website Clustal Omega. Available from: http://www.ebi.ac.uk/tools/msa/clustalo/, 2015 (Cited May 2015).
(Cited on page 220.)

[257] P. B. Osborne and J. T. Williams. Characterization of acute homologous desensitization of μ-opioid receptor-induced currents in locus coeruleus neurones. *Br J Pharmacol*, 115(6):925–32, 1995.
(Cited on page 77.)

[258] M. H. Ossipov, G. O. Dussor, and F. Porreca. Central modulation of pain. *J Clin Invest*, 120 (11):3779–87, 2010.
(Cited on page 12.)

[259] Y. Pak, B. F. O'Dowd, and S. R. George. Agonist-induced desensitization of the μ opioid receptor is determined by threonine 394 preceded by acidic amino acids in the COOH-terminal tail. *J Biol Chem*, 272(40):24961–5, 1997.
(Cited on pages 24, 27, and 192.)

[260] Y. Pak, B. F. O'Dowd, J. B. Wang, and S. R. George. Agonist-induced, G protein-dependent and -independent down-regulation of the μ opioid receptor. the receptor is a direct substrate for protein-tyrosine kinase. *J Biol Chem*, 274(39):27610–6, 1999.
(Cited on page 192.)

[261] K. Palczewski, T. Kumasaka, T. Hori, C. A. Behnke, H. Motoshima, B. A. Fox, I. Le Trong, D. C. Teller, T. Okada, R. E. Stenkamp, M. Yamamoto, and M. Miyano. Crystal structure of rhodopsin: A G protein-coupled receptor. *Science*, 289(5480):739–45, 2000.
(Cited on page 18.)

[262] L. Pan, J. Xu, R. Yu, M. M. Xu, Y. X. Pan, and G. W. Pasternak. Identification and characterization of six new alternatively spliced variants of the human μ opioid receptor gene, Oprm. *Neuroscience*, 133(1):209–20, 2005.
(Cited on page 44.)

[263] Z. Pan, N. Hirakawa, and H. L. Fields. A cellular mechanism for the bidirectional pain-modulating actions of orphanin FQ/nociceptin. *Neuron*, 26(2):515–22, 2000.
(Cited on page 8.)

[264] C. A. Paronis and S. G. Holtzman. Development of tolerance to the analgesic activity of μ agonists after continuous infusion of morphine, meperidine or fentanyl in rats. *J Pharmacol Exp Ther*, 262(1):1–9, 1992.
(Cited on page 14.)

[265] Y. C. Patel, R. Panetta, E. Escher, M. Greenwood, and C. B. Srikant. Expression of multiple somatostatin receptor genes in AtT-20 cells. evidence for a novel somatostatin-28 selective receptor subtype. *J Biol Chem*, 269(2):1506–9, 1994.
(Cited on page 95.)

[266] H. Pathan and J. Williams. Basic opioid pharmacology: an update. *British Journal of Pain*, 6 (1):11–16, 2012.
(Cited on pages 6, 7, 10, and 12.)

[267] M. Pawar, P. Kumar, S. Sunkaraneni, S. Sirohi, E. A. Walker, and B. C. Yoburn. Opioid agonist efficacy predicts the magnitude of tolerance and the regulation of μ -opioid receptors and dynamin-2. *Eur J Pharmacol*, 563(1-3):92–101, 2007.
(Cited on page 14.)

[268] D. Peckys and G. B. Landwehrmeyer. Expression of mu, kappa, and delta opioid receptor messenger RNA in the human CNS: a ^{33}P *in situ* hybridization study. *Neuroscience*, 88(4): 1093–135, 1999.
(Cited on page 12.)

[269] R. S. Pedersen, P. Damkier, and K. Brosen. Enantioselective pharmacokinetics of tramadol in CYP2D6 extensive and poor metabolizers. *Eur J Clin Pharmacol*, 62(7):513–21, 2006.
(Cited on pages 1 and 100.)

[270] C. B. Pert and S. H. Snyder. Opiate receptor: demonstration in nervous tissue. *Science*, 179 (4077):1011–4, 1973.

(Cited on page 12.)

[271] M. Petraschka, S. Li, T. L. Gilbert, R. E. Westenbroek, M. R. Bruchas, S. Schreiber, J. Lowe, M. J. Low, J. E. Pintar, and C. Chavkin. The absence of endogenous β-endorphin selectively blocks phosphorylation and desensitization of mu opioid receptors following partial sciatic nerve ligation. *Neuroscience*, 146(4):1795–807, 2007.
(Cited on page 36.)

[272] M. Pfeiffer, T. Koch, H. Schroder, M. Laugsch, V. Hollt, and S. Schulz. Heterodimerization of somatostatin and opioid receptors cross-modulates phosphorylation, internalization, and desensitization. *J Biol Chem*, 277(22):19762–72, 2002.
(Cited on pages 22, 95, 96, 183, 186, 187, and 209.)

[273] S. Pierre, T. Eschenhagen, G. Geisslinger, and K. Scholich. Capturing adenylyl cyclases as potential drug targets. *Nat Rev Drug Discov*, 8(4):321–35, 2009.
(Cited on page 29.)

[274] F. Poll, D. Lehmann, S. Illing, M. Ginj, S. Jacobs, A. Lupp, R. Stumm, and S. Schulz. Pasireotide and octreotide stimulate distinct patterns of sst_{2A} somatostatin receptor phosphorylation. *Mol Endocrinol*, 24(2):436–46, 2010.
(Cited on page 96.)

[275] R. K. Portenoy. Tolerance to opioid analgesics: clinical aspects. *Cancer Surv*, 21:49–65, 1994.
(Cited on page 14.)

[276] P. S. Portoghese. A new concept on the mode of interaction of narcotic analgesics with receptors. *J Med Chem*, 8(5):609–16, 1965.
(Cited on page 7.)

[277] L. S. Premkumar and G. P. Ahern. Induction of vanilloid receptor channel activity by protein kinase C. *Nature*, 408(6815):985–990, 2000.
(Cited on pages 248 and 252.)

[278] D. Provasi, M. B. Boz, J. M. Johnston, and M. Filizola. Preferred supramolecular organization and dimer interfaces of opioid receptors from simulated self-association. *PLoS Comput Biol*, 11 (3):e1004148, 2015.
(Cited on pages 22, 141, and 214.)

[279] N. Quillinan, E. K. Lau, M. Virk, M. von Zastrow, and J. T. Williams. Recovery from μ -opioid receptor desensitization after chronic treatment with morphine and methadone. *J Neurosci*, 31 (12):4434–43, 2011.
(Cited on page 41.)

[280] K. M. Raehal, J. K. Walker, and L. M. Bohn. Morphine side effects in β-arrestin 2 knockout mice. *J Pharmacol Exp Ther*, 314(3):1195–201, 2005.
(Cited on page 43.)

[281] K. M. Raehal, C. L. Schmid, C. E. Groer, and L. M. Bohn. Functional selectivity at the μ -opioid receptor: implications for understanding opioid analgesia and tolerance. *Pharmacol Rev*, 63(4):1001–19, 2011.
(Cited on page 43.)

[282] R. B. Raffa, R. P. Martinez, and C. D. Connelly. G-protein antisense oligodeoxyribonucleotides and μ -opioid supraspinal antinociception. *Eur J Pharmacol*, 258(1-2):R5–7, 1994.
(Cited on page 43.)

[283] D. S. Ramsay and S. C. Woods. Clarifying the roles of homeostasis and allostasis in physiological regulation. *Psychol Rev*, 121(2):225–47, 2014.
(Cited on page 12.)

[284] S. G. Rasmussen, H. J. Choi, D. M. Rosenbaum, T. S. Kobilka, F. S. Thian, P. C. Edwards, M. Burghammer, V. R. Ratnala, R. Sanishvili, R. F. Fischetti, G. F. Schertler, W. I. Weis, and B. K. Kobilka. Crystal structure of the human β_2 adrenergic G-protein-coupled receptor. *Nature*, 450(7168):383–7, 2007.
(Cited on page 18.)

[285] S. G. Rasmussen, H. J. Choi, J. J. Fung, E. Pardon, P. Casarosa, P. S. Chae, B. T. Devree, D. M. Rosenbaum, F. S. Thian, T. S. Kobilka, A. Schnapp, I. Konetzki, R. K. Sunahara, S. H. Gellman, A. Pautsch, J. Steyaert, W. I. Weis, and B. K. Kobilka. Structure of a nanobody-stabilized active state of the β_2 adrenoceptor. *Nature*, 469(7329):175–80, 2011.
(Cited on pages 20, 21, 179, 181, and 218.)

[286] A. Raveh, A. Cooper, L. Guy-David, and E. Reuveny. Nonenzymatic rapid control of GIRK channel function by a G protein-coupled receptor kinase. *Cell*, 143(5):750–60, 2010.
(Cited on pages 37, 96, 187, 209, and 215.)

[287] A. Ravindranathan, G. Joslyn, M. Robertson, M. A. Schuckit, J. L. Whistler, and R. L. White. Functional characterization of human variants of the mu-opioid receptor gene. *Proc Natl Acad Sci U S A*, 106(26):10811–6, 2009.
(Cited on pages 42, 44, 101, 126, 127, 128, 134, 142, 144, 146, and 147.)

[288] K. Raynor, H. Kong, Y. Chen, K. Yasuda, L. Yu, G. I. Bell, and T. Reisine. Pharmacological characterization of the cloned κ-, δ-, and μ -opioid receptors. *Mol Pharmacol*, 45(2):330–4, 1994.
(Cited on pages 9 and 10.)

[289] R. K. Reinscheid, H. P. Nothacker, A. Bourson, A. Ardati, R. A. Henningsen, J. R. Bunzow, D. K. Grandy, H. Langen, Jr. Monsma, F. J., and O. Civelli. Orphanin FQ: a neuropeptide that activates an opioidlike G protein-coupled receptor. *Science*, 270(5237):792–4, 1995.
(Cited on page 8.)

[290] T. Reisine. Opiate receptors. *Neuropharmacology*, 34(5):463–72, 1995.
(Cited on page 16.)

[291] E. Reiter and R. J. Lefkowitz. GRKs and β-arrestins: roles in receptor silencing, trafficking and signaling. *Trends Endocrinol Metab*, 17(4):159–65, 2006.
(Cited on page 205.)

[292] E. Reiter, S. Ahn, A. K. Shukla, and R. J. Lefkowitz. Molecular mechanism of β-arrestin-biased agonism at seven-transmembrane receptors. *Annu Rev Pharmacol Toxicol*, 52:179–97, 2012.
(Cited on pages 31, 35, 43, and 205.)

[293] Q. Ren, H. Kurose, R. J. Lefkowitz, and S. Cotecchia. Constitutively active mutants of the α_2-adrenergic receptor. *J Biol Chem*, 268(22):16483–7, 1993.
(Cited on page 181.)

[294] G. Rivero, J. Llorente, J. McPherson, A. Cooke, S. J. Mundell, C. A. McArdle, E. M. Rosethorne, S. J. Charlton, C. Krasel, C. P. Bailey, G. Henderson, and E. Kelly. Endomorphin-2: a biased agonist at the μ -opioid receptor. *Mol Pharmacol*, 82(2):178–88, 2012.
(Cited on pages 38, 43, 94, 108, 120, 205, and 207.)

[295] A Roos and W F Boron. *Intracellular pH*, volume 61. 1981.
(Cited on page 179.)

[296] D. M. Rosenbaum, V. Cherezov, M. A. Hanson, S. G. Rasmussen, F. S. Thian, T. S. Kobilka, H. J. Choi, X. J. Yao, W. I. Weis, R. C. Stevens, and B. K. Kobilka. GPCR engineering yields high-resolution structural insights into β_2-adrenergic receptor function. *Science*, 318(5854): 1266–73, 2007.
(Cited on page 18.)

[297] D. M. Rosenbaum, S. G. Rasmussen, and B. K. Kobilka. The structure and function of G-protein-coupled receptors. *Nature*, 459(7245):356–63, 2009.
(Cited on page 18.)

[298] D. M. Rosenbaum, C. Zhang, J. A. Lyons, R. Holl, D. Aragao, D. H. Arlow, S. G. Rasmussen, H. J. Choi, B. T. Devree, R. K. Sunahara, P. S. Chae, S. H. Gellman, R. O. Dror, D. E. Shaw, W. I. Weis, M. Caffrey, P. Gmeiner, and B. K. Kobilka. Structure and function of an irreversible agonist-β_2 adrenoceptor complex. *Nature*, 469(7329):236–40, 2011.
(Cited on page 20.)

[299] A. Rosenblum, L. A. Marsch, H. Joseph, and R. K. Portenoy. Opioids and the treatment of chronic pain: controversies, current status, and future directions. *Exp Clin Psychopharmacol*, 16(5):405–16, 2008.
(Cited on pages 10 and 11.)

[300] N. Rouvinen-Lagerstrom, J. Lahti, H. Alho, L. Kovanen, M. Aalto, T. Partonen, K. Silander, D. Sinclair, K. Raikkonen, J. G. Eriksson, A. Palotie, S. Koskinen, and S. T. Saarikoski. μ -opioid receptor gene (OPRM1) polymorphism A118G: lack of association in finnish populations with alcohol dependence or alcohol consumption. *Alcohol Alcohol*, 48(5):519–25, 2013.
(Cited on pages 15 and 102.)

[301] S. Roy, H. C. Liu, and H. H. Loh. μ -opioid receptor-knockout mice: the role of μ -opioid receptor in gastrointestinal transit. *Brain Res Mol Brain Res*, 56(1-2):281–3, 1998.
(Cited on page 13.)

[302] P. Salmi, J. Kela, U. Arvidsson, and C. Wahlestedt. Functional interactions between δ- and μ -opioid receptors in rat thermoregulation. *Eur J Pharmacol*, 458(1-2):101–6, 2003.
(Cited on page 12.)

[303] A. Salvi, J. M. Quillan, and W. Sade. Monitoring intracellular pH changes in response to osmotic stress and membrane transport activity using 5-chloromethylfluorescein. *AAPS PharmSci*, 4(4): 21–28, 2002.
(Cited on page 179.)

[304] C. F. Samer, Y. Daali, M. Wagner, G. Hopfgartner, C. B. Eap, M. C. Rebsamen, M. F. Rossier, D. Hochstrasser, P. Dayer, and J. A. Desmeules. Genetic polymorphisms and drug interactions modulating CYP2D6 and CYP3A activities have a major effect on oxycodone analgesic efficacy and safety. *Br J Pharmacol*, 160(4):919–30, 2010.
(Cited on pages 1, 44, and 100.)

[305] C. F. Samer, K. I. Lorenzini, V. Rollason, Y. Daali, and J. A. Desmeules. Applications of CYP450 testing in the clinical setting. *Mol Diagn Ther*, 17(3):165–84, 2013.
(Cited on page 1.)

[306] P. Sanchez-Blazquez, A. Garcia-Espana, and J. Garzon. In vivo injection of antisense oligodeoxynucleotides to G α subunits and supraspinal analgesia evoked by μ and δ opioid agonists. *J Pharmacol Exp Ther*, 275(3):1590–6, 1995.
(Cited on page 43.)

[307] B. Sauer. Site-specific recombination: developments and applications. *Curr Opin Biotechnol*, 5 (5):521–7, 1994.
(Cited on page 117.)

[308] A. K. Schreiber, C. F. Nones, R. C. Reis, J. G. Chichorro, and J. M. Cunha. Diabetic neuropathic pain: Physiopathology and treatment. *World J Diabetes*, 6(3):432–44, 2015.
(Cited on page 11.)

[309] S. A. Schug and C. Goddard. Recent advances in the pharmacological management of acute and chronic pain. *Ann Palliat Med*, 3(4):263–75, 2014.
(Cited on page 11.)

[310] K. Schuhmann, C. Voelker, G. F. Hfer, H. Pflgelmeier, N. Klugbauer, F. Hofmann, C. Romanin, and K. Groschner. Essential role of the beta subunit in modulation of C-class L-type Ca^{2+} channels by intracellular pH. *FEBS Letters*, 408(1):75–80, 1997.
(Cited on page 179.)

[311] S. Schulz, D. Mayer, M. Pfeiffer, R. Stumm, T. Koch, and V. Hollt. Morphine induces terminal μ -opioid receptor desensitization by sustained phosphorylation of serine-375. *EMBO J*, 23(16): 3282–9, 2004.
(Cited on pages 27, 112, 120, 190, and 191.)

[312] S. Schulz, A. Lehmann, A. Kliewer, and F. Nagel. Fine-tuning somatostatin receptor signalling by agonist-selective phosphorylation and dephosphorylation: IUPHAR Review 5. *Br J Pharmacol*, 171(7):1591–9, 2014.
(Cited on page 95.)

[313] V. Segredo, N. T. Burford, J. Lameh, and W. Sadee. A constitutively internalizing and recycling mutant of the μ -opioid receptor. *J Neurochem*, 68(6):2395–404, 1997.
(Cited on page 181.)

[314] T. Seki, M. Minami, T. Nakagawa, Y. Ienaga, A. Morisada, and M. Satoh. DAMGO recognizes four residues in the third extracellular loop to discriminate between μ - and κ-opioid receptors. *Eur J Pharmacol*, 350(2-3):301–10, 1998.
(Cited on page 18.)

[315] A. W. Serohijos, S. Yin, F. Ding, J. Gauthier, D. G. Gibson, W. Maixner, N. V. Dokholyan, and L. Diatchenko. Structural basis for μ -opioid receptor binding and activation. *Structure*, 19 (11):1683–90, 2011.
(Cited on pages 21 and 212.)

[316] G. Shahane, C. Parsania, D. Sengupta, and M. Joshi. Molecular insights into the dynamics of pharmacogenetically important N-terminal variants of the human β_2-adrenergic receptor. *PLoS Comput Biol*, 10(12):e1004006, 2014.
(Cited on page 123.)

[317] Y. Shang, V. LeRouzic, S. Schneider, P. Bisignano, G. W. Pasternak, and M. Filizola. Mechanistic insights into the allosteric modulation of opioid receptors by sodium ions. *Biochemistry*, 53(31):5140–9, 2014.
(Cited on page 19.)

[318] J. Shim, A. Coop, and Jr. MacKerell, A. D. Molecular details of the activation of the μ opioid receptor. *J Phys Chem B*, 117(26):7907–17, 2013.
(Cited on pages 21, 181, 184, 206, and 214.)

[319] E. J. Simon, J. M. Hiller, and I. Edelman. Stereospecific binding of the potent narcotic analgesic (^{3} H) etorphine to rat-brain homogenate. *Proc Natl Acad Sci U S A*, 70(7):1947–9, 1973.
(Cited on page 12.)

[320] F. Simonin, O. Valverde, C. Smadja, S. Slowe, I. Kitchen, A. Dierich, M. Le Meur, B. P. Roques, R. Maldonado, and B. L. Kieffer. Disruption of the κ-opioid receptor gene in mice enhances sensitivity to chemical visceral pain, impairs pharmacological actions of the selective κ-agonist U-50,488H and attenuates morphine withdrawal. *EMBO J*, 17(4):886–97, 1998.
(Cited on page 13.)

[321] F. L. Smith, B. H. Gabra, P. A. Smith, M. C. Redwood, and W. L. Dewey. Determination of the role of conventional, novel and atypical *pkc* isoforms in the expression of morphine tolerance in mice. *Pain*, 127(1-2):129–39, 2007.
(Cited on pages 37 and 77.)

[322] H. S. Smith and J. F. Peppin. Toward a systematic approach to opioid rotation. *J Pain Res*, 7: 589–608, 2014.
(Cited on page 14.)

[323] M. Sobczak, M. Salaga, M. A. Storr, and J. Fichna. Physiology, signaling, and pharmacology of opioid receptors and their ligands in the gastrointestinal tract: current concepts and future perspectives. *J Gastroenterol*, 49(1):24–45, 2014.
(Cited on page 12.)

[324] D. G. Soergel, R. A. Subach, N. Burnham, M. W. Lark, I. E. James, B. M. Sadler, F. Skobieranda, J. D. Violin, and L. R. Webster. Biased agonism of the mu-opioid receptor by TRV130 increases analgesia and reduces on-target adverse effects versus morphine: A randomized, double-blind, placebo-controlled, crossover study in healthy volunteers. *Pain*, 155(9): 1829–35, 2014.
(Cited on page 44.)

[325] J. Craig Venter Institute. PROVEAN software. Available from: http://provean.jcvi.org/index.php, 2015 (Cited 20 June 2015).
(Cited on page 140.)

[326] S. M. Spampinato. Overview of genetic analysis of human opioid receptors. *Methods Mol Biol*, 1230:3–12, 2015.
(Cited on page 2.)

[327] J. M. Stadel, P. Nambi, T. N. Lavin, S. L. Heald, M. G. Caron, and R. J. Lefkowitz. Catecholamine-induced desensitization of turkey erythrocyte adenylate cyclase. structural alterations in the beta-adrenergic receptor revealed by photoaffinity labeling. *J Biol Chem*, 257 (16):9242–5, 1982.
(Cited on page 33.)

[328] C. Stein. Targeting pain and inflammation by peripherally acting opioids. *Front Pharmacol*, 4: 123, 2013.
(Cited on pages 12 and 31.)

[329] C. Stein and H. Machelska. Modulation of peripheral sensory neurons by the immune system: implications for pain therapy. *Pharmacol Rev*, 63(4):860–81, 2011.
(Cited on page 12.)

[330] C. Stein, M. Schafer, and H. Machelska. Attacking pain at its source: new perspectives on opioids. *Nat Med*, 9(8):1003–8, 2003.
(Cited on page 29.)

[331] C. Sternini, M. Spann, B. Anton, Jr. Keith, D. E., N. W. Bunnett, M. von Zastrow, C. Evans, and N. C. Brecha. Agonist-selective endocytosis of mu opioid receptor by neurons in vivo. *Proc Natl Acad Sci U S A*, 93(17):9241–6, 1996.
(Cited on page 126.)

[332] Jr. Stockton, S. D. and L. A. Devi. Functional relevance of μ -δ opioid receptor heteromerization: a role in novel signaling and implications for the treatment of addiction disorders: from a symposium on new concepts in mu-opioid pharmacology. *Drug Alcohol Depend*, 121(3):167–72, 2012.
(Cited on page 22.)

[333] C. D. Strader, T. M. Fong, M. R. Tota, D. Underwood, and R. A. Dixon. Structure and function of G protein-coupled receptors. *Annu Rev Biochem*, 63:101–32, 1994.
(Cited on page 150.)

[334] P. G. Strange. Agonist binding, agonist affinity and agonist efficacy at G protein-coupled receptors. *Br J Pharmacol*, 153(7):1353–63, 2008.
(Cited on pages 146 and 215.)

[335] E. C. Tan, C. H. Tan, U. Karupathivan, and E. P. Yap. Mu opioid receptor gene polymorphisms and heroin dependence in Asian populations. *Neuroreport*, 14(4):569–72, 2003.
(Cited on page 101.)

[336] L. Terenius. Stereospecific interaction between narcotic analgesics and a synaptic plasm a membrane fraction of rat cerebral cortex. *Acta Pharmacol Toxicol (Copenh)*, 32(3):317–20, 1973.
(Cited on page 12.)

[337] A. Terskiy, K. M. Wannemacher, P. N. Yadav, M. Tsai, B. Tian, and R. D. Howells. Search of the human proteome for endomorphin-1 and endomorphin-2 precursor proteins. *Life Sci*, 81 (23-24):1593–601, 2007.
(Cited on page 8.)

[338] H. Teschemacher. Opioid receptor ligands derived from food proteins. *Curr Pharm Des*, 9(16): 1331–44, 2003.
(Cited on page 9.)

[339] M. Torrecilla, C. L. Marker, S. C. Cintora, M. Stoffel, J. T. Williams, and K. Wickman. G-protein-gated potassium channels containing Kir3.2 and Kir3.3 subunits mediate the acute inhibitory effects of opioids on locus ceruleus neurons. *J Neurosci*, 22(11):4328–34, 2002.
(Cited on page 30.)

[340] J. Traynor. μ -opioid receptors and regulators of G protein signaling (RGS) proteins: from a symposium on new concepts in mu-opioid pharmacology. *Drug Alcohol Depend*, 121(3):173–80, 2012.
(Cited on page 93.)

[341] J. M. Trigo, E. Martin-Garcia, F. Berrendero, P. Robledo, and R. Maldonado. The endogenous opioid system: a common substrate in drug addiction. *Drug Alcohol Depend*, 108(3):183–94, 2010.
(Cited on page 15.)

[342] M. S. Trivedi, J. S. Shah, S. Al-Mughairy, N. W. Hodgson, B. Simms, G. A. Trooskens, W. Van Criekinge, and R. C. Deth. Food-derived opioid peptides inhibit cysteine uptake with redox and epigenetic consequences. *J Nutr Biochem*, 25(10):1011–8, 2014.
(Cited on page 9.)

[343] A. Troisi, G. Frazzetto, V. Carola, G. Di Lorenzo, M. Coviello, F. R. D'Amato, A. Moles, A. Siracusano, and C. Gross. Social hedonic capacity is associated with the A118G polymorphism of the mu-opioid receptor gene (OPRM1) in adult healthy volunteers and psychiatric patients. *Soc Neurosci*, 6(1):88–97, 2011.
(Cited on page 102.)

[344] C. W. Vaughan, S. L. Ingram, M. A. Connor, and M. J. Christie. How opioids inhibit GABA-mediated neurotransmission. *Nature*, 390(6660):611–4, 1997.
(Cited on page 28.)

[345] J. P. Vilardaga, V. O. Nikolaev, K. Lorenz, S. Ferrandon, Z. Zhuang, and M. J. Lohse. Conformational cross-talk between α_{2A}-adrenergic and μ -opioid receptors controls cell signaling. *Nat Chem Biol*, 4(2):126–31, 2008.
(Cited on pages 22 and 142.)

[346] M. S. Virk, S. Arttamangkul, W. T. Birdsong, and J. T. Williams. Buprenorphine is a weak partial agonist that inhibits opioid receptor desensitization. *J Neurosci*, 29(22):7341–8, 2009.
(Cited on page 122.)

[347] M. von Zastrow, A. Svingos, H. Haberstock-Debic, and C. Evans. Regulated endocytosis of opioid receptors: cellular mechanisms and proposed roles in physiological adaptation to opiate drugs. *Curr Opin Neurobiol*, 13(3):348–53, 2003.
(Cited on pages 39, 40, and 126.)

[348] E. A. Walker and A. M. Young. Differential tolerance to antinociceptive effects of μ opioids during repeated treatment with etonitazene, morphine, or buprenorphine in rats. *Psychopharmacology (Berl)*, 154(2):131–42, 2001.
(Cited on page 14.)

[349] W. Walwyn, C. J. Evans, and T. G. Hales. β-arrestin2 and c-Src regulate the constitutive activity and recycling of μ opioid receptors in dorsal root ganglion neurons. *J Neurosci*, 27(19): 5092–104, 2007.
(Cited on page 32.)

[350] D. Wang, J. M. Quillan, K. Winans, J. L. Lucas, and W. Sadee. Single nucleotide polymorphisms in the human μ opioid receptor gene alter basal G protein coupling and calmodulin binding. *J Biol Chem*, 276(37):34624–30, 2001.
(Cited on pages 151 and 185.)

[351] D. J. Webb and R. Nuccitelli. Direct measurement of intracellular pH changes in *Xenopus* eggs at fertilization and cleavage. *J Cell Biol*, 91(2 Pt 1):562–7, 1981.
(Cited on page 179.)

[352] L. L. Werling, P. S. Puttfarcken, and B. M. Cox. Multiple agonist-affinity states of opioid receptors: regulation of binding by guanyl nucleotides in guinea pig cortical, NG108-15, and 7315c cell membranes. *Mol Pharmacol*, 33(4):423–31, 1988.
(Cited on page 20.)

[353] J. L. Whistler, H. H. Chuang, P. Chu, L. Y. Jan, and M. von Zastrow. Functional dissociation of μ opioid receptor signaling and endocytosis: implications for the biology of opiate tolerance and addiction. *Neuron*, 23(4):737–46, 1999.
(Cited on page 94.)

[354] J. M. White and R. J. Irvine. Mechanisms of fatal opioid overdose. *Addiction*, 94(7):961–72, 1999.
(Cited on page 14.)

[355] A. M. Wilbanks, S. A. Laporte, L. M. Bohn, L. S. Barak, and M. G. Caron. Apparent loss-of-function mutant GPCRs revealed as constitutively desensitized receptors. *Biochemistry*, 41 (40):11981–9, 2002.
(Cited on pages 128 and 145.)

[356] J. T. Williams, S. L. Ingram, G. Henderson, C. Chavkin, M. von Zastrow, S. Schulz, T. Koch, C. J. Evans, and M. J. Christie. Regulation of μ -opioid receptors: desensitization, phosphorylation, internalization, and tolerance. *Pharmacol Rev*, 65(1):223–54, 2013.
(Cited on pages 26, 32, 33, 41, 144, 160, 190, 193, 206, and 220.)

[357] R. Wolf, T. Koch, S. Schulz, M. Klutzny, H. Schroder, E. Raulf, F. Buhling, and V. Hollt. Replacement of threonine 394 by alanine facilitates internalization and resensitization of the rat μ opioid receptor. *Mol Pharmacol*, 55(2):263–8, 1999.
(Cited on page 192.)

[358] T. M. Wong and J. Shan. Modulation of sympathetic actions on the heart by opioid receptor stimulation. *J Biomed Sci*, 8(4):299–306, 2001.
(Cited on page 28.)

[359] H. Wu, D. Wacker, M. Mileni, V. Katritch, G. W. Han, E. Vardy, W. Liu, A. A. Thompson, X. P. Huang, F. I. Carroll, S. W. Mascarella, R. B. Westkaemper, P. D. Mosier, B. L. Roth, V. Cherezov, and R. C. Stevens. Structure of the human κ-opioid receptor in complex with JDTic. *Nature*, 485(7398):327–32, 2012.
(Cited on page 23.)

[360] Z. Xie, Z. Li, L. Guo, C. Ye, J. Li, X. Yu, H. Yang, Y. Wang, C. Chen, D. Zhang, and L. Y. Liu-Chen. Regulator of G protein signaling proteins differentially modulate signaling of μ and δ opioid receptors. *Eur J Pharmacol*, 565(1-3):45–53, 2007.
(Cited on page 93.)

[361] J. Xu, M. Xu, Y. L. Hurd, G. W. Pasternak, and Y. X. Pan. Isolation and characterization of new exon 11-associated N-terminal splice variants of the human mu opioid receptor gene. *J Neurochem*, 108(4):962–72, 2009.
(Cited on page 44.)

[362] T. Yamamoto, K. Shono, and S. Tanabe. Buprenorphine activates μ and opioid receptor like-1 receptors simultaneously, but the analgesic effect is mainly mediated by μ receptor activation in the rat formalin test. *J Pharmacol Exp Ther*, 318(1):206–13, 2006.
(Cited on page 122.)

[363] K. Yasuda, K. Raynor, H. Kong, C. D. Breder, J. Takeda, T. Reisine, and G. I. Bell. Cloning and functional comparison of κ and δ opioid receptors from mouse brain. *Proc Natl Acad Sci U S A*, 90(14):6736–40, 1993.
(Cited on page 7.)

[364] A. Yousuf, E. Miess, S. Sianati, Y. P. Du, S. Schulz, and M. Christie. The role of phosphorylation sites in desensitization of μ -opioid receptor. *Mol Pharmacol*, 2015.
(Cited on pages 25, 35, 37, 41, 193, 206, 208, and 216.)

[365] Y. Yu, L. Zhang, X. Yin, H. Sun, G. R. Uhl, and J. B. Wang. μ opioid receptor phosphorylation, desensitization, and ligand efficacy. *J Biol Chem*, 272(46):28869–74, 1997.
(Cited on page 190.)

[366] J. E. Zadina, L. Hackler, L. J. Ge, and A. J. Kastin. A potent and selective endogenous agonist for the μ -opiate receptor. *Nature*, 386(6624):499–502, 1997.
(Cited on page 8.)

[367] J. Zhang, S. S. Ferguson, L. S. Barak, S. R. Bodduluri, S. A. Laporte, P. Y. Law, and M. G. Caron. Role for G protein-coupled receptor kinase in agonist-specific regulation of mu-opioid receptor responsiveness. *Proc Natl Acad Sci U S A*, 95(12):7157–62, 1998.
(Cited on pages 36 and 185.)

[368] J. Zhang, L. S. Barak, P. H. Anborgh, S. A. Laporte, M. G. Caron, and S. S. Ferguson. Cellular trafficking of G protein-coupled receptor/β-arrestin endocytic complexes. *J Biol Chem*, 274(16): 10999–1006, 1999.
(Cited on page 39.)

[369] L. Zhang, Y. Yu, S. Mackin, F. F. Weight, G. R. Uhl, and J. B. Wang. Differential μ opiate receptor phosphorylation and desensitization induced by agonists and phorbol esters. *J Biol Chem*, 271(19):11449–54, 1996.
(Cited on pages 76 and 77.)

[370] L. Zhang, H. Zhao, Y. Qiu, H. H. Loh, and P. Y. Law. Src phosphorylation of μ -receptor is responsible for the receptor switching from an inhibitory to a stimulatory signal. *J Biol Chem*, 284(4):1990–2000, 2009.
(Cited on pages 26 and 30.)

[371] L. Zhang, H. H. Loh, and P. Y. Law. A novel noncanonical signaling pathway for the μ -opioid receptor. *Mol Pharmacol*, 84(6):844–53, 2013.
(Cited on page 30.)

[372] P. Zhang, P. S. Johnson, C. Zollner, W. Wang, Z. Wang, A. E. Montes, B. K. Seidleck, C. J. Blaschak, and C. K. Surratt. Mutation of human μ opioid receptor extracellular "disulfide

cysteine" residues alters ligand binding but does not prevent receptor targeting to the cell plasma membrane. *Brain Res Mol Brain Res*, 72(2):195–204, 1999.
(Cited on page 19.)

[373] Y. Zhang, D. Wang, A. D. Johnson, A. C. Papp, and W. Sadee. Allelic expression imbalance of human mu opioid receptor (OPRM1) caused by variant A118G. *J Biol Chem*, 280(38):32618–24, 2005.
(Cited on pages 102, 117, and 119.)

[374] H. Zheng, J. Chu, Y. Zhang, H. H. Loh, and P. Y. Law. Modulating micro-opioid receptor phosphorylation switches agonist-dependent signaling as reflected in PKCϵ activation and dendritic spine stability. *J Biol Chem*, 286(14):12724–33, 2011.
(Cited on pages 78 and 208.)

[375] H. Zheng, E. A. Pearsall, D. P. Hurst, Y. Zhang, J. Chu, Y. Zhou, P. H. Reggio, H. H. Loh, and P. Y. Law. Palmitoylation and membrane cholesterol stabilize μ -opioid receptor homodimerization and G protein coupling. *BMC Cell Biol*, 13:6, 2012.
(Cited on page 23.)

[376] Y. Zhu, M. A. King, A. G. Schuller, J. F. Nitsche, M. Reidl, R. P. Elde, E. Unterwald, G. W. Pasternak, and J. E. Pintar. Retention of supraspinal delta-like analgesia and loss of morphine tolerance in δ opioid receptor knockout mice. *Neuron*, 24(1):243–52, 1999.
(Cited on page 13.)

[377] Y. Zhu, Q. Dong, B. J. Tan, W. G. Lim, S. Zhou, and W. Duan. The PKCα-D294G mutant found in pituitary and thyroid tumors fails to transduce extracellular signals. *Cancer Res*, 65 (11):4520–4, 2005.
(Cited on page 97.)